



UNIVERSITÀ
DEGLI STUDI
FIRENZE

DOTTORATO DI RICERCA IN
Scienze della Salute (psicologia e terapia del dolore)

CICLO XXI

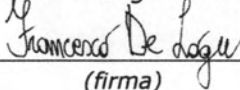
COORDINATORE Prof. Marco Matucci Cerinic

Caratterizzazione del ruolo fisiopatologico e funzionale dei canali
Transient Receptor Potential (TRP) nelle patologie dolorose di origine
infiammatoria e neuropatica"

Settore Scientifico Disciplinare MED/41

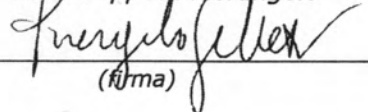
Dottorando

Dott. De Logu Francesco


(firma)

Tutore

Prof. Geppetti Pierangelo


(firma)

Coordinatore

Prof. (Matucci Cerinic Marco)


(firma)

Anni 2015/2018

Introduction

Historical Background: Transient Receptor Potential (TRP) channels and sensory neurons

The original discovery that vision in *Drosophila* is produced by an initial activation of a transient inward current associated with receptor stimulation (Montell et al., 1989) has led, with an unprecedented pace, to the identification of the TRP channels. TRPs represents one of the largest families of ion channels with more than 56 subtypes, which are widely distributed within the phylogeny and contribute to an array of different physiological functions and are implicated in a large series of pathological conditions. In mammals TRPs comprise 28 membrane proteins mainly behaving as non-selective cation permeable channels. TRPs are classified into seven subfamilies: TRPC ('Canonical'), TRPV ('Vanilloid'), TRPM ('Melastatin'), TRPP ('Polycystin'), TRPML ('Mucolipin'), TRPA ('Ankyrin'), and TRPN ('NOMP-C') (Clapham et al., 2003; Nilius, 2007).

TRP channels: Structure and Mechanism of Activation

TRP general structure recapitulates that of voltage gated channels with six transmembrane domains (S1-6) and the intracellular N- and C-terminal regions of variable length with a pore loop between S5 and S6 (Clapham et al., 2003; Owsianik et al., 2006). Whereas the C-terminus region, usually, possesses highly conserved domains, in most TRP channels, the N-terminus region is characterized by the presence of ankyrin repeats (33-residue motifs consisting of pairs of antiparallel α -helices connected by β -hairpin motifs). Ankyrin repeats have been associated with different features, including channel assembly in tetramers and interactions with ligands and protein partners (Gaudet, 2008). The number of ankyrin repeats is variable between different TRP subfamilies: 3 to 4 in TRPC, 6 in TRPV, 14 to 15 in TRPA and about 29 in TRPN. TRPs may contain other specific domains and motifs, such as coiled coils, calmodulin-binding sites, lipid-interaction domains, calcium-binding EF-hand-like motif, helix-loop-helix motif able to bind calcium ions, or phosphorylation sites that regulate channel functions.

It has been reported that four subunits, each composed by 6 transmembrane domains, may assemble in homo- and/or hetero-tetramers to form the functional channel,

where each subunit contributes to a shared selectivity filter and ion-conducting pore (Schaefer, 2005). Heteromultimeric channels between members of the same subfamily or different subfamilies can be also formed (Hofmann et al., 2002), suggesting that a wide variety of functionally diverse channels could be potentially formed. Although several TRPs may be weakly voltage-dependent they lack the hallmark of voltage-gated channels, e.g. the voltage sensor (Vannier et al., 1998; Voets et al., 2001). Beyond their general membrane topology and permeability to cations, TRP channels are strikingly diverse. Unlike other families of ion channels, the sequence homology of mammalian TRP channels is low. However, they exhibit a wide variety of modes of activation of both chemical and physical nature (exogenous chemical compounds, lipids, oxidative stress, acids, pheromones, osmolarity, mechanical stimulation, light, temperature and others), regulation (transcription, alternative splicing, glycosylation, phosphorylation), ion selectivity, tissue distribution (virtually all cells tested express at least one member of the superfamily). These features underline the unprecedented diversity of physiological and pathophysiological functions mediated by TRPs and their definition as polymodal sensors.

Despite this heterogeneity TRP activation may be summarized by three main general modalities: i. direct activation, operated by ligands, which encompass exogenous small organic molecules, including synthetic compounds and natural products, including capsaicin, icilin, allyl isothiocyanate (AITC), and others, endogenous lipids or products of lipid metabolism (diacylglycerols, phosphoinositides, eicosanoids, endocannabinoids, oxidative stress byproducts, and others) acting as allosteric modulators. It should be underlined that although many endogenous ligands for TRPs have been discovered, only for a very few numbers measured concentrations can suggest a physiological and pathophysiological role via TRP channel activation; ii. direct activation, operated by changes in ambient temperature (as in the case of vanilloid receptors) and by application of mechanical forces (as for cell swelling by hypoosmotic stimuli) although with a poorly understood mechanism, including conformational coupling to inositol trisphosphate (IP₃) receptors, and channel phosphorylation (Vriens et al., 2004); iii. indirect activation, produced through G protein-coupled receptors (GPCRs) and receptor tyrosine kinases stimulation thereby stimulating phospholipases C (PLCs) with a subsequent liberation of Ca²⁺ from intracellular stores (Clapham, 1995). Inorganic ions also regulate channel function, Ca²⁺ and Mg²⁺ being the most likely to have physiological relevance.

Posttranslational modification (i.e., phosphorylation) may affect TRP channel activation or deactivation. Protein kinases A, C, and G (PKA, PKC, and PKG, respectively) modulate TRP channel activity (Yao et al., 2005) and by Ca^{2+} /calmodulin (Ca^{2+} /CaM) (Zhu, 2005) may directly affect the TRP channel functioning, whereas indirect regulation of TRP potency is provided, as for GPCR, thus sensitizing or desensitizing the channels. Because most TRPs appear to be responsive to multiple stimuli, they may be defined as a sort of signal integrators. Channels are also high-gain signal amplifiers in that they function to enzymatically couple a single gating event (channel opening) to the flux of millions of ions per second. The combined properties of signal integrator and amplifier suggest that TRPs are adapted to function as cellular coincidence detectors. As such, TRP channels are inherently suited to serving broadly defined roles as cellular sensors (Clapham, 2003). This concept would be of particular relevance when describing the role of specific TRP channels in pain signalling.

TRP channels and nociceptors

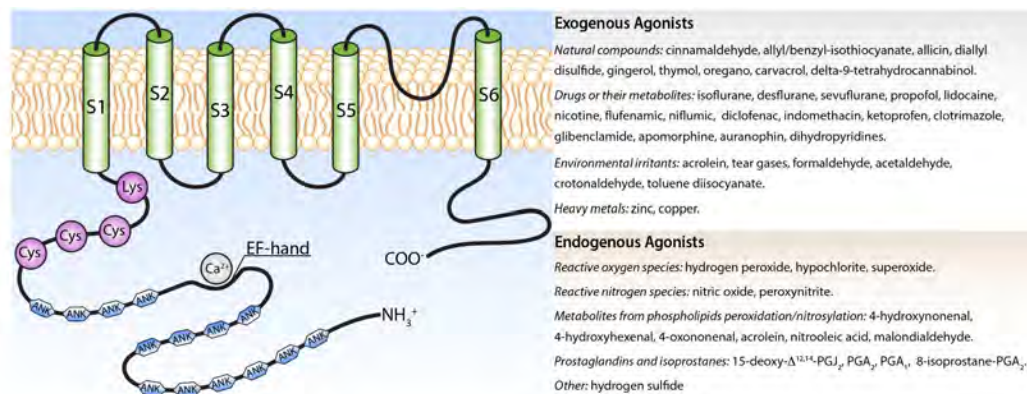
TRP channels are expressed in cellular membranes, with the exception of the nuclear envelope and mitochondria, of almost every excitable and non-excitable cell type. Object of the present review is to describe physiological and pathophysiological functions of the TRPs localized to a subset of primary sensory neurons (Szallasi et al., 2007), where they result highly involved in sensing physiological and noxious agents and, more generally, in pain perception. Just about a century ago, Sherrington proposed the existence of nociceptors, a subgroup of primary sensory neurons which are activated by tissue damaging stimuli, such as heat, intense pressure or irritant chemicals, but not by innocuous stimuli such as warming or light touch (Julius et al., 2001; Sherrington, 1906). The heterogeneous populations of primary sensory neurons and the fibres that they originate can be differentiated according to morphological, electrophysiological, neurochemical, functional and other criteria. In particular, neurons with the largest diameter cell bodies give rise to myelinated, rapidly conducting $\text{A}\beta$ fibres, which detect innocuous stimuli and normally do not contribute to nociceptive stimulus transduction. In contrast, neurons with small- and medium-diameter cell bodies give rise to unmyelinated, slowly conducting C-fibres and thinly myelinated, more rapidly conducting $\text{A}\delta$ -fibres. Both are highly involved in nociception. $\text{A}\delta$ - and C-nociceptive fibres either respond to a single type of physical stimuli, or more commonly integrate and generate

responses to potentially damaging thermal, mechanical and/or chemical stimuli, and for this reason are also defined as polymodal nociceptors (Julius et al., 2001).

A specific subset of C-fibre and A δ -fibre nociceptors is exquisitely sensitive to capsaicin, the pungent ingredient in hot peppers, and for this reason they have been labelled as ‘capsaicin-sensitive’ sensory neurons. The selective excitatory role of capsaicin is associated in a time- and concentration/dose-dependent manner with the ability of the compound to desensitize the channel and to defunctionalize TRPV1-positive nociceptors to capsaicin itself and to any other stimulus. This unique property of capsaicin, most likely derives by excessive Ca²⁺ influx through the channel, which, in adult rats transiently and in newborn rats permanently, alters nociceptor morphology and functioning (Bevan et al., 1992; Szallasi et al., 2007). TRPV1-expressing neurons comprise a subcategory defined as peptidergic because they produce the neuropeptides calcitonin gene-related peptide (CGRP) and the tachykinins, substance P (SP) and neurokinin A (NKA), which in response to depolarization, capsaicin or other excitatory stimuli are released from central and peripheral neuronal terminals. Upon peripheral neuropeptide release, activation of CGRP and tachykinin (NK₁, NK₂ and NK₃) receptors on effector cells, particularly at the vascular level, causes a series of inflammatory responses, collectively referred to as “neurogenic inflammation” (Geppetti et al., 1996). The peculiar property of capsaicin to first excite and thereafter desensitize both the afferent (nociception) and the efferent (neurogenic inflammation) responses, has given an unprecedented contribution to our current understanding of the role of these neurons in health and disease. In addition to TRPV1, peptidergic nociceptors also express other TRPs, including the TRPV2, TRPV3 and TRPV4 channels and the TRPA1 (Story et al., 2003), whereas TRPM8 seems to be confined to non-peptidergic sensory neurons (Bhattacharya et al., 2008). Because of the property to sense temperatures from cold (A1 and M8) to warm (V3 and V4) and hot (V1 and V2) temperatures, these channels have been collectively labelled as thermoTRPs (Guler et al., 2002; Story et al., 2003; Watanabe et al., 2002). Exogenous agents, early recognized as thermoTRP simulants include camphor for TRPV3 and TRPV4 (Moqrich et al., 2005), menthol for TRPM8 (McKemy et al., 2002; Peier et al., 2002), mustard and cinnamon oil for TRPA1 (Bandell et al., 2004; Jordt et al., 2004). The ability to sense, in addition to variations in temperature, physical and chemical changes within nerve terminal milieu indicates thermoTRPs as molecular integrators of multiple sensory modalities. Finally, coexistence of

neuropeptides and TRPs in the same sensory nerve terminals implies that different channel (TRPV1, TRPV4 or TRPA1) activation may drive the release mechanism that eventually results in the protective and/or detrimental process promoted by neurogenic inflammation (Geppetti et al., 1996).

Transient receptor potential ankyrin 1 (TRPA1)



Transient Receptor Potential Cation Channel Subfamily A Member 1 (TRPA1), Schematic representation of TRPA1 structure

The ankyrin-1 subtype of the transient receptor potential (TRPA1) is the only member of TRP channel superfamily in mammals. Initially identified in human lung fibroblasts (Jaquemar et al., 1999), as an ankyrin-like protein with transmembrane domains protein 1 (ANKTM1), the protein was successively recognized as a TRP channel for its homology with several members of the same superfamily (Story et al., 2003). TRPA1 that has been cloned in invertebrates, such as *Caenorhabditis elegans* and fruit fly and in variety of species, including zebrafish, chicken, mouse, rat, dog and humans (Nilius et al., 2014), is a protein of about 1,100 aminoacids (120-130 kDa), although shorter splice variants have also been reported. The human *trpa1* gene is in chromosome 8q13 and consists of 27 exons and spans 55,701 base pairs. Like others TRPs, TRPA1 is composed by 6 transmembrane domains with a pore region between domains 5 and 6 and 2 intracellular cytoplasmic regions located to the N- and C-terminals. Its name derives from an abundant number (14-19) of ankyrin repeat regions within the N-terminal, which appear to play a major role in protein-protein interactions, as they connect transmembrane proteins to the cytoskeleton and are involved in channel trafficking to the plasma

membrane. Another important functional site of TRPA1 is represented by at least 11 (of a total 31) reactive cysteines and lysine residues in the N-terminal domain. This region is required for activation operated by electrophilic molecules (Macpherson et al., 2007), as well as for channel desensitization.

TRPA1 also contains a Ca^{2+} -binding helix-loop-helix structural domain (EF-hand domain) which represents the most common mechanism for many Ca^{2+} -interacting proteins. Intracellular Ca^{2+} ions can directly activate the channel or potentiate agonist-induced responses probably through this mechanism. The C-terminal region contains positively charged domains for interaction with negatively charged ligands, including phosphoinositides or inorganic polyphosphates, that are generally considered to modulate TRPA1. The TRPA1, like many TRPs, is a non-selective cation channel with a characteristically inward depolarizing current prevalently due to Na^+ and Ca^{2+} ions (Nilius et al., 2014). TRPA1 activation by selective electrophilic agonists results in large inward currents whereas the outward rectification results mostly abolished (Nilius et al., 2014). In contrast, TRPA1 activation with non-electrophilic compounds maintains outward rectification. The reason for these differences remains to be elucidated, but it has been suggested that the extracellular Ca^{2+} level affects TRPA1 currents. In the presence of extracellular Ca^{2+} , activated TRPA1 currents decline rapidly (desensitization) whereas in its absence, both current activation and decay are delayed. TRPA1 channel arranges in subunits as tetramers, usually homo-tetramers, resulting in a permeable cation-selective channel functionally active. TRPA1 subunits may often co-localize with another TRP channel, the vanilloid 1 (TRPV1), thereby assembling into hetero-tetramers to adapt the single channel biophysical properties in native sensory neurons (Nilius et al., 2014).

Localization

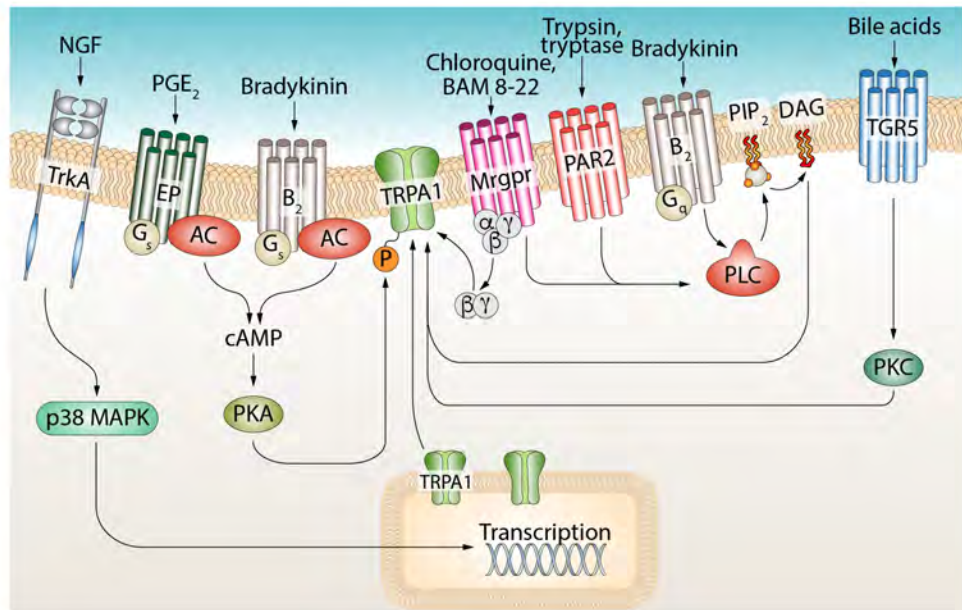
TRPA1 protein is abundantly expressed in a subpopulation of primary sensory neurons of the dorsal root (DRG), trigeminal (TG), and vagal (VG) ganglia. TRPA1-expressing neurons have unmyelinated C- and thinly myelinated $\text{A}\delta$ -fibres, and only occasionally large myelinated fibres (Bhattacharya et al., 2008; Story et al., 2003). However, the original proposal that TRPA1 expression is confined to peptidergic nociceptors (Bhattacharya et al., 2008; Story et al., 2003) has been challenged by recent evidence of co-localization of TRPA1 with markers of non-peptidergic neurons, including the purinergic P2X3 receptor, isolectin B4 (IB4), or the $\text{Na}(\text{V})1.8$ channel. The neuropeptides expressed by TRPA1-positive nociceptors are the tachykinins, substance P

(SP) and neurokinin A (NKA) and calcitonin gene-related peptide (CGRP) that mediate neurogenic inflammatory responses, when released from peripheral nerve terminals.

In the central nervous system, TRPA1 is expressed in hippocampal neurons, where it seems to be linked with the cannabinoid receptor CB1, in astrocytes, where it appears to contribute to resting intracellular Ca^{2+} levels and regulating inhibitory synapses modulating the extracellular concentration of γ -aminobutyric acid and in oligodendrocytes, with possible detrimental roles in ischemia and neurodegeneration (Hamilton et al., 2016). TRPA1 has been also identified in a variety of extra-neuronal cells tissues. These include the inner ear and the organ of Corti, where it may contribute to mechanical transduction, vascular endothelial cells, where it modulates vessel tone, keratinocytes and skin fibroblasts, where it mediates secretion of eicosanoids, such as prostaglandin E_2 (PGE_2) and leukotriene B_4 (LTB_4), thereby promoting, dental pulp fibroblasts, where it contributes to the perception of noxious cold and to cold hypersensitivity, airway and lung fibroblasts and epithelial and smooth muscle cells, where it modulates interleukin-8 release, rat pancreatic islets, where it facilitates insulin release, and enterochromaffin cells where it modulates gastrointestinal motility. TRPA1 is also expressed on taste cells, where it associates with the bitter taste receptor TAS2R60.

Channel modulation and intracellular pathways

G protein-coupled receptors (GPCRs) through second-messenger signalling cascades affect TRPA1 function. Thus, stimulation of the bradykinin receptor 2 (B2), the protease-activated receptor 2 (PAR2), the MAS-related GPCRs (MrgprA3 and MrgprC11) and the bile acid receptor (TGR5) with respective agonists have been found to activate/sensitize the TRPA1 channel. TRPA1 sensitivity was potentiated through phospholipase C (PLC)-coupled B2 receptor activation. The pathway that ultimately results in TRPA1 signalling requires the removal of the inhibitory effect of phosphatidylinositol-4,5-bisphosphate (PIP₂) and the inositol triphosphate (IP₃)-dependent Ca^{2+} release from intracellular stores. GPCR-dependent TRPA1 potentiation was inhibited by protein kinase A (PKA) blockers, indicating an additive potentiating effect mediated by the PKA pathway.



Transient Receptor Potential Cation Channel Subfamily A Member 1 (TRPA1), Intracellular pathways of TRPA1 modulation

PAR2 receptor expressed on sensory nerves is functionally coupled to TRPA1 by a PLC dependent pathways similar to that described for the B₂ receptor. PAR2 cleaved and activated by the proinflammatory agents, trypsin and mast cell tryptase, induces PLC activation and by this mechanism increases TRPA1 sensitivity to agonists. Pruritogens that induce histamine-independent itch activates the MrgprA3 and MrgprC11 receptors, which *via* Gβγ and PLC signalling, respectively, sensitize TRPA1 and exacerbate scratching behaviour in mice model of itch. Protein kinase C (PKC) activated by TGR5, co-expressed with TRPA1 by a subpopulation of cutaneous afferents, seems necessary for TRPA1 sensitization mediated by bile acids-

Neurotrophic factors receptors, expressed in peptidergic nociceptors, contribute to regulate TRPA1 expression and function under pathophysiological circumstances. In particular, increased nerve growth factor (NGF) levels by activating tyrosine kinase A (TrkA) receptor enhance phosphorylated p38 mitogen-activated protein kinase (MAPK), thus regulating TRPA1 expression and functional responses to augment pain hypersensitivity. MAPK activation may also occur downstream to the TRPA1 signalling pathway as activation of extracellular regulated kinase 1/2 (ERK1/2) and p38 MAPKs in DRG neurons correlated with TRPA1 activation.

Modes of activation and functions

TRPA1, initially described as a sensor of noxious cold (<15°C) (Story et al., 2003), in some species appears to mediate acute cold responses, being directly activated by cold either *via* Ca²⁺-dependent or Ca²⁺-independent mechanisms. Exposure to cold temperature sensitizes the channel, either native or expressed in heterologous systems, *via* an allosteric kinetic and Ca²⁺-independent process. *In vivo* observation confirmed that cold-like response by TRPA1 agonists detected in wild-type animals was absent in TRPA1-deficient mice. However, the TRPA1 role in cold sensation remain controversial with remarkable variability across species, as indicated by the fact that a single residue in S5 transmembrane domain accounts for the different response to cold stimuli between rodent and primate TRPA1. In contrast, the contribution of TRPA1 to cold hypersensitivity has been established in a variety of rodent models.

The role of TRPA1 has been also advocated in mechanosensation and, particularly, in mechanical hypersensitivity. The TRPA1 worm orthologue is sensitive to mechanical pressure, and several amphipathic molecules, such as trinitrophenol and chlorpromazine, produce a membrane curvature that leads to TRPA1 activity modulation. Whereas channel ability to mediate the acute painful consequences of mechanical pressure is still matter of debate, increasing evidence indicates a key role for TRPA1 in mechanical allodynia and hyperalgesia in rodent models of both inflammatory and neuropathic pain. What is not disputable is the TRPA1 sensitivity for an unprecedented series of chemical compounds, which has led to define TRPA1 as an ideal chemosensor. In the last 10 years, a plethora of chemical mediators that, produced by tissue or nerve injury, by targeting TRPA1 promote inflammatory and neuropathic pain have been identified. These can be divided into two main groups according to the mechanism of channel activation. The first group comprises all the molecules which gate the channel by modifying or interacting with nucleophilic cysteine and lysine residues of the channel N-terminus (Macpherson et al., 2007), by several chemical modes of covalent modification of the aminoacidic residues, including Michael addition, formation of a thiocarbamate intermediate and of cysteine-disulfide products or alkylation. The second group encompasses non-electrophilic compounds which activate the channel through a non-covalent protein modification, which act *via* bimodal mechanism that usually at low concentrations activate, whereas higher concentrations inhibit channel activity. In more general terms TRPA1 is among the various TRP channel that one more sensitive to change in the redox state of the milieu.

Channel agonists

Another way to classify TRPA1 agonists derives from their origin that can be either from exogenous sources or produced endogenously under inflammatory or tissue injury conditions. Exogenous agonists include a large variety of chemical species, such as molecules derived from natural or alimentary origin, drugs or drug metabolites, and environmental irritant molecules. Among natural compounds, the best-known activators, with moderate to severe irritant properties, are cinnamaldehyde, extracted from the *Cinnamomum*, several isothiocyanate compounds, such as allyl isothiocyanate (mustard oil) or benzyl obtained from the *Brassica* seeds, and contained in mustard or wasabi, allicin and diallyl disulfide, contained in garlic (*Allium sativum*) (Macpherson et al., 2005). Additional less potent or selective TRPA1 activators are gingerol, contained in ginger, which also gates TRPV1, thymol, a major component of thyme (*Thymus vulgari*) and oregano (*Origanum vulgare*), and carvacrol, contained in oregano. All these compounds have a common reactive chemical nature, which enables them to covalently modify specific cysteine residues within the cytoplasmic N-terminal region of the channel, resulting in TRPA1 activation. The non-electrophilic compound, delta-9-tetrahydrocannabinol (THC), contained in *Cannabis sativa*, or other phytocannabinoids, activate TRPA1 without any requirement of covalent modification. Environmental irritants described as TRPA1 channel stimulants include among others acrolein (Bautista et al., 2006) tear gases, toluene diisocyanate, formaldehyde (McNamara et al., 2007), acetaldehyde and crotonaldehyde, contained in cigarette smoke (Andre et al., 2008).

Another subgroup of exogenous TRPA1 activators is represented by drugs or their metabolites. General anaesthetics, including isoflurane, desflurane, sevoflurane and propofol, directly activate TRPA1 thereby producing irritation and neurogenic inflammatory responses in the respiratory tract. Local anaesthetics, including lidocaine (at high concentrations), can activate TRPA1 by both covalent and irreversible modification of intracellular cysteine residues and by interacting with the S5 transmembrane domain. Nicotine activates TRPA1 in nociceptors in a membrane-delimited manner, stabilizing the open state and destabilizing the closed state of the channel. Very high concentrations of non-steroidal anti-inflammatory drugs (NSAIDs) including flufenamic and niflumic acid, diclofenac, indomethacin and ketoprofen, have been shown to activate the rodent and human TRPA1, *in vitro*. Other currently used drug,

such as the antimycotic clotrimazole, the antidiabetic glibenclamide the non-narcotic morphine derivative, apomorphine, the antirheumatic medicine, auranophin, the antihypertensive and antianginal dihydropyridines have been also shown to activate TRPA1, albeit with low potency.

The second main group of TRPA1 activators is represented by endogenous mediators generated at sites of inflammation or tissue injury. The TRPA1 channel has been denoted as a sensor (Bessac et al., 2008) of a wide array of byproducts of oxidative stress, including reactive oxygen (ROS) and nitrogen (RNS) species. Among ROS, hydrogen peroxide (H_2O_2) hypochlorite (OCl^-), and superoxide (O_2^-), activate TRPA1. Among RNS, NO and ONOO $^-$ are TRPA1 stimulants. The peroxidation or nitrosylation of plasma membrane phospholipids generate reactive metabolites, including 4-hydroxy-nonenal (4-HNE), 4-hydroxy-hexenal (4-HHE), 4-oxo-nonenal (4-ONE), and nitrooleic acid (9-OA-NO $_2$), all identified as remarkable TRPA1 activators. ROS gate TRPA1 through a cysteine oxidation or disulfide formation, whereas RNS use a S-nitrosylation reaction. The reactive aldehydes, 4-HNE and acrolein, gate the channel by a Michael-addition reaction between their electrophilic C=C double bond and the sulfhydryl group of cysteine, the ϵ -amino group of lysine or the imidazole group of histidine residues (Macpherson et al., 2007; Trevisani et al., 2007). Cyclopentenone prostaglandins (PGs) and isoprostanes (iso-PGs), including 15-deoxy- $\Delta^{12,14}$ -PGJ $_2$ (15-d-PGJ $_2$), PGA $_2$ and PGA $_1$, and 8-isoprostane-PGA $_2$ generated *via* a non-enzymatic dehydration from proinflammatory and proalgesic prostaglandins and isoprostanes directly target the. Finally, hydrogen sulfide (H_2S), produced by cysteine metabolism and endowed with vasodilatory and other properties, has also been shown to stimulate TRPA1.

Thermal and Mechanical Activation

Although initially TRPA1 has been described as a sensor for noxious cold ($<15^\circ C$) (Bandell et al., 2004; Story et al., 2003) its role as a cold pain sensor has not been always confirmed. In particular, cold sensation was similar in wild type and TRPA1 deleted mice and TRPA1 blockade did or did not inhibit cold-evoked response in cinnamaldehyde sensitive nociceptors (Bautista et al., 2006; Caspani et al., 2009; McKemy et al., 2002). Some reports showed that TRPA1 contributes to acute cold responses, (Kwan et al., 2006), and TRPA1 seems to be directly activated by cold either *via* a Ca^{2+} -dependent (Zurborg et al., 2007) and a Ca^{2+} -independent mechanism (Karashima et al., 2009). If

different views are still present regarding the role of TRPA1 in acute transduction of cold sensation, increasing evidence suggests that TRPA1 channel plays a key role in cold hyperalgesia. Exposure to cold temperature sensitizes the channel, either native or expressed in heterologous systems *via* an allosteric kinetic and Ca²⁺-independent model (del Camino et al., 2010). *In vitro* results were confirmed by the *in vivo* observation that cold response by TRPA1 agonists was dramatically increased in wild-type animals, an effect that was absent in TRPA1-deficient mice (del Camino et al., 2010). Similarly, pharmacological channel inhibition reduced exaggerated cold response evoked by TRPA1 agonists (cinnamaldehyde, menthol, and icilin) (Fajardo et al., 2008). Furthermore, mice in which NaV1.8-expressing sensory neurons were eliminated by diphtheria toxin A exhibited a strongly reduced expression of TRPA1 in DRG neurons and lacked TRPA1-mediated nociceptive responses to formalin and cold (Abrahamsen et al., 2008), suggesting that noxious cold sensing *in vivo* requires somatosensory neurons that express both NaV1.8 and TRPA1.

One possible explanation for the conflicting results derives from the tenet that heterologous expression systems do not seem well suited to discriminate the specific role of TRPA1 in the transduction of cold stimuli. However, data obtained with TRPA1 or TRPM8-deficient mice propose that a population of neurons exists in both trigeminal and nodose ganglia that are activated by noxious cold and are not responsive to TRPA1 agonists (Fajardo et al., 2008; Karashima et al., 2009). Species differences may also contribute to this complex scenario, as a single residue in S5 transmembrane domain seems to account for the different response to cold stimuli between rodent and primate TRPA1 (Chen et al., 2011). Importantly, genetic deletion, or pharmacological inhibition, does not alter noxious cold sensation or body temperature regulation (Chen et al., 2011). This suggests that clinical development of TRPA1 antagonists may not be spoiled by temperature regulation problems that have severely hampered the clinical development of TRPV1 antagonists.

Another puzzling issue is represented by the role of TRPA1 in mechanosensation and mechanical hypersensitivity. The observations that TRPA1 channel is activated by hypertonic solution, that the TRPA1 worm orthologue is sensitive to mechanical pressure (Kindt et al., 2007), and that several amphipathic molecules, such as trinitrophenol and chlorpromazine, cause a membrane curvature that leads to TRPA1 activity modulation (Hill et al., 2007), supported the channel role in mechanosensitivity (Corey et al., 2004).

More importantly, increasing *in vivo* evidence suggests a key role for TRPA1 in mechanical allodynia or hyperalgesia. In rodent models of both inflammatory and neuropathic pain, mechanical hypersensitivity has been completely or partially dependent from TRPA1. The role in mechanical hypersensitivity of TRPA1 seems to be confined to the channel expressed by nociceptors. However, the specific subset of nociceptors (peptidergic, non-peptidergic), the contribution of neuropeptide-mediated neurogenic inflammation, or the influence of non-nociceptive fibres in TRPA1-mediated hypersensitivity, are all issues that remain to be defined. To add further complication, a recent study reports TRPA1 expression in epidermal and hair follicle keratinocytes as part of the mechanotransduction system (Kwan et al., 2009) In conclusion, current available data do not support an established and primary role for TRPA1 in acute mechanosensation. However, it should be carefully considered that emerging findings placed TRPA1 in a key position as the mediator of cold and mechanical hypersensitivity in different models of painful diseases.

Antagonists and desensitizing agents

Because of its pivotal role in several painful and inflammatory conditions, TRPA1 has recently been considered as a highly attractive target for the development of analgesic and anti-inflammatory drugs. Unfortunately, striking differences between human and rodent TRPA1 homologues have complicated TRPA1-targeted drug discovery. Many compounds that show antagonistic effects with the human TRPA1 can behave as agonists or show no activity when examined in the rat and mouse homologues. From a careful analysis it has emerged that the pharmacological profile of the rhesus monkey TRPA1 channel (rhTRPA1) is similar to the human TRPA1 channel (hTRPA1). In contrast, the rat TRPA1 and mouse TRPA1 channels are closely related but are pharmacologically distinct from either hTRPA1 or rhTRPA1 channels (Bianchi et al., 2012). These findings reveal that TRPA1 function differs between primate and rodent species and this should be considered in evaluating the predictive value of animal studies for clinical development (Bianchi et al., 2012).

The first rather selective TRPA1 antagonist, HC-030031, has been proposed by Hydra Biosciences in 2007. The compound in addition to inhibit responses by known TRPA1 agonists, as AITC, abated the nociceptive response typical of both the first and

second phase of formalin test, a key model of inflammatory pain (McNamara et al., 2007). Chemically, HC-030031 contains a xanthine alkaloid core similar to caffeine, a low potency TRPA1 activator, and covalently binds to the receptor (McNamara et al., 2007). From its discovery, HC-030031 has been widely used as a pharmacological tool to probe the role of TRPA1 channel in a variety of physiological functions and in a number of models of disease. The low potency of HC-030031 (AITC- and formalin evoked calcium influx *via* the hTRPA1 was inhibited with IC₅₀ values of 6.2 ± 0.2 and 5.3 ± 0.2 μM, respectively), is compensated by a good selectivity, which allows its effective use for parenteral or oral administration to specifically target TRPA1. A second antagonist, AP-18, was identified in the same year (Petrus et al., 2007). It is an oxime derivative that covalently binds to the channel. The first use of this compound allowed supporting a role of TRPA1 in mechanical hyperalgesia, as AP18 reverted complete Freund adjuvant-induced mechanical hyperalgesia in mice (Petrus et al., 2007).

A few years later Abbott disclosed a family of TRPA1 antagonists belonging to the α,β-unsaturated oxime series, identified by using a high-throughput screening program (>1,000,000 compounds) and their optimization. This class of compounds exhibits comparable pharmacology at human and rodent TRPA1, but pharmacokinetic profiles were often poor allowing insufficient drug exposure, as for the structural analogue, AP18 (Petrus et al., 2007). Iterative synthesis and screening led to subsequent identification of A-967079, (Chen et al., 2011), which for the first time, showed that TRPA1 antagonism does not affect body temperature or noxious cold sensation (Chen et al., 2011). This finding suggests that the preclinical and clinical development of TRPA1 antagonists may be safer regarding temperature regulation issues than those of TRPV1 antagonists. Chembridge-5861528, a derivative of HC-030031 was successfully used in a model of diabetic neuropathy (Wei et al., 2010), where it reduced pain-related behaviour and hypersensitivity (Koivisto et al., 2012). Lastly, a new series of compounds based on 7-substituted-1,3-dimethyl-1,5-dihydro-pyrrolo[3,2-d]pyrimidine-2,4-dione derivatives, which showed antagonistic properties at both rodent and human TRPA1 channel comparable to those of HC-030031 has been reported (Baraldi et al., 2012). Although at its infancy, TRPA1 antagonist research has been of great value for a better understanding of the main mechanisms of activation of TRPA1 channel, and in particular the role of the channel in a broad series of models of disease.

A series of herbal extracts used for the treatment of pain or migraine have been identified as TRPA1 agonists. Albeit this action would conflict with the beneficial effects of these compounds, they have been also characterized as partial agonists that peculiarly desensitize the channel and the sensory nerve terminal that mediate pain and neurogenic inflammation (Nassini et al., 2014). Parthenolide, the active constituent of *Tanacetum parthenium* recommended for migraine treatment, is a partial TRPA1 agonist, with the ensuing capability of antagonizing endogenous full channel agonists (Materazzi et al., 2013). Furthermore, parthenolide produced a prolonged desensitization of the TRPA1 channel and of the dual function of primary sensory neurons (neurogenic inflammatory and nociceptive responses). Ligustilide, used to treat pain and headaches, is contained in elevated concentrations in herbal medicines, and like parthenolide, by activating TRPA1 promotes nociceptor desensitization. Acetaminophen (paracetamol) is a universally used analgesic that, owe to its excellent safety profile, is prescribed in children and pregnant women to control fever and pain. However, the mechanism of action of its therapeutic action is unknown. The main acetaminophen metabolite, N-acetyl-p-benzoquinone imine (NAPQI), is a highly reactive molecule responsible for the major toxic effects if APAP is overdosed. NAPQI probably by its remarkable reactivity targets TRPA1, thereby causing channel desensitization and inhibiting pain transmission at relay structures of the dorsal spinal cord (Nassini et al., 2010). More importantly, antipyrine, propyphenazone and dipyron (metamizole), old analgesics still successfully used by hundreds of millions of patients, whose mechanism of action remained disputable, are potent and selective TRPA1 antagonists at concentrations fully compatible with human plasma levels, and by this mechanism inhibit inflammatory and neuropathic pain (Nassini et al., 2015).

TRPA1 and inflammatory pain

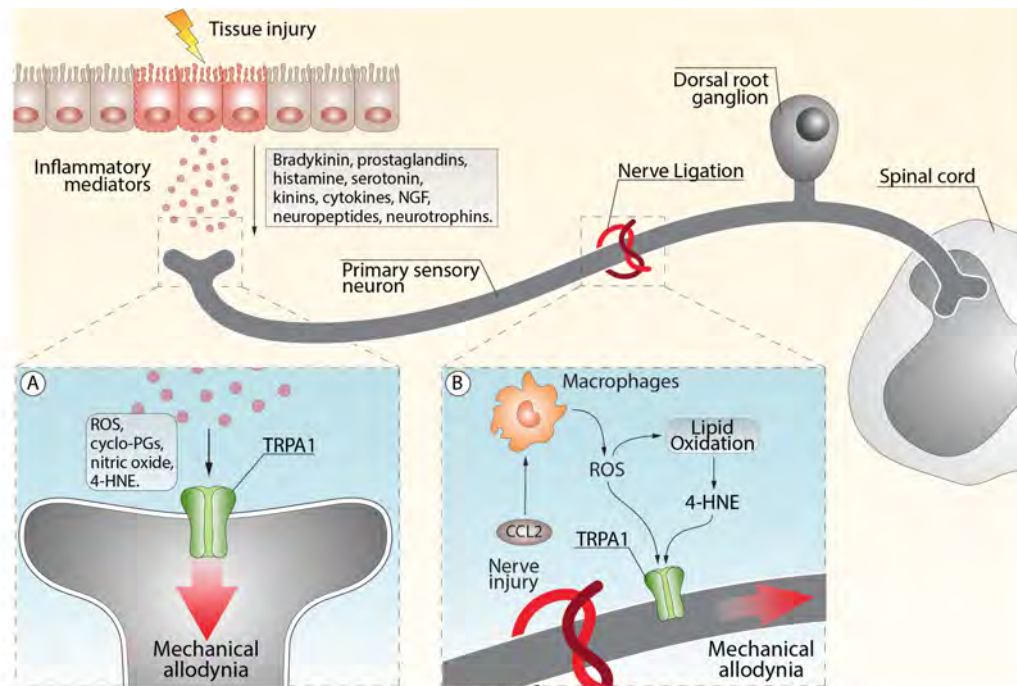
The role of TRPA1 channel in inflammatory pain should be considered twofold. On one side, proinflammatory agents activate and/or sensitize nociceptors via TRPA1. On the other side, TRPA1 stimulation is generally associated to the release of the proinflammatory neuropeptides SP/NKA and CGRP, which orchestrate a sort of feed-forward proinflammatory mechanism by promoting vasodilation, plasma protein leak, and stimulatory effects on immune cells (Geppetti et al., 1996). Of the heterogeneous pattern of agents found at sites of inflammation and collectively defined as ‘inflammatory soup’, many have been identified as activators or modulators of the TRPA1 channel. First

evidence on the role of TRPA1 in inflammatory hypersensitivity derived from cellular findings that TRPA1 via a PLC/Ca²⁺ signalling pathway contributes to bradykinin excitatory effects (Bandell et al., 2004), thus, representing an essential downstream target of bradykinin to induce nociceptor hypersensitivity (Bautista et al., 2006).

First reports on the role of TRPA1 in models of inflammatory pain have been described in rodent injected intradermally or intra-articularly with complete Freund's adjuvant (CFA). CFA-induced cold and mechanical hyperalgesia were associated with up-regulation of TRPA1 in DRG neurons (Obata et al., 2005) and sensitization of TRPA1 expressing neurons (Dunham et al., 2008). Pharmacological experiments corroborated this early evidence, as HC-030031 or AP-18 remarkably reduced CFA-evoked mechanical and cold hypersensitivity (da Costa et al., 2010; Eid et al., 2008; McGaraughty et al., 2010; Petrus et al., 2007). A seminal paper that underscored the unique role of TRPA1 in inflammatory nociception reported that either pharmacological blockade or gene deletion of the TRPA1 channel abrogated both the first and second phase of the nociceptive response induced by formalin in rat and mouse paw (McNamara et al., 2007).

While the involvement of TRPA1 to establish an acute hyperalgesic condition associated with an early inflammatory response has been well documented, more recent evidence supports channel contribution to the maintenance of nociceptor hypersensitivity. TRPA1 was found to mediate hypersensitivity associated with chronic inflammation, even days or weeks after the administration of the harmful stimulus, when damaging agents are removed or inflammation presumably resolved. TRPA1 gene deletion or selective antagonism reduced neuronal sensitization in models of osteoarthritis, induced by complete Freund adjuvant, carrageenan, monosodium iodoacetate, and monosodium urate (Bonet et al., 2013; Chen et al., 2008; da Costa et al., 2010; Fernandes et al., 2011; McGaraughty et al., 2010; Moilanen et al., 2012; Okun et al., 2012; Petrus et al., 2007). In particular, the ability of antisense mRNA for TRPA1 to prevent carrageenan-induced inflammatory hyperalgesia suggests that channel activation is necessary for both the development and the maintenance of this phenomenon (Bonet et al., 2013). However, the molecular mechanisms governing the key process, which, under inflammatory circumstances, results in a TRP-driven chronic painful phenotype, are not known. The role of oxidative stress and its byproducts, as observed in models of neuropathic pain (see

the following section), in this phenomenon either has not emerged or has not been exhaustively scrutinized yet.



Transient Receptor Potential Cation Channel Subfamily A Member 1 (TRPA1), Central role of TRPA1 in inflammatory and neuropathic pain. (a) Tissue injury generates an array of inflammatory agents, including reactive oxygen (ROS), nitrogen (nitric oxide) and carbonylic (4-hydroxy-2-nonenal, 4-HNE) species, bradykinin, prostaglandins, nerve growth factor (NGF), histamine, serotonin, kinins, cytokines, neuropeptides, and neurotrophins. Some of these agents such as ROS, cyclopentenone-prostaglandins (cyclo-PGs), nitric oxide, and 4-HNE directly gate the channel, whereas other agents modulate TRPA1 activity indirectly, promoting intracellular signaling cascades. Activation of both pathways contributes to increased mechanical allodynia typical of inflammatory pain. (b) The injured nerve trunk releases protective chemokines, including the chemoattractant chemokine (C-C motif) ligand 2 (CCL2), that recruits activated macrophages within the lesioned area. Phagocyte dependent oxidative stress (ROS) and the ensuing byproducts (4-HNE) target TRPA1 in nociceptor to produce mechanical allodynia typical of neuropathic pain.

TRPA1 and neuropathic pain

Unlike inflammatory pain, neuropathic pain is not associated with an overt tissue inflammatory condition, but rather is dependent from a damage or dysfunction of the nervous system and is most frequently due to peripheral nerve injury. The involvement of TRPA1 in different patterns of neuropathic pain has been proposed by recent results obtained in different animal models. Growing evidence is robustly building up the hypothesis that TRPA1 plays a major role in the hypersensitivity to chemical, thermal

and mechanical stimuli, which characterizes a variety of models of neuropathic pain, such as nerve injury, diabetic neuropathy and neuropathy induced by the chemotherapeutic agents (CIPN). Supporting data have been obtained by using both pharmacological and genetic tools.

Nerve injury and diabetes painful neuropathy

The contribution of TRPA1 channel to neuropathic pain has been first studied in model of lumbar spinal nerve ligation in which a down-regulation of TRPA1 expression in L5/DRG has been observed (Obata et al., 2005). Concomitant channel up-regulation in the adjacent L4/DRG characterized the presence of a compensatory mechanism of neuronal plasticity, based on an extensive TRPA1 expression and sensitization following nerve injury. Both dysregulation and adaptation of TRPA1 receptor in DRG neurons have been further described in other nerve-injury models, such as sciatic nerve injury by chronic constriction or transection (Caspani et al., 2009). The mechanism underlying TRPA1 upregulation at sites of nerve injuries remains unknown, although it is apparently associated with mechanical and thermal hyperalgesia. Studies based on pharmacological interventions have further corroborated this hypothesis. First, antisense knockdown of TRPA1, suppressed cold hypersensitivity developed after spinal nerve ligation in rats. Secondly, in a rat model of L5/L6 nerve ligation the mechanical hypersensitivity, detected six weeks post-surgery, was reversed by oral administration of HC-030031 (Eid et al., 2008). These results were confirmed by using a different, selective receptor antagonist, A-967079, which reduced cold hypersensitivity after injury without altering the normal cold perception in nerve injury models (Chen et al., 2011).

The contribution of TRPA1 channel has been proposed in conditions of neuropathic pain, which do not result from mechanical trauma, such as the pain secondary to diabetic neuropathy and CIPN (Wei et al., 2010). Painful peripheral neuropathy, a frequent complication of diabetes mellitus, is described as a superficial burning pain associated with mechanical and thermal hypersensitivity. In rodent model of streptozotocin-induced diabetes, acute blockade of TRPA1 was shown to reduce mechanical hypersensitivity (Wei et al., 2010). The role of oxidative stress that generates reactive carbonyl species, as HNE and methylglyoxal, is underscored by the recommendation in Germany of the antioxidant, α -lipoic acid, for the treatment of diabetic. In particular, methylglyoxal, held responsible for the development of long-term diabetic complications including diabetic

neuropathy (Vander Jagt, 2008), may exert this action by targeting the TRPA1 channel. More recently, it has been hypothesized that the reactive compounds produced in diabetes induce a sustained TRPA1 channel-mediated activation of nociceptive nerve fibres, causing both the pain hypersensitivity and the subsequent loss of cutaneous nerve fibre function, responsible for the detrimental long-term effects (Koivisto et al., 2012).

Chemotherapeutic induced neuropathy

CIPN is a major dose-limiting adverse reaction of anticancer therapeutics, characterized a prolonged pain condition and functional disability which negatively affects the quality of life of a relevant portion of treated patients and often results in therapy discontinuation (Cavaletti et al., 2010). Chemically diverse chemotherapeutic agents with different anticancer mechanisms, however, share the common ability to induce CIPN. These include platinum-based compounds (e.g., cisplatin and oxaliplatin), taxanes (e.g., paclitaxel), vinca alkaloids (e.g., vincristine), and the first-in-class proteasome inhibitor, bortezomib. The most common sensory symptoms of CIPN include paresthesias and dysesthesias to the extremities, spontaneous pain, and mechanical and thermal hypersensitivity. Treatment to improve the symptoms of CIPN is currently unsatisfactory and patients are undertreated (Cavaletti et al., 2010). The ability of chemotherapeutic agents to produce oxidative stress is considered an additional and collective property that, if from one side contributes to their anticancer action, on the other side seems to be responsible for major adverse reactions, including CIPN. In line with this assumption, it has been reported that oxaliplatin-induced mechanical hyperalgesia and heat- and cold-evoked allodynia in rats are attenuated by antioxidants, including acetyl-L-carnitine, α -lipoic acid or vitamin C, suggesting the contribution of oxidative stress to these painful conditions (Joseph et al., 2008).

A series of mechanisms have been advocated to explain the bothersome and dose-limiting painful CIPN, however, the neurochemical pathway(s) underlying the neuronal hyperexcitability and pain remains unrecognized. In recent years much attention has been paid to the peculiar interactions of chemotherapeutic agents with ion channels located on the membrane of the very terminal region of sensory nerve fibres. Voltage sensitive channels and more recently TRP channels, have been the object of intense investigation, mainly because their prevalent localization in nociceptors. The first report of the involvement of a TRP channel in a rodent model of CIPN was obtained by studying

cisplatin. Paradoxically, TRPV1 was found to protect against mechanical allodynia, because channel deletion worsened cisplatin-induced neurotoxicity (Bolcskei et al., 2005). Due to its primary localization to nociceptive sensory neurons, and its nociceptive role as a sensor of oxidative stress (Bessac et al., 2008), TRPA1 results perfectly suited to contribute to CIPN. Indeed, a single dose of oxaliplatin produces either in rats or mice a rapid-onset and time-dependent mechanical and cold hypersensitivities, which are reduced or abolished by TRPA1 genetic deletion or pharmacological inhibition (Gauchan et al., 2009; Joseph et al., 2009; Nassini et al., 2011). TRPA1 contribution to mechanical hypersensitivity does not seem confined to oxaliplatin, as TRPA1-deficient mice also developed a much-reduced mechanical allodynia after administration of the closely related drug, cisplatin. These early series of events may occur rapidly after oxaliplatin administration, but there is indirect evidence that oxidative stress may outlast for days after exposure to oxaliplatin. In fact, the antioxidants, acetyl L-carnitine, α -lipoic acid and vitamin C profoundly reduced oxaliplatin-evoked mechanical hyperalgesia, when given on the fifth day after oxaliplatin administration (Joseph et al., 2008).

The role of TRPA1 in models of CIPN, although prevalent, does not seem exclusive. In a mouse model of neuropathy induced by paclitaxel, mechanical hyperalgesia derives in part by the activation of the TRPV4 channel (Alessandri-Haber et al., 2008). However, both cold allodynia and the TRPV4-resistant mechanical hyperalgesia evoked by paclitaxel are entirely mediated by TRPA1 (Materazzi et al., 2012). Moreover, in a rat model of diabetes, paclitaxel significantly enhanced cold hyperalgesia in comparison to normoglycemic paclitaxel-treated control animals (Barriere et al., 2012). In diabetic and control rats, paclitaxel treatment was associated with accumulation of atypical mitochondria, and increased mitochondrial ROS production (Barriere et al., 2012). Paclitaxel potentiation of cold hyperalgesia in diabetes may result from the combination of increased mitochondrial ROS production and poor radical detoxification (Barriere et al., 2012). The observation that sensory hypersensitivity evoked by paclitaxel (Barriere et al., 2012; Materazzi et al., 2012) was prevented by pretreatment with antioxidant molecules or TRPA1 antagonists, corroborates the hypothesis that the common final pathway activated by chemically different chemotherapeutics produces notable oxidative stress (Joseph et al., 2008), that in turn activates and sensitizes TRPA1 channel.

More recent reports showed that a single dose of oxaliplatin or bortezomib is followed 1-3 days after administration by the onset of mechanical and cold hypersensitivity that lasts for 11-15 days (Trevisan et al., 2013a). Platinum-derived drugs, paclitaxel, or bortezomib do not directly target TRPA1 and there is evidence that cisplatin and oxaliplatin gate the channel by producing ROS most likely from cells other than primary sensory neurons (Nassini et al., 2011). Hypersensitivity, when established, is totally although transiently reverted by the antioxidant, α -lipoic acid or the TRPA1 antagonist, HC-030031 (Nassini et al., 2011; Trevisan et al., 2013a). However, hypersensitivity was completely absent if chemotherapeutic agents were administered to TRPA1 deleted mice (Nassini et al., 2011; Trevisan et al., 2013a). This finding implies that TRPA1 is necessary and sufficient for establishing a prolonged (10 days) hypersensitivity condition, which by no means outlasts the presence of the chemotherapeutic agent in plasma and/or tissues. Treatment with oxaliplatin or bortezomib transiently (1-6 hours) increased a marker of oxidative stress (Trevisan et al., 2013b), suggesting that both events (increased oxidative stress and its ability to target TRPA1) are required to establish the hypersensitivity condition. This hypothesis was confirmed by the following experiment. Treatment with a ROS scavenger or TRPA1 antagonist just before and for 6 hours after bortezomib or oxaliplatin administration completely and permanently protected mice from the development of the hypersensitivity (Trevisan et al., 2013b). Altogether, the described findings propose the unifying hypothesis that oxidative stress byproducts produced systemically or in the proximity of sensory neurons following exposure to chemotherapeutic agents activate/sensitize TRPA1 to induce a chronic hypersensitivity state (Nassini et al., 2011; Trevisan et al., 2013a). In this perspective TRPA1 may represent a unique pharmacological target for treating cancer patients who undergoing chemotherapeutic treatment, unfortunately develop CIPN.

TRPA1 and Migraine Headache

The original proposal by William Bayliss (Bayliss, 1901) and later by Sir Tomas Lewis (Lewis, 1937) of the existence of a ‘nocifensor system’, which, made up by a subset of somatosensory neurons, senses tissue injury and immediately orchestrates a local, inflammatory and defensive response, has only recently obtained a too long waited neurochemical demonstration. The CGRP receptor antagonist, telcagepant (Salvatore et

al., 2008), inhibited the neurogenic flare response induced by capsaicin application to the human forearm skin. This mechanism appears to be relevant in migraine headaches. While the proposal that meningeal plasma extravasation (mediated by SP acting at the NK1 receptor) contributes to migraine headache was not confirmed by different clinical trials (Goldstein et al., 1997), the component of neurogenic inflammation produced by CGRP released from perivascular trigeminal nerve endings seems to represent the underlying mechanism of migraine headaches. Indeed, various chemically unrelated CGRP receptor antagonists have been shown to ameliorate the pain and the associated symptoms of migraine attacks (Diener, 2003; Ho et al., 2008). As a consequence, stimuli, which acting at different receptors/channels, excite peptidergic nociceptors to release CGRP, may be expected to trigger migraine attacks. Recently, TRPA1 has emerged as a specific target for a number of migraine triggers and there is also evidence that some antimigraine medicines have an inhibitory action on channel activity.

TRPA1 is Activated by Migraine Producing Agents

It is a common notion for clinicians and a general experience for patients that a series of exogenous stimuli, including environmental agents, foods, medicines and other stimuli either provoke or favour headache in migraineurs. A proportion of migraineurs is particularly sensitive to inhalation of cigarette smoke, which increases the frequency of migraine and cluster headache (a rare and particularly severe type of primary headache) attacks. Crotonaldehyde, acetaldehyde (Bang et al., 2007), formaldehyde (McNamara et al., 2007), hydrogen peroxide (Sawada et al., 2008), nicotine (Talavera et al., 2009), and acrolein (Bautista et al., 2006) are, among the thousands of components of cigarette smoke, those which have been investigated and identified as TRPA1 activators. Cigarette smoke exposure in rodents causes a neurogenic inflammatory response in the airways (Lundberg et al., 1983) that is entirely mediated by TRPA1 activation (Andre et al., 2008). In line with these findings, it has been showed that application to the rat nasal mucosa of acrolein, a reactive α,β -unsaturated aldehyde, which gates TRPA1, produces a TRPA1-dependent and CGRP-mediated increase in meningeal blood flow (Kunkler et al., 2011). In clinical settings it is, thus, possible that inhalation of cigarette smoke through its TRPA1-acting components, as acrolein, crotonaldehyde, formaldehyde, acetaldehyde, hydrogen peroxide and nicotine promote CGRP release, e.g the process now recognized to trigger migraine attacks (Kunkler et al., 2011). Acrolein, which is also present in

vehicle exhaust and tear gas, because of its ability to excite TRPA1, could be responsible for the irritant responses evoked by tear gas, which in addition to cough, chest pain and dyspnoea, include headache. Additional molecules, identified as TRPA1 agonists, which have been long known as migraine or cluster headache provocative agents, include ammonium chloride (Bessac et al., 2009), and formalin (formaldehyde) (McNamara et al., 2007).

Nitroglycerine and its analogues exert cardioprotective effect through the release of the active vasodilator gaseous compound, nitric oxide (NO). Intra- and extra-cranial vasodilatation is considered one possible mechanism responsible for the common adverse reaction produced by nitroglycerine and congeners. Reversal of nitroglycerine-evoked headache/migraine by sumatriptan, presumably mediated by a direct vasoconstrictor action through serotonin 5-HT_{1B} receptor activation (Amin et al., 2013), strengthens the hypothesis of a major pro-headache role of NO-mediated vasodilatation of cranial arteries. Nitroglycerine/NO have been reported to release CGRP *in vitro* (Wei et al., 1992) and *in vivo* (Fanciullacci et al., 1995), and more recently NO has been found to act as a TRPA1 agonist (Miyamoto et al., 2009). Typically, nitroglycerine evokes an early and transient moderate headache in both migraineurs and healthy controls, while only migraineurs after a 4-5 hours delay develop an almost genuine migraine attack (Iversen et al., 1996). Thus, vasodilation *in vivo* (Iversen et al., 1996) and CGRP release *in vitro* (Wei et al., 1992), cannot easily account for the postponed migraine onset. However, it is not known whether a TRPA1-dependent mechanism contributes to the neuronal sensitization or other pathways responsible for the ability of NO and NO-donors to trigger migraine attacks.

Umbellulone is the major constituent of the California bay laurel, *Umbellularia californica*, which is also known as “headache tree” because of the headache provoking properties of its scent. Cluster headache like-attacks may also be triggered by exposure to the scent of *Umbellularia californica* (Benemei et al., 2009). Umbellulone, in a manner not immediately predictable from its chemical structure, reacts in a “click-fashion” with the biogenic thiol cysteamine, producing a Michael adduct (Nassini et al., 2012a), a prerequisite to exert a TRPA1 agonistic activity. Indeed, umbellulone gated TRPA1, thereby releasing CGRP. These *in vitro* responses were recapitulated *in vivo* by intranasal application of umbellulone, which, as for acrolein (Kunkler et al., 2011), produced a TRPA1-mediated and CGRP-dependent neurogenic meningeal vasodilation (Nassini et

al., 2012a). The reflex pathway or other possible neural mechanisms responsible for acrolein- and umbellulone-evoked meningeal vasodilatation following intranasal exposure to TRPA1 agonists remain to be investigated.

Additional Pathophysiological Roles of TRPA1 Related to Primary Sensory Neurons

Because of its wide neuronal and extra-neuronal distribution and the large number of activators, TRPA1 channel has been implicated, beside pain syndromes, in a broader series of pathological conditions. In particular, the ability of TRPA1 to release proinflammatory neuropeptides (Andre et al., 2008; Bautista et al., 2013; Nassini et al., 2012a; Trevisani et al., 2007), has suggested a role of TRPA1 not only in pain disease, but also in a series of pathophysiological models which feature sensory hypersensitivities along with neurogenic inflammatory responses. As an extreme example of novel proinflammatory activity, stimulation of TRPA1 in sensory neurons has been associated with the release of tumour necrosis factor- α (TNF- α) (Fernandes et al., 2011). Furthermore, there is now increasing evidence that TRPA1 activation in non neuronal cells contributes to non-neurogenic inflammation. Thus TRPA1, in both sensory neurons and non-neuronal cells, represents a molecular sensor for several chemical and irritant molecules (Atoyan et al., 2009; Moilanen et al., 2012; Nassini et al., 2010; Shapiro et al., 2013; Wei et al., 2010). For instance, TRPA1 localized to epithelial or smooth muscle pulmonary cells, elicits the release of interleukin-8 (IL-8) (Nassini et al., 2012b). Thus, TRPA1 activation may integrate both neuronal and extra-neuronal protective responses and also, by these same mechanisms, if become protracted and uncontrolled, may represent the underlying mechanism of chronic inflammatory and painful diseases.

The Airways

The pathophysiological role of TRPA1 in the respiratory tract seems to be primarily dependent from neurogenic inflammation (Nassenstein et al., 2008). The respiratory tract is highly innervated by vagal primary afferents, which can be activated by mechanical stimuli, environmental irritants or mediators produced by several patophysiological events. This pathway may mediate central reflexes, such as dyspnoea, changes in breathing pattern and cough and provoke local neurogenically mediated responses (Caceres et al., 2009). Clinical trials with SP receptor antagonists have not supported a

role for neurogenic plasma extravasation (which is mediated by SP and NK-1 receptors) in asthma. This hypothesis is reinforced by the observation that TRPV1 deleted mice do not show any protection in model of ovalbumin evoked asthma (Caceres et al., 2009). However, the same paper showed that TRPA1 pharmacological inhibition or gene deletion produced a mouse phenotype almost completely resistant to both airway inflammatory cell infiltration and hyperresponsiveness (Caceres et al., 2009). This finding challenges the proposal that oxidative stress (Bessac et al., 2008) and the ensuing activation of both sensory and non-sensory TRPA1 airway channel orchestrate the asthmatic response. In this context, it should be recalled that the increased prevalence of asthma in late childhood has been associated with the worldwide larger use of APAP during pregnancy, and early infancy. These otherwise robust epidemiological data, however, lack of a mechanistic explanation. The ability of NAPQI to promote mild to moderate and reversible airway inflammation, *via* TRPA1 (Nassini et al., 2010) may contribute to the pro-asthmatic action of APAP in susceptible individuals.

It is widely accepted that cigarette smoke habit is the major causative agent of chronic obstructive pulmonary disease (COPD) (Andre et al., 2008). Several major components of cigarette smoke, including crotonaldehyde (Andre et al., 2008), formaldehyde (McNamara et al., 2007), acrolein (Bautista et al., 2006) and nicotine (Talavera et al., 2009), are TRPA1 agonists. More importantly, the early inflammatory response produced by cigarette smoke inhalation, which has been defined entirely neurogenic in the past (Lundberg et al., 1983), is completely absent in TRPA1 knockout mice (Andre et al., 2008). Thus, it may be proposed that TRPA1 activation and the ensuing neurogenic responses are important in the pathogenesis of COPD. However, it should be underscored that also mouse and human pulmonary cells express functional TRPA1 (Jaquemar et al., 1999; Mukhopadhyay et al., 2011; Nassini et al., 2012b) and that channel activation in these cells promotes the release of several proinflammatory mediators, including certain chemokines, as the IL-8 (Nassini et al., 2012b; Shapiro et al., 2013). It is therefore possible that extra-neuronal TRPA1 cooperates with the neuronal channel to drive the chronic condition underlying asthma and COPD.

Itch and Skin Inflammation

Itch is a complex and multifactorial phenomenon interpreted as a primary and early defensive mechanism that, however, may develop either as a primary condition, a

symptom of underlying diseases or as an adverse drug reaction. Independently from the aetiology, itch, when chronic or associated with a chronic condition, may severely affect the quality of life of patients. Classically, histamine and serotonin and their receptors are considered major pruritogenic pathways (Cevikbas et al., 2014). Additional itch mechanisms encompass cascades mediated by Mas-related G protein-coupled receptor A3 (MrgprA3, activated by chloroquine) and MrgprC11, the receptor for the endogenous pruritogen BAM8-22. Recently, TRPA1 has been claimed to mediate chloroquine and BAM8-22 induced pruritus (Wilson et al., 2011) and it is required substantially for both transduction of chronic itch signals and for the skin changes triggered by dry-skin-evoked itch and scratching (Wilson et al., 2011). Additional mechanisms have been implicated in itch, as those activated by bile acids and their receptor (TGR5) (Alemi et al., 2013). However, there is no information as to whether TRPA1 contributes also to this latter pathway. Recent studies, in different itch models in rodent, demonstrated that additional neuronal pathways contribute to the response by implicating TRPA1 activation in a histamine-independent manner (Wilson et al., 2011).

Genetic diseases

Few studies have explored whether pain conditions associated with genetic TRPA1 variants. In 2010 in a Colombian family a point mutation in the S4 domain of TRPA1 that induced an autosomal dominant Mendelian heritable episodic pain syndrome, was identified (Kremeyer et al., 2010). Patients show severe episodes of pain triggered by conditions of fatigue, fasting and cold and mainly affecting the thorax and arms and occasionally radiating to the abdomen and legs. Affected patients displayed hypersensitivity to mustard oil and this effect correlated with a gain of function of the mutant TRPA1 channel inducing channel hypersensitivity to agonists and cold *in vitro* (Kremeyer et al. 2010). Another study has identified a single nucleotide mutation in N-terminal of TRPA1 channel (E179K) linked to paradoxical heat sensation in patient suffering from neuropathic pain (May et al., 2012).

Aim of the study

The TRPA1 receptor has been identified as a pivotal molecular entity in sensory biology, especially as a sensor of chemical species/irritants present in foods, atmospheric pollutants and toxicants. Rapid progress is being made in characterizing the function of TRPA1 in various tissues and organs under normal and pathophysiological conditions. TRPA1 receptor is an excitatory ion channel expressed by a subpopulation of primary afferent somatosensory neurons that contain SP and CGRP. Environmental irritants (mustard oil, allicin, acrolein) can activate TRPA1, causing acute pain, neuropeptide release, and neurogenic inflammation. Genetic studies indicate that TRPA1 is also activated downstream of one or more proalgesic agents that stimulate phospholipase C signaling pathways, thereby implicating this channel in peripheral mechanisms controlling pain hypersensitivity.

The commonly accepted paradigm is that TRPA1 expressed in primary sensory neurons is directly activated by ROS/RNS/RCS, thus signalling pain from the PNS to the CNS. While direct stimulation of nociceptor TRPA1 mediates acute spontaneous pain, recent findings from our laboratory also, have shifted the focus to the TRPA1 expressed in non-neuronal cells as the critical factor to sustain allodynia and chronic pain. In our study we aim at identifying the role of TRPA1 in different model of pain ranging from inflammatory to neuropathic pain.

The first aim of the present study was to identify the role of TRPA1 in a mouse model of trigeminal neuropathic pain produced by the constriction of the infraorbital nerve (CION) and to explore the molecular and cellular pathways that, from the initial nerve injury, result in channel engagement. The monocyte chemoattractant protein 1 (MCP-1), also known as chemoattractant chemokine (C-C motif) ligand 2 (CCL2), by binding to the chemotactic cytokine receptor 2 (CCR-2), promotes monocyte transendothelial migration to the site of nerve injury. In various paradigms of peripheral nerve injury, CCL2 inhibition and CCR-2 genetic ablation abrogates mechanical allodynia. In addition, antioxidants have been reported to attenuate neural hypersensitivity in various models of neuropathic pain, such as sciatic chronic constriction injury and spinal nerve ligation. Thus, the contribution of monocyte/macrophage infiltration and the ensuing oxidative stress in the TRPA1-mediated pain-like behaviors was investigated in the CION model.

However, while exploring a similar model (partial sciatic nerve ligation, pSNL), we surprisingly observed that mice with genetic deletion or pharmacological blockade of TRPA1 not only showed the expected reduced mechanical allodynia, but also exhibited a marked reduction in macrophages infiltration and H₂O₂ generation in the injured nerve trunk. Thus, by a series of genetic and pharmacological interventions and, more importantly, by generating mice with conditional TRPA1 deletion in different cells, we aim at identifying a possible expression of TRPA1 in cells other than neurons and its possible role in molecular events that sustain allodynia after a damaged of the nerve trunk.

Since TRPA1 is involved in multiple painful condition, we also investigate the role of TRPA1 in pain symptoms associated with the treatment of the third-generation AIs, which include the steroidal agent exemestane (Aromasin) the triazoles anastrozole (Arimidex) and letrozole (Femara), currently recommended for adjuvant endocrine treatment as primary, sequential, or extended therapy with tamoxifen, for postmenopausal women diagnosed with estrogen receptor-positive breast cancer (Burstein et al., 2010; Cuzick et al., 2013; Gibson et al., 2009). Among these, the AI-associated musculoskeletal symptoms (AIMSS) are characterized by morning stiffness and pain of the hands, knees, hips, lower back, and shoulders. In addition to musculoskeletal pain, pain symptoms associated with AIs have recently been more accurately described with the inclusion of neuropathic, diffused, and mixed pain (Laroche et al., 2014). The chemical structure of exemestane includes a system of highly electrophilic conjugated Michael acceptor groups, which might react with the thiol groups of reactive cysteine residues. Michael addition reaction with specific cysteine residues is a major mechanism that results in TRPA1 activation by a large variety of electrophilic compounds (Hinman et al., 2006; Macpherson et al., 2007; Trevisani et al., 2007). In addition, aliphatic and aromatic nitriles can react with cysteine to form thiazoline derivatives and accordingly the tear gas 2-chlorobenzylidene malononitrile (CS) has been identified as a TRPA1 agonist. We noticed that both letrozole and anastrozole possess nitrile moieties. Thus, we hypothesized that exemestane, letrozole and anastrozole may produce neurogenic inflammation, nociception and hyperalgesia by targeting TRPA1. The ability to gate TRPA1 in vitro was confirmed in vivo by the observation that the pain-like behaviors evoked by AIs in mice are abrogated by genetic deletion or pharmacological blockade of the channel. However, AI concentrations required for TRPA1 gating in vitro are 1-2 order of magnitude higher than those found in patient plasma. In addition, an important

proportion (30-40%), but not all, of treated patients develop the painful condition. These observations suggest that exposure to AIs is necessary, but not sufficient, to produce AIMSS, and that additional factors should cooperate with AIs to promote pain symptoms. Aromatase inhibition, while reducing downstream production of estrogens, moderately increases upstream plasma concentrations of androgens, including androstenedione (ASD) (Gallicchio et al., 2011). Exemestane, a false aromatase substrate, blocks enzymatic activity by accommodating in the binding pocket that snugly encloses ASD. We reasoned that ASD, which retains some of the reactive chemical features of exemestane, such as the α,β -carbonyl moiety of the A ring and the ketone group at the 17 position, might target TRPA1.

Another painful condition is represented by migraine pain. Occupational exposure to, or treatment with, organic nitrates has long been known to provoke headaches. These observations have led to the clinical use of glyceryl trinitrate (GTN) as a reliable provocation test for migraine attacks (Iversen et al., 1989; Olesen, 2008; Sicuteri et al., 1987). In most subjects, including healthy controls, GTN administration causes a mild headache that develops rapidly and is short-lived. However, after a remarkable time lag (hours) from GTN exposure, migraineurs develop severe headaches that fulfill the criteria of a typical migraine attack (Iversen et al., 1989; Olesen, 2008; Sicuteri et al., 1987).

GTN administration to rodents and humans produces a delayed and prolonged (hours) hyperalgesia that temporally correlates with GTN-induced migraine-like attacks in humans (Ferrari et al., 2016; Tassorelli et al., 2003). Several mechanisms have been proposed to explain the mechanism, including degranulation of meningeal mast cells (Ferrari et al., 2016), delayed meningeal inflammation sustained by induction of NO synthase and prolonged NO generation, and the release of CGRP (Ramachandran et al., 2014), a primary migraine neuropeptide (Edvinsson, 2015), but the precise mechanisms was not identified. In our study we aim at identifying a possible role of TRPA1 expressed in trigeminal ganglion neurons in the delayed mechanical allodynia induced by GTN administration, which recapitulate the migraine attack.

Material and Methods

Animals and Drugs

In vivo experiments and tissue collection were carried out according to the European Union (EU) guidelines for animal care procedures and the Italian legislation (DLgs 26/2014) application of the EU Directive 2010/63/EU. Studies were conducted under the University of Florence research permit #204/2012-B. C57BL/6 mice (male, 20-25 g, age 5 weeks) (Harlan Laboratories, Milan, Italy), littermate wild type (wt, *Trpa1*^{+/+}) and TRPA1-deficient (*Trpa1*^{-/-}) mice (25-30 g, 5-8 weeks) (Kwan et al., 2006); wt (*Trpv4*^{+/+}) and TRPV4-deficient (*Trpv4*^{-/-}) mice (25-30 g, 5-8 weeks); and TRPV1-deficient mice (*Trpv1*^{-/-}; B6.129X1-*Trpv1*^{tm1Jul/J}) backcrossed with C57BL/6 mice (*Trpv1*^{+/+}) for at least 10 generations (Jackson Laboratories, 25-30 g, 5-8 weeks). To selectively delete *Trpa1* gene in primary sensory neurons, 129S-*Trpa1*^{tm2Kykw/J} mice (*floxed TRPA1*, *Trpa1*^{fl/fl}, Stock No: 008649; Jackson Laboratories), which possess loxP sites on either side of the S5/S6 transmembrane domains of the *Trpa1* gene, were crossed with hemizygous *Advillin-Cre* male mice (Guan et al., 2016; Zurborg et al., 2011). The progeny was genotyped by standard PCR for *Trpa1* ([PCR Protocol 008650](#)) and *Advillin-Cre* (Guan et al., 2016). Mice negative for *Advillin-Cre* (*Adv-Cre*⁻; *Trpa1*^{fl/fl}) were used as control. Successful *Advillin-Cre* driven deletion of TRPA1 mRNA was confirmed by RT-qPCR (Zappia et al., 2017)}. B6.Cg-Tg(Plp1-CreERT)3Pop/J mice (*Plp1-Cre*^{ERT}, Stock No: 005975), expressing a tamoxifen-inducible Cre in myelinating cells (Plp1, proteolipid protein myelin 1) (Doerflinger et al., 2003), and 129S-*Trpa1*^{tm2Kykw/J} mice (*floxed TRPA1*, *Trpa1*^{fl/fl}, Stock No: 008649), which possess loxP sites on either side of the S5/S6 transmembrane domains of the *Trpa1* gene, were obtained from Jackson Laboratories (Bar Harbor, ME, USA). To generate mice in which the *Trpa1* gene was conditionally silenced in Schwann cells/oligodendrocytes homozygous *Trpa1*^{fl/fl} mice were crossed with hemizygous *Plp1-Cre*^{ERT} mice. The progeny was genotyped by standard PCR for *Cre*^{ERT} alleles. Both positive or negative mice to *Cre*^{ERT} and homozygous for floxed *Trpa1* (*Plp1-Cre*^{ERT}; *Trpa1*^{fl/fl} and *Plp1-Cre*^{ERT}; *Trpa1*^{fl/fl}, respectively) were treated with intraperitoneal (i.p.) 4-hydroxytamoxifen (1 mg/100 µl in corn oil, once a day, for 5 consecutive days) (Doerflinger et al., 2003) resulting in Cre-mediated ablation of *Trpa1* in PLP-expressing Schwann cells/oligodendrocytes. Successful Cre-driven deletion of

TRPA1 mRNA was confirmed by RT-qPCR. Mice negative to *CreERT* (*Plp1-Cre^{ERT}-;Trpa1^{fl/fl}*) were used as control. Behavioral experiments were performed, after 1 hour of animal acclimation, in a quiet, temperature-controlled room (20-22°C) between 9 a.m. and 5 p.m. with a randomized order by an operator blinded to genotype and drug treatments. Animals were euthanized with a high dose of sodium pentobarbital (200 mg/kg intraperitoneal, i.p.). HC-030031 (2-(1,3-Dimethyl-2,6-dioxo-1,2,3,6-tetrahydro-7H-purin-7-yl)-N-(4-isopropylphenyl) acetamide) was synthesized as previously described (Andre et al., 2008). If not otherwise indicated, reagents were obtained from Sigma-Aldrich (Milan, Italy).

Constriction of the Infraorbital Nerve

CIION was performed in C57BL/6, *Trpa1^{+/+}* or *Trpa1^{-/-}* mice as previously described (Luiz et al., 2010; Vos et al., 1994). Briefly, mice were anesthetized with an i.p. injection of a mixture of ketamine (90 mg/kg) and xylazine (3 mg/kg) and an incision was made in the left upper lip skin lateral to the nose, and the rostral end of the infraorbital nerve was exposed. Then, two loosely constrictive ligatures (#6/0 silk suture) were placed around the infraorbital nerve with a distance of 2 mm. In the sham procedure, the left infraorbital nerve was exposed but not ligated. To verify whether an inflammatory component, due to a foreign body, contributes to immune cell accumulation and mechanical and cold hypersensitivity, in a series of experiments a silk thread was inserted close to the ION without any ligature. Neomycin sulfate and sulfathiazole (powder, 0.05 g and 9.95 g, respectively; Boehringer Ingelheim Italia S.p.A, Reggello, Italy) were applied to the wound and the incision was sutured. Mice were monitored, adequately rehydrated, and maintained in a controlled temperature (37°C) until fully recovered from anesthesia.

Partial ligation of the sciatic nerve (pSNL)

pSNL was performed in C57BL/6, in *Trpa1^{+/+}* or *Trpa1^{-/-}*, in *Trpv1^{+/+}* or *Trpv1^{-/-}*, in *Trpv4^{+/+}* or *Trpv4^{-/-}* and in *Plp1-Cre^{ERT};Trpa1^{fl/fl}* or control mice as previously described (Malmberg et al., 1998). Briefly, mice were anesthetized with i.p. injection of a mixture of ketamine (90 mg/kg) and xylazine (3 mg/kg), the right sciatic nerve was

exposed, and a partial ligation was made by tying one-third to one half of the dorsal portion of the sciatic nerve. In sham-operated mice, used as controls, the right sciatic nerve was exposed, but not ligated. Mice were monitored, adequately rehydrated, and maintained in a controlled temperature (37°C) until fully recovered from anesthesia.

Assessment of Pain-like Behaviors

Non-evoked nociceptive behavior. As previously reported, the CION induces non-evoked, continuous or recurring pain in the cutaneous region innervated by the damaged nerve, a behavioral response indicative of neuropathic pain. To assess changes in spontaneous facial rubbing, C57BL/6, *Trpa1*^{+/+} or *Trpa1*^{-/-} mice were placed individually in clear plexiglass boxes (7×9×11 cm) on elevated wire mesh platforms. After 1 hour of adaptation, the time spent rubbing (time that forelimbs touched ears or facial region) was recorded for 30 minutes.

Mechanical allodynia. Mechanical threshold was measured using the up-and-down paradigm, previously reported. Mice were habituated to the room temperature for at least 1 hour before the test. Then, a series of 7 Von Frey hairs in logarithmic increments of force (0.008, 0.02, 0.04, 0.07, 0.16, 0.4, 0.6 g) was used to stimulate the infraorbital nerve region, *i.e.* near the center of the vibrissal pad on hairy skin of the left upper lip (ipsilateral to the surgery side). The response was considered positive when the mouse strongly withdrew its head. The stimulation initiated with the 0.16 g filament. The von Frey hairs were applied with sufficient force to cause slight buckling, and held for approximately 2-4 seconds. Absence of response after 5 seconds led to use the filament with increased weight, whereas a positive response led to use a weaker (*i.e.* lighter) filament. Six measurements were collected for each mouse or until four consecutive positive or negative responses occurred. The 50% mechanical withdrawal threshold (expressed in g) response was then calculated from these scores. Basal values were recorded before CION or sham procedure. Mechanical allodynia was considered as a decrease in the mechanical threshold in comparison to basal (intra-animal) or sham animal (inter-animal) values.

Nociceptive response. To measure nociceptive responses, mice were placed in a Plexiglas chamber immediately after the injection compounds, and the total time spent licking and lifting (nociception time, s) the injected right hind limb and paw was recorded

for 5 min.

Cold hypersensitivity. Mice were placed individually in clear Plexiglas boxes (7×9×11cm) on elevated wire mesh platforms and habituated for at least 1 hour before the test. After, 15 µl of acetone was gently applied to the left vibrissa pad skin surface (ipsilateral to the surgery side), and the time spent grooming the region over a 60 second period was measured. Acetone was applied three times at 10-15 minute intervals, and the average nociceptive (*i.e.* grooming) time was calculated. Cold allodynia was considered as an increase in the nociceptive time observed after exposure to acetone when compared with basal (intra-animal) or sham-operated animal (inter-animal) values.

Chemical hyperalgesia. Basal nociceptive behavior was assessed by measuring spontaneous nociceptive responses induced by s.c. (10 µl) injection into the left upper lip (ipsilateral to the surgery side) of increasing doses of allyl isothiocyanate (AITC, 0.1-30 nmol/site) or vehicle (DMSO 3%), hydrogen peroxide (H₂O₂, 0.01-1 µmol/site) or vehicle (isotonic saline), capsaicin (0.01-1 nmol/site) or vehicle (ethanol 1%) or concentrations of hypotonic saline (NaCl, 0.63%-0% NaCl/site) in non-operated C57BL/6 mice, in order to identify the minimal suprathreshold dose. Each animal was tested with 1 dose of 1 substance. The identified suprathreshold doses of AITC (1 nmol/site), H₂O₂ (0.1 µmol/site), capsaicin (0.01 nmol/site) or hypotonic saline (0.45% NaCl/site) were tested in CION- or sham-operated mice on day 10 after surgery. Animals were placed individually in chambers (transparent glass cylinders of 20 cm in diameter) and were adapted for 20 minutes before algogen or vehicle injection. Each animal was tested with 1 suprathreshold dose of 1 substance or vehicles, according to a random allocation. Immediately after the injection, mice were placed inside a plexiglass box and the total time of ipsilateral facial rubbing was recorded for 5 minutes.

Rotarod test. Locomotor function, coordination, and sedation of animals were tested by using a rotarod apparatus (UgoBasile). Briefly, 24 hours before the experiments, the animals were trained on the rotarod apparatus, programmed at 8 rpm, until they remained without falling for 60 sec. The day of the experiment, the latency (sec) to the first fall and the number of falls were recorded. Cut-off time was 240 sec. The results of the rotarod test indicated that the various pharmacological interventions did not affect the

forced locomotion of animals.

Orofacial thermal heat hyperalgesia. Thermal heat hyperalgesia of the orofacial area was measured with a radiant heat (50 ± 1 °C) placed on the surface of the vibrissal pad. The latency to display either head withdrawal or vigorous flicking of the snout was recorded (in seconds). A 20 seconds cut-off time was used to prevent tissue damage. Reductions in the response latency to heat stimulation were considered to be indicative of thermal hyperalgesia.

Paw thermal heat hyperalgesia. Thermal hyperalgesia was measured by exposing the mid plantar surface of the hind paw to a beam of radiant heat through a transparent surface, using a plantar analgesimeter for paw stimulation (Ugo Basile, Comerio, Italy). Paw withdrawal latency was recorded as the time from onset of the thermal stimulus to the withdrawal response. In each paw mean withdrawal latency of three measures was calculated. The interval between trials on the same paw was at least 5 min. The cut-off latency was set at 20 s to avoid tissue damage in case of failure to remove the paw.

Plasma protein extravasation

After different stimuli, the extravasated dye was extracted from synovial tissue of the knee joint by overnight incubation in formamide, and assayed by spectrophotometry at 620 nm.

Synovial fluid lavage

Synovial fluid was collected by instilling 3 times 0.1 ml of Hank's Buffer plus 10 mM HEPES and 10 mM EDTA in the knee 15 minutes after letrozole. The neutrophil count was performed using standard morphological criteria on Diff-Quick stained cytopins. Data are expressed as total number of neutrophils in 100 μ l of solution.

Cell culture, primary culture of Schwann cells and neurons, and culture of peritoneal macrophages

Human embryonic kidney (HEK293) cells stably transfected with the cDNA for human TRPA1 (hTRPA1-HEK293), kindly donated by A.H. Morice (University of Hull, Hull, UK) or with the cDNA for human TRPV1 (hTRPV1-HEK293), kindly donated by Martin J. Gunthorpe (GlaxoSmithKline, Harlow, UK), and naive untransfected HEK293 cells (American Type Culture Collection, Manassas, VA, USA) were cultured as previously described (Sadofsky et al., 2014).

HEK293 cells (ATCC® CRL-1573™), cultured according to the manufacturer's instructions, were transiently transfected with the cDNAs (1 µg) codifying for wild type (Wt) (hTRPA1-HEK293) or mutant 3C/K-Q human TRPA1 (C619S, C639S, C663S, K708Q; 3C/K-Q hTRPA1-HEK293) (Hinman et al., 2006) using the jetPRIME transfection reagent (Poliplus-transfection® SA) according to the manufacturer's protocol. For all cell lines, the cells were used when received without further authentication.

Schwann cells were isolated from sciatic nerves of C57BL/6, *Trpa1*^{+/+}, *Trpa1*^{-/-}, *Plp1-Cre^{ERT};Trpa1^{fl/fl}* or control mice. Briefly, the *epineurium* was removed, and nerve explants were divided into 1 mm segments and dissociated enzymatically using collagenase (0.05%) and hyaluronidase (0.1%) in HBSS (2 h, 37°C). Cells were collected by centrifugation (800xrpm, 10 min, RT) and the pellet was resuspended and cultured in DMEM containing: 10% FCS, 2mM L-glutamine, 100 U/ml penicillin/100 mg/ml streptomycin or 50 mg/ml gentamycin. Three days later, cytosine arabinoside (10 mM) was added to remove fibroblasts. To enhance Schwann cell proliferation, forskolin (2 µM) was added to the culturing medium.

Primary dorsal root ganglion (DRG) neurons were isolated from Sprague-Dawley rats and C57BL/6 or *Trpa1*^{+/+} and *Trpa1*^{-/-} adult mice, Ganglia were bilaterally excised under a dissection microscope and enzymatically digested using 2 mg/ml of collagenase type 1A and 1 mg/ml of trypsin, for rat DRG neurons, or 1 mg/ml of papain, for mouse DRG neurons, in Hank's Balanced Salt Solution (HBSS) for 25-35 minutes at 37 °C. Rat and mouse DRG neurons were pelleted and resuspended in Dulbecco's Modified Eagle's Medium (DMEM) supplemented with 10% heat inactivated horse serum or Ham's-F12, respectively, containing 10% heat-inactivated fetal bovine serum (FBS), 100 U/ml of penicillin, 0.1 mg/ml of streptomycin, and 2 mM L-glutamine for mechanical digestion. In this step, ganglia were disrupted by several passages through a series of syringe needles (23-25G). Neurons were then pelleted by centrifugation at 1200 g for 5 minutes,

suspended in *medium* enriched with 100 ng/ml mouse-NGF and 2.5 mM cytosine-b-D-arabino-furanoside free base, and then plated on 25 mm glass coverslips coated with poly-L-lysine (8.3 μ M) and laminin (5 μ M). DRG neurons were cultured for 3-4 days before being used for calcium imaging experiments.

To obtain cultured peritoneal macrophages, C57BL/6 mice were i.p. injected with thioglycolate (3%, 1 ml). After 3 days, cells were harvested from sacrificed animals by peritoneal lavage for a total of 10 ml PBS and centrifuged (400 \times g, 10 min, 4°C). Cells were cultured in DMEM supplemented with 10% FBS. After incubation at 37°C for 24 h, non-adherent cells were removed by repeated washing. Before each experiment, cells were tested with specific kits for cells mycoplasma contamination based on PCR (EMK090020, N-GARDE kit, Euroclone, Milan, Italy).

To obtain trigeminal neuronal and satellite glial cells (SGCs)-mixed cultures or SGCs-enriched cultures the protocol reported previously (Chung et al., 2015) was used.

Calcium Imaging Assay

Intracellular calcium was measured in transfected and untransfected HEK293 cells or in DRG neurons. Plated cells were loaded with 5 μ M Fura-2AM-ester (Alexis Biochemicals, Lausen, Switzerland) added to the buffer solution (37 °C) containing the following (in mM): 2 CaCl₂; 5.4 KCl; 0.4 MgSO₄; 135 NaCl; 10 D-glucose; 10 HEPES and 0.1% bovine serum albumin at pH 7.4. After 40 minutes, cells were washed and transferred to a chamber on the stage of a Nikon Eclipse TE-2000U microscope for recording. Cells were excited alternatively at 340 nm and 380 nm to indicate relative intracellular calcium changes by the Ratio_{340/380} recorded with a dynamic image analysis system (Laboratory Automation 2.0, RCSsoftware, Florence, Italy). Results are expressed as or the percentage of increase of Ratio_{340/380} over the baseline normalized to the maximum effect induced by ionomycin (5 μ M) added at the end of each experiment (% Change in R_{340/380}) or Ratio_{340/380}.

Electrophysiology

Whole-cell patch-clamp recordings were performed on hTRPA1-HEK293, vector-HEK293 cells or rat DRG neurons grown on a poly-L-lysine-coated 13 mm-diameter

glass coverslips. Each coverslip was transferred to a recording chamber (1 ml volume) mounted on the platform of an inverted microscope (Olympus CKX41, Milan, Italy) and superfused at a flow rate of 2 ml/min with a standard extracellular solution containing (in mM): 10 HEPES, 10 D-glucose, 147 NaCl, 4 KCl, 1 MgCl₂, and 2 CaCl₂ (pH adjusted to 7.4 with NaOH). Borosilicate glass electrodes (Harvard Apparatus, Holliston, MA, USA) were pulled with a Sutter Instruments puller (model P-87) to a final tip resistance of 4–7 MΩ. Pipette solution used for HEK293 cells contained (in mM): 134 K-gluconate, 10 KCl, 11 EGTA, 10 HEPES (pH adjusted to 7.4 with KOH). When recordings were performed on rat DRG neurons, 5 mM CaCl₂ was present in the extracellular solution and pipette solution contained (in mM): CsCl 120, Mg₂ATP 3, BAPTA 10, HEPES-Na 10 (pH adjusted to 7.4 with CsOH). Data were acquired with an Axopatch 200B amplifier (Axon Instruments, CA, USA), stored and analyzed with a pClamp 9.2 software (Axon Instruments, CA, USA). All the experiments were carried out at 20–22°C. Cells were voltage-clamped at –60 mV. Cell membrane capacitance was calculated in each cell throughout the experiment by integrating the capacitive currents elicited by a ± 10 mV voltage pulse.

Protein Extraction and Western Immunoblot Assay

Tissue samples were homogenized in a lysis buffer containing (mM): 50 Tris, 150 NaCl, 2 EGTA, 100 NaF, 1 Na₃VO₄, 1% Nonidet P40 (pH 7.5) and complete protease inhibitor cocktail (Roche Diagnostics, Mannheim, Germany). Lysates were centrifuged at 14,000xg at 4°C for 45 minutes. Protein concentration in supernatants was determined using DC protein assay (Bio-Rad, Milan, Italy). Samples with equal amounts of proteins (30 µg) were then separated by NuPAGE 4-12% Bis-Tris gel electrophoresis (Life Technologies, Carlsbad, USA), and the resolved proteins were transferred to a polyvinylidenedifluoride membrane (Merck Millipore Billerica, USA). Membranes were incubated with 5% dry milk in Tris buffer containing 0.1% Tween 20 (TBST; 20 mM Tris at pH 7.5, 150 mM NaCl) for 1 hour at room temperature, and incubated with rat polyclonal primary antibody for TRPA1 detection (1:200, Novus Biologicals, Littleton, USA), or mouse monoclonal primary antibody for β-actin (1:6000, Thermo Scientific, Rockford, USA), at 4°C overnight. Membranes were then probed with goat anti-mouse or donkey anti-rabbit IgG conjugated with horseradish peroxidase (HRPO) (Bethyl

Laboratories Inc., Cambridge, UK) for 50 minutes at room temperature. Finally, membranes were washed three times with TBST, and bound antibodies were detected using chemiluminescence reagents (ECL, Pierce, Thermo Scientific, Rockford, USA). Negative controls were obtained by overnight preadsorption at 4°C with 1 µg peptide/1 µg antibody of the immunizing peptide (Novus Biological, Littleton, USA). The density of specific bands was measured using an image processing program (ImageJ 1.32J, Wayne Rasband, USA) and normalized to β-actin.

CCL2 Enzyme-Linked Immunosorbent Assay, H₂O₂ Level and Superoxide Dismutase Activity

The CCL2 content was measured by using a mouse CCL2/MCP-1 quantikine ELISA Kit (R&D system, Minneapolis, USA). Samples were homogenized in PBS at 4°C containing a protease inhibitor cocktail tablet (Roche Diagnostics, Mannheim, Germany). The homogenate was then centrifuged at 10,000xg for 20 minutes at 4°C, supernatants were collected and assayed according to the manufacturer's instructions. The concentration of CCL2 was expressed in pg/mg of total protein content.

H₂O₂ levels were detected by using the phenol red-HRPO method. Samples were homogenized in 50 mM phosphate buffer (pH 7.4) containing 5 mM of sodium azide at 4°C for 60 seconds, centrifuged at 12,000xg for 20 minutes at 4°C, and the supernatant was used to determine the H₂O₂ content. H₂O₂ levels were expressed as µmol on the basis of a standard curve of HRPO-mediated oxidation of phenol red by H₂O₂, corrected by protein content (expressed in mg).

The superoxide dismutase (SOD) activity was assayed using a Nitro Blue Tetrazolium (NBT)-based assay (Abcam, Cambridge, UK) Tissues were homogenized in a Tris-HCl buffer (100 mM, pH 7.4) containing 0.5% Triton X-100, 5 mM beta-mercaptoethanol, 0.1 g/ml phenylmethanesulfonyl fluoride, centrifuged at 14,000xg at 4°C for 5 minutes and assayed according to the manufacturer's instructions. Results were expressed as the percent inhibition of the rate of NBT-diformazan formation.

Immunofluorescence assay

Mice were anesthetized with a mixture of ketamine (90 mg/kg) and xylazine (3

mg/kg) and transcardially perfused with PBS (phosphate buffer saline), followed by 4% paraformaldehyde. Immunofluorescence staining was performed according to standard procedures. Cryosections (10 μm) were stained with hematoxylin and eosin (H&E) for histological examination or incubated with the following primary antibodies: F4/80 (MA516624, rat monoclonal [Cl:A3-1], 1:50, Thermo Fisher Scientific, Rockford, USA), CD8 (ab22378, rat monoclonal [YTS169.4], 1:200, Abcam, Cambridge, UK) and Ly6G (ab25377, rat monoclonal [RB6-8C5], 1:200, Abcam, Cambridge, UK) (1 h, RT), diluted in fresh blocking solution (PBS, pH 7.4, 10% normal goat serum, NGS). Formalin fixed paraffin-embedded sections (5 μm) were incubated with the following primary antibodies: protein gene product 9.5 (PGP9.5, ab8189, mouse monoclonal [13C4/I3C4], 1:600, Abcam, Cambridge, UK), TRPA1 (ab58844, rabbit polyclonal, 1:400, Abcam, Cambridge, UK), S100 (ab14849, mouse monoclonal [4B3], 1:300, Abcam, Cambridge, UK), SOX10 (ab216020, mouse monoclonal [SOX10/1074], 1:300, Abcam, Cambridge, UK), 4- HNE (ab48506, mouse monoclonal [HNEJ-2], 1:40, Abcam, Cambridge, UK) or NOX1 (ab131088, rabbit polyclonal, 1:250, Abcam, Cambridge, UK) (1 h, RT) diluted in antibody diluent (Roche Diagnostics, Mannheim, Germany). Sections were then incubated with fluorescent secondary antibodies: polyclonal Alexa Fluor 488, polyclonal Alexa Fluor 594, polyclonal Alexa Fluor 546, and polyclonal Alexa Fluor 647 (1:600, Invitrogen, Milan, Italy) (2 h, RT, protected from light). Sections were coverslipped using a water-based mounting medium with 4'6'-diamidino-2-phenylindole (DAPI) (Abcam, Cambridge, UK). The analysis of negative controls (non-immune serum) was simultaneously performed to exclude the presence of non-specific immunofluorescent staining, cross-immunostaining, or fluorescence bleed-through. Tissues were visualized, and digital images were captured using an Olympus BX51 or confocal scan a LEICA TCS SP5. High power 3D renderings of the images were obtained using ImageJ 3D viewer. The number of F4/80⁺ cells was counted in 10⁴ μm^2 boxes within the dashed lines of the injured branches of the infraorbital nerve. The 4-HNE staining was evaluated as the fluorescence intensity measured by an image processing program (ImageJ 1.32J, National Institutes of Health, Bethesda, USA).

Real-Time PCR

RNA was extracted from different tissues. The standard Trizol® extraction method was used. RNA concentration and purity was assessed spectrophotometrically by measuring the absorbance at 260 nm and 280 nm. The RNA (100 ng) was reverse-transcribed using the iScript™ cDNA Synthesis kit (Bio-Rad, Hercules, USA) according to the manufacturer's protocol. For relative quantification of mRNA, real time PCR was performed on Rotor Gene® Q (Qiagen, Hilden, GE). The sets of primers-probes were as follows: 18S-FW (forward): 5'-CGCGGTTCTATTTTGTGGT-3', 18S-RE (reverse): 5'-AGTCGGCATCGTTTATGGTC-3' (NCBI Ref Seq: NR_003278.3); TRPA1-FW: 5'-CAGGATGCTACGGTTTTTTCATTACT-3', TRPA1-RE: 5'-GCATGTGTCAATGTTTGGTACTTCT-3' (NCBI Ref Seq: NM_177781.4); S100-FW: 5'-TGGATGAAAACGGAGATGGGG-3', S100-RE: 5'-ACAGACTGTGCTCAACTGGT-3' (NCBI Ref Seq: NM_011309); SOX10-FW: 5'-AGATCCAGTTCGGTGTCAATAA-3', SOX10-RE: 5'-GCGAGAAGAAGGCTAGGTG-3' (NCBI Ref Seq: U70441.1); NOX1-FW: 5'-CACTCACCAATGCCCAGGAT-3', NOX1-RE: 5'-TGGAAGCAAAGGGAGTGACC-3' (NCBI Ref Seq: NM_172203.2); NOX2-FW: 5'-GAGGTTGGTTCGGTTTTGGC-3', NOX2-RE: 5'-CAGGAGCAGAGGTCAGTGTG-3' (NCBI Ref Seq: NM_007807.5); NOX4-FW: 5'-TGTTGGGCCTAGGATTGTGT-3', NOX4-RE: 5'-TCCTGCTAGGGACCTTCTGT-3' (NCBI Ref Seq: NM_015760.5); F4/80-FW: 5'-CCCAGCTTATGCCACCTGCA-3', F4/80-RE: 5'-TCCAGGCCCTGGAACATTGG-3' (NCBI Ref Seq: NC_000083.6); Floxed TRPA1-FW: 5'-GGGCAGCTTATTGCCTTCAC-3', Floxed TRPA1-RE: 5'-TTGCGTAAGTACCAGAGTGGC-3' (NCBI Ref Seq: NM_177781.4)

The chosen reference gene was the 18S. The SsoAdvanced™ Universal SYBR® Green Supermix (Bio-Rad, Hercules, USA) was used for amplification, and the cycling conditions were the following: samples were heated to 95°C for 1 min followed by 40 cycles of 95°C for 10 s, and 65°C for 20 s. PCR reaction was carried out in triplicate. Relative expression of TRPA1 mRNA was calculated using the $2^{-\Delta(\Delta CT)}$ comparative method, with each gene normalized against the internal endogenous reference 18S gene for the same sample.

Live animal imaging (Near infrared, NIR)

Macrophage localization *in vivo* was obtained by NIR imaging of the fluorescent label macrophage mice by using PhotonImager (Biospace Laboratory, Paris, France). Mouse thioglycollate-elicited peritoneal macrophages were harvested (up to 250×10^6 cells/ml) and incubated for 15 min at RT with VivoTrack 680 (PerkinElmer, Inc., Waltham, USA), dissolved in sterile PBS, washed, centrifuged (400xg, 10 min) and diluted to a final concentration of 5×10^6 cells/40 μ l. Retro-orbital vein injection (40 μ l) of labeled macrophages was performed in pSNL/sham C57BL/6 mice at day 9 after surgery. Twenty-four h later, anesthetized mice were put inside the pre-heated chamber. NIR imaging was performed before and 1 and 3 h after HC030031 (100 mg/kg, i.p.) administration. Images were acquired with *Photo Acquisition* software and processed with *M3 Vision* software (Biospace Laboratory, Paris, France). The NIR pixel area was measured by ImageJ 1.32J from a region of the same size over the sciatic nerve, identifying an area of interest (ROI) around the fluorescent signal evident in the pSNL. That ROI perimeter was then reported to other images derived from different experimental settings. Data were expressed as NIR pixel area/ROI pixel area.

Proximity ligation assay (PLA)

Colocalization of TRPA1 and NOX2 in mouse TG was obtained using an *in situ* PLA detection kit (Duolink, Olink Biosciences Inc.) as previously described (Sullivan et al., 2015). In TG sections (5 μ m) fluorescence images were obtained using Olympus BX51 and a 100X oil-immersion objective. Negative control was performed by omitting primary antibodies or PLA probes.

Blood flow experiments

Cutaneous blood flow was assessed using a laser doppler flowmeter (Perimed Instruments) in anaesthetized in C57BL/6, *Trpa1*^{+/+} and *Trpa1*^{-/-} mice. Cutaneous blood flow was monitored by a probe (cutaneous type) fixed to the shaved periorbital area, before and after the systemic administration of GTN (10 mg/kg, i.p.) or its vehicle. Before

(0.5 h) GTN injection, mice were treated with i.p. HC-030031, disulfiram (both, 100 mg/kg) and BIBN4096BS (1 mg/kg) or their vehicles and cutaneous blood flow was monitored for at least 0.5 h. Baseline blood flow was calculated by the mean flow value measured during a 5-min period before the stimulus. The increase in cutaneous blood flow was calculated as the percentage change over the baseline.

Androstenedione and letrozole level determination

ASD levels were measured in mouse serum by using the Active® ASD Radioimmunoassay (Beckman Coulter, CA, USA), a competitive RIA with a sensitivity of 0.1 nmol/L. Radiometric detection was performed using a 2470 WIZARD Automatic Gamma Counter (Perkin Elmer, IL, USA). Letrozole levels were measured by LC-MS/MS. Briefly, plasma samples (50 µl) were obtained from the blood collected at different time points (1 and 3 hours) after i.g. administration of letrozole (0.1 and 0.5 mg/kg). At 50 µl of plasma sample, 200 pg of d4-letrozole was added. The sample was vortex-mixed for 10 seconds, then 50 µl of ZnSO₄ (90 mg/ml) diluted 1:4 with methanol was added, vortex-mixed for 30 seconds, and centrifuged at 12,000 rpm for 10 minutes. Supernatant (50 µl) was injected in On-line column-switching SPE (CS-SPE). The CS-SPE consists of two high-performance-liquid chromatography (HPLC) systems connected by a six-port switching valve. In the first step, analytes of interest are retained on column 1 (trapping column, SPE Strata C18 20µm, 20 x 2 mm, Phenomenex, Torrance, CA, USA), whereas the matrix components can be washed off. In the second step, column 1 is switched in back-flush to column 2 (analytical column, LUNA, 3 µm, C18 20 x 2 mm, Mercury MS Phenomenex, Torrance, CA, USA). The mobile phases were the same for the trapping column and the analytical column, eluent A water with 0.1% formic acid and eluent B methanol. Samples were measured with a Perkin Elmer Sciex (Thornhill, Canada) API 365 triple quadrupole mass spectrometer equipped with a Turbo IonSpray source, operating in positive ion mode, interfaced with a HPLC Perkin Elmer pump series 200. The capillary voltage was set to 5.5 kV. Heated turbo gas (450° C, air) at a flow rate of 10 l/minutes was used. The ion transitions recorded in Multiple Reaction Monitoring (MRM) were m/z 286.2→217.2 for letrozole and 290.2→221.2 for d4-letrozole. A calibration curve was constructed for letrozole using the appropriate internal standard (d4-letrozole). Plasma samples (50 µl) from control mice were spiked with different

concentrations of letrozole (from 2 to 16 ng/ml). A satisfying linearity was obtained for letrozole ($r^2=0.994$).

Statistical Analysis

Data are presented as mean \pm SEM. Statistical analysis was performed by the unpaired two-tailed Student's t-test for comparisons between two groups, the 1- or 2- way ANOVA, followed by the post-hoc Bonferroni's test for comparisons of multiple groups. $P < 0.05$ was considered statistically significant (GraphPad Prism version 5.00, La Jolla, USA). To meet ANOVA assumptions, mechanical allodynia data were subjected to log transformation before statistical analysis.

Results

TRPA1, downstream to monocytes/macrophages and oxidative stress, mediates trigeminal neuropathic pain in mice

The aim of the present study was to identify the role of TRPA1 in a mouse model of trigeminal neuropathic pain produced by the constriction of the infraorbital nerve (CION) (Fig. 1A) and to explore the molecular and cellular pathways that, from the initial nerve injury, result in channel engagement. The monocyte chemoattractant protein 1 (MCP-1), also known as chemoattractant chemokine (C-C motif) ligand 2 (CCL2), by binding to the chemotactic cytokine receptor 2 (CCR-2), promotes monocyte transendothelial migration to the site of nerve injury. In various paradigms of peripheral nerve injury, CCL2 inhibition and CCR-2 genetic ablation abrogates mechanical allodynia. In addition, antioxidants have been reported to attenuate neural hypersensitivity in various models of neuropathic pain, such as sciatic chronic constriction injury and spinal nerve ligation. Thus, the contribution of monocyte/macrophage infiltration and the ensuing oxidative stress in the TRPA1-mediated pain-like behaviors was investigated in the CION model. Results propose that CCL2-driven monocyte/macrophage accumulation within the injured nerve and the neighboring tissue generates oxidative burst that, by TRPA1 targeting, promotes and maintains CION-evoked pain-like behaviors.

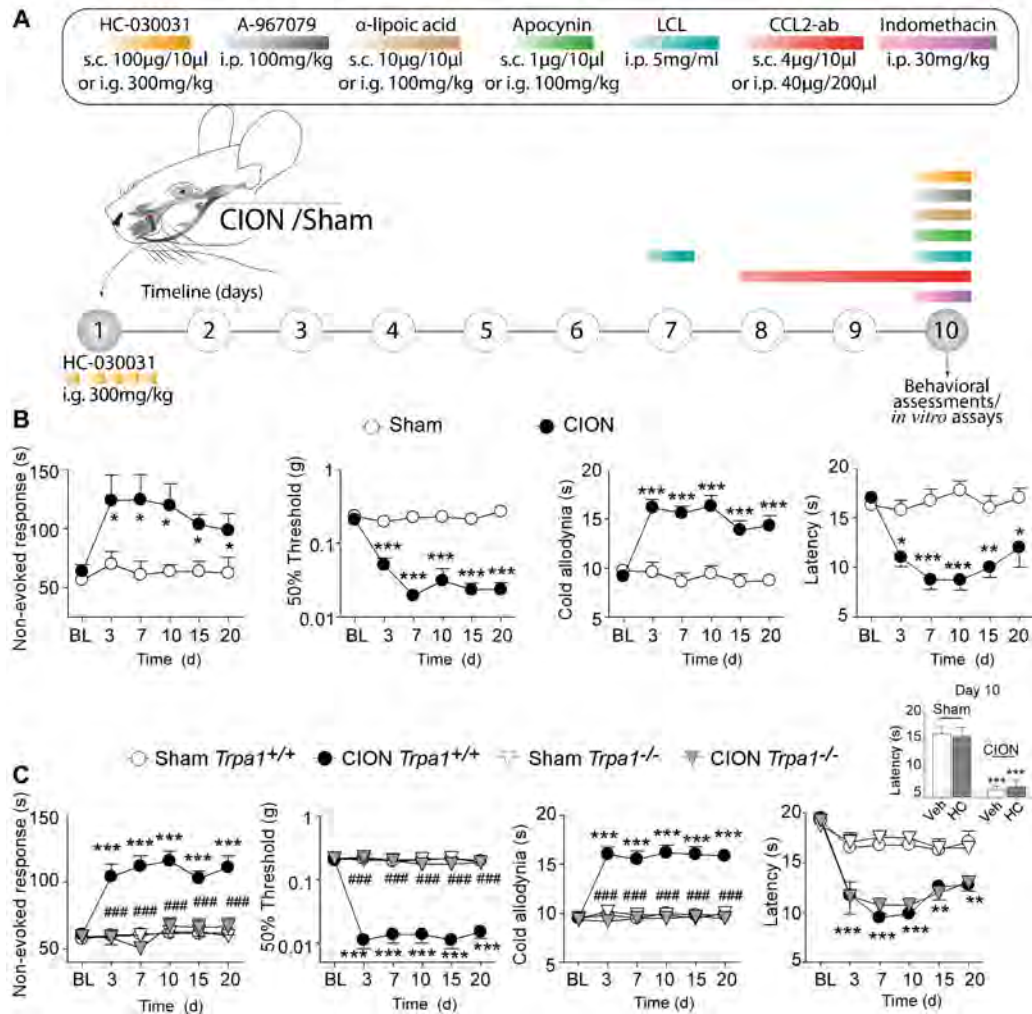


Figure 1 The constriction of the infraorbital nerve (CION) induces a non-evoked nociceptive behavior, mechanical allodynia and cold hypersensitivity, via TRPA1 activation in mice. (A) Scheme of the experimental procedure and timeline. C57BL/6, *Trpa1*^{+/+} or *Trpa1*^{-/-} mice underwent constriction of the infraorbital nerve (CION) or sham surgery on day 1. At day 10 mice received intragastric (i.g.) or subcutaneous (s.c.) HC-030031, A-967079, indomethacin, apocynin or α -lipoic acid. In another group of C57BL/6 mice, HC-030031 was administered (i.g.) 30 minutes before and shortly (4 times at 90 minutes interval each) after CION- or sham- procedure. Additional mice were treated with an antibody directed to the CCL2 chemokine (CCL2-ab) or its vehicle (IgG2B) at day 8, 9 and 10, or liposome-encapsulated clodronate (LCL) or its vehicle (liposome-encapsulated phosphate buffer saline) at day 7 and 10. On day 10, in all animals, pain-like behaviors (non-evoked nociceptive behavior, mechanical allodynia, cold hypersensitivity, chemical hyperalgesia, heat hyperalgesia) were assessed and tissues were collected for *in vitro* assays. **(B)** In C57BL/6 mice, CION induces non-evoked nociceptive behavior, mechanical allodynia, cold and heat hypersensitivity starting at day 3 and still persisting at day 20 after surgery. **(C)** The non-evoked nociceptive behavior, mechanical allodynia, and cold hypersensitivity induced by CION surgery in *Trpa1*^{+/+} mice are completely absent in *Trpa1*^{-/-} mice. The heat hypersensitivity was similar in both *Trpa1*^{+/+} and *Trpa1*^{-/-} CION-operated mice. Sham-operated animals do not show any hypersensitivity when compared to basal values. **P* < 0.05, ***P* < 0.01 and ****P* < 0.001 vs. Sham, Student's T test; *****P* < 0.001 and ***P* < 0.01 vs. Sham *Trpa1*^{+/+} and Sham/veh, one-way ANOVA and Bonferroni *post hoc* test; #####*P* < 0.001 vs. CION *Trpa1*^{+/+}; one-way ANOVA and Bonferroni *post hoc* test. BL, baseline assessment before surgery.

CION induces non-evoked nociceptive behavior, mechanical allodynia, and cold and chemical hypersensitivity via TRPA1 activation

CION induced significant changes in non-evoked nociceptive response and mechanical allodynia in C57BL/6 mice at day 3 after surgery and throughout the 20 days of observation, whereas in sham-operated mice the three outcomes remained stable over the entire period of observation (Fig. 1B). CION also induced hypersensitivity to cold (Fig. 1B). CION- and sham-operation did not affect the normal body weight increase (not shown). As previously reported (Luiz et al., 2010), in C57BL/6 mice, CION decreased the response latency to the application of the heat stimulus compared to the sham-operated group (Fig. 1B). Treatment with HC-030031 did not affect heat hyperalgesia at day 10 after surgery (Fig. 1C). In addition, heat hyperalgesia produced by CION was similar in both *Trpa1*^{+/+} and *Trpa1*^{-/-} mice (Fig. 1C).

In wild-type (*Trpa1*^{+/+}) mice, changes in non-evoked nociceptive behavior and mechanical allodynia/cold hypersensitivity produced by CION were similar to those observed in C57BL/6 mice (Fig. 1C). In contrast, and most importantly, littermate *Trpa1*^{-/-} mice were completely protected from all pain-like behaviors evoked by CION (Fig. 1C). At day 10 after surgery, systemic (i.g.) treatment with the TRPA1 selective antagonist, HC-030031, completely reverted the non-evoked nociceptive behavior, mechanical allodynia, and cold hypersensitivity (Fig. 2A).

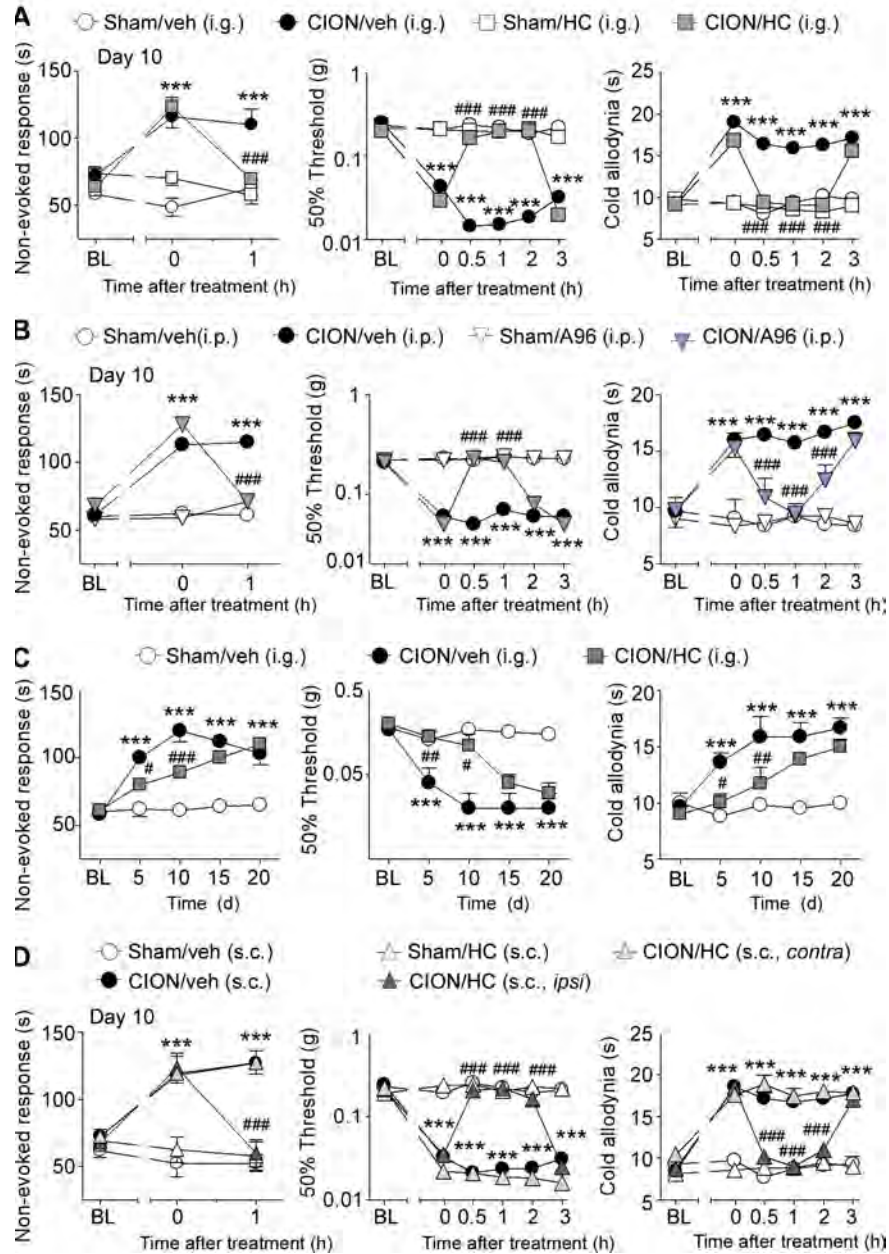


Figure 2 Pharmacological inhibition of TRPA1 prevents the non-evoked nociceptive behavior, mechanical allodynia and cold hypersensitivity induced by constriction of the infraorbital nerve (CION). (A,B) At day 10 after surgery, the systemic administration of selective TRPA1 receptor antagonists, HC-030031 (HC, 300 mg/kg intragastric, i.g.) or A-967079 (A96, 100 mg/kg intraperitoneal, i.p.), transiently reverses the non-evoked nociceptive behavior, mechanical allodynia and cold hypersensitivity 1 hour post dosing. (C) HC-030031 (300 mg/kg, i.g.) administered just before and 4 times (every 90 minutes) after CION or sham procedure prevents the early, but not the late phase of non-evoked nociceptive behavior, mechanical allodynia, and cold hypersensitivity induced by CION. (D) At day 10 after CION surgery, the subcutaneous (s.c.) administration of HC-030031 (100 μ g/10 μ l) in the left upper lip, ipsilateral (*ipsi*) to CION surgery, but not its injection in the contralateral (*contra*) upper lip, completely reverses the non-evoked nociceptive behavior, mechanical allodynia and cold hypersensitivity. (A-D) HC-030031 (s.c. and i.g.) and A-967079 (i.p.) do not affect the non-evoked nociceptive behavior, mechanical allodynia and cold hypersensitivity 30 minutes, 1 and 2 hours post dosing at day 10 after Sham procedure. *** $P < 0.001$ vs. Sham/veh, Sham/HC and Sham/A96, one-way

ANOVA and Bonferroni *post hoc* test; [#]*P* < 0.05, ^{##}*P* < 0.01 and ^{###}*P* < 0.001 vs. CION/veh; one-way ANOVA and Bonferroni *post hoc* test. BL, baseline assessment before surgery.

HC-030031 did not affect baseline values in sham-operated animals (Fig. 2A). The same results were obtained with another TRPA1 selective antagonist, A-967079. Systemic (i.p.) A-967079 completely reverted non-evoked nociceptive behavior, mechanical allodynia, and cold hypersensitivity evoked by CION (Fig. 2B). As for HC-030031, A-967079 did not affect baseline values in sham-operated animals (Fig. 2B). In addition, to assess whether TRPA1 inhibition prevents the development of non-evoked nociceptive behavior, mechanical allodynia, and cold hypersensitivity, HC-030031 was administered just before and 4 times (every 90 minutes) after CION or sham procedure. Such treatment delayed by about 15 days the onset of all pain-like behaviors (Fig. 2C), which fully recurred 15-20 days after CION.

To identify the site of TRPA1 engagement, HC-030031 was administered locally. At day 10 after surgery, local (s.c.) injection of HC-030031 in the left upper lip, ipsilateral to the surgery, reverted the non-evoked nociceptive behavior, mechanical allodynia and cold hypersensitivity (Fig. 2D). Importantly, HC-030031 injection in the right upper lip, contralateral to the surgery side, did not affect any pain-like behaviors measured in the ipsilateral upper lip (Fig. 2D). HC-030031 (s.c.) did not change any pain-like parameters in sham-operated mice (Fig. 2D). However, due to the vicinity of the injection site to both the ligature site and the skin area where Von Frey hairs are applied, it is possible that HC-030031 diffuses to both of them. Accordingly, these experiments cannot distinguish if only one of the two areas along the nerve fiber or both are targeted by the channel antagonist.

There is evidence that nerve injury associated with surgical procedures affect channel expression in different sections of sensory nerves (Jiang et al., 2014; Li et al., 2013). We evaluated, by Western blotting, TRPA1 protein content in the infraorbital nerve both ipsilateral and contralateral to the surgery in either CION- or sham-operated mice. Two major bands were identified, one slightly above 100 kDa and the other slightly below 140kDa. In the presence of the immunizing peptide, the 100 kDa band disappeared, thus indicating this band as the one most likely to correspond to the TRPA1 (Fig. 3A). At day 10 after surgery TRPA1 protein expression was not changed in infraorbital nerve (Fig. 3A) across the four different experimental conditions.

Selective chemical hypersensitivity to TRPA1 agonists has been reported in

experimental neuropathic pain (Trevisan et al., 2013a). Local injection (s.c.) in the left upper lip of the TRPA1 agonists, AITC or H₂O₂, the transient receptor potential vanilloid 1 selective agonist, capsaicin, and hypotonic saline, which stimulates the transient receptor potential vanilloid 4 channel (Trevisan et al., 2013a), evoked a dose-dependent increase in the nociceptive behavior in naïve, non-operated C57BL/6 mice (not shown). The nociceptive responses produced by suprathreshold doses of AITC, H₂O₂, but not those evoked by capsaicin or hypotonic saline, were more intense in CION-operated mice than in sham-operated mice (Fig. 3B-E). Notably, *Trpa1*^{-/-} mice showed neither acute nociception in response to suprathreshold doses of AITC and H₂O₂, nor increased responses to these stimuli after CION (Fig. 3F,G). However, in CION-operated *Trpa1*^{+/+} mice the nociceptive responses produced by suprathreshold doses of AITC, H₂O₂ were similar to those observed in C57BL/6 mice (Fig. 3F,G).

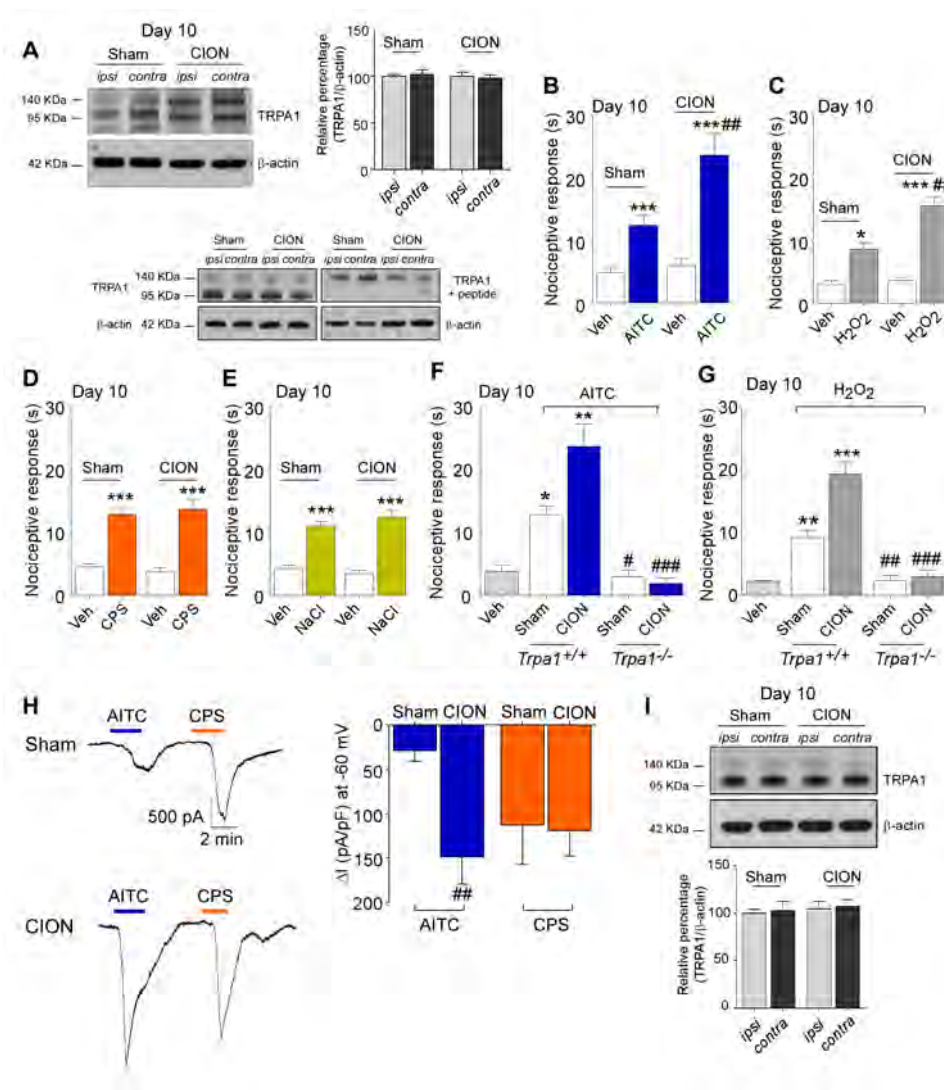


Figure 3 The constriction of the infraorbital nerve (CION) does not increase TRPA1 expression of, but enhances, TRPA1 activity. (A) TRPA1 protein content analyzed by Western blotting is not different in infraorbital nerve tissue homogenates obtained from the side ipsilateral (*ipsi*) and contralateral (*contra*) to the surgery in sham and CION mice 10 days after the surgery. Equally loaded protein was checked by expression of β -actin. Representative blots show TRPA1 protein expression in the infraorbital nerve and negative control obtained by preadsorption with the immunizing peptide. (B, C) The nociceptive response induced by a suprathreshold subcutaneous (s.c., 10 μ l) dose of the TRPA1 agonists, AITC (1 nmol/site) or H₂O₂ (0.1 μ mol/site) injected in the left upper lip, ipsilateral to CION surgery, is enhanced in CION mice compared to sham mice 10 days after surgery. (D, E) The responses to suprathreshold doses of capsaicin (CPS, 0.01 nmol/site) or hypotonic saline (NaCl, 0.45%/site) are not changed in CION mice. (F, G) AITC (1 nmol/site) or H₂O₂ (0.1 μ mol/site) injection induces nociceptive behaviors that are increased in *Trpa1*^{+/+} CION vs. sham mice. (F, G) Both the nociceptive behavior and its potentiation in CION mice are completely absent in *Trpa1*^{-/-} mice. *Trpa1*^{-/-} mice do not show any nociceptive behavior, including CION potentiation of nociceptive response, when the two TRPA1 agonists are administered. (H) A low concentration of AITC (30 μ M) elicits an inward current in trigeminal neurons isolated from sham mice, a response that results potentiated in neurons taken from CION mice, at day 10 after surgery. (I) TRPA1 protein content analyzed by Western blotting is not different in trigeminal ganglion homogenates obtained from the side ipsilateral (*ipsi*) and contralateral (*contra*) to the surgery in sham and CION mice 10 days after the surgery. Equally loaded protein was checked by expression of β -actin. Representative blot are shown. Values are mean \pm SEM of 6 to 8 mice. **P* < 0.05 vs. Sham/veh or veh or Sham *Trpa1*^{+/+}, ***P* < 0.01 vs. CION/veh or Sham *Trpa1*^{+/+}, ****P* < 0.001 vs. Sham/ veh or Sham *Trpa1*^{+/+}, #*P* < 0.05 vs. Sham *Trpa1*^{+/+}, ##*P* < 0.05 vs. Sham AITC or Sham H₂O₂ or Sham *Trpa1*^{+/+}, ###*P* < 0.001 vs. CION *Trpa1*^{+/+}; one-way ANOVA and Bonferroni *post hoc* test.

The primary role of TRPA1 in CION-evoked hypersensitivity is further supported by *in vitro* electrophysiological experiments performed in cultured TG neurons obtained 10 days after CION or sham procedure. Inward currents produced in neurons from CION-operated mice by a suprathreshold concentration of AITC were higher than those obtained in neurons from sham-operated mice (Fig. 3H). In contrast, the response to capsaicin was similar in neurons from CION- or sham-operated mice (Fig. 3H). In spite of the exaggerated functional response, TRPA1 protein expression was unchanged in TGs of CION or sham mice (Fig. 3I). Thus, TRPA1 hypersensitivity in CION does not seem to depend on increased protein expression.

Oxidative stress mediates non-evoked nociceptive behavior, mechanical allodynia and cold hypersensitivity induced by CION

At day 10 after CION surgery, changes in non-evoked nociceptive behavior, mechanical allodynia, and cold hypersensitivity were abrogated 1 hour after the systemic (i.g.) administration of the antioxidant agent, α -lipoic acid (Fig. 4A). A similar complete

attenuation was obtained after local treatment (s.c.) with α -lipoic acid into the left upper lip, ipsilateral to the surgery (Fig. 4B). Instead, local administration of α -lipoic acid to the contralateral side did not afford any protection against pain-like behaviors (Fig. 4B). In addition, at day 10 after CION surgery and 1 hour after i.g. or s.c. (in the left upper lip, ipsilateral to the surgery side) administration of the non selective NOX inhibitor, apocynin, abated the non-evoked nociceptive behavior, mechanical allodynia and cold hypersensitivity (Fig. 4C,D). Thresholds of sham-operated mice were not affected by either α -lipoic acid or apocynin, independently from their route of administration (i.g. or s.c.) (Fig. 4A-D).

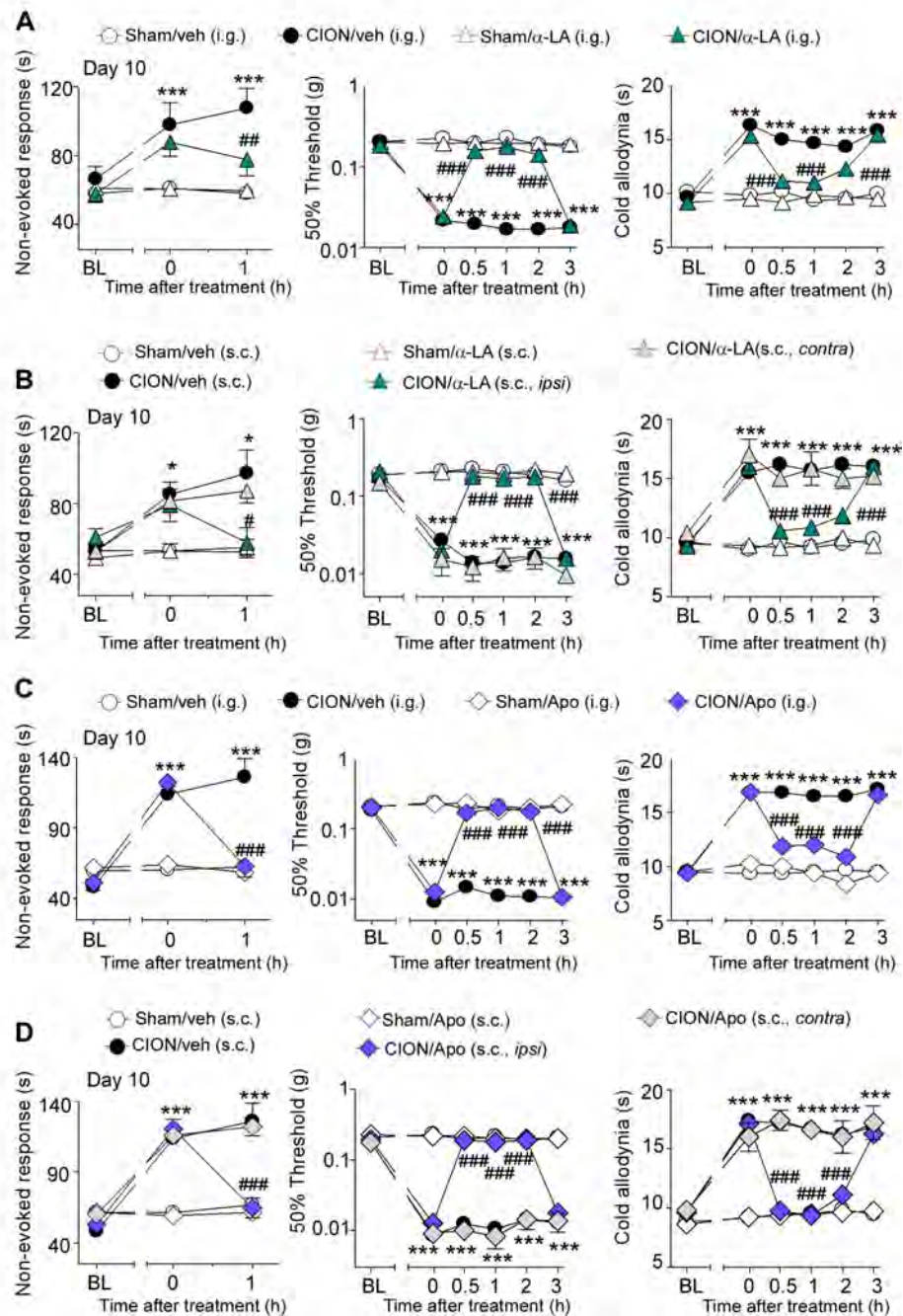


Figure 4 Systemic and local administration of α -lipoic acid (α -LA) or NADPH oxidase inhibitor, apocynin (Apo) transiently reverts the non-evoked nociceptive behavior, mechanical allodynia and cold hypersensitivity evoked by the constriction of the infraorbital nerve (CION). (A, B) In C57BL/6 mice, 10 days after CION surgery, both intragastric (i.g.) α -LA (100 mg/kg) and subcutaneous (s.c.) administration in the left upper lip, ipsilateral (ipsi) to CION surgery, but not in the contralateral (contra) upper lip, of α -LA (100 μ g/site) transiently (for 2 hours starting from 30 minutes post dosing) abates the non-evoked nociceptive behavior, mechanical allodynia and cold hypersensitivity. (C) At day 10 after CION surgery, Apo (i.g., 100 mg/kg), one hour after its injection, transiently reverts the non-evoked nociceptive behavior, mechanical allodynia and cold hypersensitivity. (D) A similar complete reduction in non-evoked nociceptive behavior, mechanical allodynia and cold hypersensitivity is observed one hour after subcutaneous administration in the left upper lip, ipsilateral (ipsi) to CION surgery, but not in the contralateral (contra) upper lip, of Apo (s.c., 1 μ g/site). Either i.g. or s.c. injection of α -LA or

Apo does not affect any nociceptive behavior evaluated in sham mice. Values are mean \pm SEM of 6 to 8 mice $^*P < 0.05$ and $^{***}P < 0.001$ vs. Sham/veh. $^{\#}P < 0.05$, $^{\#\#}P < 0.01$ and $^{\#\#\#}P < 0.001$ vs. CION/veh; one-way ANOVA and Bonferroni *post hoc* test. BL, baseline assessment, before surgery.

CION induces local monocyte/macrophage infiltration

At day 10 after surgery, a number of infiltrating monocytes/macrophages were observed in infraorbital nerve of CION-operated mice. At day 10 after the sham-operation or sham-operation with the insertion of the silk thread without ligature, only a few macrophages were found in infraorbital nerve (Fig. 5A,B). In addition, CCL2 levels in ION tissue homogenates from CION-operated mice were markedly augmented (Fig. 5C). In addition, CCL2 levels in homogenates of the nerve trunk and the surrounding tissue were augmented in CION-operated mice (Fig. 5C). A reduction in monocyte/macrophage content was observed in CION-operated mice treated systemically (i.p.) with the macrophage-depleting agent, LCL, which, as expected, did not affect CCL2 levels (Fig. 5B,C). In addition, the number of infiltrating monocytes/macrophages and CCL2 tissue levels were significantly reduced by the systemic (i.p.) administration at days 8 and 10 of the CCL2-ab as compared to the administration of the inactive IgG2B isotype (Fig. 5B,C). Finally, the failure of indomethacin to affect pain-like behaviors evoked by CION indicates that infiltrating monocytes/macrophages do not promote pain-like behaviors due to a cyclooxygenase-dependent inflammatory response (Fig. 5D).

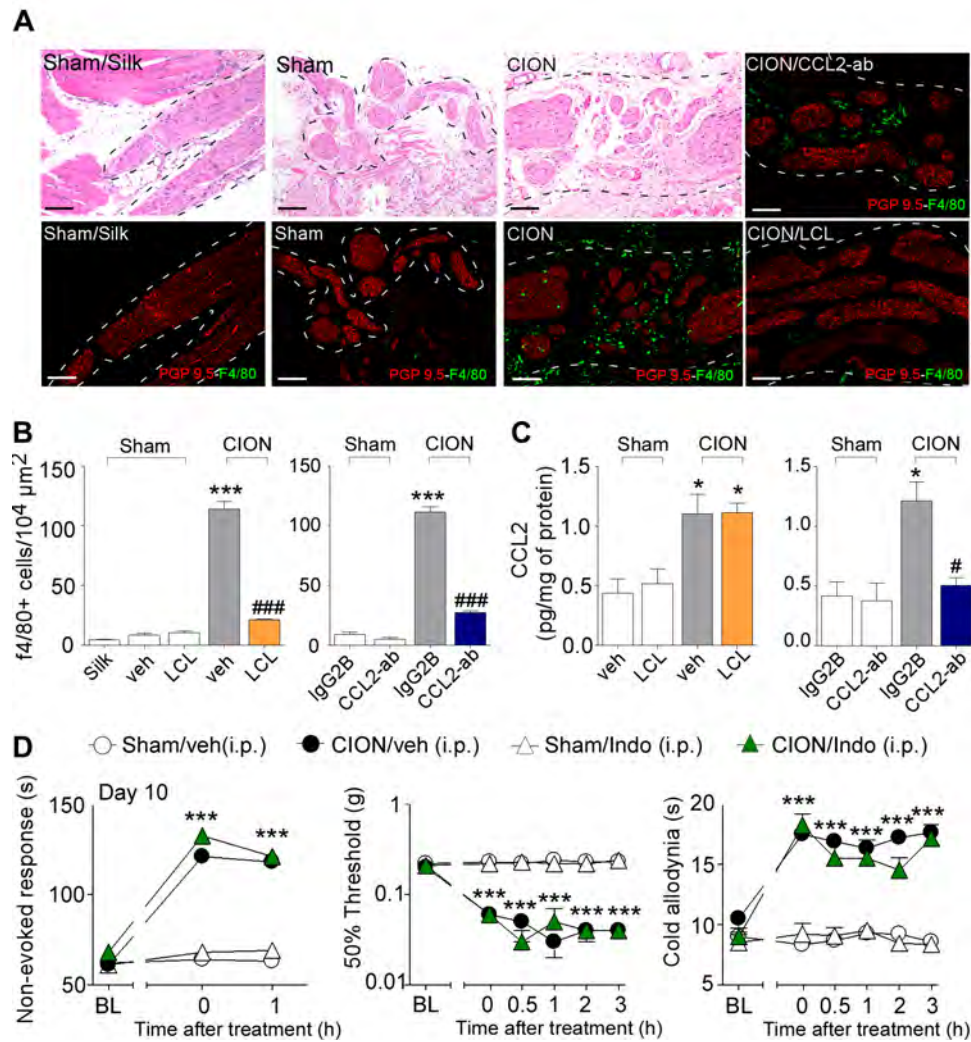


Figure 5 The constriction of the infraorbital nerve (CION) induces monocyte/macrophage infiltration in the site of ligature, which is reduced by macrophage depletion. (A,B) Representative images and pooled data of monocytes/macrophages infiltrating the nerve trunk in CION, sham or sham/silk (insertion of the silk thread without ligature) mice. Dashed lines represent the *epineurium* border of one of the injured branches of the infraorbital nerve. **(B)** Systemic (i.p.) liposome-encapsulated clodronate (LCL, 5 mg/ml, injected at day 7 and day 10 after surgery) or an antibody directed to CCL2 chemokine (CCL2-ab, 40 μg/200 μl, injected from day 8 to day 10 after surgery) prevent macrophage infiltration. **(C)** Pooled data of the increase in CCL2 content in tissue (infraorbital nerve and surrounding tissue) taken from the ipsilateral side to the surgery in CION mice on day 10 after surgical procedure compared to the sham. CCL2-ab, but not LCL, prevents the increase in CCL2 content. **(D)** At day 10 after surgery, intraperitoneal (i.p.) administration of indomethacin (Indo, 30 mg/kg) does not affect non-evoked nociceptive behavior, mechanical allodynia and cold hypersensitivity induced by CION. Values are mean ± SEM of 6 to 8 mice. **P* < 0.05 and ****P* < 0.001 vs. Sham/Veh or Sham/Silk or Sham/IgG2B, #*P* < 0.05 vs. CION/IgG2B, ###*P* < 0.001 vs. CION/Veh or CION/IgG2B; one-way ANOVA and Bonferroni *post hoc* test. The number of F4/80⁺ cells was counted in 10⁴ μm² boxes in left upper lip sections.

Monocyte/macrophage infiltration increases oxidative stress markers in the infraorbital nerve and perineural tissue, and drives pain-like behaviors

At day 10 after surgery, SOD activity and H₂O₂ levels were increased in the peripheral infraorbital nerve and perineural tissue homogenates from CION-operated mice as compared to sham-operated mice (Fig. 6A,B). Treatment with systemic (i.p.) LCL or CCL2-ab significantly reduced SOD activity and H₂O₂ levels in CION-operated mice (Fig. 6A,B), without affecting baseline levels of sham-operated mice. To identify the site of origin of the oxidative burst, associated with the TRPA1-dependent pain-like behaviors, we measured the content of 4-HNE, a final product of peroxidation of plasma membrane phospholipids (Csala et al., 2015). 4-HNE staining was markedly increased within the ligated infraorbital nerve and in the surrounding tissue of CION-operated mice as compared to sham-operated mice (Fig. 6E). Importantly, 4-HNE accumulated within or in the vicinity of TRPA1-expressing nerve bundles (Fig. 6E). TRPA1 staining was found within nerve bundles (PGP9-5 positive) of the infraorbital nerve and in some cells surrounding the nerve trunk in slices from *Trpa1*^{+/+}, but not from *Trpa1*^{-/-} mice (Fig. 6C). The ability of the antibody to label TRPA1 was further proved by the intense staining observed in TG from *Trpa1*^{+/+}, and the absence of staining in TGs from *Trpa1*^{-/-} mice (Fig. 6D). The increased 4-HNE content associated with CION surgery was attenuated by systemic (i.p.) administration of either the CCL2-ab or LCL (Fig. 6E).

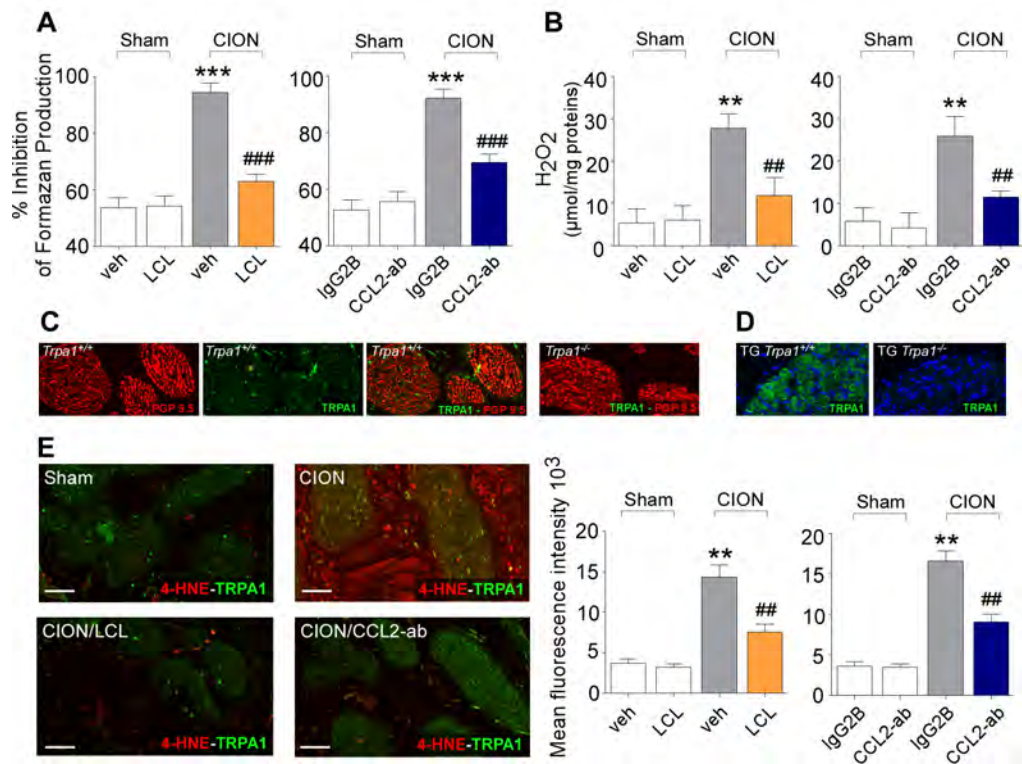


Figure 6 The constriction of the infraorbital nerve (CION) induces the increase in superoxide dismutase activity, hydrogen peroxide (H₂O₂) levels, and 4-hydroxynonenal (4-HNE) content in peripheral infraorbital nerve and perineural tissue, ipsilateral to the surgery. (A,B) Superoxide dismutase activity and H₂O₂ content measured at day 10 after sham or CION surgery, are reduced by intraperitoneal (i.p.) liposome-encapsulated clodronate (LCL, 5 mg/ml, injected at day 7 and 10 after surgery) or the antibody against CCL2 (CCL2-ab, 40 μg/200 μl, injected at day 8 and 10 after surgery), but not by their respective vehicles. (C) TRPA1 staining is present both in PGP9-5 positive nerve bundles of infraorbital nerve and in some cells of the surrounding tissue, and in TG (D) from *Trpa1*^{+/+}, but not from *Trpa1*^{-/-} mice. (E) Representative images and pooled data of the 4-HNE content. 4-HNE staining is markedly increased within the ligated infraorbital nerve and in the surrounding tissue of CION-operated mice as compared to sham-operated mice, and that increase is reverted by treatment with LCL or CCL2-ab. Values are mean ± SEM of 6 mice. ***P* < 0.01 and ****P* < 0.001 vs. Sham/Veh or Sham/IgG2B, ##*P* < 0.01 and ###*P* < 0.001 vs. CION/Veh or CION/IgG2B; one-way ANOVA and Bonferroni *post hoc* test. BL, baseline assessment, before surgery.

Importantly, monocyte/macrophage reduction by LCL or CCL2-ab was associated with a remarkable inhibition of non-evoked nociceptive behavior, mechanical allodynia and cold hypersensitivity (Fig. 7A,B). To determine whether pain-like behaviors were dependent from monocytes/macrophages accumulated at the site of nerve injury, we administered the CCL2-ab locally. Injection (s.c.) of CCL2-ab in the left upper lip, ipsilateral to the surgery, reverted the non-evoked nociceptive behavior, mechanical allodynia and cold hypersensitivity (Fig. 7C). In contrast, when the CCL2-ab was injected

in the right upper lip, contralateral to the surgery side, no change in pain-like behaviors was found in the ipsilateral left upper lip (Fig. 7C). These data indicate that the invasion of the infraorbital nerve and perineural tissue by monocytes/macrophages is a necessary and sufficient condition for the development of pain-like behaviors produced by the CION surgery.

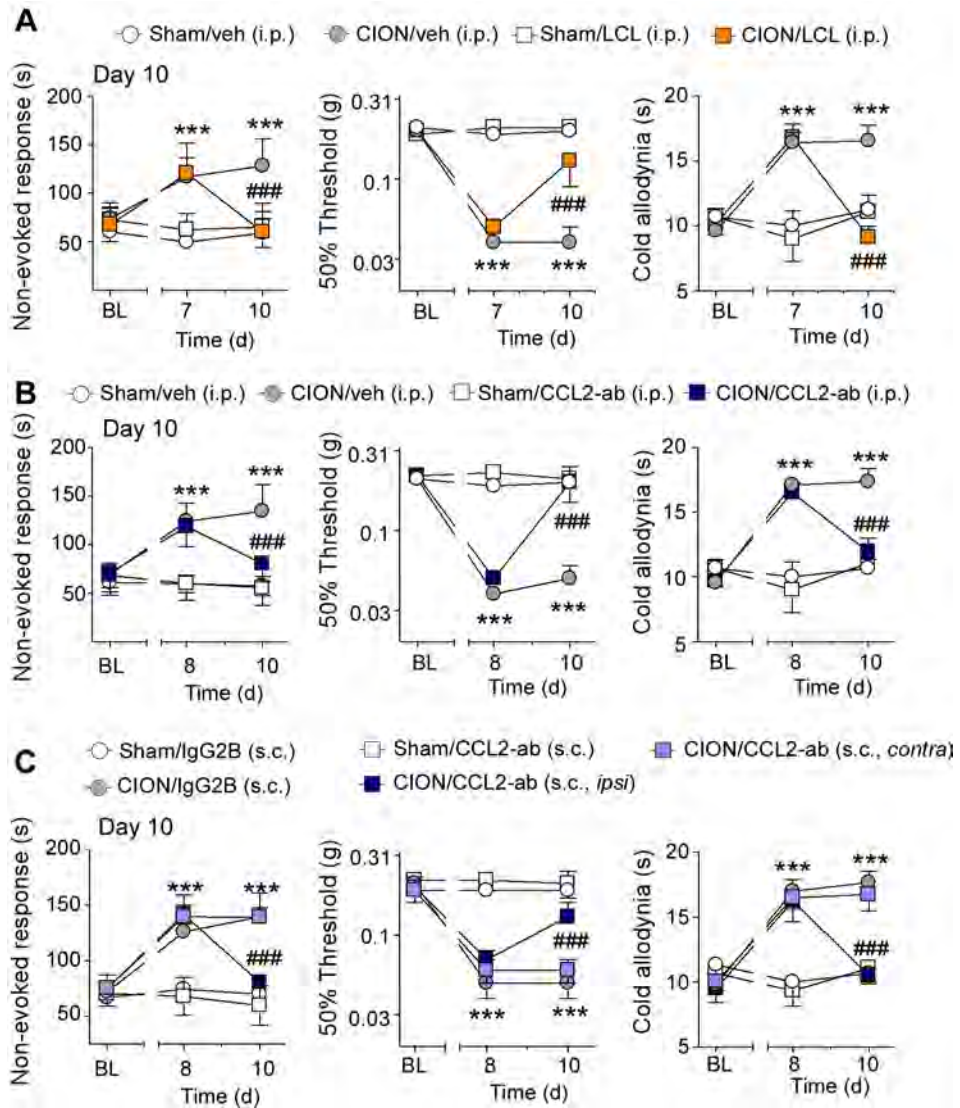


Figure 7 Systemic and local administration of liposome-encapsulated clodronate (LCL) or the antibody against CCL2 (CCL2-ab) reverts the non-evoked nociceptive behavior, mechanical allodynia and cold hypersensitivity evoked by the constriction of the infraorbital nerve (CION). (A,B) Effect of the intraperitoneal (i.p.) treatment with LCL (5 mg/ml, injected at day 7 and 10 after surgery), the CCL2-ab (40 μ g/200 μ l, injected at day 8 and 10 after surgery) and their respective vehicles in sham and CION-operated mice. Both treatments revert the non-evoked nociceptive behavior, mechanical allodynia and cold hypersensitivity induced by CION. (C) At day 10 after surgery and one hour post dosing, subcutaneous (s.c.) administration of CCL2-ab (4 μ g/10 μ l, two injections starting from day 8 after surgery) in the left upper lip, ipsilateral (ipsi) to CION surgery, but not its injection in the contralateral (contra) upper lip, completely reverts the non-evoked nociceptive behavior, mechanical allodynia and cold hypersensitivity. Values are mean \pm SEM of 6 to 8 mice. *** P < 0.001 vs. Sham/Veh or Sham/IgG2B, ### P < 0.001 vs. CION/Veh or CION/IgG2B; one-way ANOVA and Bonferroni *post hoc* test. BL, baseline assessment, before surgery.

Schwann cell TRPA1 mediates neuroinflammation that sustains macrophage-dependent neuropathic pain in mice

Our previous data showed that in mice with trigeminal nerve injury (CION) macrophages, recruited by a CCL2-dependent process, increase H₂O₂ levels within the site of nerve injury. The resulting oxidative stress and the ensuing increases in RCS were proposed to mediate prolonged mechanical allodynia by gating TRPA1 in trigeminal nerve fibers. Thus, TRPA1, expressed by primary sensory neurons, appears to be the target of the macrophage-dependent oxidative burst required to promote neuropathic pain. We, surprisingly, also found that pharmacological blockade or genetic deletion of TRPA1 not only induced the expected inhibition of mechanical allodynia, but also suppressed macrophage infiltration and H₂O₂ generation in the injured nerve.

Thus, we aimed at identifying the cellular and molecular mechanisms responsible for this TRPA1-mediated macrophage infiltration and generation of oxidative stress.

TRPA1 mediates neuroinflammation

In C57BL/6 mice pSNL, but not sham surgery (Fig 8a), induced prolonged (3-20 days) mechanical allodynia (Fig. 8b) accompanied by macrophage (F4/80⁺ cells)

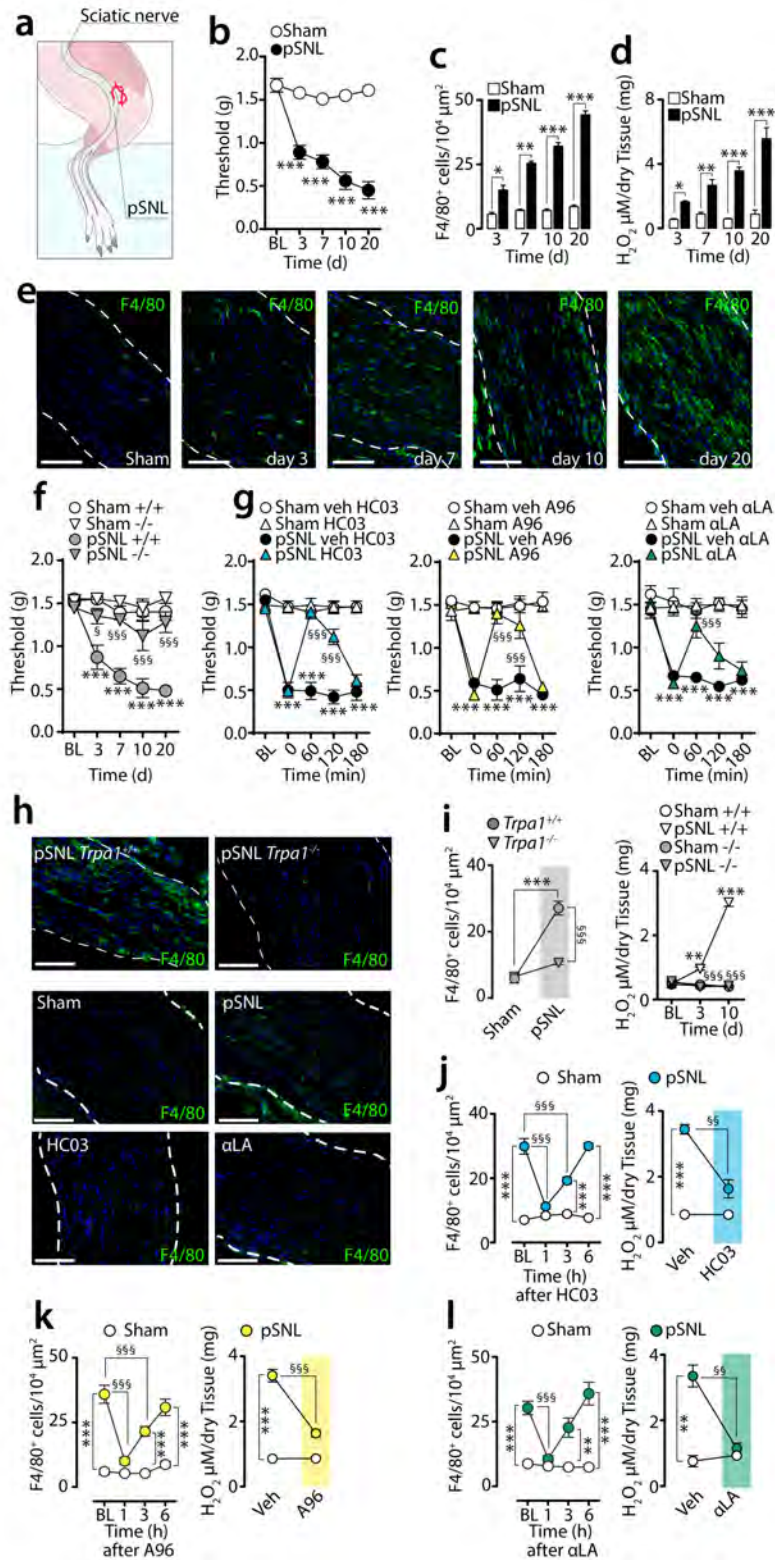


Figure 8. TRPA1 mediates pSNL-evoked allodynia and neuroinflammation. (a) Drawing representing the pSNL surgery in mice. (b-e) Time-dependent (3-20 days, d) mechanical allodynia (b), number and representative images of macrophages (F4/80⁺ cells) (c,e) and H₂O₂ content (d) in the sciatic nerve trunk induced by pSNL in C57BL/6 compared to sham mice (n=6, *P<0.005, **P<0.01, ***P<0.001 pSNL vs. Sham; two-way ANOVA followed by Bonferroni post hoc analyses and unpaired two-tailed Student's t-test). (f) Time-dependent (3-20 d)

mechanical allodynia in sham/pSNL *Trpa1*^{+/+}/*Trpa1*^{-/-} mice (n=8, ***P <0.001 pSNL^{+/+} vs. Sham^{+/+}; n=6, ^{\$}P <0.05 and ^{\$\$\$}P<0.001 pSNL^{-/-} vs. pSNL^{+/+}; two-way ANOVA followed by Bonferroni post hoc analyses). (g) Mechanical allodynia (at day 10 after surgery) in sham/pSNL mice after HC-030031 (HC03, 100 mg kg⁻¹, i.p.), A-967079 (A96, 100 mg/kg, i.p.) and α -lipoic acid (α LA, 100 mg kg⁻¹, i.p.) or respective vehicles (veh, 4% DMSO and 4% tween80 in isotonic saline) (n=6, ***P<0.001 pSNL veh vs. Sham veh; ^{\$\$\$}P<0.001 pSNL-HC03, A96 or α LA vs. pSNL-veh; two-way ANOVA followed by Bonferroni post hoc analyses). (h-i) Representative images, number of F4/80⁺ cells, and H₂O₂ content in the sciatic nerve of sham/pSNL *Trpa1*^{+/+}/*Trpa1*^{-/-} and C57BL/6 mice, before (BL) and 1-6 h after HC03, A96, α LA (all, 100 mg kg⁻¹, i.p.) or respective vehicles (veh, 4% DMSO and 4% tween80 in isotonic saline) (n=6, **P<0.01 and ***P<0.001 pSNL *Trpa1*^{+/+} vs. Sham-*Trpa1*^{+/+} and pSNL veh vs. Sham veh; ^{\$\$}P<0.01 and ^{\$\$\$}P<0.001 pSNL *Trpa1*^{-/-} vs. pSNL-*Trpa1*^{+/+} and pSNL HC03, A96 or α LA vs. pSNL-veh; two-way and one-way ANOVA followed by Bonferroni post hoc analyses). (Scale bars: 50 μ m; e,h dashed lines, *perineurium*). Data are represented as mean \pm s.e.m.

recruitment (Fig. 8c,e) and oxidative stress (H₂O₂) generation (Fig. 8d) within the injured nerve. *Trpa1* (Fig 8f), but not *Trpv1* or *Trpv4*, deletion prevented mechanical allodynia. *Trpa1*, but not *Trpv1* or *Trpv4*, deletion also attenuated cold allodynia, but this response was not further investigated in the present study. Heat hyperalgesia was unaffected by *Trpa1*, *Trpv1* and *Trpv4* deletion. As previously reported (Eid et al., 2008; Kim et al., 2004) in similar models, at day 10 after pSNL (all measurements were at 10 days unless otherwise specified), TRPA1 antagonists (HC-030031, A-967079) and antioxidants (α -lipoic acid [α LA] and phenyl-N-tert-butyl nitron [PBN]) (Fig. 8g) reversed mechanical allodynia. Treatments for 3 days with the monocyte-depleting agent clodronate (Liu et al., 2000) or an anti-CCL2 antibody (CCL2-Ab) (Zhu et al., 2011) attenuated allodynia, macrophage infiltration and H₂O₂ generation, confirming the proalgesic role of these cells.

Other inflammatory cells, which are recruited to sites of nerve injury, may also contribute to mechanical allodynia (Perkins et al., 2000). To explore their role in the delayed phase of mechanical allodynia, the number of neutrophils and T lymphocytes was evaluated in the nerve trunk at day 10 after surgery. Although both neutrophils (Ly6g⁺ cells) and T lymphocytes (CD8⁺ cells) were increased by pSNL, treatment with clodronate, which markedly attenuated both the infiltration macrophages and allodynia, did not affect the number of neutrophils or T lymphocytes. In agreement with a previous report (Perkins et al., 2000), these data exclude the contribution of neutrophils and T cells to mechanical allodynia assessed 10 days after pSNL.

The hypothesis that oxidative stress produced by infiltrating macrophages targets neuronal TRPA1 to signal neuropathic pain implies that the channel inhibition reduces

allodynia but does not affect neuroinflammation. Surprisingly, *Trpa1* deletion prevented infiltration of F4/80⁺ cells and H₂O₂ generation in the injured sciatic nerve (Fig. 8h,i). TRPA1 antagonists (Fig. 8h,j,k) and antioxidants (Fig. 8h,l) also transiently reversed macrophage infiltration and H₂O₂ production. Thus, the TRPA1-oxidative stress pathway mediates both neuropathic pain and neuroinflammation in the injured nerve.

CCL2 induces neuroinflammation via TRPA1

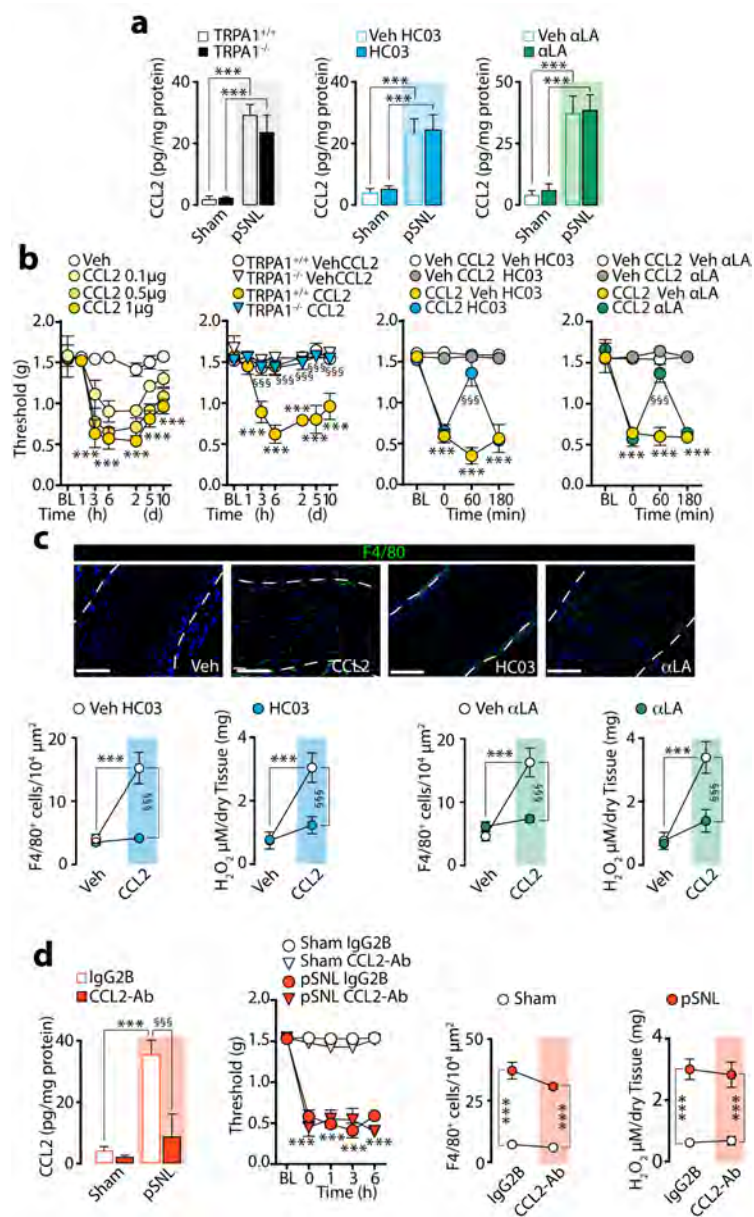


Figure 9. TRPA1 mediates CCL2-evoked allodynia and neuroinflammation. (a) CCL2 levels in sciatic nerves (at day 10 after surgery) of sham/pSNL *Trpa1*^{+/+}/*Trpa1*^{-/-} and C57BL/6 mice after HC-030031 (HC03, 100 mg kg⁻¹, i.p.), α-lipoic acid (αLA, 100 mg kg⁻¹, i.p.) or respective vehicles (veh, 4% DMSO and 4% tween80 in isotonic saline) (n=6, ***P<0.001 pSNL-*Trpa1*^{+/+} vs. sham-*Trpa1*^{+/+} and pSNL-veh vs. sham-veh; one-way ANOVA followed by Bonferroni post hoc analyses). (b) Mechanical allodynia induced by perineural CCL2 (0.1-1 μg) or vehicle (veh, isotonic saline) in C57BL/6 mice (n=4, ***P<0.001 veh vs. CCL2 (1 μg), two-way ANOVA followed by Bonferroni post hoc analyses) and CCL2 (1 μg) in *Trpa1*^{+/+}/*Trpa1*^{-/-} and after HC03, αLA (both, 100 mg/kg, i.p.) or respective vehicles (veh, 4% DMSO and 4% tween80 in isotonic saline) in C57BL/6 mice (n=4, ***P<0.001 *Trpa1*^{+/+} CCL2 vs. *Trpa1*^{+/+}veh; CCL2 veh HC03, αLA vs. veh CCL2; §§§P<0.001 *Trpa1*^{-/-} CCL2 vs. *Trpa1*^{+/+} CCL2 and CCL2 HC03, αLA vs. CCL2 veh HC03, αLA; two-way ANOVA followed by Bonferroni post hoc analyses). (c) Representative images, F4/80⁺ cell number and H₂O₂ content in sciatic nerves of mice treated with

perineural CCL2 (1 μg) after HC03, αLA (both, 100 mg kg^{-1} , i.p.) or respective vehicles (veh, 4% DMSO and 4% tween80 in isotonic saline) ($n=5$, *** $P<0.001$ CCL2 vs. veh HC03, αLA ; §§§ $P<0.001$ CCL2 HC03, αLA vs. CCL2 veh HC03, αLA ; one-way ANOVA followed by Bonferroni post hoc analyses) (Scale bars: 50 μm , dashed lines indicate *perineurium*). **(d)** CCL2 levels, mechanical allodynia, F4/80⁺ cell number and H₂O₂ content in sciatic nerves (at day 10 after surgery) of sham/pSNL C57BL/6 mice after an anti-CCL2 antibody (CCL2-Ab) or IgG2B control (120 $\mu\text{g 200 } \mu\text{l}^{-1}$, i.p., single administration) ($n=6$, *** $P<0.001$ pSNL-CCL2-Ab vs. sham-CCL2-Ab; §§§ $P<0.001$ pSNL-CCL2-Ab vs. pSNL-IgG2B; one-way ANOVA followed by Bonferroni post hoc analyses). Data are represented as mean \pm s.e.m.

One possible explanation may be that TRPA1 mediates the release of the monocyte chemoattractant, CCL2, generated by injured nerves (Van Steenwinckel et al., 2014). However, as neither TRPA1 deletion or antagonism nor antioxidants affected CCL2 increases in ligated sciatic nerves (Fig. 9a), the chemokine should originate from a TRPA1–oxidative stress-independent pathway. As previously shown (Van Steenwinckel et al., 2014), local perineural CCL2 administration induced mechanical allodynia, as well as producing F4/80⁺ cell infiltration and H₂O₂ generation (Fig. 2b,c). TRPA1 deletion or antagonism and antioxidants prevented or reversed the effects of CCL2 (Fig. 9b,c). Pretreatment with clodronate, which depletes circulating monocytes and thereby inhibits their neural accumulation, prevented mechanical allodynia evoked by CCL2. Furthermore, in mice with pSNL clodronate treatment depleted macrophages and attenuated mechanical allodynia, but did not affect the increased CCL2 levels within the ligated nerve trunk. Together, the present findings support the view that oxidative stress and TRPA1 induce neuroinflammation downstream from CCL2. There was a distinct temporal difference between the effects of CCL2-Ab and TRPA1 antagonists/antioxidants on pSNL-induced neuroinflammation and allodynia. One-hour after HC-030031, A-967079, αLA or PBN, pSNL-induced F4/80⁺ cell infiltration, H₂O₂ formation and allodynia were all prominently inhibited (Fig. 8g,h,j-l), whereas a high dose of the CCL2-Ab, which at 1 hour already attenuated neural CCL2 levels, was completely ineffective (over 6 hours) in reducing mechanical allodynia (Fig. 9d). Successful inhibition of pain and inflammation required the administration of a lower CCL2-Ab dose for 3 consecutive days that, as expected, also reduced CCL2 levels in the nerve trunk. Thus, while TRPA1-antagonism/antioxidants rapidly (within 1 hour) reversed neuroinflammation, CCL2-blockade required a much longer time (3 days) to produce the same inhibitory effects.

Schwann cells express TRPA1 that releases H₂O₂

Nerve fibers, macrophages and Schwann cells within the injured nerve trunk could potentially mediate TRPA1-dependent oxidative stress. By targeting TRPV1, resiniferatoxin (RTX) defunctionalizes TRPV1⁺/TRPA1⁺ neurons. RTX abolished nociceptive responses to TRPV1 (capsaicin) and AITC and reversed pSNL-evoked allodynia, but did not affect F4/80⁺ cell infiltration and H₂O₂ generation. Thus, TRPV1⁺/TRPA1⁺ nerve fibers mediate neuropathic pain but not neuroinflammation. Naïve or lipopolysaccharide-activated mouse peritoneal macrophages in culture neither expressed TRPA1 mRNA (RT-qPCR), TRPA1 protein (immunocytochemistry) nor responded to AITC (Ca²⁺-signaling). Thus, macrophages infiltrating the injured nerve cannot generate TRPA1-dependent oxidative stress.

Schwann cells ensheath nerve fibers, including C-fiber nociceptors, and represent 90% of the nucleated cells of the nerve trunk (Campana, 2007). We localized immunoreactive TRPA1 to PGP9.5⁺ nerve fibers and to S-100⁺ or SOX10⁺

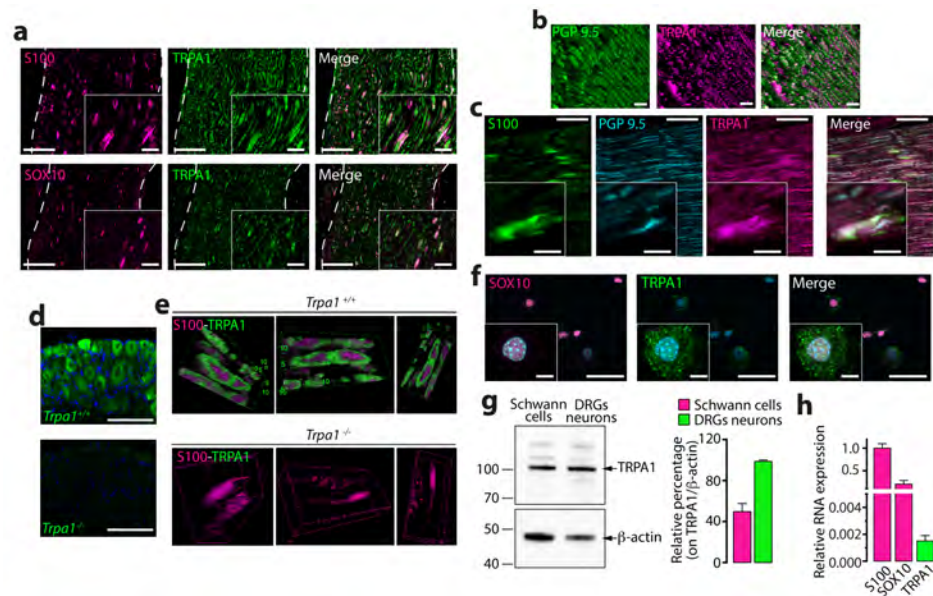


Figure 10. Schwann cells express TRPA1. (a) Double immunofluorescence staining of TRPA1 and S-100 and SOX10 (two specific markers for detecting Schwann cells), in sciatic nerve from C57BL/6 mice (Scale bars: 50 μ m and inset 20 μ m). (b) 3D confocal images of TRPA1 and PGP9.5 staining in Schwann cells from sciatic nerve trunks of C57BL/6 mice (Scale bars: 20 μ m). (c) Triple immunofluorescence staining of S-100, PGP9.5 and TRPA1 in sciatic nerve trunks from C57BL/6 mice (Scale bars: 20 μ m and inset 10 μ m). (d) TRPA1 staining in DRGs neurons from *Trpa1*^{+/+} and *Trpa1*^{-/-} mice (Scale bars: 50 μ m). (e) 3D confocal image reconstructions of TRPA1 and S100 in Schwann cells from sciatic nerve trunks of *Trpa1*^{+/+} and *Trpa1*^{-/-} mice. (f) TRPA1 and SOX-10 immunoreactivity in cultured C57BL/6 mouse Schwann cells (Scale bars: 50 μ m and

inset 10 μm). **(g)** Representative blot and TRPA1 protein content in cultured Schwann cells and DRGs neurons taken from C57BL/6 mice. Equally loaded protein was checked by expression of β -actin (n=4 independent experiments). **(h)** TRPA1 mRNA relative expression in cultured C57BL/6 mouse Schwann cells (n=3 replicates from 2 independent experiments). Data are represented as mean \pm s.e.m.

Schwann cells in the sciatic nerve trunk from C57BL/6 mice (Fig 10a-c). TRPA1 immunoreactivity was not detected in dorsal root ganglia (DRG, L4-L6) (Fig. 10d) or in S-100⁺ cells in the sciatic nerve trunk (Fig. 10e) from *Trpa1*^{-/-} mice, which confirms antibody selectivity. Expression of TRPA1 (protein and mRNA) in cultured mouse Schwann cells was confirmed by immunofluorescence, western blotting and RT-qPCR (Fig. 10f-h). Furthermore, AITC induced intracellular Ca²⁺ response in cultured Schwann cells from wild type mice, which was attenuated by HC-030031 (Fig. 11a). In contrast, capsaicin or a TRPV4 agonist (GSK1016790A) failed to produce any Ca²⁺ response (Fig. 11a). Importantly, Schwann cells from *Trpa1*^{+/+} mice, but not from *Trpa1*^{-/-} mice, responded to AITC (Fig. 11B). The ability of TRPA1 to promote oxidative stress was explored by measuring H₂O₂ generation. Both AITC and H₂O₂, which has been shown to gate TRPA1 (Sawada et al., 2008), stimulated H₂O₂ release from HEK293 cells expressing the human TRPA1 (hTRPA1-HEK293 cells), but not from untransfected HEK293 cells (Fig. 4c,d). AITC or H₂O₂ also produced a time- and Ca²⁺-dependent H₂O₂ generation in Schwann cells, which was prevented by HC-030031 (Fig. 11e). Thus, Schwann cells generate H₂O₂ in response to TRPA1 activation.

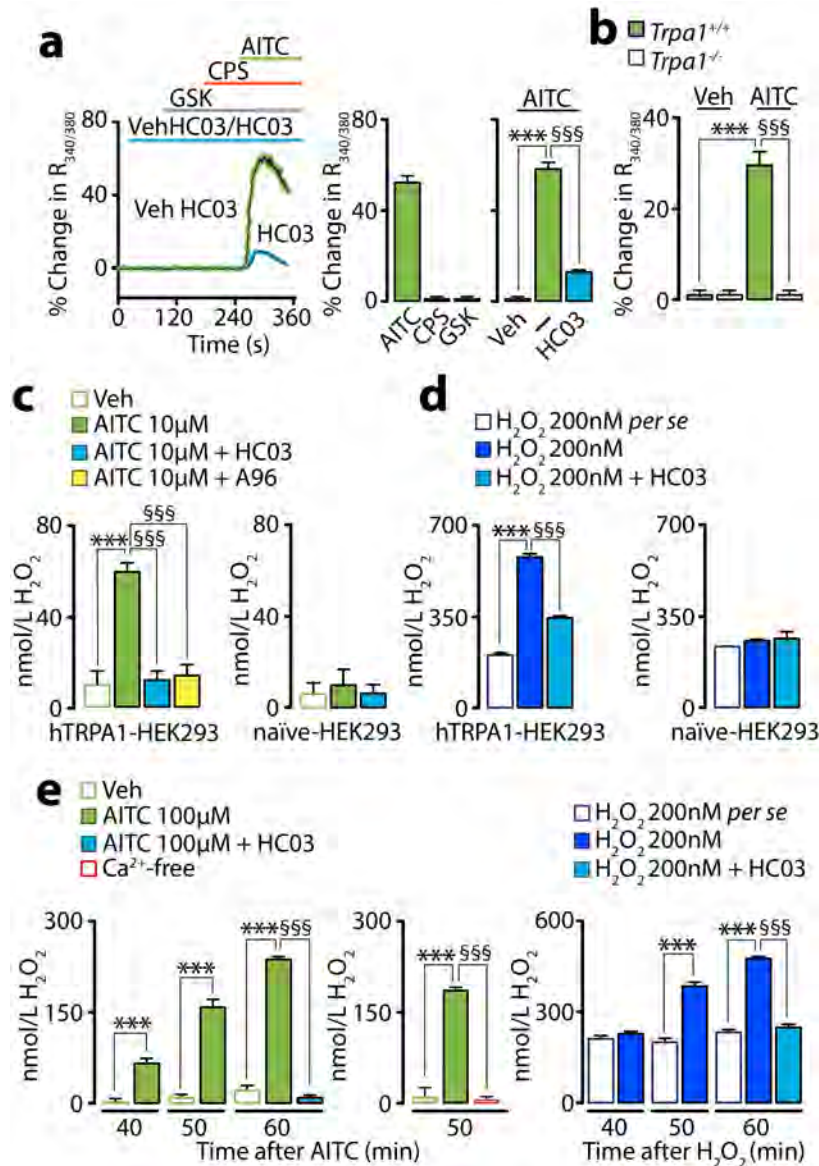


Figure 11. Schwann cells expressing TRPA1 release H_2O_2 . (a) Ca^{2+} responses to AITC (1 mM) in cultured Schwann cells with HC-030031 (HC03, 30 μ M) or its vehicle (veh, 0.3% DMSO) and to TRPV1- (capsaicin, CPS, 0.5 μ M) or TRPV4- (GSK1016790A, GSK, 50 nM) agonists (n=25 cells from 3 independent experiments, *** P <0.001 AITC vs. veh; §§§ P <0.001 HC03 vs. AITC; one-way ANOVA followed by Bonferroni post hoc analyses). (b) AITC (1 mM)-evoked calcium response in Schwann cells from $Trpa1^{+/+}$, but not from $Trpa1^{-/-}$ mice (n=25 cells from 3 independent experiments, *** P <0.001 $Trpa1^{+/+}$ AITC vs. $Trpa1^{+/+}$ veh; §§§ P <0.001 $Trpa1^{-/-}$ AITC vs. $Trpa1^{+/+}$ AITC; one-way ANOVA followed by Bonferroni post hoc analyses). (c,d) H_2O_2 release from hTRPA1-HEK293 or untransfected (naïve-HEK293) cells induced by AITC (10 μ M) or H_2O_2 (200 nM) and effect of HC03 (30 μ M), A-967079 (A96, 30 μ M) or respective vehicles (veh, 0.3% DMSO) (n=8 replicates from 3 independent experiments, *** P <0.001 AITC, H_2O_2 vs. veh; §§§ P <0.001 AITC, H_2O_2 + HC03/A96 vs. AITC, H_2O_2 ; one-way ANOVA followed by Bonferroni post hoc analyses; H_2O_2 200 nM *per se* represents the value of H_2O_2 over the time, not in presence of cells). (e) H_2O_2 release from cultured mouse Schwann cells evoked by AITC (100 μ M) or H_2O_2 (200 nM) and effect of HC03 (30 μ M) and Ca^{2+} free medium (Ca^{2+} -free) (n=8 replicates from 3 independent experiments, *** P <0.001, veh-AITC/ H_2O_2 vs. AITC/ H_2O_2 ; §§§ P <0.001 HC03 vs. AITC, H_2O_2 ; one-way ANOVA followed by Bonferroni post hoc analyses; H_2O_2 200 nM *per se* represents the value of H_2O_2 without cells). Data are represented as mean \pm s.e.m.

Schwann cells generate oxidative stress via TRPA1 and NOX1

Different NOXs play a key role in oxidative stress (Bedard et al., 2007). While we observed that macrophages contain exclusively NOX2 (mRNA and protein), cultured Schwann cells expressed NOX1, NOX2 and NOX4 mRNAs. Yet, only NOX1 protein was detected by immunofluorescence (Fig. 12a). Functional data corroborated the molecular/morphological findings as the selective NOX2-inhibitor (Gp91ds-tat peptide), but not the NOX1/NOX4-inhibitor (GKT13783), attenuated phorbol myristate acetate-stimulated H₂O₂ release from cultured peritoneal macrophages. However, GKT13783, but not gp91ds-tat peptide, inhibited AITC-induced H₂O₂ release from cultured Schwann cells, indicating a major role for NOX1. One hour after the administration of 2-acetylphenothiazine (ML171, selective NOX1-inhibitor) or GKT13783, pSNL-induced allodynia and neuroinflammation were attenuated (Fig. 12b), whereas gp91ds-tat peptide was ineffective. Perineural administration of antisense oligonucleotides (AS-ODN) for NOX1, NOX2 or NOX4 effectively knocked down respective mRNA expression (Fig. 12c). However, only NOX1 AS-ODN attenuated pSNL-induced allodynia, macrophage infiltration and H₂O₂ generation (Fig. 12d).

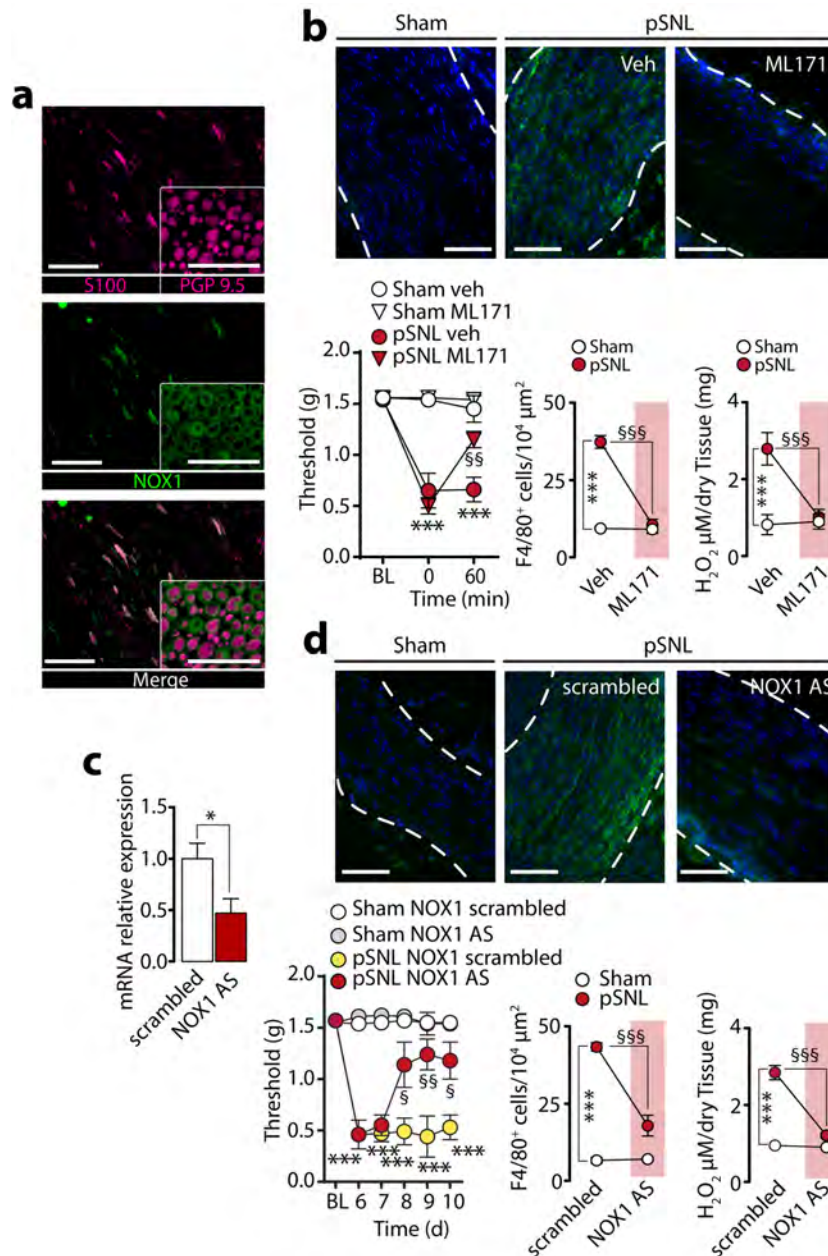


Figure 12. NOX1 blockade inhibited pSNL-evoked allodynia and neuroinflammation. (a) Images of S100/PGP9.5 and NOX1 immunofluorescence in sciatic nerves (Scale bars: 50 μm and inset 20 μm). (b) Mechanical allodynia, representative images and F4/80⁺ cell number, and H₂O₂ content (at day 10 after surgery) in sham/pSNL mice after NOX1-inhibitor (ML171, 60 mg kg⁻¹, i.p) or vehicle (veh, 4% DMSO and 4% tween80 in isotonic saline) (n=6, ***P<0.001 pSNL-veh vs. sham-veh; \$\$\$P<0.01 and \$\$\$P<0.001 pSNL-ML171 vs. pSNL-veh; two-way ANOVA followed by Bonferroni post hoc analyses) (Scale bars: 50 μm; dashed lines, *perineurium*). (c) NOX1 mRNA relative expression in sciatic nerve after perineural NOX1 antisense oligonucleotides (AS-ODN) or scrambled-ODN (both, 10 nmol 10μl⁻¹) (n=3 replicates from 2 independent experiments, *P<0.05 AS-ODN vs. scrambled-ODN; unpaired two-tailed Student's t-test). (d) Mechanical allodynia, representative images and F4/80⁺ cell number, and H₂O₂ content (at day 10 after surgery) in sham/pSNL mice after NOX1 AS-ODN or scrambled-ODN (both, 10 nmol 10μl⁻¹) (n=6, ***P<0.001 pSNL-NOX1-scrambled vs. sham-NOX1scrambled; \$P<0.05, \$\$\$P<0.01 and \$\$\$P<0.001 pSNL-NOX1 AS-ODN vs. pSNL-NOX1scrambled; two-way ANOVA followed by Bonferroni post hoc analyses) (Scale bars: 50 μm; dashed lines, *perineurium*). Data are represented as mean±s.e.m.

To define the contribution of the TRPA1/NOX1 pathway of Schwann cells to neuroinflammation and neuropathic pain evoked by pSNL, antisense TRPA1 oligonucleotide (TRPA1 AS-ODN) or their mismatched (TRPA1 MM-ODN) analogues were administered to pSNL mice by perineural or intrathecal route (Fig. 6a,f). Perineural treatment with TRPA1 AS-ODN did not affect expression of TRPA1 mRNA and immunoreactivity in DRGs (L4-L6), or acute nociceptive responses to perineural AITC or capsaicin (Fig. 13b). However, it markedly reduced TRPA1 mRNA and the TRPA1/S-100 overlap (Fig. 13c) in injured sciatic nerves, and inhibited pSNL-evoked allodynia, neural F4/80⁺ cell infiltration, and H₂O₂ generation (Fig. 13d,e). Thus, Schwann cell TRPA1 silencing preserved TRPA1-mediated acute nociceptive signaling, but disrupted pSNL-evoked neuroinflammation and allodynia. Intrathecal administration of TRPA1 AS-ODN (Fig 13f) down-regulated TRPA1 mRNA and immunoreactivity in DRGs (L4-L6), suppressed the acute nociception by perineural AITC, but not capsaicin, and inhibited pSNL-evoked allodynia (Fig. 13g,i). However, TRPA1 mRNA, the TRPA1/S-100 overlap, and pSNL-evoked F4/80⁺ cell infiltration and H₂O₂ generation in injured nerves were unaffected (Fig. 13h,j).

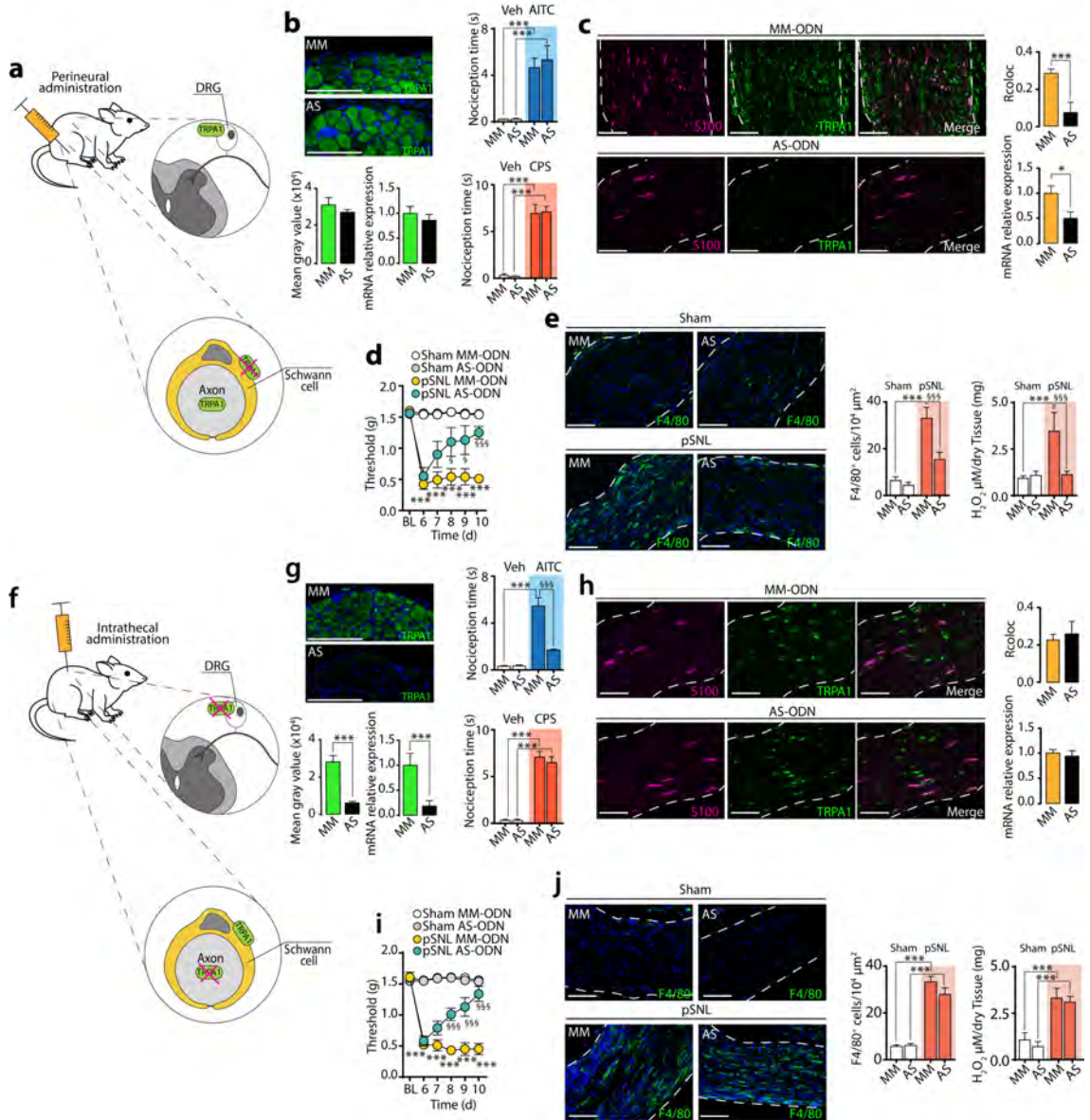


Figure 13. Oxidative stress from Schwann cell TRPA1 recruits macrophages and signal pain in C57BL/6 mice. (a,f) Schematic representation of perineural/intrathecal injection of TRPA1 antisense/mismatch oligonucleotides (AS/MM-ODN). (b,g) TRPA1 immunofluorescence (mean gray value) and TRPA1 mRNA relative expression in DRGs and acute nociception after perineural AITC (20 nmol 10 μ l⁻¹) or capsaicin (CPS, 1 nmol 10 μ l⁻¹) following perineural (10 nmol 10 μ l⁻¹) (b) or intrathecal (5 nmol 5 μ l⁻¹) (g) TRPA1 AS/MM-ODN treatment (once/day for 4 consecutive days) in C57BL/6 (n=6, ***P<0.001 MM/AS AITC, CPS vs. MM/AS veh; §§§P<0.001 AS AITC vs. MM AITC; one-way ANOVA followed by Bonferroni post hoc analyses, Scale bars: 20 μ m). (c,h) Representative images (Scale bars: 50 μ m; dashed lines, *perineurium*), (j) colocalization value (Rcoloc) of S100/TRPA1 and mRNA-TRPA1 expression in sciatic nerve after perineural (c) and intrathecal (h) AS/MM-ODN (n=6, *P<0.05; ***P<0.001 AS vs MM; unpaired two-tailed Student's t-test). (d,i) Mechanical allodynia, and (e,j) representative images, F4/80⁺-cells, and H₂O₂-content (at day 10 after surgery) in sham/pSNL mice after perineural (d,e) and intratechal (i,j) AS/MM-ODN (n=8, ***P<0.001 pSNL-MM-ODN vs. sham-MM-ODN; §P<0.05 and §§§P<0.001 pSNL-AS-ODN vs. pSNL-MM-ODN; (d,i) two-way ANOVA followed by Bonferroni post hoc analyses and (e,j) one-way ANOVA followed by Bonferroni post hoc analyses) (Scale bars: 50 μ m; dashed lines, *perineurium*). Data are represented as mean \pm s.e.m.

HC-030031 reduced the number of fluorescent macrophages accumulated at the site of pSNL by ~50% (Fig. 14a), assessed by *in vivo* imaging. Increased F4/80⁺ cells were found in the tissue surrounding the injured nerve trunk (Fig. 14b). HC-030031 or α LA reduced F4/80⁺ cells in the pSNL-injured nerve trunk and neighboring tissue, but not in perineural tissue distant from the injury site (Fig. 14b). The Schwann cell-mediated TRPA1/NOX1 pathway regulates the final stages of macrophage migration from the circulation into the injured nerve trunk, in a manner dependent on the H₂O₂ concentration gradient.

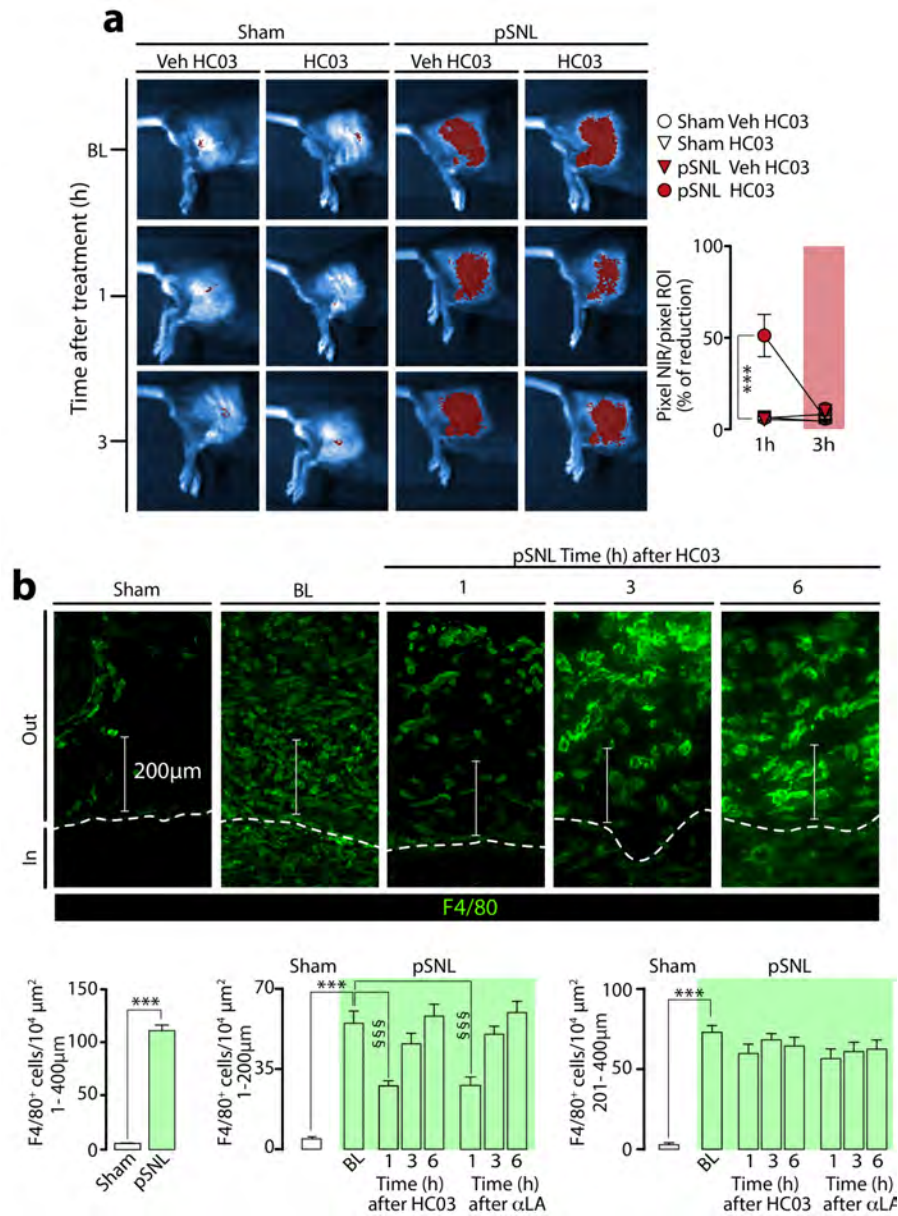


Figure 14. TRPA1 blockade and antioxidant reduced the number of fluorescent macrophages accumulated at the site of pSNL. (a) *In vivo* imaging and quantitative data (NIR area/total ROI) of NIR labeled macrophages (at day 10 after surgery) in sham/pSNL mice at baseline (BL), 1 and 3 h after HC-030031 (HC03, 100 mg kg⁻¹, i.p.) (n=4, ***P<0.001 pSNL HC03 vs. pSNL Veh HC03; two-way ANOVA followed by Bonferroni post hoc analyses). (b) Representative images and F4/80⁺-cell number surrounding the injured nerve trunk (at day 10 after surgery) of sham/pSNL-mice at BL and 1, 3 and 6 h after HC03 or alpha-lipoic acid (αLA) (both, 100 mg kg⁻¹, i.p.). (n=4, ***P<0.001 pSNL vs sham; \$\$\$P<0.001 pSNL HC03, αLA vs. pSNL veh; one-way ANOVA followed by Bonferroni post hoc analyses) (Scale bars, 200 μm; inside [in] and outside [out] sciatic nerves). Data are represented as mean±s.e.m.

To provide further support for the involvement of Schwann cell TRPA1 in orchestrating neuroinflammation and ensuing neuropathic pain in the pSNL model, we selectively deleted TRPA1 from Schwann cells. We crossed a floxed TRPA1 mouse (TRPA1^{fl/fl}) with a *Plp1-Cre/ERT* mouse in which Cre recombinase is expressed in Schwann cells/oligodendrocytes (*Plp1-Cre^{ERT};Trpa1^{fl/fl}* mice). *Plp1-Cre^{ERT};Trpa1^{fl/fl}* mice were treated with tamoxifen to induce TRPA1 deletion in Schwann cells. In *Plp1-Cre^{ERT};Trpa1^{fl/fl}* mice, the ability of intraplantar injection of AITC to evoke acute nociception was unaffected (Fig. 15a). In nerve trunks from *Plp1-Cre^{ERT};Trpa1^{fl/fl}* mice, immunoreactive TRPA1 was detected in PGP9.5⁺ nerve fibers, indicating preservation of TRPA1 expression in sensory nerve fibers (Fig 15b). In contrast, immunoreactive TRPA1 was markedly down-regulated in S100⁺ cells, but not in PGP9.5⁺ nerve fibers, confirming effective channel deletion in Schwann cells (Fig 15b). Functional confirmation of the selective conditional *Trpa1* gene knock-out was obtained by the failure of AITC to increase [Ca²⁺]_i in Schwann cells from *Plp1-Cre^{ERT};Trpa1^{fl/fl}* mice (Fig. 15c). In *Plp1-Cre^{ERT};Trpa1^{fl/fl}* mice, mechanical allodynia (Fig. 15d) and macrophage recruitment and oxidative stress (H₂O₂ generation) in the injured nerve (Fig. 15e) were markedly attenuated. Thus, tissue-selective deletion shows that Schwann cell TRPA1 promotes macrophage infiltration and oxidative stress in injured nerve trunks, whereas nociceptor TRPA1 does not contribute to neuroinflammation.

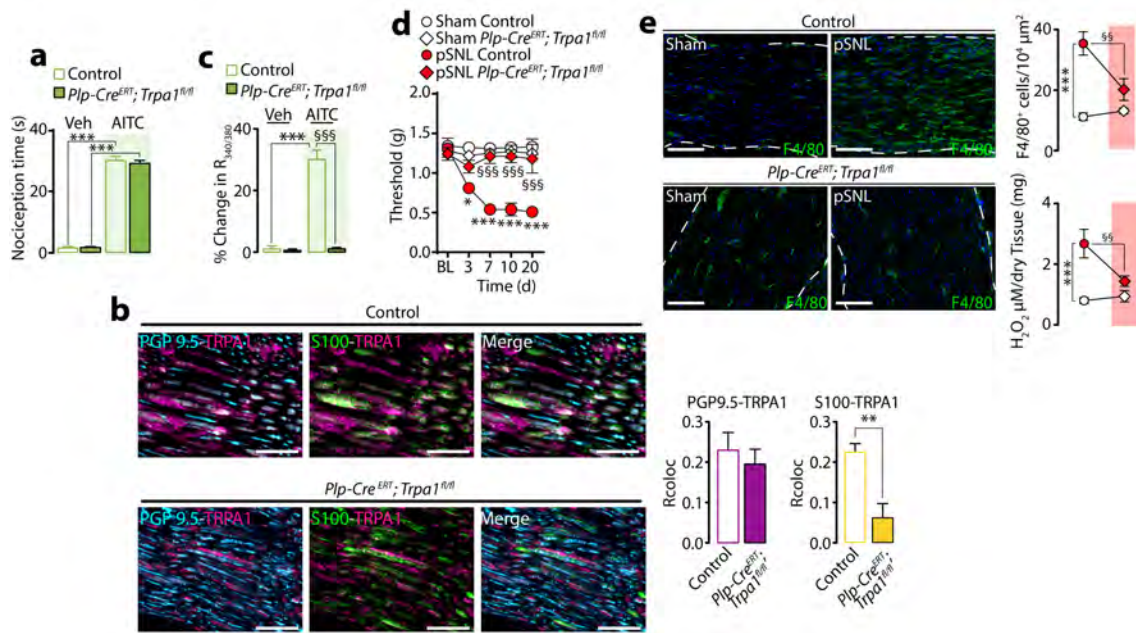


Figure 15. Plp1-Cre/ERT-mediated *Trpa1* deletion from Schwann cells prevented the partial sciatic nerve ligation (pSNL)-evoked allodynia and neuroinflammation. (a) Acute nociception response induced by intraplantar AITC (10 nmol 20 μl^{-1}) or vehicle (veh, 0.5% DMSO) in *Plp1-Cre^{ERT}; Trpa1^{fl/fl}* and control mice (n=6, ***P<0.001 AITC vs. veh; one-way ANOVA followed by Bonferroni post hoc analyses). **(b)** Triple immunofluorescence staining and colocalization value (Rcoloc) of TRPA1, PGP9.5 and S100 (Scale bars: 20 μm) in sciatic nerve trunks obtained from *Plp1-Cre^{ERT}; Trpa1^{fl/fl}* (n=5) and control mice (n=4), (**P<0.01; *Plp1-Cre^{ERT}; Trpa1^{fl/fl}* vs. control; unpaired two-tailed Student's t-test). **(c)** Ca^{2+} responses to AITC (1 mM) or vehicle (veh, 1% DMSO) in cultured Schwann cells from sciatic nerve trunks of *Plp1-Cre^{ERT}; Trpa1^{fl/fl}* and control mice (n=25 cells/2 independent experiments, ***P<0.001 AITC vs. veh; §§§P<0.001 AITC *Plp1-Cre^{ERT}; Trpa1^{fl/fl}* vs. AITC control; one-way ANOVA followed by Bonferroni post hoc analyses). **(d)** Mechanical allodynia, and **(e)** representative images, F4/80⁺-cells, and H₂O₂-content (at day 10 after surgery) in sham/pSNL *Plp1-Cre^{ERT}; Trpa1^{fl/fl}* and control mice (n=8, *P<0.05 and ***P<0.001 pSNL control vs. sham control; §§P<0.01 and §§§P<0.001 pSNL *Plp1-Cre^{ERT}; Trpa1^{fl/fl}* vs. pSNL control; **(d)** two-way ANOVA followed by Bonferroni post hoc analyses and **(e)** one-way ANOVA followed by Bonferroni post hoc analyses) (Scale bars: 50 μm). Data are represented as mean \pm s.e.m.

Steroidal and non-steroidal third-generation aromatase inhibitors induce pain-like symptoms via TRPA1

Since TRPA1 is involved in multiple painful condition, we also investigated the role of TRPA1 in pain symptoms associated with the treatment of the third-generation aromatase inhibitors (AIs), exemestane, anastrozole and, letrozole currently

recommended for adjuvant endocrine treatment for postmenopausal women diagnosed with estrogen receptor-positive breast cancer.

AIs are currently recommended for adjuvant endocrine treatment as primary, sequential, or extended therapy with tamoxifen, for postmenopausal women diagnosed with estrogen receptor-positive breast cancer (Burstein et al., 2010; Cuzick et al., 2013; Gibson et al., 2009). AIs include the steroidal exemestane and non-steroidalazole derivatives, letrozole and anastrozole, which, via a covalent (exemestane) and non-covalent (azoles) binding, inactivate aromatase, the enzyme which catalyzes the conversion of androgens to estrogens in peripheral tissue. The use of AIs is, however, associated with a series of relevant side effects which are reported in 30%-60% of treated patients (Connor et al., 2013; Mouridsen, 2006). Among these, the AI-associated musculoskeletal symptoms (AIMSS) are characterized by morning stiffness and pain of the hands, knees, hips, lower back, and shoulders. In addition to musculoskeletal pain, pain symptoms associated with AIs have recently been more accurately described with the inclusion of neuropathic, diffused, and mixed pain (Laroche et al., 2014). The whole spectrum of painful conditions has been reported to affect up to 40% of patients, and to lead 10-20% of patients to non-adherence or discontinuation of treatment (Burstein et al., 2010; Laroche et al., 2014; Mao et al., 2013). Although it has been proposed that estrogen deprivation and several other factors, including a higher level of anxiety, may contribute to the development of AIMSS and related pain symptoms, none of these hypotheses has been confirmed (Laroche et al., 2014; Sestak et al., 2008). Thus, the exact mechanism of such conditions is still unclear and, consequently, patients are undertreated.

The chemical structure of exemestane includes a system of highly electrophilic conjugated Michael acceptor groups, which might react with the thiol groups of reactive cysteine residues. Michael addition reaction with specific cysteine residues is a major mechanism that results in TRPA1 activation by a large variety of electrophilic compounds. Aliphatic and aromatic nitriles can react with cysteine to form thiazoline derivatives and accordingly the tear gas 2-chlorobenzylidene malononitrile (CS) has been identified as a TRPA1 agonist. We noticed that both letrozole and anastrozole possess nitrile moieties. Thus, we hypothesized that exemestane, letrozole and anastrozole may produce neurogenic inflammation, nociception and hyperalgesia by targeting TRPA1. Data showed that AIs directly stimulate TRPA1, and *via* this pathway provoke neurogenic inflammatory edema, acute nociception, mechanical allodynia, and reduced grip strength,

indicating a new mechanism through which AIs induce cytokine-independent inflammation and pain, and suggesting TRPA1 antagonists as possible innovative therapies for pain-like symptoms associated with the use of AIs.

Aromatase inhibitors selectively activate the recombinant human and the native rodent TRPA1 channel.

To explore whether AIs gate the human TRPA1 channel, we first used cells stably transfected with human TRPA1 cDNA (hTRPA1-HEK293). In hTRPA1-HEK293 cells, which respond to the selective TRPA1 agonist AITC (30 μ M), but not in untransfected HEK293 cells, the three AIs, exemestane, letrozole, and anastrozole evoked concentration-dependent calcium responses that were inhibited by the selective TRPA1 antagonist, HC-030031 (30 μ M) (Fig. 16a,b,c). EC₅₀ of AIs ranged between 58 and 134 μ M (Fig. 16b). The calcium response was abated in a calcium-free medium, thus supporting the hypothesis that the increase in intracellular calcium originates from extracellular sources. In HEK293 cells stably transfected with human TRPV1 cDNA (hTRPV1-HEK293) all AIs (100 μ M) were ineffective. Key aminoacid residues are required for channel activation by electrophilic TRPA1 agonists. Notably, HEK293 cells expressing a mutated TRPA1 channel (3C/K-Q), which presents substitutions of three cysteine with serine (C619S, C639S, C663S) and one lysine with glutamine (K708Q) residues, were insensitive to both AITC and all three AIs, while maintaining sensitivity to the non-electrophilic agonists, menthol or icilin (Fig. 16d). This finding supports the hypothesis that the ability of AIs to target TRPA1 derives from their electrophilic nature. Electrophysiology experiments recapitulated findings obtained by means of the calcium assay. Exemestane, letrozole, and anastrozole selectively activated a concentration-dependent inward current in hTRPA1-HEK293 cells, a response that was abated by HC-030031. AIs did not evoke any current in untransfected HEK293 cells.

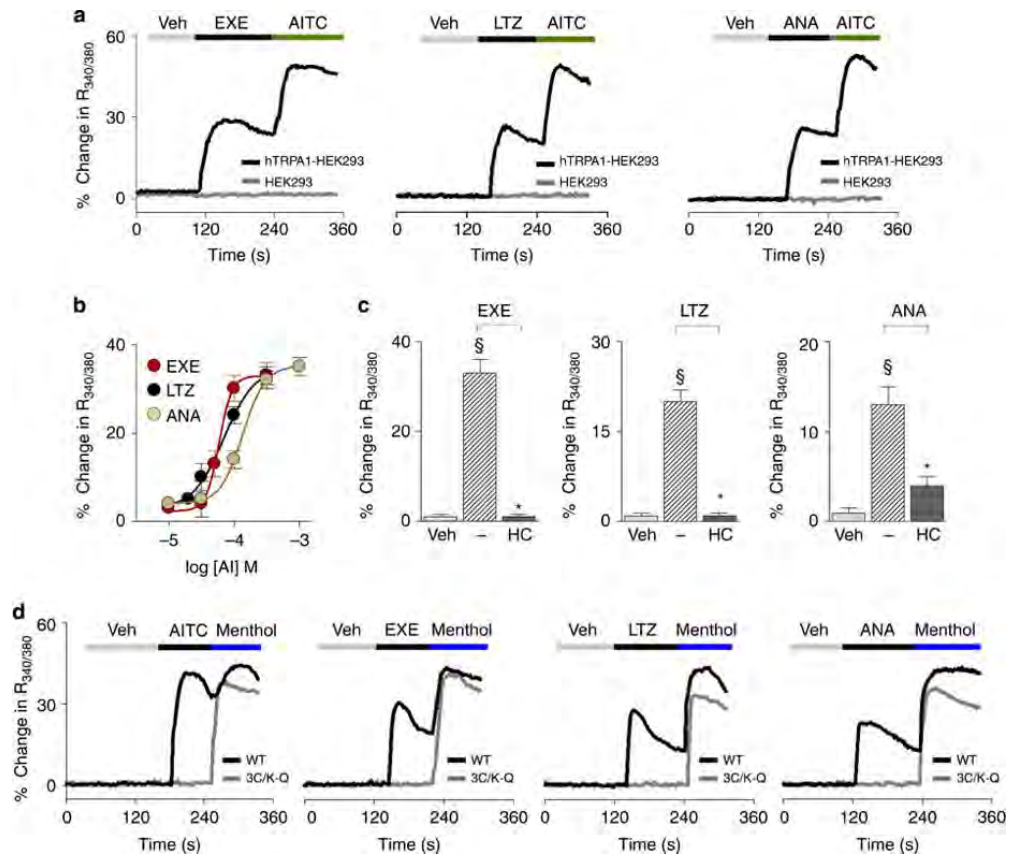


Figure 16. Exemestane (EXE), letrozole (LTZ) and anastrozole (ANA) selectively activate the human TRPA1 channel. (a) Representative traces of intracellular calcium response evoked by the aromatase inhibitors (AIs), EXE (100 μ M), LTZ (100 μ M) and ANA (100 μ M), in HEK293 cells transfected with the cDNA for human TRPA1 (hTRPA1-HEK293) which respond to the selective TRPA1 agonist, allyl isothiocyanate (AITC; 30 μ M). AITC (30 μ M), EXE, LTZ, and ANA (all 100 μ M) fail to produce any calcium response in untransfected-HEK293 cells (HEK293). (b) Concentration-response curves to EXE, LTZ and ANA, yielded EC_{50} (95% confidence interval) of 58 (46-72) μ M, 69 (43-109) μ M, and 134 (96-186) μ M, respectively. (c) AI-evoked calcium response in hTRPA1-HEK293 is abolished by the selective TRPA1 antagonist, HC-030031 (HC; 30 μ M). (d) Representative traces of cells transfected with the cDNA codifying for the mutant hTRPA1 channel (3C/K-Q), which are insensitive to AITC (30 μ M) or AIs (100 μ M), but respond to the non-electrophilic agonist, menthol (100 μ M), whereas HEK293 cells transfected with the cDNA codifying for wild type hTRPA1 (WT) respond to all the drugs. Veh is the vehicle of AIs; dash (-) indicates the vehicle of HC. Each point or column represents the mean \pm s.e.m. of at least 25 cells from 3-6 independent experiments. $^{\$}P < 0.05$ vs. Veh, $^*P < 0.05$ vs. EXE, LTZ or ANA group; ANOVA and Bonferroni *post hoc* test.

Next, to verify whether exemestane, letrozole and anastrozole stimulate nociceptive sensory neurons via TRPA1 activation, we used primary culture of both rat and mouse dorsal root ganglion (DRG) neurons. Similar to AITC, all AIs produced a concentration-dependent calcium response (Fig. 17a,b) in a proportion (about 30%) of

cells that responded to the selective TRPV1 agonist, capsaicin (0.1 μ M). All cells responding to AIs, but none of the non-responding cells, invariably responded to a subsequent high concentration of AITC (30 μ M) (Fig. 17a), further documenting TRPA1 as the target of AIs. In rat DRG neurons, EC50 ranged between 78 and 135 μ M (Fig. 17b). Calcium responses evoked by the three AIs were abated by HC-030031 (30 μ M), but were unaffected by the selective TRPV1 antagonist, capsazepine (10 μ M) (Fig. 17c). Notably, AITC and all AIs produced a calcium response in capsaicin-sensitive DRG neurons isolated from wild type (*Trpa1*^{+/+}) mice, an effect that was absent in neurons obtained from TRPA1-deficient (*Trpa1*^{-/-}) mice (Fig. 17de).

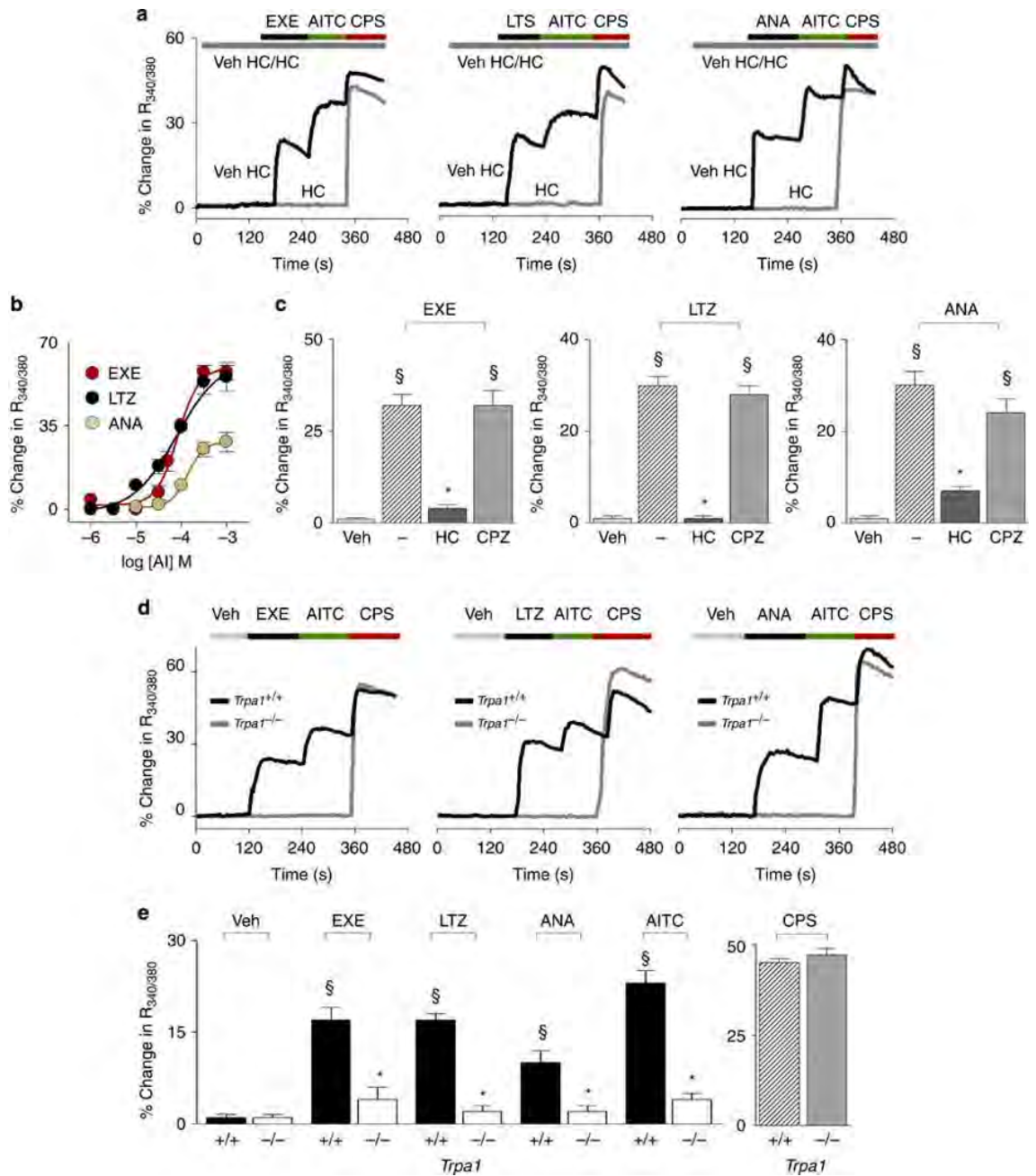


Figure 17. Exemestane (EXE), letrozole (LTZ) and anastrozole (ANA) selectively activate the native TRPA1 channel expressed in rodent dorsal root ganglion (DRG) neurons. (a) Representative traces of calcium response evoked by EXE (100 μ M), LTZ (100 μ M), ANA (300 μ M) in cultured rat DRG neurons which also respond to allyl isothiocyanate (AITC; 30 μ M) and capsaicin (CPS; 0.1 μ M). Calcium responses evoked by AIs and AITC are abolished by the selective TRPA1 antagonist, HC-030031 (HC; 30 μ M), which does not affect response to CPS. (b) Concentration-response curves of EXE, LTZ, and ANA, yielded EC_{50} (95% confidence interval) of 82 (61-108) μ M, 78 (39-152) μ M, and 135 (78-231) μ M, respectively. (c) Calcium responses induced by AIs are inhibited by HC and unaffected by the TRPV1 antagonist, capsazepine (CPZ; 10 μ M). $\$P < 0.05$ vs. Veh, $*P < 0.05$ vs. EXE, LTZ or ANA; ANOVA and Bonferroni *post hoc* test. (d) Representative traces and (e) pooled data of the calcium response evoked by EXE, LTZ, ANA (all 100 μ M) or AITC (30 μ M), in DRG neurons isolated from $Trpa1^{+/+}$ mice. Neurons isolated from $Trpa1^{-/-}$ mice do not respond to AITC, EXE, LTZ and ANA, whereas they do respond normally to CPS (0.1 μ M). $\$P < 0.05$ vs. Veh, $*P < 0.05$ vs. EXE, LTZ, ANA or AITC- $Trpa1^{+/+}$, ANOVA and Bonferroni *post hoc* test. Veh is the vehicle of AIs; dash

(-) indicates the combination of the vehicles of HC and CPZ. Each point or column represents the mean \pm s.e.m. of at least 25 neurons obtained from 3-7 independent experiments.

Local administration of exemestane and letrozole produces TRPA1-dependent acute nocifensive response and delayed mechanical allodynia.

It has been well documented that local exposure to TRPA1 agonists in experimental animals is associated with an immediate nociceptive response, lasting for a few minutes, and a delayed more prolonged mechanical allodynia (Bautista et al., 2006; Trevisani et al., 2007). To investigate whether AIs activate such a nociceptive and hyperalgesic TRPA1-dependent pathway, we used one steroidal (exemestane) and one non-steroidal (letrozole) AI. Given the chemical similarity and the hypothesized analogous mechanism of the two non-steroidal AIs, to minimize the number of animals used, anastrozole was not investigated in the following in vivo experiments. Intraplantar (i.pl.) injection (20 μ l/paw) of exemestane (1, 5, and 10 nmol) or letrozole (10, 20 nmol) evoked an acute (0-5 min) nociceptive response and a delayed (15-120 min for exemestane and 15-240 min for letrozole) mechanical allodynia in C57BL/6 mice. Both the nociceptive response and mechanical allodynia evoked by AIs were confined to the treated paw and were almost completely prevented by intraperitoneal (i.p.) pretreatment with HC-030031 (100 mg/kg), but not with capsazepine (4 mg/kg). Furthermore, similar to results obtained in C57BL/6 mice, local injection (i.pl.) of exemestane or letrozole in *Trpa1*^{+/+} mice evoked an early nociceptive response and a delayed mechanical allodynia. *Trpa1*^{-/-} mice did not develop such responses. Thus, by using both pharmacological and genetic tools, we demonstrated that local administration of both steroidal and non-steroidal AIs produces a typical TRPA1-dependent behavior, characterized by acute nociception and delayed mechanical allodynia.

Exemestane and letrozole produce neurogenic edema by releasing sensory neuropeptides

TRPA1 is expressed by peptidergic nociceptors, and its stimulation is associated with proinflammatory neuropeptide release and the ensuing neurogenic inflammatory responses. First, we explored whether AIs are able to directly promote the release of CGRP (one of the proinflammatory neuropeptides, which are usually co-released upon

stimulation of peptidergic nociceptors) *via* a TRPA1-dependent pathway. AIs increased CGRP outflow from slices of rat dorsal spinal cord (an anatomical area enriched with central terminals of nociceptors). This effect was substantially attenuated in rat slices pretreated with a desensitizing concentration of capsaicin (10 μ M, 20 min) or in the presence of HC-030031 (Fig. 18a). The increase in CGRP outflow observed in slices obtained from *Trpa1*^{+/+} mice was markedly reduced in slices obtained from *Trpa1*^{-/-} mice (Fig. 3b).

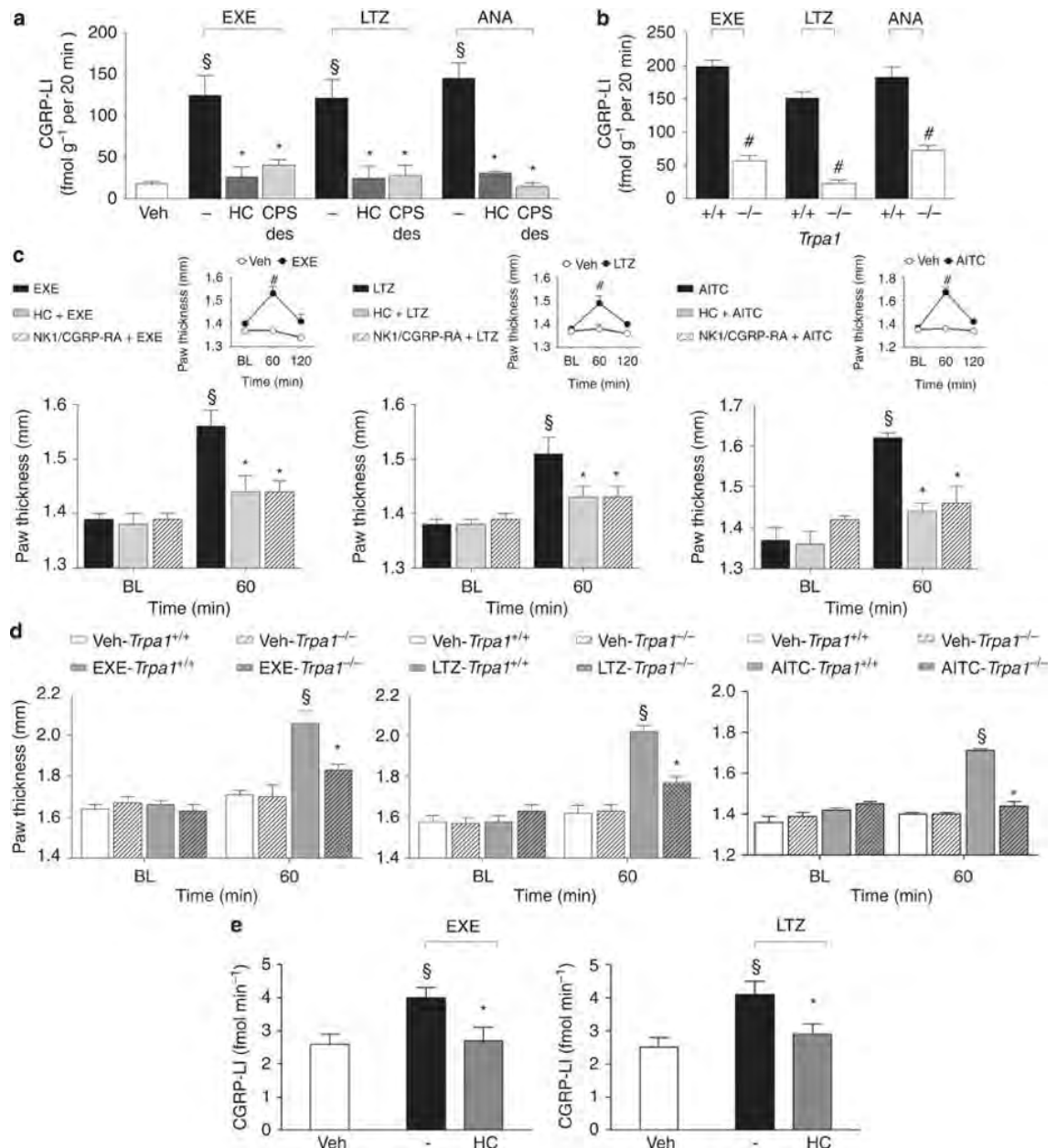


Figure 18. Aromatase inhibitors release calcitonin gene-related peptide (CGRP) and produce neurogenic edema. (a) Exemestane (EXE), letrozole (LTZ) and anastrozole (ANA) (all

100 μ M) increase the CGRP-like immunoreactivity (CGRP-LI) outflow from slices of rat dorsal spinal cord. This effect is prevented by HC-030031 (HC; 30 μ M) or after exposure to capsaicin (10 μ M, 20 minutes; CPS-des). **(b)** EXE, LTZ and ANA (all 100 μ M) increase the CGRP-LI outflow from spinal cord slices obtained from *Trpa1*^{+/+}, but not from *Trpa1*^{-/-} mice. Results are mean \pm s.e.m. of at least 4 independent experiments. Veh is the vehicle of EXE, LTZ and ANA, dash (-) indicates the vehicle of HC and CPS. $^{\S}P < 0.05$ vs. Veh, $^*P < 0.05$ vs. EXE, LTZ or ANA; ANOVA followed by Bonferroni *post hoc* test. $^{\#}P < 0.05$ vs. EXE-, LTZ-, ANA-*Trpa1*^{+/+}, Student's T test. **(c)** In C57BL/6 mice intraplantar (i.pl.) injection (20 μ l) of EXE (10 nmol), LTZ (20 nmol) or allyl isothiocyanate (AITC; 10 nmol) induces paw edema, which peaks at 60 minutes and fades 120 minutes after injection (**c**, upper insets), and is attenuated by pretreatment with HC (100 mg/kg intraperitoneal, i.p.) or the combination of the selective antagonists of the neurokinin-1 receptor, (NK1-RA), L-733,060, and of the CGRP receptor (CGRP-RA), CGRP8-37, (both, 2 μ mol/kg, intravenous). **(d)** Paw edema induced by EXE, LTZ and AITC (i.pl.) in *Trpa1*^{+/+} mice is markedly reduced in *Trpa1*^{-/-} mice. BL, baseline level. Results are mean \pm s.e.m. of at least 5 mice for each group. Veh is the vehicle of EXE, LTZ and AITC. $^{\#}P < 0.05$ vs. Veh, Student's T test; $^{\S}P < 0.05$ vs. BL values, $^*P < 0.05$ vs. EXE, LTZ, AITC or EXE-, LTZ-, AITC-*Trpa1*^{+/+}; ANOVA followed by Bonferroni *post hoc* test. **(e)** Injection (50 μ l) of EXE (5 nmol) or LTZ (10 nmol) in the rat knee increases CGRP-LI levels in the synovial fluid, an effect that is markedly attenuated by pretreatment with HC (100 mg/kg, i.p.). Results are mean \pm s.e.m. of at least 5 mice for each group. Veh is the vehicle of EXE and LTZ, dash (-) indicates the vehicle of HC. $^{\S}P < 0.05$ vs. Veh, $^*P < 0.05$ vs. EXE, LTZ; ANOVA followed by Bonferroni *post hoc* test.

These neurochemical data were corroborated by functional experiments. Injection (i.pl.) of the TRPA1 agonist, AITC (10 nmol/paw), induced paw edema that peaked at 60 min after injection. The response was abated by treatment with HC-030031 (100 mg/kg, i.p.) or a combination of the SP neurokinin-1 (NK-1) receptor antagonist, L-733,060, and the CGRP receptor antagonist, CGRP8-37 (both, 2 μ mol/kg, intravenous, i.v.) (Fig. 18c). Similarly, we found that i.pl. administration of exemestane (10 nmol/paw) and letrozole (20 nmol/paw) caused paw edema that peaked at 60 minutes and faded 120 minutes after injection (Fig. 3c, insets). Treatment with HC-030031 (100 mg/kg, i.p.) or a combination of L-733,060 and CGRP8-37 (both, 2 μ mol/kg, i.v.), markedly reduced the AI-evoked edema (Fig. 18c). No edema was found in the paw contralateral to that injected with AIs. Importantly, the edema produced in *Trpa1*^{+/+} mice by exemestane and letrozole was markedly attenuated in *Trpa1*^{-/-} mice (Fig. 18d). Next, to directly evaluate the ability of AIs to release CGRP from peripheral terminals of peptidergic nociceptors, AIs were administered to the rat knee joint. Intraarticular (i.a., 50 μ l) injection of exemestane (5 nmol) or letrozole (10 nmol) increased CGRP levels in the synovial fluid, an effect that was markedly attenuated by pretreatment with HC-030031 (100 mg/kg, i.p.) (Fig. 18e). Neurochemical and functional data indicate that AIs by TRPA1 activation release sensory

neuropeptides from sensory nerve endings, and by this mechanism promote neurogenic inflammatory responses in the innervated peripheral tissue.

Systemic exemestane and letrozole induce prolonged pain-like effects by targeting TRPA1.

AIs are given to patients by a systemic route of administration. Therefore, we explored in mice whether intraperitoneal (i.p.) or intragastric (i.g.) administration of exemestane and letrozole could produce pain-like effects via TRPA1 activation. For i.p. administration experiments, doses, corresponding to those used in humans, were selected according to the mouse to human conversion factor indicated by the National Institute of Health (Reagan-Shaw et al., 2008). Exemestane (5 mg/kg, i.p.) or letrozole (0.5 mg/kg, i.p.) injection did not produce any visible nociceptive behavior in mice. However, 3 hours after exemestane or letrozole administration, mice developed a prolonged (3 hours) mechanical allodynia and a reduction in forelimb grip strength, a test used in its clinical version for the study of musculoskeletal pain in patients (Lintermans et al., 2011). When mechanical allodynia by exemestane or letrozole was at its maximum, systemic HC-030031 administration (100 mg/kg, i.p.) transiently reverted both responses. Furthermore, mechanical allodynia and the reduction in forelimb grip strength produced by exemestane and letrozole in *Trpa1*^{+/+} mice were markedly reduced in *Trpa1*^{-/-} mice. In experiments where AIs were given by intragastric (i.g.) gavage, doses were adjusted considering the oral bioavailability in humans, which is 99% for letrozole (Jin et al., 2012), and 40% (with food) for exemestane (Jukanti et al., 2011). First, we found that after i.g. administration of exemestane (10 mg/kg) or letrozole (0.5 mg/kg) their peak plasma levels (13.2 ± 1.7 ng/ml, n=5; and 60.5 ± 12.1 ng/ml, n=5, respectively) approximated the maximum plasma concentrations found in humans. Second, results similar to those obtained after i.p. administration were reported when AIs were given by i.g. gavage. First, exemestane (10 mg/kg, i.g.) or letrozole (0.5 mg/kg, i.g.) ingestion was not associated with any spontaneous nocifensor behavior (Fig. 4a and 5a, insets). Second, exemestane or letrozole produced, with a similar time-course, mechanical allodynia and a marked reduction in forelimb grip strength (Fig. 19a,c and Fig. 20a,c). Pretreatment with HC-030031 or deletion of TRPA1 (*Trpa1*^{-/-} mice) significantly attenuated both responses (Fig. 19b,d,e,f and Fig. 5b,d,e,f).

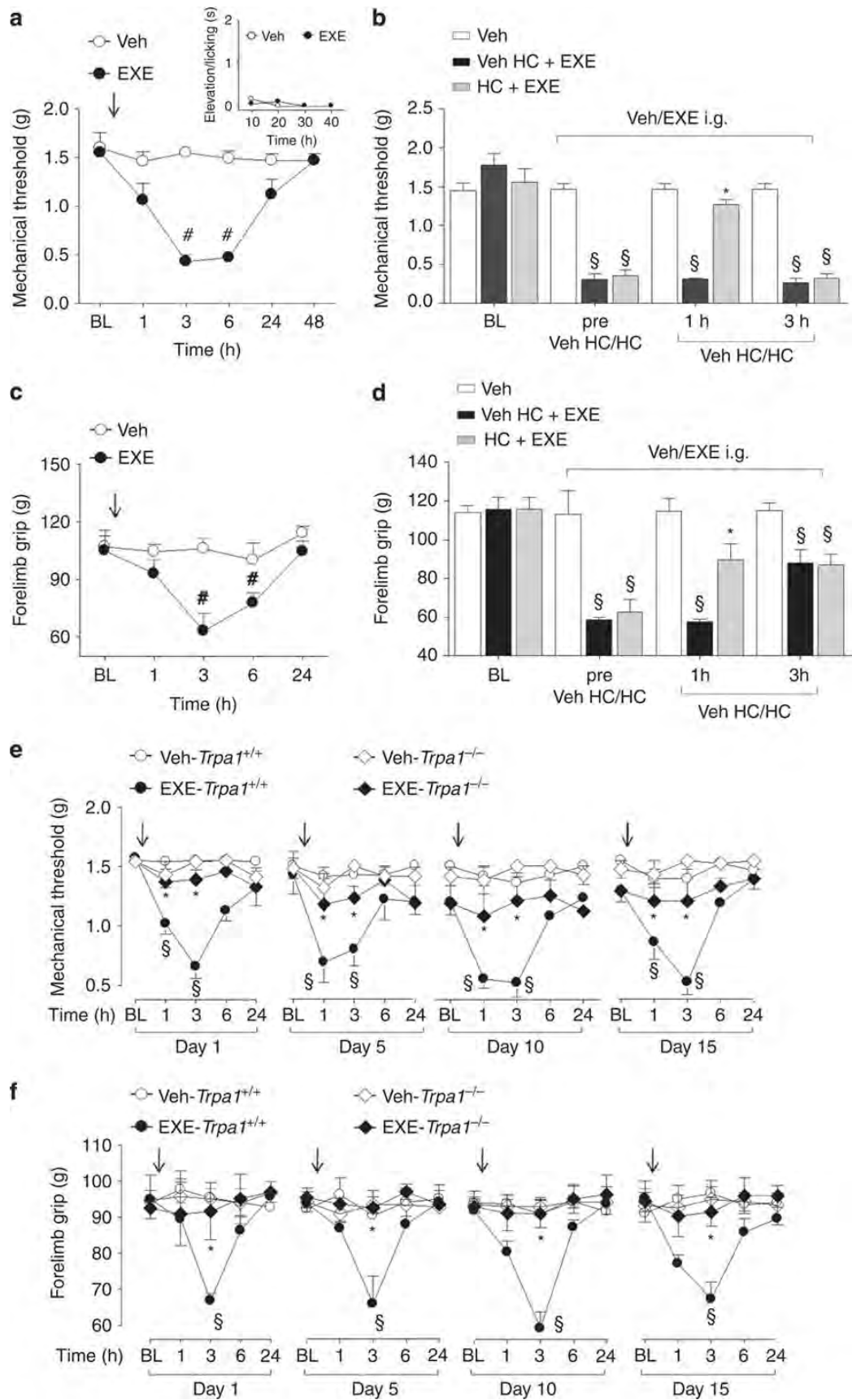


Figure 19. Intra-gastric exemestane (EXE) induces TRPA1-dependent prolonged mechanical allodynia and reduction in forelimb grip strength in mice. In C57BL/6 mice intra-gastric (i.g.) administration of EXE (10 mg/kg) induces (a) mechanical allodynia and (c) a

reduction in forelimb grip strength that last 3-6 hours after administration. EXE does not produce any acute nocifensor behavior as measured by the indicated test (**a**, inset). (**b,d**) Three hours after EXE administration, HC-030031 (HC; 100 mg/kg i.p.) reverts both mechanical allodynia and the reduction in forelimb grip strength. HC inhibition is no longer visible 3 hours after its administration. Veh is the vehicle of EXE. [#] $P < 0.05$ vs. Veh; Student's T test (**a,c**) and [§] $P < 0.05$ vs. Veh and ^{*} $P < 0.05$ vs. Veh HC-EXE; ANOVA followed by Bonferroni *post hoc* test (**b,d**). (**e,f**) EXE (once a day for 15 consecutive days, 10 mg/kg i.g.) induces reproducible mechanical allodynia and decrease in forelimb grip strength at day 1, 5, 10 and 15 in *Trpa1*^{+/+} mice. Arrows indicate Veh or EXE administration. Both these effects are markedly reduced in *Trpa1*^{-/-} mice. [§] $P < 0.05$ vs. Veh-*Trpa1*^{+/+}, ^{*} $P < 0.05$ vs. EXE-*Trpa1*^{+/+}; ANOVA followed by Bonferroni *post hoc* test. Results are mean \pm s.e.m. of at least 5 mice for each group. In all conditions, baseline (BL) levels were recorded 30 minutes before EXE administration.

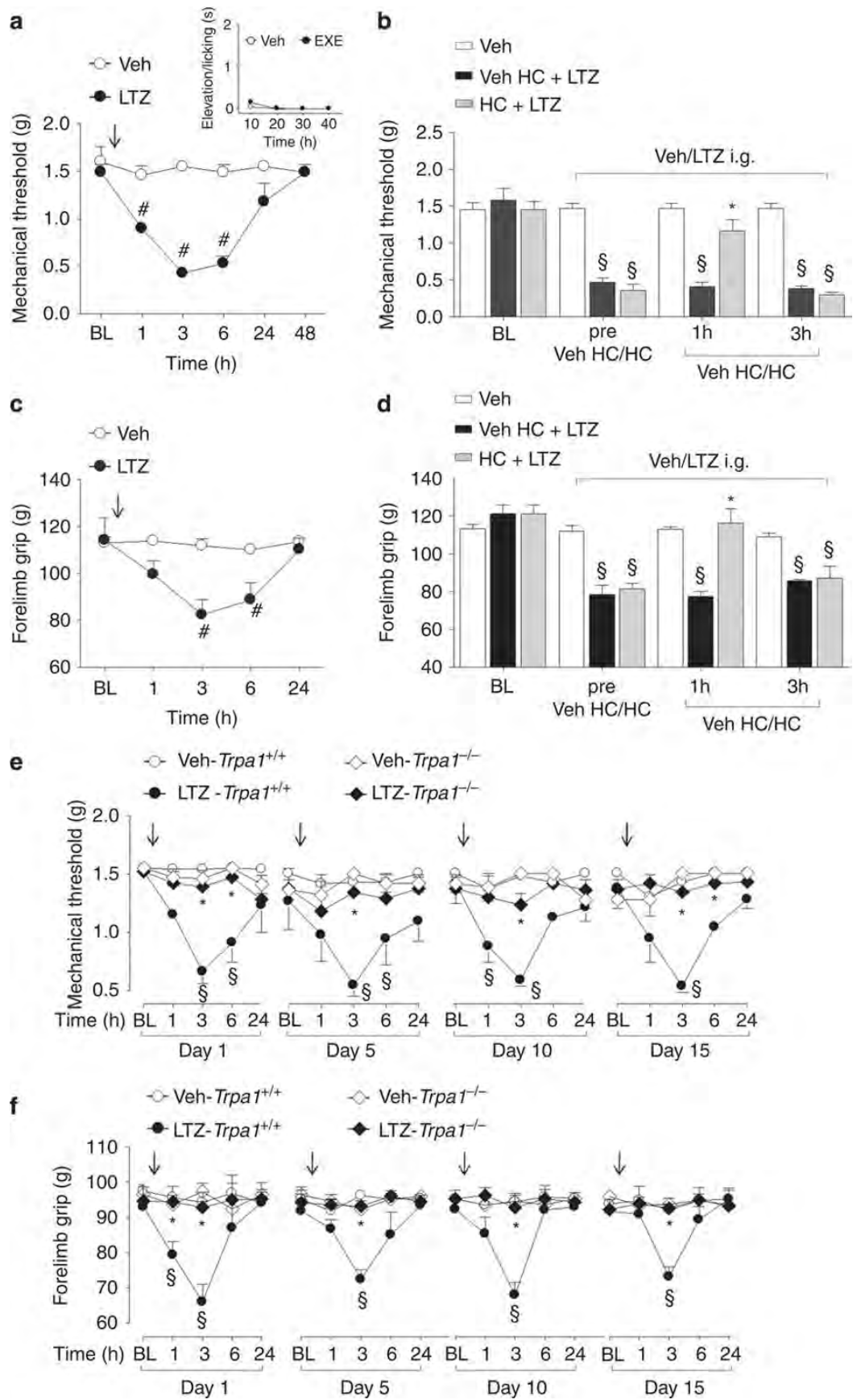


Figure 20. Intra-gastric letrozole (LTZ) induces TRPA1-dependent prolonged mechanical allodynia and reduction in forelimb grip strength in mice. In C57BL/6 mice intra-gastric (i.g.)

administration of LTZ (0.5 mg/kg) induces (a) mechanical allodynia and (c) reduction in forelimb grip strength that last 3-6 hours after administration. LTZ does not produce any acute nocifensor behavior as measured by the indicated test (a, inset). (b,d) Three hours after LTZ administration, HC-030031 (HC; 100 mg/kg i.p.) reverts both mechanical allodynia and the reduction in forelimb grip strength. HC inhibition is no longer visible 3 hours after its administration. Veh is the vehicle of LTZ. [#]*P*<0.05 vs. Veh; Student's T test (a,c) and [§]*P*<0.05 vs. Veh and **P*<0.05 vs. Veh HC-LTZ; ANOVA followed by Bonferroni *post hoc* test (b,d). (e,f) LTZ (once a day for 15 consecutive days, 0.5 mg/kg i.g.) induces reproducible mechanical allodynia and decrease in forelimb grip strength at day 1, 5, 10 and 15 in *Trpa1*^{+/+} mice. Arrows indicate Veh or LTZ administration. Both effects are markedly reduced in *Trpa1*^{-/-} mice. [§]*P*<0.05 vs. Veh-*Trpa1*^{+/+}, **P*<0.05 vs. LTZ-*Trpa1*^{+/+}; ANOVA followed by Bonferroni *post hoc* test. Results are mean ± s.e.m. of at least 5 mice for each group. In all conditions baseline (BL) levels were recorded 30 minutes before LTZ administration.

Furthermore, since in clinical practice patients are treated with AIs on a daily basis over very long periods of time (up to 5 years), we asked whether exemestane or letrozole maintain the ability to evoke a TRPA1-dependent mechanical hypersensitivity and decreased grip strength upon repeated administration. In *Trpa1*^{+/+} mice, treatment with systemic exemestane (5 mg/kg, i.p.) or letrozole (0.5 mg/kg i.p) (both once a day for 15 consecutive days) produced at day 1, 5, 10 and 15 a transient (from 1 to 6 hours) and reproducible mechanical allodynia. Importantly, in *Trpa1*^{-/-} the proalgesic action of AIs was markedly attenuated. In addition, the decrease in the grip strength was maintained, without undergoing desensitization, over the entire time period of daily i.p. administration of exemestane or letrozole. Both these effects of AIs were significantly reduced in *Trpa1*^{-/-} mice. Similar results were obtained after i.g. administration of exemestane or letrozole (once a day for 15 consecutive days at the dose of 10 mg/kg i.g. or 0.5 mg/kg i.g., respectively). Both mechanical allodynia and decreased grip strength were observed, without signs of desensitization, over the 15 days of observation in *Trpa1*^{+/+} mice, but were markedly reduced in *Trpa1*^{-/-} mice (Fig. 19e,f and Fig. 20e,f). Altogether, the present data demonstrate that both steroidal and non-steroidal third-generation AIs induce a series of pain-like effects predominantly via a TRPA1-dependent mechanism, effects that over time do not undergo desensitization, thus mimicking the chronic clinical condition.

Exemestane- and letrozole-evoked TRPA1 activation is enhanced by proinflammatory stimuli.

Although it affects a large proportion of subjects, not all patients treated with AIs develop AIMSS. One possible explanation for the peculiar susceptibility to AIMSS of

some patients is that, if TRPA1 activation is a necessary prerequisite, per se it is not sufficient, and additional proalgesic factors must contribute to the development of pain symptoms. It has been reported that stimulation of proalgesic pathways exaggerates TRPA1-dependent responses in vitro and in vivo (Dai et al., 2007; Wang et al., 2008). One example of such potentiating action has been reported for the proteinase-activated receptor-2 (PAR2), whose subthreshold activation results in an exaggerated response to the TRPA1 agonist, AITC (Dai et al., 2007). PAR2 undergoes activation upon a unique proteolytic mechanism by cleavage of its tethered ligand domain by trypsin and other proteases, thus mediating inflammation and hyperalgesia (Vergnolle et al., 2001). On this basis, and following a previously reported protocol (Dai et al., 2007), we explored, by in vivo functional experiments in C57BL/6 mice, whether PAR2 activation exaggerates TRPA1-dependent hypersensitivity induced by AIs. Prior (10 minutes) injection (i.pl.) of the PAR2 activating peptide (AP) (PAR2-AP, 1 µg/paw), but not the reverse peptide (RP) (PAR2-RP, 1 µg/paw, inactive on PAR2), markedly enhanced the duration of licks and flinches of the hind paw produced by local injection (i.pl.) of exemestane (1 nmol/paw) and letrozole (10 nmol/paw) (Fig. 21a). The injected dose of PAR2-AP, as well as PAR2-RP, did not cause per se any visible acute nocifensor response (Fig.21a). The exaggerated responses to the combination of PAR2-AP and exemestane or letrozole were inhibited by HC-030031 (100 mg/kg, i.p.) (Fig. 21a).

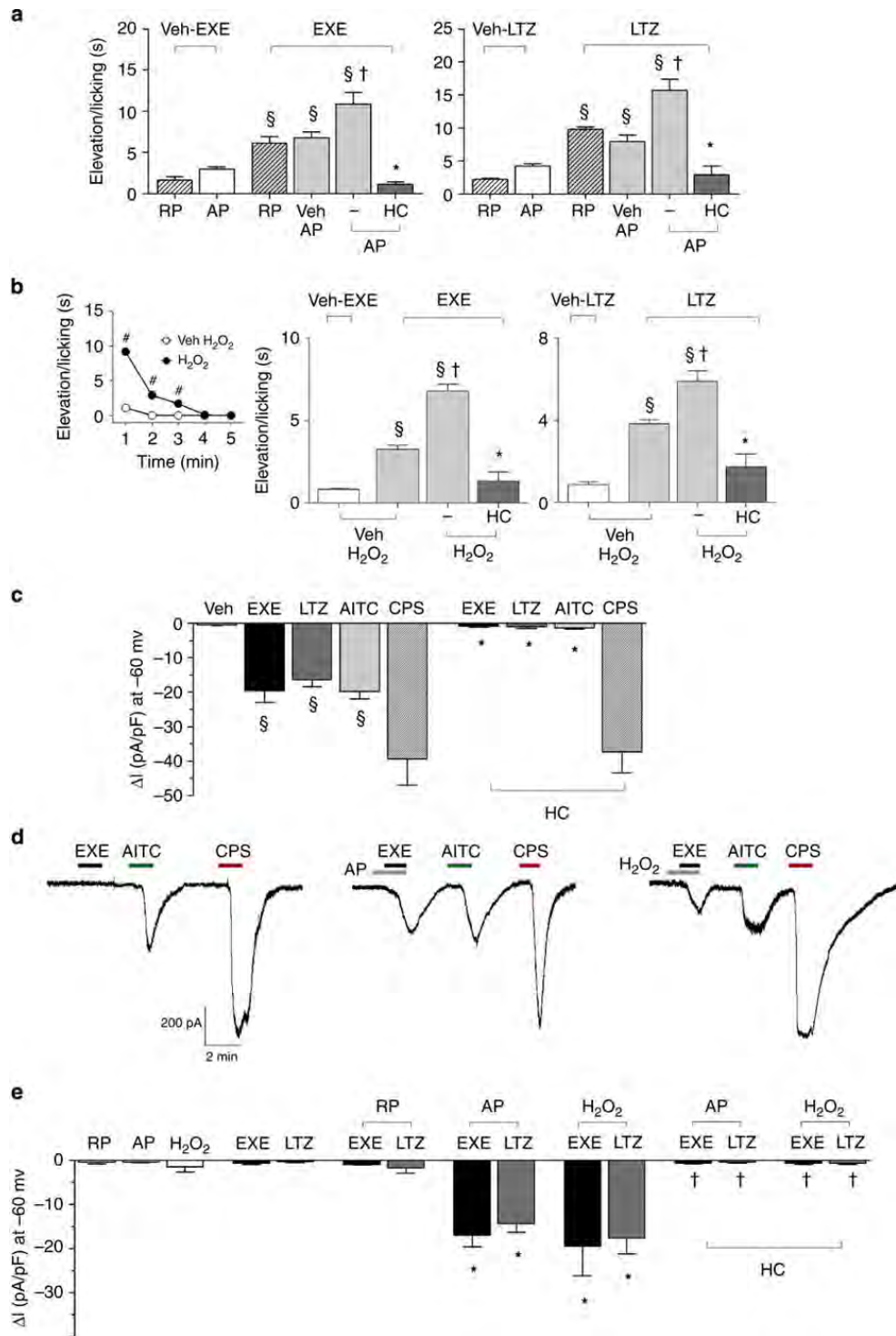


Figure 21. TRPA1-activation by exemestane (EXE) and letrozole (LTZ) is enhanced by proinflammatory stimuli. (a) Intraplantar (i.pl.; 10 μ l) pretreatment (10 minutes) with the proteinase-activated receptor 2 (PAR2) activating peptide (AP; 1 μ g), but not with the inactive PAR2 reverse peptide (RP; 1 μ g), enhances nocifensor behavior produced by EXE (1 nmol/10 μ l, i.pl.) or LTZ (10 nmol/10 μ l, i.pl.). AP and RP alone cause negligible nociception. The potentiated responses to EXE or LTZ are markedly attenuated by HC-030031 (HC; 100 mg/kg, i.p.). (b) H_2O_2 (0.5 μ mol/10 μ l, i.pl.) injection produces a transient nocifensor behavior, lasting only 5 minutes (b, inset). Pretreatment (10 minutes before AI administration) with H_2O_2 (0.5 μ mol/10 μ l, i.pl.) increases nocifensor behavior produced by EXE (1 nmol/10 μ l, i.pl.) or LTZ (10 nmol/10 μ l, i.pl.). HC (100 mg/kg, i.p.) inhibits the exaggerated responses to both EXE and LTZ. Dash (-)

indicates the vehicle of HC. Points or columns are mean \pm s.e.m. of at least 5 mice for each group. $^{\S}P < 0.05$ vs. RP or AP or Veh H₂O₂; $^{\dagger}P < 0.05$ vs. Veh AP/EXE or Veh AP/LTZ or Veh H₂O₂/EXE or Veh H₂O₂/LTZ; $^{*}P < 0.05$ vs. AP/EXE or AP/LTZ or H₂O₂/EXE or H₂O₂/LTZ; ANOVA followed by Bonferroni *post hoc* test. $^{\#}P < 0.05$ vs. Veh H₂O₂, Student's T test. (c) An active concentration of EXE or LTZ (both 100 μ M) evokes inward currents in rat dorsal root ganglion (DRG) neurons, which also respond to allyl isothiocyanate (AITC; 100 μ M) and capsaicin (CPS; 1 μ M). Inward currents evoked by EXE, LTZ or AITC are inhibited in the presence of HC (50 μ M), which does not affect CPS-evoked currents. Typical traces (d) and pooled data (e) showing that pre-exposure to AP (100 μ M) or H₂O₂ (100 μ M) exaggerates currents evoked by a subthreshold concentration of EXE and LTZ (both 20 μ M). The inactive RP does not affect responses to EXE or LTZ (both 20 μ M). The potentiated responses to EXE or LTZ are markedly attenuated by HC (50 μ M). Veh is the vehicle of EXE, LTZ and AITC. Results are mean \pm s.e.m. of at least 5 independent experiments. $^{\S}P < 0.05$ vs. Veh, $^{*}P < 0.05$ vs. EXE, LTZ or AITC and $^{\dagger}P < 0.05$ vs. EXE- or LTZ-AP and EXE- or LTZ-H₂O₂; ANOVA followed by Bonferroni *post hoc* test.

We also tested the ability of a recognized endogenous TRPA1 agonist, H₂O₂ to increase the nocifensor response of exemestane or letrozole. In addition, we explored the ability of AIs to increase either nociception or mechanical allodynia to H₂O₂. H₂O₂ (0.5 μ mol/paw) injection produced a transient nocifensor behavior that terminated within 5 min (Fig. 21b, inset). We found that 10 min after H₂O₂ injection (when baseline levels of nociception were restored) administration of exemestane (1 nmol/paw) and letrozole (10 nmol/paw) evoked nociceptive responses markedly increased as compared to vehicle-pretreated mice (Fig. 21b). The exaggerated responses to AIs were inhibited by HC-030031 (Fig. 21b). Thus, both homologous activation of the channel by the TRPA1 agonist H₂O₂, or heterologous stimulation of a classical proinflammatory pathway, such as PAR2, converge in a final common pathway, which results in the potentiation of the AI-evoked and TRPA1-dependent proalgesic mechanism. In the attempt to understand the mechanism underlying the *in vivo* potentiation between PAR2 or H₂O₂ and AIs, cultured DRG neurons were challenged with combinations of these same agents. First, in *in vitro* electrophysiological experiments, we found that AITC, exemestane and letrozole (all 100 μ M) produced inward currents in cultured DRG neurons, effects that were abated in the presence of HC-030031 (50 μ M). However, HC-030031 did not affect the inward current produced by capsaicin (Fig. 21c). Second, we showed that pre-exposure to subthreshold concentrations of PAR2-AP or H₂O₂ enhanced currents evoked by subthreshold concentrations of either exemestane or letrozole (both 20 μ M) (Fig. 21de). Third, HC-030031 inhibited the exaggerated responses (Fig 21e).

TRPA1 mediates aromatase inhibitor-evoked pain by the aromatase substrate androstenedione

AIs block the activity of aromatase cytochrome P450, an almost ubiquitous enzyme, which, however, rather selectively transforms the androgens, androstenedione and testosterone into the estrogens (estrone and 17 β -estradiol, respectively), responsible for cancer cell replication and growth. Unfortunately, one-third of patients treated with AIs develop muscular and joint pain and inflammation (aromatase inhibitor-associated musculoskeletal symptoms, AIMSS) (Crew et al., 2007; Henry et al., 2008), and also exhibit symptoms of neuropathic or mixed pain (Laroche et al., 2014). AIMSS and the associated forms of pain represent a major medical problem because they affect the quality of life of the patients, thus limiting treatment adherence, and sometimes leading to therapy discontinuation. Furthermore, AIMSS respond poorly to current analgesic therapies, and the therapeutic needs of the patients remain unmet. We reported that TRPA1, mediates the entire constellation of pain-like behaviors evoked by AIs in mice.

However, AI concentrations required for TRPA1 gating in vitro are 1-2 order of magnitude higher than those found in patient plasma (Desta et al., 2011). In addition, an important proportion (30-40%), but not all, of treated patients develop the painful condition (Presant et al., 2007; Sestak et al., 2008). These observations suggest that the sole exposure to AIs is necessary, but not sufficient, to produce AIMSS, and that additional factors should cooperate with AIs to promote pain symptoms.

Aromatase inhibition, while reducing downstream production of estrogens, moderately increases upstream plasma concentrations of androgens, including androstenedione (Gallicchio et al., 2011). Exemestane, a false aromatase substrate, blocks enzymatic activity by accommodating in the binding pocket that snugly encloses androstenedione (Ghosh et al., 2009). We reasoned that androstenedione, which retains some of the reactive chemical features of exemestane, such as the α,β -carbonyl moiety of the A ring and the ketone group at the 17 position, might target TRPA1.

Androstenedione selectively activates the recombinant and native human TRPA1 by targeting key electrophilic amino acid residues

We first explored whether androstenedione targets the human TRPA1 channel by using HEK293 cells transfected with the cDNA for the human TRPA1 (hTRPA1-HEK293). In hTRPA1-HEK293 cells, but not in untransfected HEK293 cells, androstenedione evoked calcium responses in a concentration-dependent manner (EC_{50} , 49 μ M) (Fig. 22A). Responses to both androstenedione and the TRPA1 agonist, AITC, were abrogated by the selective TRPA1 antagonist, HC-030031 (Fig. 22B). Consistently, hTRPA1-HEK293 cells superfused with androstenedione elicited concentration-dependent inward currents, an effect blocked by HC-030031 (Fig. 22C) and absent in untransfected HEK293 cells (Fig. 22D). In HEK293 cells transfected with the cDNA for the human TRPV1 (hTRPV1-HEK293) and in HEK293 cells transfected with the cDNA for the human TRPV4 (hTRPV4-HEK293), activated by the selective TRPV1 agonist, capsaicin, or the selective TRPV4 agonist, GSK1016790A, respectively, androstenedione failed to evoke calcium responses or inward currents (Fig. 22E and 22F). Notably, HEK293 cells expressing a mutated TRPA1 channel (hTRPA1 3C/K-Q HEK293 cells) with substitutions of three cysteine with serine (C619S, C639S, C663S) and one lysine with glutamine (K708Q) residues, did not respond to AITC or androstenedione, while they did respond to the non-electrophilic TRPA1 agonist, menthol (Fig. 22G).

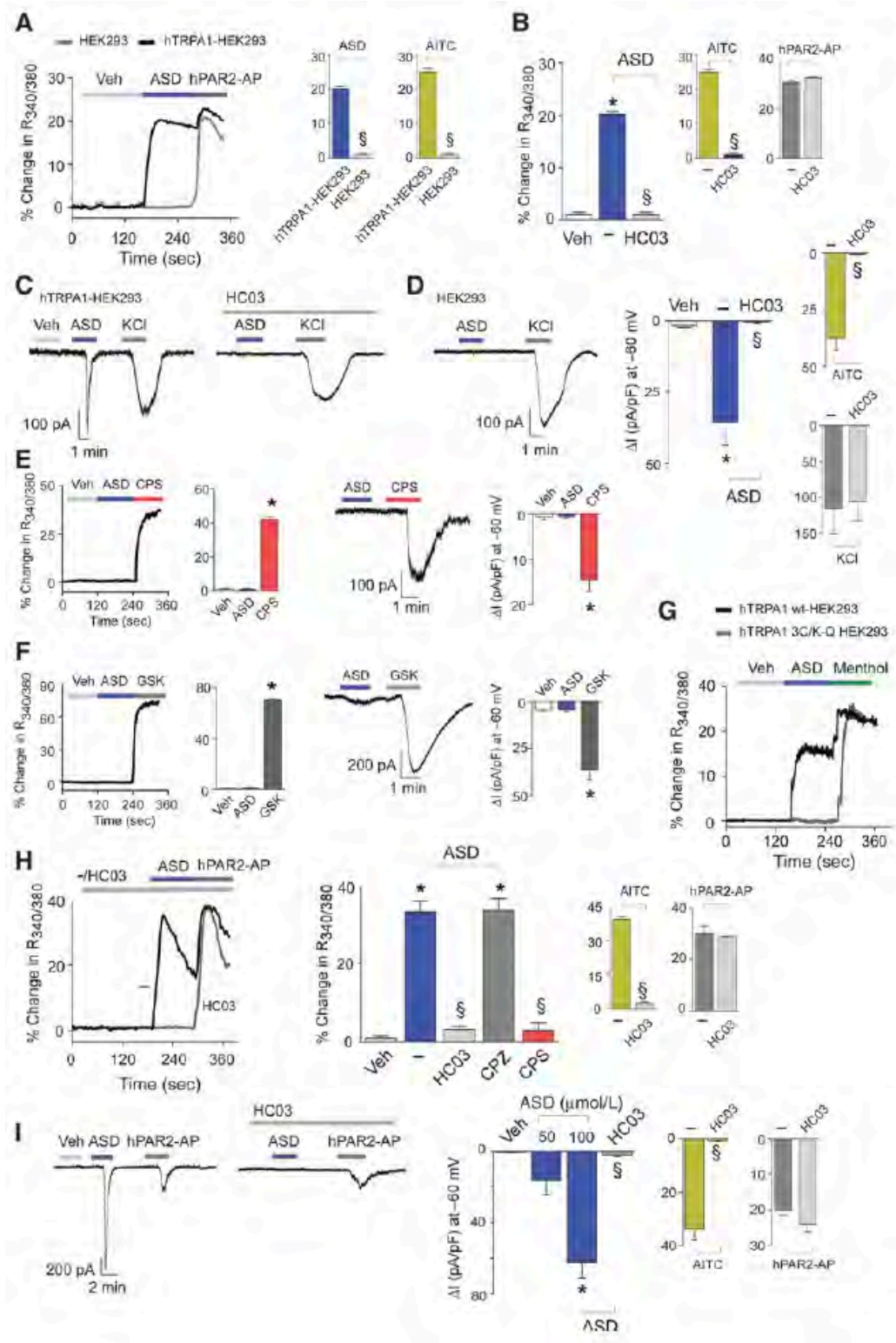


Figure 22. ASD selectively activates the human TRPA1 channel. A, calcium response evoked by ASD (100 μ M), AITC (5 μ M) and hPAR2-AP (100 μ M) in hTRPA1-HEK293 and in HEK293 cells. B, HC-030031 (HC03; 30 μ M) abates the response to both ASD and AITC, but not to hPAR2-AP. C and D, ASD (50 μ M) or AITC (100 μ M), elicit inward currents in hTRPA1-HEK293, but not in HEK293 cells. HC03 (50 μ M) does not affect responses to KCl (50 mM), but

abolishes responses to either ASD or AITC. E and F, ASD (100 μ M) is ineffective in hTRPV1-HEK293, activated by capsaicin (CPS; 0.1 μ M), and in hTRPV4-HEK293, activated by GSK1016790A (GSK; 0.1 μ M). G, hTRPA1 3C/K-Q HEK293 are insensitive to ASD (100 μ M), but respond to menthol (100 μ M), whereas wt-hTRPA1 respond to both compounds. H, IMR90 respond to ASD (100 μ M) and AITC (1 μ M), but not to CPS (5 μ M). Responses to AITC and ASD, but not to hPAR2-AP (100 μ M), are inhibited by HC03 (30 μ M), but not by capsazepine (CPZ, 10 μ M). I, In IMR90 fibroblasts ASD (100 μ M) and AITC (100 μ M), but not hPAR2-AP (100 μ M), evoke inward currents, which are abated by HC03 (50 μ M). Veh is the vehicle of ASD; (-) indicates the vehicle of antagonists. Each point/column is the mean \pm SEM of at least n=25 cells from 3-6 independent experiments for calcium recordings or of at least n=6 cells from 4-8 independent experiments for electrophysiological recordings. *P<0.05 vs. Veh, §P<0.05 vs. ASD or AITC. ANOVA and Bonferroni *post hoc* test.

In human IMR90 fibroblasts, which constitutively express the TRPA1 channel (Jaquemar et al., 1999) and do not respond to capsaicin, indicating the absence of a functional TRPV1 channel (Fig. 22H), androstenedione produced concentration-dependent (EC_{50} , 37 μ M) calcium responses that were fully and selectively inhibited by HC-030031 (Fig. 22H). Similar results were obtained in electrophysiology experiments, where androstenedione activated TRPA1-mediated inward currents that were entirely and selectively abolished by HC-030031 (Fig. 22I). TRPA1 selectivity of HC-030031 in inhibiting androstenedione-evoked responses was supported by failure to affect responses produced by the activating peptide of the human protease activated receptor 2 (hPAR2-AP) or KCl in hTRPA1-HEK293 or IMR90 cells (Fig. 22A-D, 1H, 1I). Next, we wondered whether the other aromatase substrate, testosterone, or steroid hormones upstream to aromatase that maintain the α,β -carbonyl moiety of the A ring (progesterone, 17-hydroxy-progesterone) or the ketone group at the 17 position (dehydroepiandrosterone) or other steroid hormones that retain the α,β -carbonyl moiety of the A ring (aldosterone, cortisol, corticosterone, deoxycorticosterone, 11-deoxycortisol), were able to activate hTRPA1-HEK293 cells. No hormone evoked a measurable response.

Androstenedione excites DRG neurons by a prominent role of TRPA1 and surprisingly with the contribution of TRPV1

To explore the ability of androstenedione to excite nociceptors, calcium responses were recorded in primary cultures of rat and mouse DRG neurons. Androstenedione evoked concentration-dependent (EC_{50} = 27 μ M) calcium responses in a subset of rat neurons (identified as such by their ability to respond to KCl) that also responded to AITC

and capsaicin (Fig. 23A). Capsaicin-sensitive neurons that did not respond to AITC were unresponsive also to androstenedione (Fig. 23A). The percentages of androstenedione-responding and AITC-responding neurons out of the KCl-responding neurons were similar (Fig. 23B). Superimposable findings were obtained by electrophysiological recording in rat DRG neurons (Fig. 24A). Surprisingly, the remarkable selectivity of androstenedione for TRPA1 among the different recombinant TRP channels was challenged by experiments in rat DRG neurons. The selective TRPV1 antagonist capsazepine reduced both the calcium response and the inward currents evoked by androstenedione, and abated the minor residual response observed in the presence of HC-030031 (Fig. 23C and 23D and Fig. 24A). The calcium response to androstenedione was, however, unaffected by the selective TRPV4 antagonist, HC-067047 (Fig. 23D).

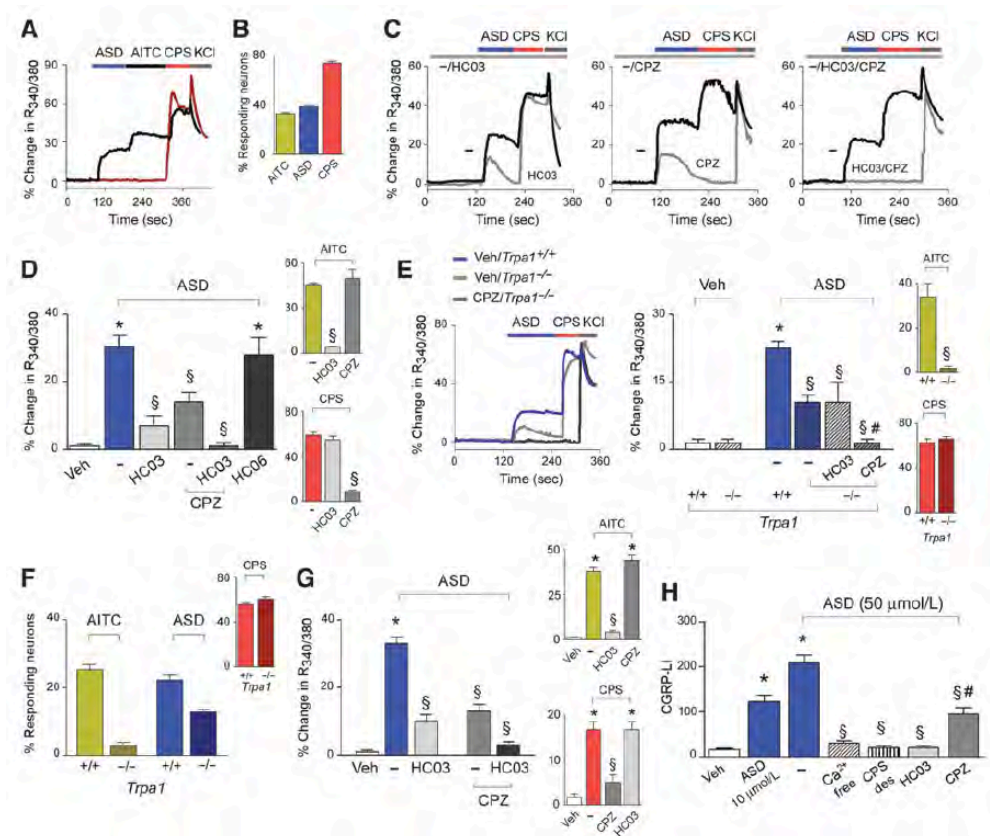


Figure 23. ASD activates the native TRPA1 channel expressed in rodent DRG neurons. A, typical tracings of calcium responses in rat DRG neurons that respond to ASD (100 μM), AITC (30 μM) and capsaicin (CPS; 0.1 μM) (black line), or solely to CPS (red line). B, percentage of DRG neurons (sensitive to 50 mM KCl) that respond to ASD, AITC or CPS. C and D, in rat DRG neurons concentrations of HC-030031 (HC03; 30 μM) and capsazepine (CPZ; 10 μM) that selectively and completely attenuated AITC and CPS responses, respectively, partially inhibit the response to ASD that, however, is abated by their combination (HC03/CPZ). HC-067047 (HC06; 10 μM) does not affect the response to ASD. E, ASD produces a calcium response in CPS-

sensitive DRG neurons isolated from *Trpa1*^{+/+} mice. The residual response to ASD in neurons from *Trpa1*^{-/-} mice is abated by CPZ. F, percentage of *Trpa1*^{+/+} or *Trpa1*^{-/-} DRG neurons responsive to AITC, ASD and CPS. G, in hTRPA1/V1-HEK293 cells the calcium response to ASD is partially inhibited by HC03 or CPZ and abated by their combination (HC03/CPZ). Calcium responses to AITC (5 μ M) and CPS (1 μ M) are abolished by HC03 and CPZ, respectively. Each point/column represents the mean \pm SEM of at least n=25 neurons from 3-7 independent experiments. *P<0.05 vs. Veh or Veh-*Trpa1*^{+/+}, §P<0.05 vs. ASD, CPS, AITC or ASD-*Trpa1*^{+/+}, #P<0.05 vs. ASD-*Trpa1*^{-/-}. H, CGRP-LI outflow elicited by ASD (10-50 μ M) from rat dorsal spinal cord slices is prevented by pre-exposure to CPS (10 μ M, 20 min; CPS-des) or by calcium removal (Ca²⁺-free) and is attenuated by HC03 (50 μ M) and only partially reduced by CPZ (10 μ M). Each column represents the mean \pm SEM of at least 4 independent experiments running in duplicate. *P<0.05 vs. Veh, §P<0.05 vs. ASD 50 μ M, #P<0.05 vs. HC03. Veh is the vehicle of ASD; (-) indicates the vehicle of antagonists. ANOVA and Bonferroni *post hoc* test.

Results obtained in rat DRG neurons were replicated in mouse DRG neurons. Cells obtained from TRPA1-deficient mice (*Trpa1*^{-/-}) exhibited a residual calcium response to androstenedione that, being consistently unaffected by HC-030031 was, however, abated by capsazepine (Fig. 23E). The percentages of androstenedione-responding and AITC-responding neurons out of the KCl-responding neurons were similar (Fig. 23F) in DRG neurons isolated from wild type mice (*Trpa1*^{+/+}). The percentage of neurons from *Trpa1*^{-/-} mice that exhibited a residual calcium response to androstenedione did not exceed the percentage obtained in neurons from *Trpa1*^{+/+} mice (Fig. 23F).

To confirm the contribution of TRPV1 in the overall response to androstenedione, we used HEK293 cells stably transfected with the cDNA for both human TRPA1 and human TRPV1 (hTRPA1/V1-HEK293 cells). In hTRPA1/V1-HEK293 cells, the calcium response evoked by androstenedione was reduced by both HC-030031 and capsazepine, and was abated solely by the combination of the two antagonists, while responses to AITC and capsaicin were fully attenuated by respective antagonists (Fig. 23G). Thus, TRPV1, when co-expressed with TRPA1, as it constitutively happens in a subpopulation of DRG neurons, appears to contribute to the overall response to androstenedione.

The release of CGRP from slices of the rat dorsal spinal cord, an anatomical site enriched with terminals of TRPA1-positive peptidergic nociceptors, was used to explore the ability of androstenedione to activate such a neuronal subpopulation. Androstenedione increased the outflow of CGRP-like immunoreactivity, a response that was abated by the removal of extracellular calcium, previous desensitization to capsaicin, or in the presence of HC-030031, but only partially reduced by capsazepine (Fig. 23H).

Thus, androstenedione elicits CGRP release from a subset of TRPV1-positive neurons *via* a neurosecretory process, mediated by TRPA1.

Androstenedione cooperates with letrozole and H₂O₂ to excite nociceptors in vitro

Next, we asked whether androstenedione cooperates with AIs and proinflammatory mediators to excite nociceptors *via* a final common pathway represented by TRPA1. Among the three AIs previously identified as TRPA1 agonists, we used letrozole, as it is currently the most prescribed in clinical practice (Kelly et al., 2015). As a prototypical proinflammatory mediator we selected H₂O₂, a byproduct of oxidative stress, because oxidative stress is increased in breast cancer, and because it is known that letrozole increases oxidative stress (Rezvanfar et al., 2012). In addition, the effect of letrozole (0.5 mg/kg, i.g.), at a dose that was previously shown to produce *per se* mechanical allodynia, was partially reduced by the antioxidant, α -lipoic acid. These observations suggest that the TRPA1-dependent letrozole-evoked mechanical hypersensitivity is partially due to the generation of oxidative stress byproducts that cooperate with the anticancer drug to target TRPA1.

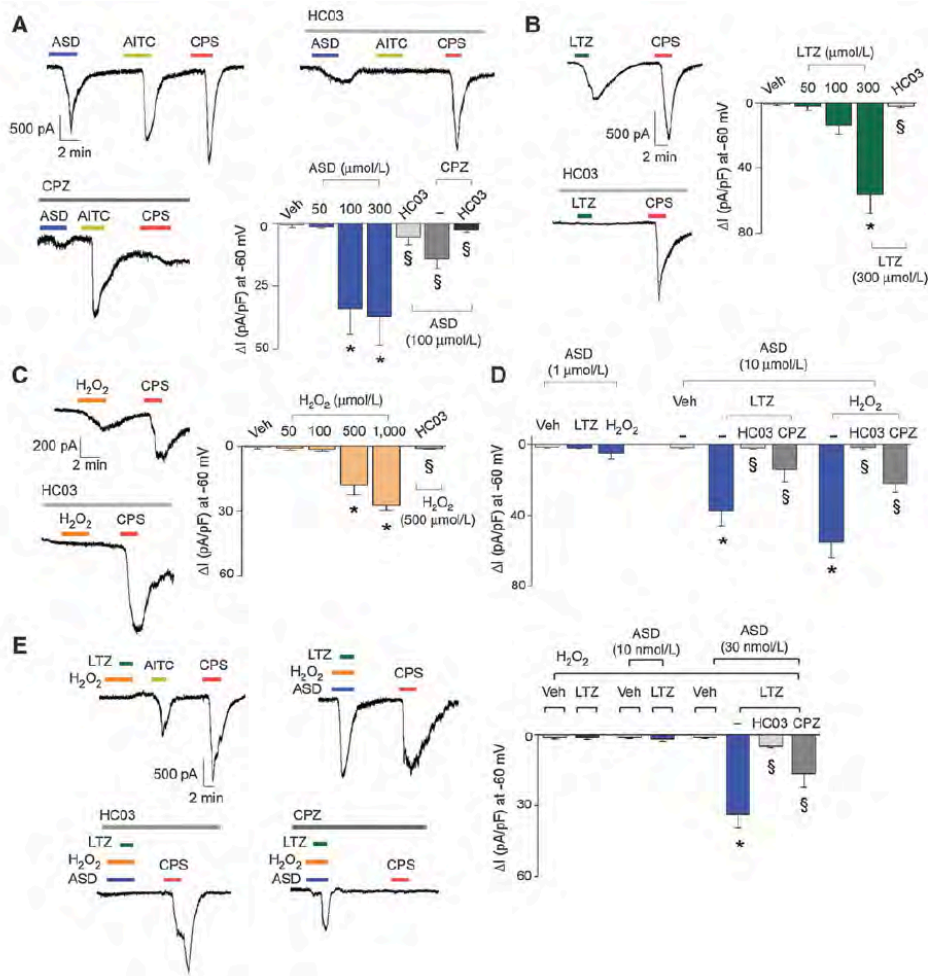


Figure 24. ASD potentiates TRPA1-mediated inward currents in the presence of subthreshold letrozole and/or proinflammatory stimuli in rat DRG neurons. A, ASD and AITC (100 μ M) evoke inward currents (whole-cell patch-clamp recordings) in capsaicin (CPS; 1 μ M)-sensitive rat DRG neurons. ASD-evoked currents are partially reduced by HC-030031 (HC03; 50 μ M) or capsazepine (CPZ; 10 μ M), which abated currents evoked by AITC or CPS, respectively. The combination of HC03 and CPZ abated the ASD-evoked currents. B and C, letrozole (LTZ) and H₂O₂ evoke concentration-dependent inward currents that are abolished by HC03 (50 μ M). D, inward currents elicited by a combination of ineffective concentrations of ASD (10 μ M)/LTZ (50 μ M) or ASD (10 μ M)/H₂O₂ (50 μ M) are abolished by HC03 and reduced by CPZ. The combination with a lower concentration of ASD (1 μ M) is ineffective. E, addition of a much lower concentration of ASD (30 nM) to the ineffective combination of LTZ (50 μ M)/H₂O₂ (50 μ M) elicits inward currents, which are abated by HC03 and reduced by CPZ. Veh is the vehicle of ASD, LTZ or H₂O₂; (-) indicates the vehicle of antagonists. Results are mean \pm SEM of at least 4 independent experiments. * P <0.05 vs. Veh; § P <0.05 vs. LTZ, H₂O₂, ASD. ANOVA and Bonferroni *post hoc* test.

From the concentration-response curves of androstenedione, letrozole, and H₂O₂ (Fig. 24A-C), we selected those subthreshold concentrations that were unable to elicit measurable inward currents in rat DRG neurons, and combined a *per se* inactive

concentration of androstenedione with inactive concentrations of letrozole or H₂O₂ (androstenedione/letrozole or androstenedione/H₂O₂). Interestingly, we found that each combination evoked inward currents, which were abated by TRPA1 antagonism and reduced by TRPV1 antagonism (Fig. 24D). Finally, we identified an inactive combination of letrozole and H₂O₂ (Fig. 24E), and we found that the addition of an inactive androstenedione concentration to letrozole and H₂O₂ triggered an inward current that was abated by HC-030031 and only partially reduced by capsazepine (Fig. 24E).

Androstenedione cooperates with letrozole and H₂O₂ to produce local TRPA1-dependent mechanical allodynia

Previous *in vitro* findings were translated to an *in vivo* experimental setting in mice. Injection of androstenedione (1-10 nmol/paw) into the mouse paw did not evoke any acute nociceptive behavior (data not shown). However, already 30 minutes after the injection and for the following 2 hours, androstenedione produced a dose-dependent mechanical allodynia (Fig. 25A and 4B) that was partially and completely abrogated by capsazepine and HC-030031, respectively (Fig. 25B). H₂O₂ injected in the mouse paw produced a dose-dependent mechanical allodynia that was entirely dependent on TRPA1 (Fig. 25C). Similar to previous findings, systemic letrozole (0.1-0.5 mg/kg, i.g.) evoked a dose-dependent, delayed (1-6 hours) mechanical allodynia that was abated by HC-030031 and unaffected by capsazepine (Fig. 25D). The combined administration of allodynia-evoking doses of intraplantar (i.pl.) androstenedione and intragastric (i.g.) letrozole produced an exaggerated pain-like response.

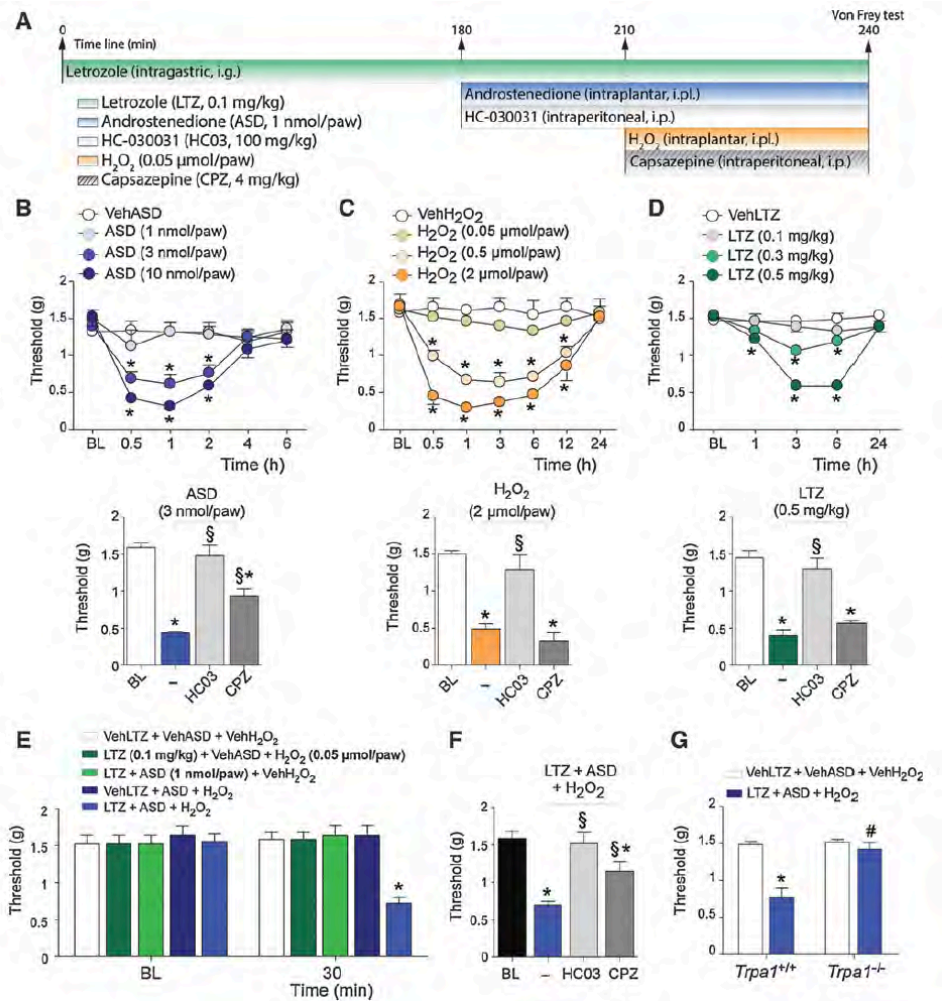


Figure 25. ASD cooperates with letrozole and H_2O_2 to produce TRPA1-dependent local mechanical allodynia. A, diagram illustrating the treatment schedule before behavioral tests. B-D, In C57BL/6 mice, injection (20 μ l) of ASD or H_2O_2 and administration of LTZ induce a dose and time-dependent mechanical allodynia that is reversed completely by HC03, and partially by CPZ. E and F, The combination of ineffective doses of LTZ, ASD and H_2O_2 evokes mechanical allodynia that is completely prevented by HC03, partially reduced by CPZ, and (G) absent in *Trpa1*^{-/-} mice. BL, baseline threshold. VehASD, VehLTZ and Veh H_2O_2 are the vehicle of ASD, LTZ and H_2O_2 , respectively; (-) is the vehicle of antagonists. Results are mean \pm SEM of at least n=5 mice for each group. *P<0.05 vs. BL; §P<0.05 vs. (-); #P<0.05 vs. *Trpa1*^{+/+}. ANOVA and Bonferroni *post hoc* test.

Next, we found doses of androstenedione and letrozole, or H_2O_2 and androstenedione, which, although *per se* ineffective, when given in combination lowered the threshold for eliciting mechanical allodynia. Finally, we identified ineffective combinations of androstenedione/letrozole, letrozole/ H_2O_2 , or H_2O_2 /androstenedione that, however, when given simultaneously (letrozole/androstenedione/ H_2O_2) caused mechanical allodynia (Fig. 25E). This response was partially reduced by capsazepine,

completely reverted by HC-030031 (Fig. 25F), and absent in TRPA1-deficient mice (Fig. 4G).

Androstenedione cooperates with letrozole and H₂O₂ to produce systemic TRPA1-dependent AIMSS-like behaviors and neurogenic inflammation

In mice, letrozole (0.5 mg/kg, i.g.) has been reported to evoke TRPA1-dependent mechanical allodynia and a decrease in grip strength, two effects reminiscent of AIMSS. The same dose of letrozole (0.5 mg/kg, i.g.) increased H₂O₂ in the sciatic nerve tissue and slightly augmented androstenedione plasma levels (Fig. 26A and 26C). D,L-buthionine sulfoximine (BSO), by inhibiting γ -glutamylcysteine synthetase, causes systemic depletion of glutathione (GSH), and the ensuing increase in reactive oxygen species (ROS). BSO (800 mg/kg, i.p.) increased mechanical allodynia and decreased forelimb grip strength through a TRPA1-dependent mechanism, while at the dose of 400 mg/kg it slightly increased H₂O₂ in the sciatic nerve tissue (Fig. 26C) without affecting pain-like behaviors. Finally, systemic administration of androstenedione (2 μ g/kg, i.p.) caused, in mice, mechanical allodynia and reduced forelimb grip strength *via* the activation of TRPA1, with a partial contribution of TRPV1. Androstenedione (2 μ g/kg, i.p.) also increased H₂O₂ levels in the sciatic nerve (Fig. 26C).

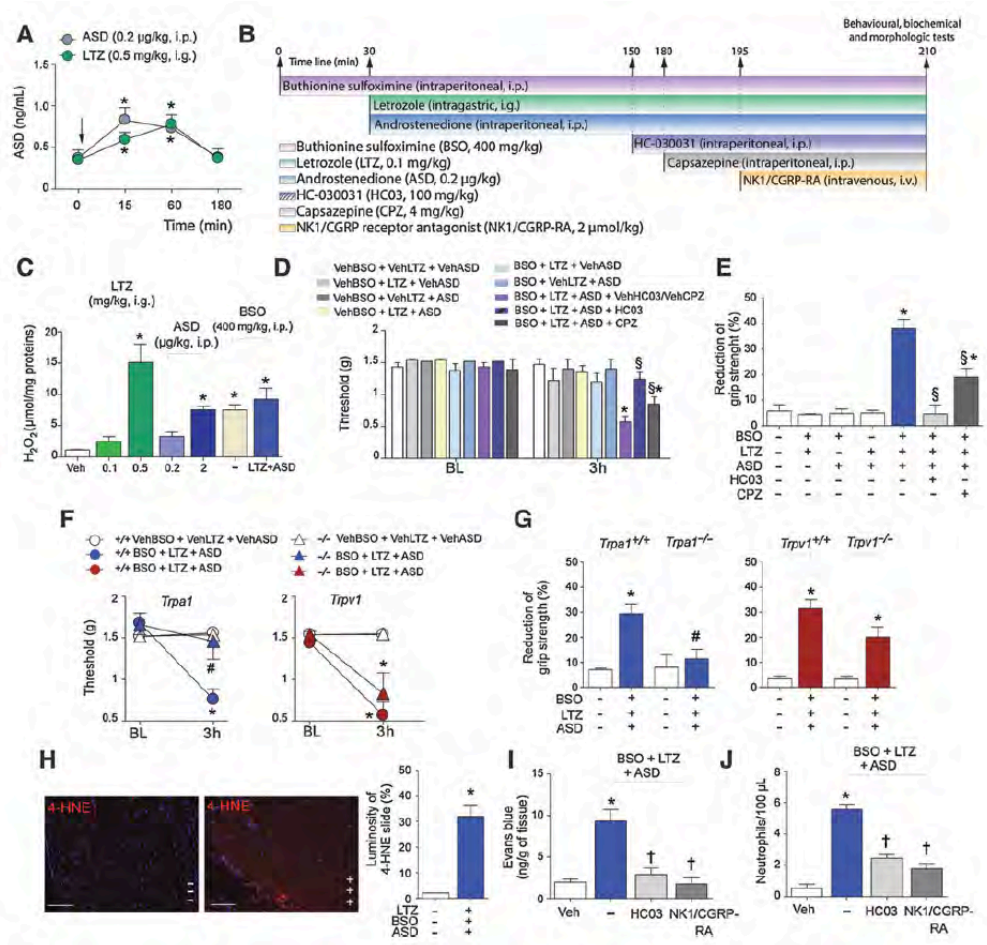


Figure 26. Androstenedione cooperates with letrozole and H₂O₂ to evoke systemic TRPA1-dependent AIMSS-like behaviors. A, ASD serum levels are similarly increased by systemic administration (↓) of ASD or letrozole (LTZ). B, diagram illustrating the treatment schedule before behavioral tests. C, LTZ or ASD increase H₂O₂ in homogenates of mouse sciatic nerve. Addition of ineffective doses of LTZ and ASD does not further increase H₂O₂ levels produced by BSO alone. D and E, ASD, LTZ and BSO alone or in dual combinations (ASD/LTZ; ASD/BSO; LTZ/BSO) do not increase mechanical allodynia or decrease grip strength. However, their combination (BSO/LTZ/ASD) increases mechanical allodynia and decreases grip strength. Both responses are reverted by HC03 and attenuated by CPZ. F and G, changes in mechanical allodynia and grip strength induced by BSO/LTZ/ASD observed in *Trpa1*^{+/-} mice are similar to those observed in *Trpv1*^{+/-} and abrogated in *Trpa1*^{-/-} mice, but not in *Trpv1*^{-/-} mice. H, BSO/LTZ/ASD (+++), but not their vehicles (---) increase 4-hydroxynonenal (4-HNE) staining within the sciatic nerve. I and J, HC03 or the combination of L-733,060 and CGRP₈₋₃₇ (NK1/CGRP-RA) attenuate increases in Evans blue dye extravasation in the knee joint synovial tissue, and in neutrophil number in synovial fluid evoked by BSO/LTZ/ASD. BL, baseline threshold. Scale bar, 100 μm. Veh is the vehicle of LTZ, ASD and BSO; VehASD, VehLTZ and VehBSO are the vehicle of ASD, LTZ and BSO, respectively; VehHC03/CPZ (D) and (-) (I, J) are the vehicle of antagonists. Results are mean±SEM of at least n=5 mice for each group. *P<0.05 vs. Veh (B), time 0 (C) or white columns or circle (D-J); †P<0.05 vs. Veh HC03/CPZ; #P<0.05 vs. *Trpa1*^{+/-}; ‡P<0.05 vs. (-). ANOVA and Bonferroni *post hoc* test.

To better understand the contribution of androstenedione and oxidative stress to the AIMSS-like behaviors, a low dose of androstenedione (0.2 $\mu\text{g}/\text{kg}$, i.p.) that failed to affect H_2O_2 generation (Fig. 26C), as well as mechanical allodynia and forelimb grip strength, was used. This same dose slightly increased hormone plasma concentration to levels comparable to those produced by a dose of letrozole (0.5 mg/kg , i.g.) that caused pain-like behaviors (Fig. 26A and Fig. 25D). Systemic BSO (400 mg/kg , i.p.), letrozole (0.1 mg/kg , i.g.) and androstenedione (0.2 $\mu\text{g}/\text{kg}$, i.p.) that *per se*, or in combinations (letrozole/androstenedione, BSO/androstenedione or BSO/letrozole), did not affect mechanical allodynia and forelimb grip strength, when given simultaneously caused remarkable mechanical allodynia and decreased forelimb grip strength (Fig. 26D and 26E). The triple combination of BSO, letrozole, and androstenedione increased H_2O_2 levels in the sciatic nerve (Fig. 26C). However, the increase was not different from the increase evoked by BSO (400 mg/kg) alone. Finally, the remarkable increase in 4-hydroxynonenal staining in the sciatic nerve allowed us to precisely localize the oxidative stress generation within the neural structure (Fig. 26H). Mechanical allodynia and decrease in forelimb grip strength evoked by the triple combination were partially and totally reverted by capsazepine and HC-030031, respectively (Fig. 26D and 26E) and were absent in TRPA1-deficient mice, but unaffected in TRPV1-deficient mice (Fig. 26F and 26G).

Finally, the combination of BSO (400 mg/kg , i.p.), letrozole (0.1 mg/kg , i.g.) and androstenedione (0.2 $\mu\text{g}/\text{kg}$, i.p.), which produced AIMSS-like behaviors, increased Evans blue dye extravasation in the synovial tissue and the number of neutrophils in the synovial fluid of mouse knee joint (Fig. 26I and 26J). Both responses were reduced by pretreatment with HC-030031 or a combination of an NK1 receptor antagonist (L733,060) and a CGRP receptor antagonist (CGRP₈₋₃₇) (both 2 $\mu\text{mol}/\text{kg}$, i.v.) (Fig. 26I and 5J). These findings indicate that the letrozole/androstenedione/BSO combination *via* TRPA1 gating promotes two typical neurogenic inflammatory responses, such as plasma protein and neutrophil extravasation (Nassini et al., 2014).

TRPA1/NOX in the soma of trigeminal ganglion neurons mediates migraine-related pain of glyceryl trinitrate in mice

Another painful condition is represented by migraine pain. Occupational exposure to, or treatment with, organic nitrates has long been known to provoke headaches (Thadani et al., 2006; Trainor et al., 1966). These observations have led to the clinical use of glyceryl trinitrate (GTN) as a reliable provocation test for migraine attacks (Iversen et al., 1989; Olesen, 2008; Sicuteri et al., 1987). In most subjects, including healthy controls, GTN administration causes a mild headache that develops rapidly and is short-lived. However, after a remarkable time lag (hours) from GTN exposure, migraineurs develop severe headaches that fulfil the criteria of a typical migraine attack (Iversen et al., 1989; Olesen, 2008; Sicuteri et al., 1987). This ability of GTN to provoke migraine is temporally dissociated from the immediate and short-lived (<10 min) release of NO (Persson et al., 1994) and the consequent cGMP-dependent vascular responses (Guo et al., 2008). Thus, while vasodilatation by GTN/NO might account for the early dull headache experienced by most subjects (Iversen et al., 1996), it cannot explain the delayed headache symptoms observed in migraineurs (Olesen, 2008).

Several mechanisms have been proposed to explain GTN-evoked headaches, including degranulation of meningeal mast cells (Ferrari et al., 2016; Reuter et al., 2001), phosphorylation of extracellular signal-regulated kinase (ERK) in meningeal arteries (Zhang et al., 2013), delayed meningeal inflammation sustained by induction of NO synthase and prolonged NO generation, and the release of calcitonin gene-related peptide (CGRP) (Ramachandran et al., 2014), a primary migraine neuropeptide (Edvinsson, 2015; Ho et al., 2010). GTN administration to rodents and humans produces a delayed and prolonged (hours) hyperalgesia that temporally correlates with GTN-induced migraine-like attacks in humans (Ferrari et al., 2016). However, the molecular processes responsible for this delayed hyperalgesia in rodents and humans are unknown.

We aim at identifying a function of nociceptor TRPA1 in sustaining GTN-induced allodynia, thereby contributing to periorbital allodynia.

GTN evokes NO-mediated TRPA1-independent vasodilatation and TRPA1-

dependent allodynia

Administration of GTN (1-10 mg/kg, i.p.) to C57BL/6 mice induced a dose-dependent and prolonged PMA (**Fig. 27A**). GTN (10 mg/kg, i.p.) also produced an early and transient (0-10 min) cutaneous increase in blood flow in the periorbital skin (**Fig. 27B**). GTN (1 mg/kg, **Fig. 27C** and 10 mg/kg, **Fig. 27D**) evoked PMA in *Trpa1*^{+/+} mice, whereas *Trpa1*^{-/-} mice were fully protected. However, the increase in cutaneous blood flow evoked by GTN (10 mg/kg) in *Trpa1*^{+/+} mice was maintained in *Trpa1*^{-/-} mice (**Fig. 27E**). Genetic deletion of TRPV1 or TRPV4 channels did not affect GTN-evoked PMA. Systemic GTN (10 mg/kg) also induced sustained mechanical allodynia in the hind paw of C57BL/6 and *Trpa1*^{+/+}, but not *Trpa1*^{-/-} mice. This response, which indicates a general proalgesic action of GTN, was not further investigated.

The TRPA1 antagonist, HC-030031, given (i.p.) 0.5 h before and 1, 3, 4 and 5 h after GTN, transiently and completely reversed PMA at all time points (**Fig. 27F**). HC-030031 (1 h after GTN) reversed PMA induced by the lowest dose of GTN (1 mg/kg). Another channel antagonist, A967079, given 0.5 h before and 1 h after GTN (10 mg/kg) also reversed allodynia. Antagonists of TRPV1 (capsazepine) and TRPV4 (HC-067047), administered before GTN did not affect GTN-induced PMA.

Mitochondrial ALDH2 is known to generate NO from GTN (Beretta et al., 2008). To determine the contribution of NO to GTN-evoked PMA, mice were treated with the ALDH2 inhibitor, disulfiram, or the specific NO scavenger, cPTIO. Both disulfiram and cPTIO, when administered (i.p.) 0.5 h before, but not 1 hour after, GTN, attenuated GTN-evoked PMA (**Fig. 27F**). The ability of disulfiram and cPTIO to prevent PMA if given before GTN indicates that NO is needed to initiate GTN-evoked PMA. However, failure of disulfiram and cPTIO to reverse established PMA suggests that additional mechanisms are required to sustain PMA. Pretreatment with disulfiram, but not with HC-030031 (both i.p., 0.5 h before GTN), attenuated the increase in periorbital blood flow evoked by GTN (10 mg/kg) (**Fig. 27G**).

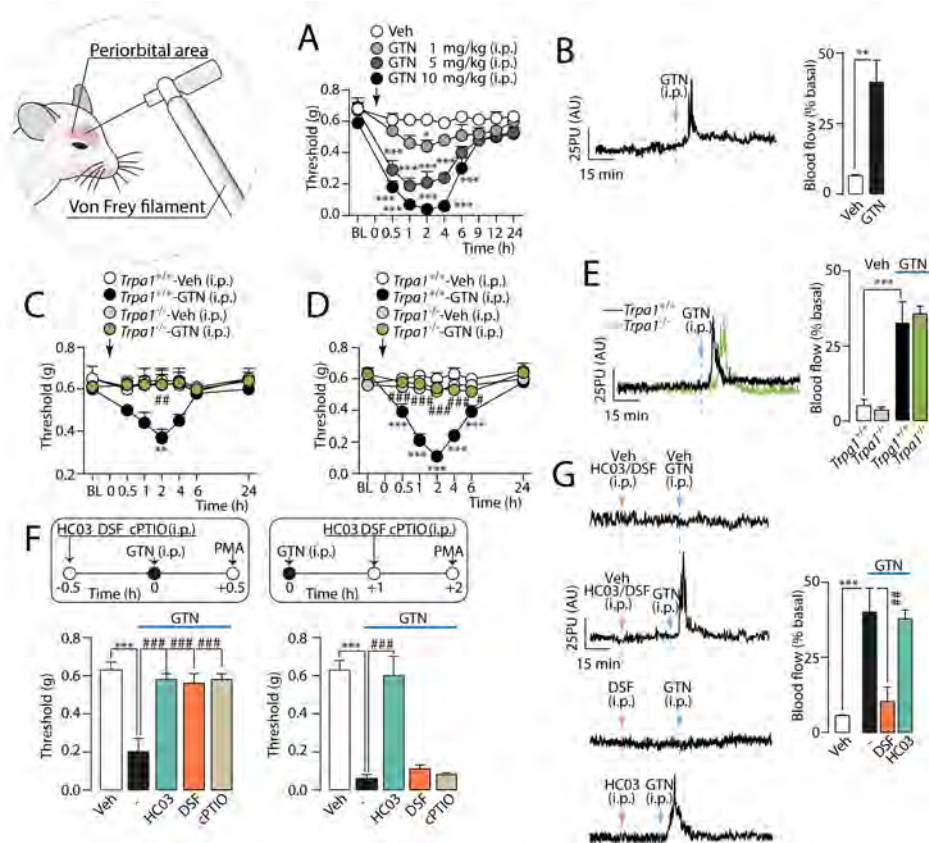


Figure 27. GTN induces periorbital mechanical allodynia (PMA) via a TRPA1-dependent mechanism. (A) Dose- and time-dependent PMA evoked by GTN in C57BL/6 mice. (B) Representative traces and pooled data of the increases in periorbital skin blood flow evoked by GTN (10 mg/kg). PMA evoked by (C) low (1 mg/kg, i.p.) and (D) high (10 mg/kg, i.p.) dose of GTN, in *Trpa1*^{+/+} and *Trpa1*^{-/-} mice. (E) Representative traces and pooled data of the increases in periorbital skin blood flow evoked by GTN (10 mg/kg) in *Trpa1*^{+/+} and *Trpa1*^{-/-} mice. (F) Pretreatment with systemic (i.p.) HC-030031 (HC03; 100 mg/kg), disulfiram (DSF, 100 mg/kg) or cPTIO (0.6 mg/kg) abates PMA measured 0.5 h after GTN (10 mg/kg). HC03 but not DSF and cPTIO (given after GTN) reduces PMA measured 2 h after GTN. (G) Representative traces and pooled data of the increases in periorbital skin blood flow evoked by GTN (10 mg/kg). DSF but not HC03, both given before GTN abolishes the increase in blood flow induced by GTN. BL, baseline mechanical threshold. Veh is the vehicle of GTN. Dash (-) indicates combined vehicles of treatments. Arrows indicate times of drug administration. PU, perfusion units. AU, arbitrary units. **Error bars indicate mean \pm SEM, 6-8 mice per group.** * $P < 0.05$, ** $P < 0.01$, *** $P < 0.001$ vs. Veh, *Trpa1*^{+/+}-Veh and # $P < 0.05$, ## $P < 0.01$, ### $P < 0.001$ vs. *Trpa1*^{+/+}-GTN or GTN; one-way or two-way ANOVA with Bonferroni post-hoc correction, and Student's t-test.

NO, but not GTN, directly targets TRPA1

To determine whether TRPA1 is directly gated by GTN and/or NO, responses to different NO donors were investigated *in vitro*. GTN caused a concentration-dependent increase in $[Ca^{2+}]_i$ in TG neurons from C57BL/6 and *Trpa1*^{+/+}, but not from *Trpa1*^{-/-} mice (**Fig. 28A and B**). The TRPA1 antagonist (HC-030031), but not the TRPV1 or TRPV4 antagonists (capsazepine or HC-067047, respectively), abolished responses (**Fig. 28A**).

Key intracellular cysteine and lysine residues of TRPA1 interact with oxidants and electrophilic agents. Whereas GTN increased $[Ca^{2+}]_i$ in hTRPA1-HEK293, HEK293 cells expressing a mutant 3C/K-Q/hTRPA1 were unresponsive (**Fig. 28C**). NO scavenger (cPTIO) or ALDH2 inhibitor (disulfiram) did not affect GTN signals in neurons from C57BL/6 mice (**Fig. 28D**). In contrast, the HC-030031-dependent Ca^{2+} -response to a different NO-donor, SNAP, was inhibited in the presence of cPTIO (**Fig. 28D**). Thus, GTN activates TRPA1 by targeting specific cysteine and lysine residues. However, conversely to SNAP, the *in vitro* action of GTN is not mediated through NO release.

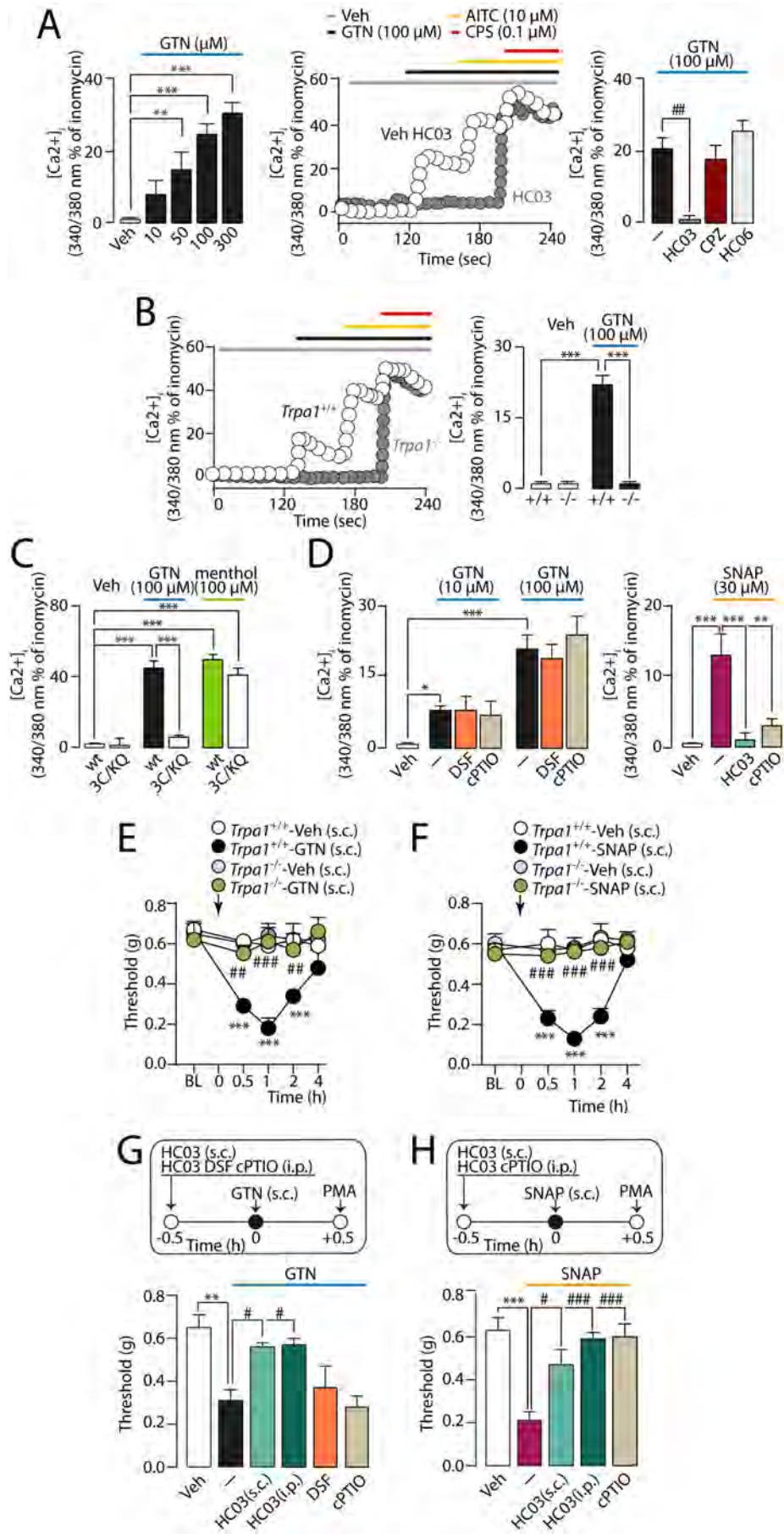


Figure 28. GTN-evoked periorbital mechanical allodynia (PMA) is mediated by NO. (A) Ca^{2+} -response to GTN in mouse trigeminal ganglion (TG) neurons, which also respond to AITC or capsaicin (CPS), is attenuated by HC-030031 (HC03), but not by HC-067047 (HC06, TRPV4 antagonist) or capsazepine (CPZ, TRPV1 antagonist), and (B) abated by TRPA1 deletion. (C) Ca^{2+} -response to GTN or menthol in HEK293-cells expressing wild type (wt) or mutant (3C/K-Q) human TRPA1. (D) GTN-evoked Ca^{2+} -response in TG neurons is unaffected by disulfiram (DSF) or cPTIO while SNAP-evoked Ca^{2+} -response is abated by cPTIO and HC03. Veh is the vehicle of GTN. Dash (-) indicates combined vehicles of treatments. Error bars indicate mean \pm SEM of $n > 15$ neurons or 50 cells (A-D). * $P < 0.05$, ** $P < 0.01$, *** $P < 0.001$; One-way ANOVA with Bonferroni post-hoc correction. (E,F) Local (s.c., 10 μl) GTN (10 μg) evokes a time-dependent PMA that is abated in *Trpa1*^{-/-} mice and by the pretreatment with local (s.c.) and systemic (i.p.) HC03 (100 μg and 100 mg/kg, respectively), but not with systemic DSF (100 mg/kg, i.p.) and cPTIO (0.6 mg/kg, i.p.). (G,H) Local (s.c., 10 μl) SNAP (40 μg) induces a time-dependent PMA that is abated in *Trpa1*^{-/-} mice and prevented by pretreatment with local (s.c.) and systemic (i.p.) HC03 (100 μg and 100 mg/kg, respectively) and systemic cPTIO (0.6 mg/kg, i.p.). BL, baseline mechanical threshold. Veh is the vehicle of GTN. Dash (-) indicates combined vehicles of treatments. Arrows indicate time of drug administration. **Error bars indicate mean \pm SEM, 6-8 mice per group.** ** $P < 0.01$, *** $P < 0.001$ vs. *Trpa1*^{+/+}-Veh, Veh and # $P < 0.05$, ## $P < 0.01$, ### $P < 0.001$ vs. *Trpa1*^{+/+}-GTN, GTN, *Trpa1*^{+/+}-SNAP or SNA, one-way or two-way ANOVA with Bonferroni post-hoc correction.

Results obtained *in vivo* by local administration of NO donors recapitulated the *in vitro* findings. Injection (s.c.) in the periorbital area of the TRPA1 agonist, AITC, evoked PMA that was reversed by local (s.c.) pretreatment with HC-030031. Local (s.c.) NO-donors, GTN or SNAP, induced PMA in *Trpa1*^{+/+}, but not *Trpa1*^{-/-} mice (**Fig. 28E and F**). Both local (s.c.) or systemic (i.p.) TRPA1 antagonism by HC-030031 reversed PMA evoked by local GTN or SNAP (**Fig. 28G and H**). Systemic (i.p.) Disulfiram or cPTIO did not affect PMA evoked by local (s.c.) GTN (**Fig. 28G**). However, cPTIO (i.p.) attenuated PMA evoked by local (s.c.) SNAP (**Fig. 28H**). Thus, GTN evokes allodynia by mechanisms that depend from the route of administration. Local GTN directly regulates TRPA1 gating, whereas systemic GTN indirectly regulates TRPA1 by a process that involves ALDH2-mediated liberation of NO.

Oxidative stress and TRPA1 sustain GTN-evoked mechanical allodynia

The NO scavenger (cPTIO) or ALDH2 inhibitor (disulfiram) prevented GTN-evoked allodynia when administered before but were ineffective when given after GTN. Thus, NO is necessary to initiate the hypersensitivity condition, but is not sufficient for its maintenance. Since GTN stimulates oxidative stress (Wenzl et al., 2009), we hypothesized that NO, liberated from GTN, initiates the process that subsequently

sustains TRPA1-dependent PMA *via* ROS generation. Two different ROS scavengers, α LA and N-tert-butyl- α -phenylnitron (PBN), reversed PMA only when given (i.p.) 1 h after, but not 0.5 h before GTN (Fig. 29A and B).

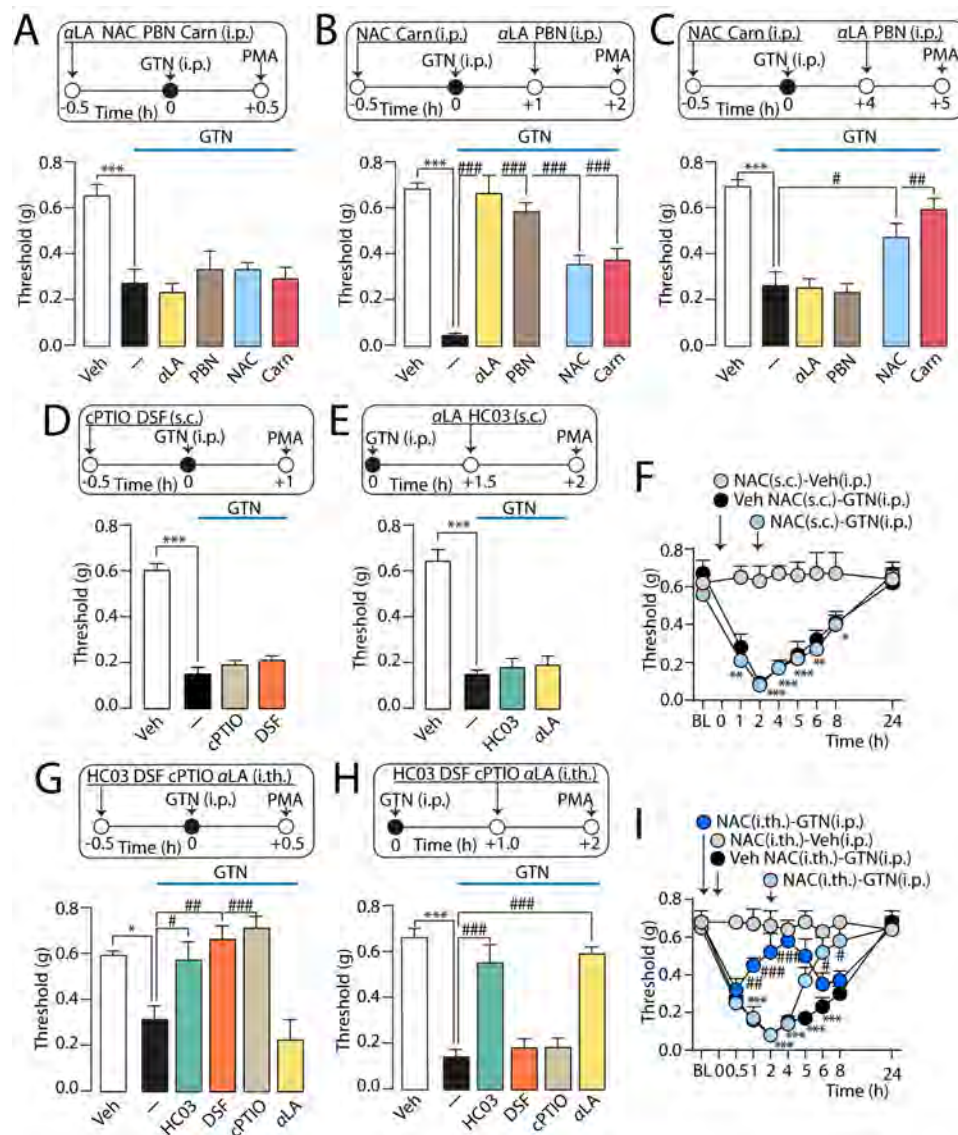


Figure 29. Prolonged periorbital mechanical allodynia (PMA) induced by GTN is mediated by oxidative stress. (A) PMA evoked by GTN (10 mg/kg) in C57BL/6 mice is not affected by the α LA (100 mg/kg), NAC (250 mg/kg), PBN (100 mg/kg) or L-carnosine (Carn, 200 mg/kg) (all pre-GTN). (B, C) α LA and PBN (all post-GTN) reduce PMA measured at 2 h not at 5 h. Pretreatment with NAC and Carn reach the maximum effect in the reduction of PMA, 5 h after GTN. (D) PMA evoked by systemic (i.p.) GTN (10 mg/kg) is unaffected by local (10 μ l, s.c.) cPTIO (60 μ g) or disulfiram (DSF; 10 μ g) (all pre-GTN), and by (E) HC-030031 (HC03; 50 μ g) and α LA (5 μ g) (all post- GTN). (F) Local (10 μ l, s.c.) administration of NAC (20 μ g, post-GTN) does not affect GTN-evoked PMA. (G) PMA evoked by systemic (i.p.) GTN (10 mg/kg) is reversed by intrathecal (5 μ l, i.th.) HC03 (10 μ g), DSF (5 μ g) and cPTIO (30 μ g) but not with α LA (10 μ g) (all pre-GTN). (H) Intrathecal (i.th.) HC03 (10 μ g) and α LA (10 μ g), but not DSF

(5 μ g) and cPTIO (30 μ g), (all post-GTN) reduce PMA measured 2 h after GTN. (I) Intrathecal (i.th.) NAC (50 μ g) (pre- or post-GTN) reduces GTN-evoked. BL, baseline mechanical threshold. Veh is the vehicle of GTN. Dash (-) indicates combined vehicles of treatments. Arrows indicate time of drug administration. Error bars indicate mean \pm SEM, 6-9 mice per group. * P <0.05, ** P <0.01, *** P <0.001 vs. Veh, NAC-Veh. # P <0.05, ## P <0.01, ### P <0.001 vs. GTN, Veh NAC-GTN; one-way or two-way ANOVA with Bonferroni post-hoc correction.

GTN-evoked PMA persisted for \sim 8 h, but α LA or PBN were unable to reverse PMA 5 h post-GTN (**Fig. 29C**), indicating that mediators other than ROS are required to sustain hypersensitivity beyond 5 h. 4-HNE is a major electrophilic aldehyde that is generated by free radical attack of 6-polyunsaturated fatty acids, and is a TRPA1 agonist. In contrast to ROS, which are short-lived, the biological activity of 4-HNE may last for hours (Brame et al., 1999). NAC and L-carnosine efficiently scavenge α,β -unsaturated aldehydes, including 4-HNE. NAC or L-carnosine (i.p.), administered before GTN, did not attenuate the first phase of GTN-evoked PMA (2 h), but strongly inhibited later phases (5 h) (**Fig. 29B and C**), indicating that carbonylic derivatives more stable than ROS, sustain the final phase of PMA.

GTN does not produce periorbital allodynia by a local mechanism

Local injections of the TRPA1 agonist, AITC and the NO-donors, GTN or SNAP, caused TRPA1-dependent PMA, suggesting the involvement of TRPA1 on cutaneous nerve terminals. However, PMA evoked by systemic GTN was unaffected by local treatment with disulfiram, cPTIO, HC-030031, α LA and NAC (**Fig. 29D-F**), excluding that systemic GTN activates TRPA1 on cutaneous afferent nerve fibres to induce PMA. Centrally administered TRPA1 antagonists, HC-030031 or A967079 (pre- or post-GTN, i.th.), attenuated PMA-evoked by systemic GTN (**Fig. 29G and H**). Disulfiram or cPTIO (pre-, but not post-GTN), α LA (post-, but not pre-GTN) and NAC (pre- or post-GTN) (all i.th.) (**Fig. 29G-I**) also attenuated PMA.

GTN/NO targets TRPA1 in the soma of TG neurons to generate oxidative stress

Failure of subcutaneous and ability of intrathecal drugs to attenuate GTN-evoked PMA suggested the involvement of central anatomical areas, including the terminals in the dorsal horn of the brainstem and nociceptor cell bodies in the TG. To determine whether systemic GTN induces oxidative stress in these locations, we measured two

markers of oxidative and carbonylic stress, H₂O₂ and 4-HNE, respectively. GTN, which failed to increase H₂O₂ and 4-HNE in brain stem, caused a rapid and transient increase in H₂O₂ (1-3 h) and a gradual and sustained increase in 4-HNE (4-6 h) in the TGs (**Fig. 30A and B**). cPTIO and disulfiram (both pre-GTN) and αLA (post-GTN) blunted the H₂O₂ increase (at 2 h) (**Fig. 30C**). cPTIO and NAC (pre-GTN), and αLA (post-GTN) blunted the 4-HNE signal (at 4 h) (**Fig. 30D**). Unexpectedly, antagonism (HC-030031) or genetic deletion of TRPA1 also attenuated GTN-induced increases in H₂O₂ or 4-HNE (**Fig. 30C-E**). These data suggest that oxidative stress generation, which seems to mediate GTN-evoked PMA, is initiated by NO-induced activation of TRPA1 within the TG.

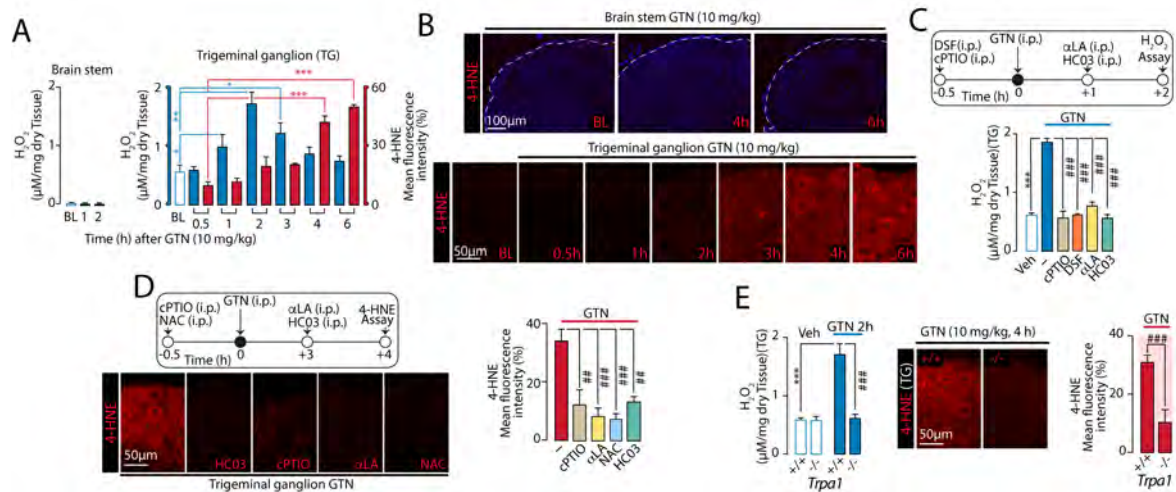


Figure 30. GTN generates oxidative stress in trigeminal ganglion (TG), via NO and TRPA1. Systemic (i.p.) GTN increases (A, B) H₂O₂ levels and 4-HNE staining in TG, but not in brain stem of C57BL/6 mice. (C) Two h after GTN the increase in H₂O₂ in TGs, is abolished by systemic (i.p.) cPTIO (0.6 mg/kg) and disulfiram (DSF, 100 mg/kg) (all pre-GTN) or αLA or HC-030031 (HC03, both 100 mg/kg) (all post-GTN). (D) Representative images and pooled data of 4-HNE staining in TGs, 4 h after GTN (10 mg/kg) administration in C57BL/6 mice treated systemically (i.p.) with cPTIO (0.6 mg/kg) or NAC (250 mg/kg) (all pre-GTN), or with HC03 and αLA (both, 100 mg/kg) (all post-GTN). (E) Systemic (i.p.) GTN (10 mg/kg) increases H₂O₂ levels and 4-HNE staining in TGs from *Trpa1*^{+/+}, but not *Trpa1*^{-/-} mice. BL, baseline level of H₂O₂ or 4-HNE. Veh is the vehicle of GTN. Dash (-) indicates combined vehicles of treatments. Error bars indicate mean ± SEM, 4-6 mice *per* group. **P*<0.05, ***P*<0.01, ****P*<0.001; ####*P*<0.001; one-way ANOVA with Bonferroni post-hoc correction and Student's *t*-test.

Sensory neurons and satellite glial cells (SGCs) are present in the TG (**Fig. 31A**). To determine which cell type generates GTN/NO-evoked oxidative stress, C57BL/6 mice were treated with resiniferatoxin, which is known to defunctionalise TRPV1-expressing neurons, which co-express TRPA1. Treatment with resiniferatoxin, which suppressed eye

wiping evoked by TRPV1 and TRPA1 agonists (capsaicin and AITC, respectively), attenuated both GTN-evoked PMA and H₂O₂ generation (**Fig. 31B**), supporting a role of TRPV1/TRPA1-positive neurons in these responses. GTN stimulated release of H₂O₂ from mixed cultures of TG neurons/SGCs (**Fig. 31C**), but not from primary cultures of isolated SGCs (**Fig. 31D**). Removal of extracellular Ca²⁺ or pre-exposure to a high capsaicin concentration, which, similar to resiniferatoxin, desensitises TRPV1/TRPA1-positive neurons (Nassini et al., 2015), attenuated GTN-evoked increase in H₂O₂ in mixed cultures of TG neurons/SGCs (**Fig. 31C**). GTN, AITC and SNAP increased H₂O₂ release from TG neurons/SGCs mixed cultures in a HC-030031-dependent manner (**Fig. 31C**).

Intrathecal administration of TRPA1 AS-ODN down-regulated TRPA1 mRNA expression in TGs (**Fig. 31E**) and reduced AITC-evoked eye wiping. TRPA1 AS-ODN attenuated GTN-evoked PMA and H₂O₂ increase in TGs (**Fig. 31E**). Further evidence for the role of neuronal TRPA1 in GTN-evoked oxidative stress and allodynia was obtained by studying *Advillin-Cre⁺;Trpa1^{f/f}* mice, which exhibited reduced TRPA1 mRNA in TGs (**Fig. 31F**) and did not respond to TRPA1-mediated eye wiping evoked by AITC. GTN failed to evoke PMA or H₂O₂ generation in TGs in *Advillin-Cre⁺;Trpa1^{f/f}* mice (**Fig. 31F**), thus supporting that GTN/NO initiates a TRPA1-dependent and oxidative stress-mediated mechanism that perpetuates nociceptor activation by an autocrine pathway that is confined to the TG.

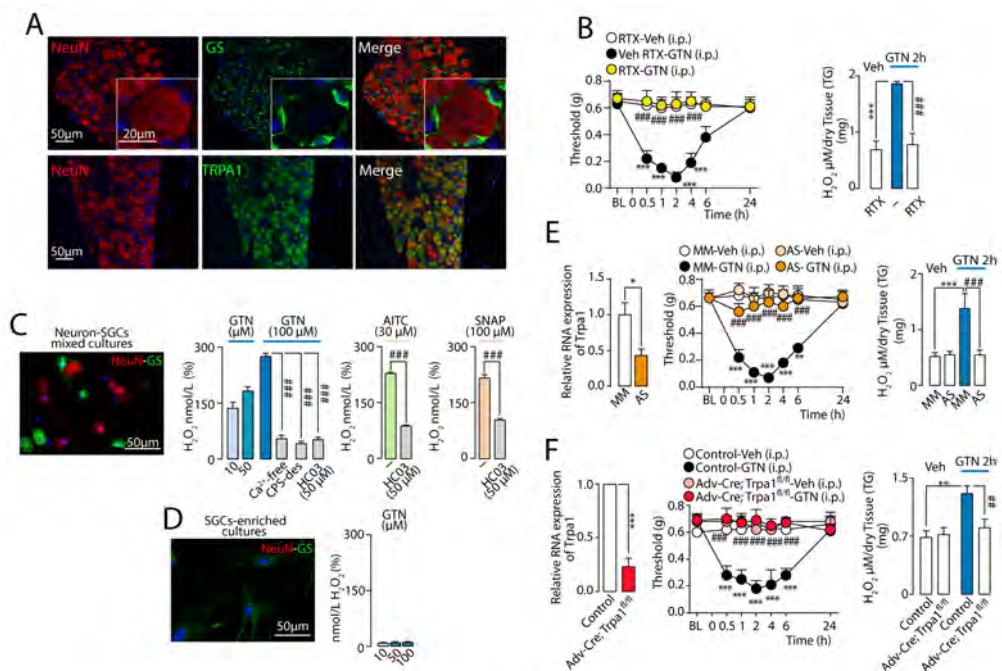


Figure 31. GTN targets neuronal TRPA1 to generate periorbital oxidative stress and

mechanical allodynia (PMA). (A) Neurons (identified by neuronal nuclei, NeuN), satellite glial cells (SGCs) (identified by glutamine synthetase, GS) and TRPA1 staining in trigeminal ganglion (TG). (B) Neuronal defunctionalization with RTX prevents systemic (i.p.) GTN-evoked PMA and H₂O₂ increase in TGs of C57BL/6 mice. (C) H₂O₂ release elicited by GTN from TG neurons-SGCs mixed cultures (see staining for NeuN/GS) is inhibited by extracellular Ca²⁺ removal (Ca²⁺-free), pre-exposure to capsaicin (CPS-des) or HC-030031 (HC03), which also inhibits H₂O₂ release elicited by AITC or SNAP. (D) In SGCs-enriched cultures (see staining for GS, but not NeuN) GTN does not release H₂O₂. (E) Intrathecal TRPA1 AS-ODN inhibits TRPA1 mRNA expression, systemic (i.p.) GTN-evoked PMA and H₂O₂ increase in TGs. (F) TRPA1 mRNA expression in TGs from control and *Advillin-Cre;Trpa1^{fl/fl}* (*Adv-Cre⁺;Trpa1^{fl/fl}*). Systemic (i.p.) GTN-evoked PMA and H₂O₂ increase in TGs are reduced in *Adv-Cre⁺;Trpa1^{fl/fl}* mice. BL, baseline mechanical threshold. Veh is the vehicle of GTN. Dash (-) indicates vehicles of treatments. Error bars indicate mean ± SEM, 6-8 mice *per* group or 2-7 replicates from 3 independent experiments. **P*<0.05, ***P*<0.01, ****P*<0.001 *vs.* RTX-Veh, MM-Veh and control-Veh; ##*P*< 0.01, ###*P*< 0.001 *vs.* Veh RTX-GTN, MM-GTN, control-GTN, GTN, AITC or SNAP, one-way or two-way ANOVA with Bonferroni post-hoc correction and Student's t-test.

TRPA1 and NOXs in the soma of TG nociceptors maintain GTN-evoked allodynia

To explore the mechanism by which oxidative stress sustains GTN-evoked allodynia within TG neurons we localized immunoreactivity for NOX1, NOX2, and NOX4 in mouse TG neurons but not in SGCs, confirming previous studies (Bedard et al., 2007). Immunoreactivities for the three NOX isoforms colocalized with that for TRPA1 (**Fig. 32A**). The non-selective NOX inhibitor, apocynin (i.p., post- but not pre-GTN) reversed GTN-evoked allodynia (**Fig. 32B and C**). Selective NOX2 (gp91ds-tat) or NOX1 (ML171) inhibitors (i.p., post- but not pre-GTN), attenuated, and their combination abolished GTN-evoked PMA (**Fig. 32B and C**). The NOX4 inhibitor, GKT137831, reduced, and the combination of GKT137831 and gp91ds-tat, abolished GTN-evoked allodynia. However, since GKT137831 also inhibits NOX1, the role of NOX4 remains uncertain. Furthermore, a proximity ligation assay showed that NOX2 and TRPA1 are closely located in TG neuronal cell bodies (**Fig. 32D**), suggesting that their interaction could underlie efficient ROS release. Thus, the soma of TRPA1-expressing TG neurons possesses the biochemical machinery required to initiate and sustain oxidative stress evoked by GTN.

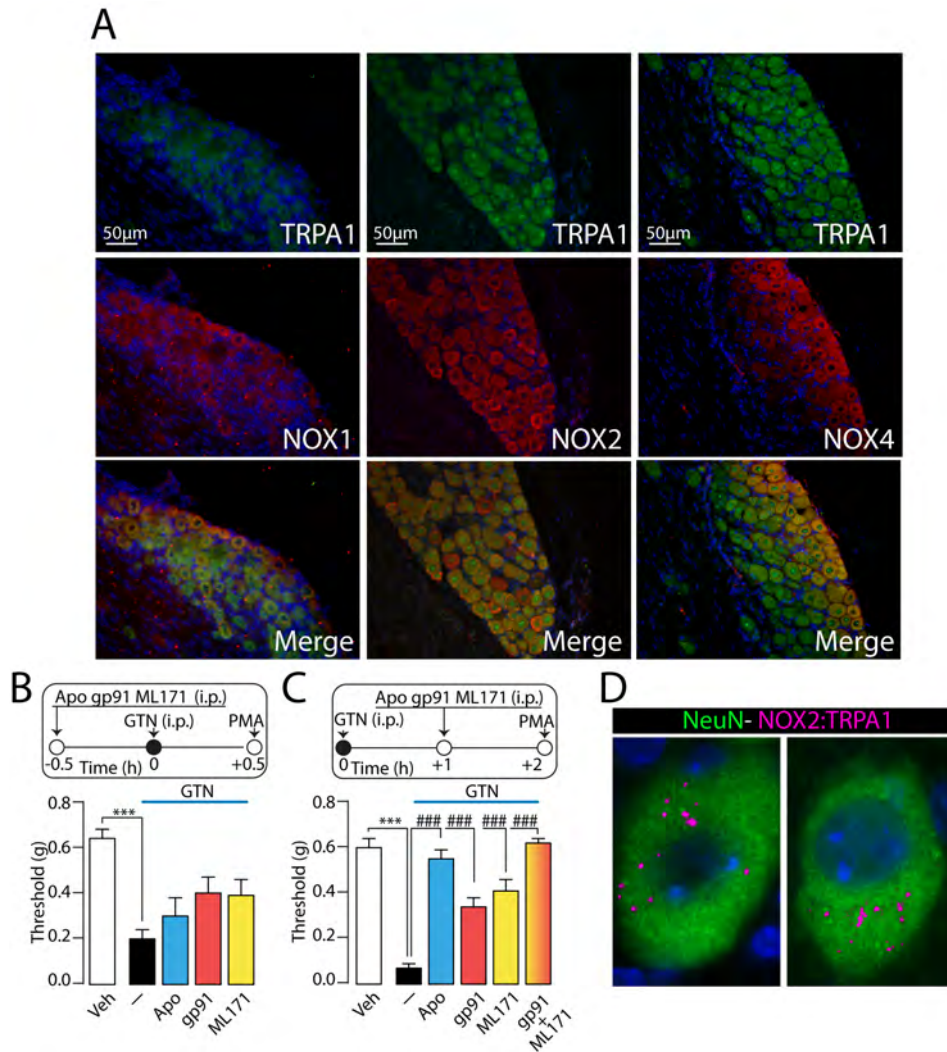


Figure 32. GTN evokes periorbital mechanical allodynia (PMA) via NADPH oxidase dependent mechanism. (A) Representative images of TRPA1, NOX1, NOX2 and NOX4 staining in mouse trigeminal ganglion (TG). (B) The unselective NOX inhibitor, apocynin (APO; 100 mg/kg), the selective (C) NOX2 (gp91ds-tat peptide, gp91; 10 mg/kg) or the selective NOX1 (ML171; 60 mg/kg) (i.p., all pre-GTN) do not affect PMA evoked by systemic (i.p.) GTN (10 mg/kg). (C) APO (100 mg/kg), gp91 (10 mg/kg) or ML171 (60 mg/kg) (i.p., all post-GTN) partially reduce PMA. The combination of gp91 and ML171 (i.p., post-GTN) reverses PMA measured 2 h after GTN. (D) *In situ* proximity ligation assays (PLAs) for TRPA1:NOX2 in mouse TG labelled with NeuN. Veh is the vehicle of GTN. Dash (-) indicates vehicles of treatments. Error bars indicate mean \pm SEM, 7-8 mice per group. *** $P < 0.001$ vs. Veh. #### $P < 0.001$ vs. GTN; one-way ANOVA with Bonferroni post-hoc correction.

CGRP contributes only in part to GTN-evoked allodynia

As CGRP is a key mediator of migraine headaches the contribution of CGRP to GTN-induced vasodilation and PMA was explored. Two different CGRP receptor antagonists, CGRP₈₋₃₇ and BIBN4096BS (olcegepant) given (i.p.) after, but not before GTN partially inhibited PMA (Fig. 33A). CGRP₈₋₃₇ or BIBN4096BS administered

centrally (i.th.) either before or after GTN did not affect GTN-evoked PMA (**Fig. 33B**). Local CGRP (s.c., 0.5-5 $\mu\text{g}/10\mu\text{l}$) in the periorbital area induced a dose-dependent and sustained (4 h) PMA (**Fig. 33C**). Local (s.c.) pretreatment with CGRP₈₋₃₇ or BIBN4096BS prevented CGRP-induced PMA (**Fig. 33D**). Local administration of CGRP₈₋₃₇ or BIBN4096BS after, but not before GTN, partially attenuated PMA in a manner similar to that produced by their systemic administration (**Fig. 33E**). GTN-evoked increase in cutaneous blood flow was unaffected by the pretreatment with BIBN4096BS (**Fig. 33F**). Thus, the early vasodilation evoked by GTN is unrelated to CGRP.

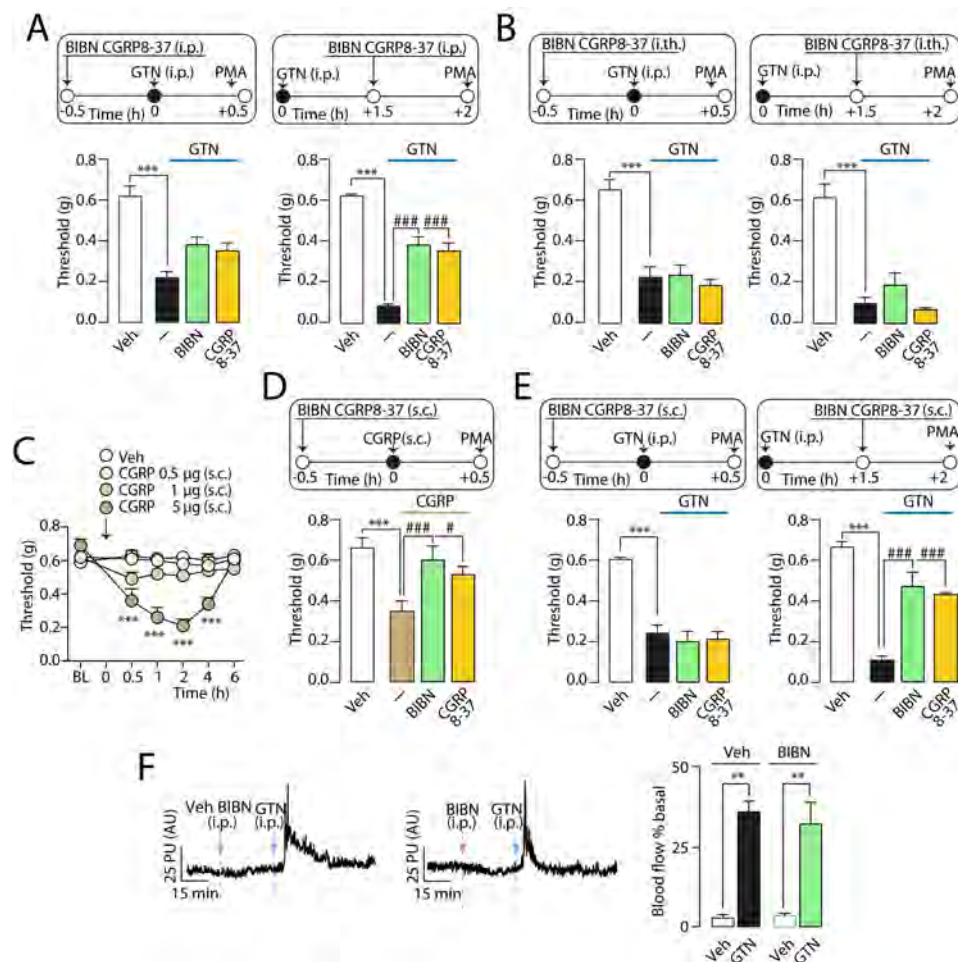


Figure 33. CGRP released from periorbital nerve terminals contributes to GTN evoked periorbital mechanical allodynia (PMA). (A) PMA evoked by systemic (i.p.) GTN (10 mg/kg) is partially reduced by i.p. administration of CGRP₈₋₃₇ (4 $\mu\text{mol}/\text{kg}$) or BIBN4096BS (BIBN; 1 mg/kg), when given post-, but not pre-GTN. (B) Intrathecal (i.th.) administration of CGRP₈₋₃₇ (5 nmol) or BIBN (1 μg) pre- and post-GTN (10 mg/kg) does not affect GTN-evoked PMA. (C) Local (s.c.) CGRP (0.5-5 μg) evokes a dose- and time-dependent PMA. (D) Pretreatment with local (s.c.) BIBN (4 nmol) or CGRP₈₋₃₇ (10 nmol) prevents CGRP (5 μg)-evoked PMA. (E) Local (s.c.) CGRP₈₋₃₇ (10 nmol) or BIBN (4 nmol) reduce PMA when given post-, but not pre-GTN

(i.p., 10 mg/kg). BL, baseline mechanical threshold. Veh is the vehicle of GTN or CGRP. Dash (-) indicates vehicles of treatments. Data are presented as mean \pm SEM of 6-8 mice per group. *** $P < 0.001$ vs. Veh. # $P < 0.05$, ### $P < 0.001$ vs. GTN or CGRP; one-way and two-way ANOVA with Bonferroni post-hoc correction. (F) Representative traces and pooled data of the increases in periorbital skin blood flow evoked by GTN (i.p., 10 mg/kg). Pretreatment with systemic (i.p.) BIBN (1 mg/kg) does not affect the early increase in blood flow. Data are presented as mean \pm SEM of 6-7 mice per group. ** $P < 0.01$ vs. Veh; one-way ANOVA with Bonferroni post-hoc correction.

Discussion

TRPA1 expressed by primary sensory neurons exhibits the distinctive property to detect and to be sensitized by a series of endogenous molecules, which play a major role in inflammation and tissue injury. These molecules are by products of oxidative and nitrative stress which affect and damage a vast array of molecules, but only recently have been identified as a major pathway, that by TRPA1, signal pain and neurogenic inflammation. Thus, TRPA1 seems to be involved in different types of pain, as inflammatory pain, neuropathic pain and migraine headache.

The present findings show for the first time that TRPA1 is essential in generating pain-like behaviors in a model of mechanical injury of the trigeminal nerve, as genetic ablation of this channel totally prevented non-evoked nociceptive behavior, mechanical allodynia, and cold and chemical hypersensitivity produced by CION. Remarkably, TRPA1-deleted mice were fully protected from all CION-evoked pain-like behaviors over the entire period of observation (20 days). Since the effect of TRPA1 genetic deletion in preventing, and TRPA1 pharmacological blockade in reverting cold hypersensitivity parallels the results obtained with mechanical hypersensitivity, it may be concluded that channel engagement mediates in mice responses that recapitulate the major symptoms observed in trigeminal neuropathic pain.

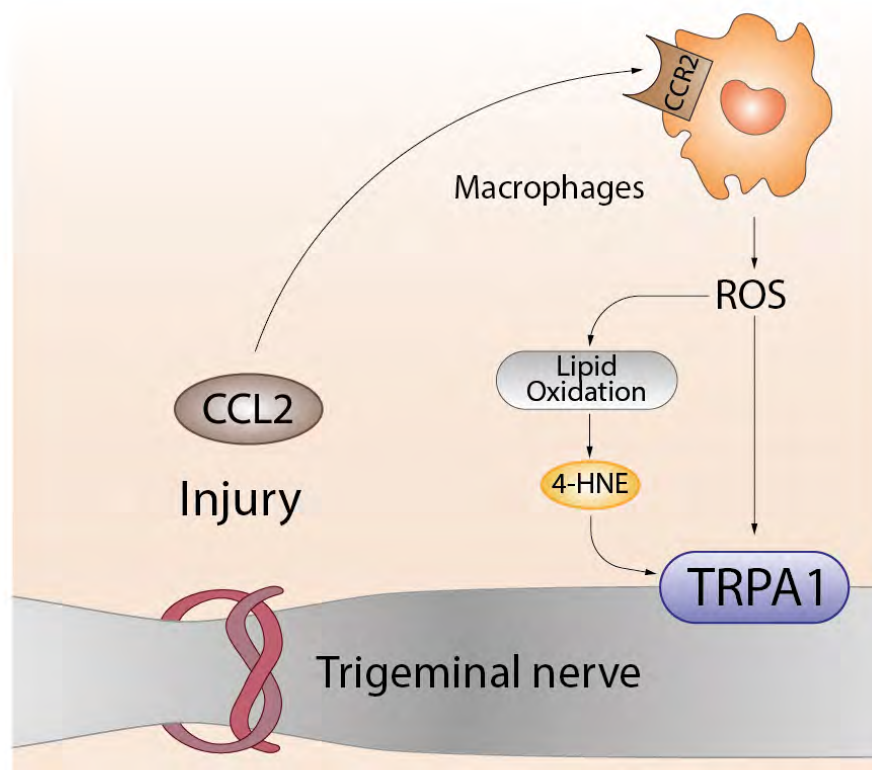
The key role of TRPA1 in the maintenance of CION-evoked nociception and mechanical/cold hypersensitivity is further corroborated by pharmacological findings. At day 10, when nociception and hypersensitivity robustly persisted, systemic administration of the selective TRPA1 antagonists, HC-030031 and A-967079, completely reverted all pain-like behaviors, thus indicating that some hitherto undefined endogenous mechanisms promote the ongoing channel activation that maintains the altered condition. Furthermore, repeated systemic treatment with HC-030031 at the time of nerve injury delayed, but did not prevent, the onset of pain-like behaviors, thus suggesting that a possible therapy with channel antagonists must consider a chronic schedule of treatment. The observation that local HC-030031 attenuated pain-like behaviors only when injected ipsilaterally to the injury indicates that TRPA1 targeting is confined to the damaged nerve. However, due to the close proximity of the injection site to both the injured nerve trunk and the skin area where hypersensitivity is assayed, the precise site of action of the TRPA1 antagonist remains unidentified.

Although fluctuations in the expression of transient receptor potential channels have been described in some rodent models of nerve injury (Jiang et al., 2014; Li et al., 2013), no change in TRPA1 protein expression was found in the infraorbital nerve under the present experimental circumstances. However, we observed a selective hypersensitivity in behavioral responses to TRPA1 agonists in CION mice. One possible interpretation is that, rather than TRPA1 upregulation, some unidentified mechanism, activated within the injured nerve trunk or in the neighboring tissue, engages the channel to cause the hypersensitivity. The finding that the putative endogenous channel agonist, H₂O₂, caused an exaggerated response in CION mice points to oxidative stress byproducts as possible mediators of the perpetuation of the TRPA1 activation.

The current observation that α -lipoic acid reverted CION-evoked spontaneous nociception and mechanical and cold hypersensitivity indicates that oxidative stress byproducts, generated by nerve injury, promote pain-like behaviors. It is well established that reactive molecules activate TRPA1, which, for this reason, is considered a sensor of oxidative stress (Bessac et al., 2008; Nassini et al., 2014). Thus, as both TRPA1 blockade and oxidative stress inhibition diminished non-evoked nociceptive behavior and mechanical/cold hypersensitivity, it can be proposed that oxidative stress byproducts *via* TRPA1 mediate CION-evoked pain-like behaviors. As for HC-030031, also in the case of α -lipoic acid ipsilateral, but not contralateral, treatment recapitulated the protective effects obtained with the systemic antioxidant administration. Thus, oxidative stress byproducts necessary and sufficient to develop the TRPA1-dependent hyperalgesic phenotype must be produced in the vicinity of the injured nerve trunk. Biochemical and morphological evidence robustly supports this hypothesis.

CION increased both SOD activity and H₂O₂ levels in tissue homogenates of perineural tissue, containing the injured nerve. In addition, CION remarkably augmented 4-HNE staining, which appeared mostly localized within and around TRPA1-expressing nerve bundles. The close proximity of 4-HNE and TRPA1 channels supports the hypothesis that oxidative stress byproducts are the mediators that initiate and maintain the ongoing TRPA1-dependent pain-like condition. Attenuation of nociception/hypersensitivity by apocynin, indicates NOX-dependent production of superoxide anion as the early and upstream step in the enzymatic chain that eventually results in the increased H₂O₂ and 4-HNE tissue levels and the ensuing pain-like behaviors. Reduced nociception provided by perineural application of apocynin further reinforces

the proposal that oxidative stress produced locally is the main contributing factor in CION-evoked pain-like behaviors. Thus, the most parsimonious hypothesis originated by data reported so far indicates that in the CION mouse model increased oxidative stress byproducts are required to activate neuronal TRPA1, which promotes pain-like behaviors, and that these events are initiated and persist over time within and in the vicinity of the ligated nerve trunk. Nevertheless, present findings do not exclude that after initial events occurring at the injured nerve trunk, upstream sites in the pain pathway exaggerate nociceptive signals. Although TRPA1 protein expression was not increased in TG neurons after CION, the observation that freshly dissociated TG neurons are selectively hypersensitive to TRPA1 activation is in line with this hypothesis. However, the identification of additional contributing mechanisms to the CION-evoked hypersensitivity in the TG or in the central nervous system is beyond the purpose of the present study.



TRPA1-dependent mechanisms in the constriction of the infraorbital nerve (CION). The drawing depicts the possible cellular and molecular events contributing to TRPA1-dependent pain-like behaviors induced by the CION. CION surgery promotes, within the injured area, the release of the chemoattractant chemokine (C-C motif) ligand 2 (CCL2), which, in turn, stimulates monocyte/macrophage recruitment and activation to generate oxidative stress (reactive oxygen species, ROS) and lipid peroxidation (4-hydroxynonenal, 4-HNE) byproducts, which engage TRPA1 in nociceptors, thus evoking pain-like behaviors.

Neuropathic pain, which follows nerve injury, has long been known to be associated

with Wallerian degeneration, whose hallmark is represented by local infiltration of inflammatory cells (Gaudet, 2008). However, much uncertainty remains regarding the mechanisms that from such cellular recruitment and activation result in pain symptoms. In the present mouse model, we found a remarkable increase in the monocytes/macrophages, which accumulated at the site of nerve damage. The ability of the monocyte/macrophage depleting agent, clodronate, to attenuate the increase in H₂O₂, 4-HNE tissue levels and nociception/hypersensitivity underlines the essential role of the cellular infiltration in CION-evoked pain-like behaviors. Present observations that CION increased CCL2 levels within the injured area, and that both a systemic and perineural anti-CCL2 antibody attenuated monocyte/macrophage accumulation, H₂O₂ and 4-HNE increases, and nociception/hypersensitivity, indicate that local CCL2 release is a major contributing mechanism, most likely placed upstream to the cascade of cellular and molecular events that drive TRPA1-dependent pain-like behaviors.

Thus, the present study identifies for the first time the mechanisms that, from the original nerve insult, determine the pain-producing engagement of TRPA1 in a model of trigeminal neuropathic pain. However, a number of questions remain to be addressed, and some study limitations should be mentioned. While TRPA1 or oxidative stress blockade fully abrogated CION-evoked pain-like behaviors, CCL2 immunological inhibition and monocyte/macrophage depletion were associated with a substantial, but incomplete, attenuation of such responses. Residual effects could be due to inadequacy in terms of dosing or timing of the pharmacological interventions (CCL2-ab and clodronate), or because additional cell type(s) and mediator(s) give a minor, but still meaningful, contribution to the overall phenomenon. Indeed, while CCL2, which is released by a variety of resident or inflammatory cells, seems to play a major role, it is possible that other chemokines or additional proinflammatory mediators, upstream to CCL2, may contribute. Trigeminal neuropathic pain affects a substantial proportion of the general population (Zakrzewska, 2013; Zakrzewska et al., 2014), and patient treatment remains unsatisfactory (Renton et al., 2012). Present findings that CCL2-dependent monocyte/macrophage accumulation and the ensuing oxidative stress byproducts that engage TRPA1 are key factors for the development and maintenance of pain-like behaviors in a mouse model of trigeminal neuropathic pain offer a new interpretation of the pathophysiology of this condition.

However, while exploring a similar model (partial sciatic nerve ligation, pSNL), we surprisingly observed that mice with genetic deletion or pharmacological blockade of TRPA1 not only showed the expected reduced mechanical allodynia, but also exhibited marked reduction of macrophages infiltration and H₂O₂ generation in the injured nerve. By a series of genetic and pharmacological interventions and, more importantly, by generating mice with conditional TRPA1 deletion in Schwann cells (SCs) (*Plp1-CreERT;Trpa1^{fl/fl}*) or nociceptors (*Adv-CreERT;Trpa1^{fl/fl}*), we found that Schwann cells ensheathing fibres of the damaged nerve trunk orchestrate a series of molecular events that sustain allodynia. SCs are recognized as indispensable components to maintain neuronal structure and function, nourish axons, and promote survival and growth upon injury. Schwann cells also regulate local immune responses by secreting cytokines and chemokines, which will further attract immune cells to the site of injury, thus shaping immune responses that can lead to inflammatory neuropathies. We report the discovery of a critical, yet unexpected, role for TRPA1 in Schwann cells in neuroinflammation and ensuing neuropathic pain. The results support the view that nociceptor TRPA1 is the ultimate peripheral target to signal pSNL-evoked allodynia to the brain. However, our findings demonstrate that Schwann cell TRPA1, rather than neuronal TRPA1, orchestrates the neuroinflammation and oxidative stress that sustain neuropathic pain.

Diverse lines of evidence support the hypothesis that Schwann cell TRPA1 is necessary and sufficient to mediate neuroinflammation and neuropathic pain. TRPA1 blockade, achieved with chemically unrelated antagonists, markedly decreased macrophage accumulation and the oxidative burden in the injured nerve. Studies of *Trpa1^{-/-}* mice confirmed the findings obtained with pharmacological antagonists. Although in the present model of neuropathic pain both approaches unequivocally demonstrated the key role of TRPA1, they could not discriminate between the specific contribution of neuronal vs. non-neuronal channels. TRPA1 is expressed by peptidergic primary sensory neurons that, by releasing SP and CGRP, promote neurogenic inflammation. Stimulants of neurogenic inflammation, including the prototypic TRPV1 agonist capsaicin, evoke a transient and moderate inflammatory response, which is chemokine/cytokine-independent and is characterized by CGRP-mediated arteriole vasodilatation and SP-mediated plasma protein and leukocyte extravasation from postcapillary venules (Nassini et al., 2014). Neuroinflammation is a localized and persistent inflammatory process that is confined to the injured nerve and neighboring tissues. The hallmarks of

neuroinflammation encompasses chronic infiltration of leukocytes, activation of glial cells, and increased production of inflammatory mediators, including a series of cytokines and chemokines and neuropathic pain. Experiments with RTX, which defunctionalizes TRPV1/TRPA1-expressing neurons and abrogate their sensory and proinflammatory efferent functions (Szallasi et al., 2007), exclude the possibility that TRPA1-dependent neurogenic inflammation contributes to pSNL-evoked neuroinflammation. RTX attenuated mechanical allodynia, but not macrophage number or H₂O₂ levels, which suggests that TRPA1 present in TRPV1⁺ peptidergic neurons may signal allodynia, but does not promote the neuroinflammatory component.

We observed that the site-specific (perineural vs. intrathecal) administration of TRPA1 AS-ODN efficiently disrupted TRPA1 expressed in nociceptors or Schwann cells, respectively, as demonstrated by behavioral and molecular studies. A reduced expression of the nociceptor TRPA1 was associated with attenuation of pain, whereas diminished expression of Schwann cell TRPA1 inhibited both pain and neuroinflammation. These findings support the hypothesis that non-neuronal TRPA1 channels exert a key role in inflammatory cell recruitment and oxidative stress generation. Confirmation of this proposal was derived from experiments with *Plp1-Cre^{ERT};Trpa1^{fl/fl}* mice, which exhibited selective depletion of *Trpa1* in Schwann cells and markedly attenuated neuroinflammation and mechanical allodynia. This novel and critical localization of TRPA1 in Schwann cells represents a plausible explanation for the widely-reported efficacy of TRPA1 antagonists in different models of neuropathic pain produced by nerve injury (Obata et al., 2005), where neuroinflammation is the underlying mechanism of the ongoing pain condition.

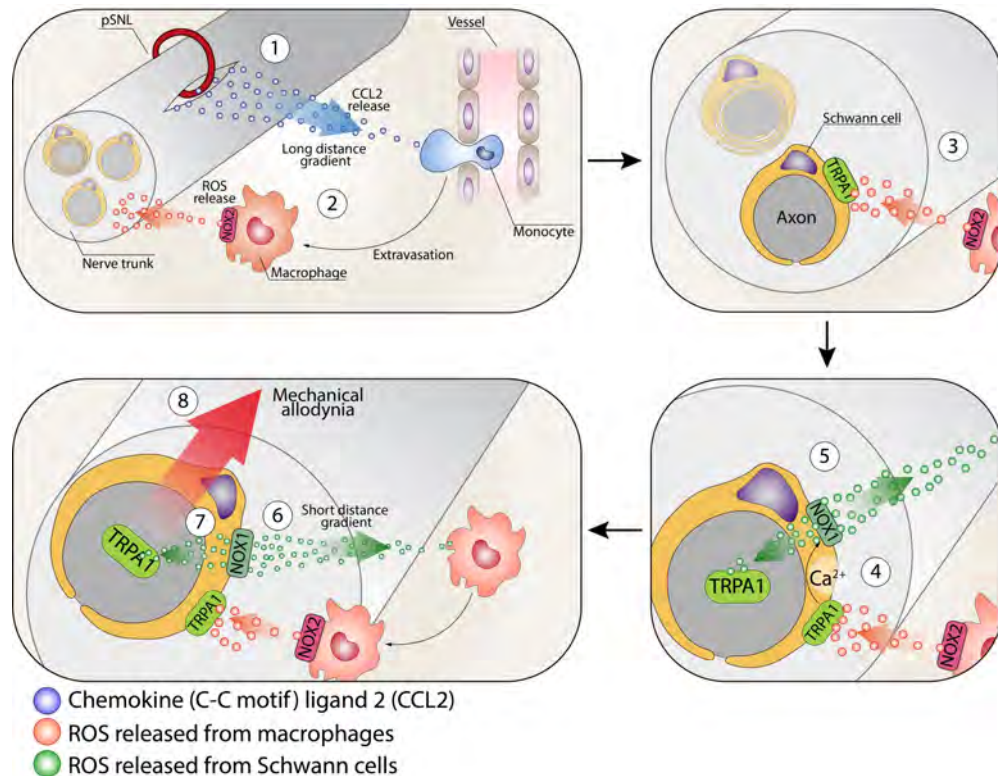
The CCL2 receptor (CCR2) is expressed by primary sensory neurons and is upregulated during neuronal injury, and may activate its cognate receptor CCR2 on TRPV1-positive nociceptors (Kao et al., 2012). The CCL2 system has been reported to augment nociceptor sensitivity by increasing TRPV1 expression (Kao et al., 2012) and TRPA1 and TRPV1 function (Jung et al., 2008). The present findings, showing that CCL2 rapidly increases neuronal hypersensitivity, support the view that this chemokine may directly stimulate primary sensory neurons, thereby enhancing mechanical allodynia under short-lived experimental conditions (Jung et al., 2008). However, as indicated by studies with monocyte/macrophage depletion, CCL2 requires the contribution of infiltrated macrophages within the injured nerve trunk to sustain the allodynia in a

prolonged model of neuropathic pain, such as the pSNL in mice.

Our results reveal distinct kinetics of monocyte/macrophage accumulation by CCL2 and the TRPA1/oxidative stress pathways. Despite its ability to suppress perineural CCL2 levels within 1 hour, a high dose of the CCL2-Ab failed to affect macrophage number, oxidative stress, and allodynia over 6 hours. In contrast, a prolonged, 3-day antibody treatment was required for successful inhibition of neuroinflammation and pain. The persistent temporal frame necessary for CCL2 inhibition to attenuate neuroinflammation and pain is, therefore, markedly different from the very short time-period (1-3 hours) required by TRPA1 antagonists or antioxidants to produce the same inhibitory responses. Oxidative burst has been reported to exert a chemoattractant activity toward monocytes/macrophages (Tauzin et al., 2014), which is limited by time and spatial constraints. Leukocyte-induced H₂O₂ release is a rapid event, lasting a few seconds and is spatially confined to a range that does not exceed a few hundred μm (Niethammer et al., 2009). Our data, including those obtained by genetic or pharmacological manipulation of NOXs, are consistent with previous observations. Macrophages express solely NOX2, while Schwann cells, which potentially express mRNAs for NOX1, NOX2 and NOX4, apparently express only the NOX1 protein. Since NOX1, but not NOX2 or NOX4, inhibitors or AS-ODNs attenuated neuroinflammation and allodynia, it is possible to propose that Schwann cell TRPA1 activates intracellular pathways, including Ca²⁺ transients, resulting in NOX1-dependent release of oxidant molecules. Furthermore, the prominent role of NOX1, but not of NOX2, in generating allodynia excludes phagocyte-derived oxidative burst in the final activation of nociceptor TRPA1.

The most parsimonious explanation of the present results is that oxidative stress generated by Schwann cell TRPA1/NOX1 has bidirectional effects. The inwardly released H₂O₂ targets TRPA1 on adjacent nociceptor nerve fibers in a paracrine fashion to sustain allodynia. The outwardly released H₂O₂ promotes the final part (about 200 μm) of the journey of macrophages, which, deriving from the blood stream, slowly accumulate into the perineural space following the CCL2 gradient. Thereafter, following the Schwann cell derived oxidative stress gradient, macrophages rapidly pass across the perineurium to enter the damaged nerve trunk. TRPA1 has been identified in oligodendrocytes, with possible detrimental roles in ischemia and neurodegeneration (Hamilton et al., 2016). Herein, we extend this observation to Schwann cells, the peripheral analogues of oligodendrocytes, which, *via* TRPA1, orchestrate

neuroinflammation and ensuing neuropathic pain. Amelioration of neuropathic pain by currently developed TRPA1 antagonists may derive from their ability to attenuate macrophage-dependent neuroinflammation.



Cellular and molecular events contributing to TRPA1-mediated mechanical allodynia and neuroinflammation in a neuropathic pain model. Partial sciatic nerve ligation (pSNL) by releasing CCL2 (1) promotes the extravasation of hematogenous monocytes (2) that, *via* their rapid NOX2-dependent oxidative burst (red dots) target the TRPA1 channel localized in Schwann cells (3). TRPA1 activation in Schwann cells evokes a Ca^{2+} -dependent, NOX1-mediated (4) prolonged H_2O_2 (green dots) generation (5) with a dual function. The outward H_2O_2 release (6) produces a space-scaled gradient that determines the final macrophage influx to the injured nerve trunk, whereas the inward H_2O_2 release (7) targets nociceptor TRPA1 to produce mechanical allodynia (8). ROS, reactive oxygen species.

TRPA1 is involved in multiple painful condition, thus we also investigate the role of TRPA1 in pain symptoms associated with the treatment of the third-generation AIs, which include the steroidal agent exemestane, anastrozole and letrozole, currently recommended for adjuvant endocrine treatment as primary, sequential, or extended therapy with tamoxifen, for postmenopausal women diagnosed with estrogen receptor-positive breast cancer. Pain symptoms associated with AIs have recently been more accurately described with the inclusion of neuropathic, diffused, and mixed pain (Laroche

et al., 2014). In our study, we provide for the first time evidence that third-generation steroidal and non-steroidal AIs, selectively target the TRPA1 channel. This conclusion derives from a series of experiments in cells expressing the recombinant human TRPA1 or in rodent DRG neurons expressing the native channel. Indeed, calcium responses and currents evoked by AIs are confined to TRPA1-expressing cells, and are selectively abolished by HC-030031, or absent in neurons obtained from TRPA1-deficient mice. We further show that key cysteine and lysine residues, required for channel activation by electrophilic agonists are also required for TRPA1 activation by AIs. Exemestane exhibits a chemical structure with a system of highly electrophilic conjugated Michael acceptor groups. A variety of known TRPA1 agonists, including acrolein and other α,β -unsaturated aldehydes, possess an electrophilic carbon or sulfur atom that is subject to nucleophilic attack (Michael addition) by cysteine, lysine or histidine residues of TRPA1 (Dalle-Donne et al., 2006). Nitriles also exhibit electrophilic properties, which may result in TRPA1 gating. Non-steroidal letrozole and anastrozole possess nitrile moieties that underscore their potential ability to activate TRPA1. Thus, the three AIs, most likely because of their electrophilic nature, selectively target TRPA1, whereas TRPV1, TRPV2, TRPV3 and TRPV4, all co-expressed with TRPA1, and other channels or receptors in DRG neurons, do not seem to play a relevant role in the direct excitation of nociceptors by AIs.

In vivo stimulation of the irritant TRPA1 receptor in rodents produces an early nociceptive behavior, followed by a delayed and prolonged mechanical allodynia. Subcutaneous exemestane and letrozole recapitulated the two effects produced by TRPA1 agonists, and produced such responses in a TRPA1-dependent way.

As TRPA1 is expressed by a subpopulation of peptidergic nociceptors, which mediate neurogenic inflammation (Bhattacharya et al., 2008; Geppetti et al., 1996), we anticipated that AIs, by targeting TRPA1, release proinflammatory neuropeptides, thereby causing neurogenic plasma extravasation. Pharmacological and genetic findings indicate that AIs produce a specific type of edema, which is neurogenic in nature, a conclusion corroborated by the direct observation that exemestane and letrozole evoke TRPA1-dependent CGRP release in peripheral tissues. The neurogenic component, mediated by TRPA-activation and sensory neuropeptide release, may thus represent an important mechanism contributing to the cytokine-independent inflammation observed in AI users.

When AIs were given to mice by systemic (intraperitoneal or intragastric) administration, no acute nocifensive response was observed, but, after ~1 hour delay they produced a prolonged condition (up to 6 hours) of mechanical allodynia and a decrease in grip strength. Also, in this case, pharmacological and genetic results indicate that AI-evoked pain-like responses are principally TRPA1-dependent. Although the present experimental conditions cannot fully mimic the clinical setting in cancer patients, our findings suggest that the TRPA1-dependent ability of AIs to produce mechanical allodynia and to decrease grip strength is maintained and does not undergo desensitization over a time period of 15 days, which broadly corresponds to a 1-year time in humans. Despite a general good tolerability, AIs produce in number of treated patients some form of pain, including AIMSS, neuropathic pain, diffuse pain and mixed pain (Laroche et al., 2014). The reason why only one tenth-fifth of the patients exposed to AIs develop these severe pain conditions, which may lead to non-adherence or therapy discontinuation, is unknown. Here, we reveal the key role of TRPA1 as the main mediator of exemestane- and letrozole-evoked nociceptor stimulation. However, it is likely that additional factors contribute to determine the development of AIMSS and related pain symptoms, particularly in those susceptible patients (10-20%) who suffer from the more severe form of this adverse reaction. Further, *in vitro* and *in vivo* experiments with the co-administration of AIs and pro-algesic stimuli, such as PAR2-AP, an agonist of the pro-inflammatory receptor, PAR2, and the TRPA1 agonist, H₂O₂ suggest that additional factors cooperate to increase the sensitivity of TRPA1 expressing nociceptors to AIs. Enhancement by PAR2 activation of the proalgesic activity of exemestane and letrozole suggests that under inflammatory conditions the potency of AIs to produce TRPA1-dependent pain-like symptoms is significantly increased. These findings are fully consistent and closely mimic previous observations that PAR2 activation increases the pro-algesic response evoked by TRPA1 agonists (Dai et al., 2007). Both AIs and H₂O₂ are TRPA1 agonists and their combination exaggerates TRPA1 mediated currents in DRG neurons *in vitro* and nociceptive responses *in vivo*. This implies that if oxidative stress byproducts are increased by inflammation, tissue injury by cancer, the AI ability to promote AIMSS and related pain symptoms may be increased. Our present investigation on the cooperation between AIs and proinflammatory mediators has been limited to PAR2 and H₂O₂. However, it is possible that similar cooperating pathways can be activated by additional pro-inflammatory and pro-algesic mediators. Altogether, the present findings

indicate that AIs *per se* or, most likely, in cooperation with other proinflammatory mediators, promote TRPA1-dependent neurogenic inflammation, mechanical hypersensitivity, and decreased grip force.

Aromatase inhibition, while reducing downstream production of estrogens, moderately increases upstream plasma concentrations of androgens, including androstenedione (ASD) (Gallicchio et al., 2011). Exemestane, a false aromatase substrate, blocks enzymatic activity by accommodating in the binding pocket that snugly encloses ASD (Ghosh et al., 2009). We reasoned that ASD, which retains some of the reactive chemical features of exemestane, such as the α,β -carbonyl moiety of the A ring and the ketone group at the 17 position, might target TRPA1.

The major finding of our investigation is that androstenedione, unique among several steroid hormones, activates the TRPA1 channel and *via* this mechanism produces pain-like behaviors, reminiscent of AIMSS. Androstenedione behaves as a TRPA1 agonist across species, as it engages both the recombinant and native human channel and the rat and mouse channel. Androstenedione properties in gating TRPA1 exhibit specific features in as much as channel binding and activation require the presence of key aminoacid residues, namely, three cysteine (C619, C639, C663) and one lysine (K708) residues. As these residues have been found essential for channel activation by electrophilic agonists, androstenedione may be included in this chemical category.

A peculiar feature of androstenedione resides in its unique selectivity profile. In recombinant systems (HEK293 cells) expressing one single channel, androstenedione stimulated TRPA1, but not TRPV1 and TRPV4. Likewise, human lung fibroblasts (IMR90 cells), which constitutively express TRPA1, but not TRPV1, responded to androstenedione in a fully TRPA1-dependent manner. Surprisingly, in rat and mouse DRG neurons, which notoriously express multiple TRP channels, TRPV1 contributes to androstenedione response, as both calcium responses and currents, in addition to HC-030031, were partially reduced by capsazepine, and complete attenuation was only attained by the combination of the two antagonists. Notably, DRG neurons from TRPA1-deficient mice maintained a residual responsiveness to androstenedione, but not to AITC, and the residual response was abolished by capsazepine. One possible explanation for this unexpected finding is that the TRPA1 protein remaining after the homologous recombination, while lacking the domain required for channel activation by most agonists (Nilius et al., 2012), including androstenedione itself, still maintains the domain essential

for TRPV1-dependent androstenedione activity. Further proof of the key role of TRPV1 to the TRPA1-mediated response derives from the observation that the simultaneous antagonism of both TRPA1 and TRPV1 was required for complete inhibition of the response to androstenedione in hTRPA1V1 HEK293 cells.

Tenosynovitis and joint swelling are included within the constellation of symptoms reported by patients treated with AIs. However, association with proinflammatory markers, including cytokines, such as interleukin-6, has been excluded so far (Henry et al., 2008). The ability of androstenedione to release the sensory neuropeptides that mediate neurogenic inflammation or, in combination with letrozole and BSO, to provoke SP and CGRP release *via* TRPA1 activation and the ensuing edema and neutrophil infiltration in the knee joint, suggest that neurogenic inflammatory mechanisms contribute to the inflammatory component of AIMSS. These findings offer further explanations for the absence of correlation between proinflammatory cytokines and the inflammatory component of AIMSS.

The underlying mechanism that causes AIMSS, a complex painful condition that includes myalgias, arthralgias associated with joint swelling, and neuropathic and mixed pain, is unknown. The consequent unsatisfactory patient treatment leads to poor adherence to, or discontinuation of, anticancer therapy. The previous observation that, due to their electrophilic and reactive properties, all three AIs, exemestane, anastrozole and letrozole, target TRPA1, thus evoking pain-like responses and neurogenic inflammation, supported the hypothesis that channel activation in peptidergic nociceptors promotes AIMSS. However, while the three AIs target TRPA1 with remarkable selectivity, they all exhibit low potency at both human and rat/mouse channels. In particular, threshold concentrations of letrozole, able to gate TRPA1 ($>10 \mu\text{M}$), are about 1-2 orders of magnitude higher than those found in mouse and human plasma after therapeutic dosing. This gap between plasma levels and threshold concentrations at TRPA1 argues against the hypothesis that AIs *per se* cause AIMSS. Thus, a direct cause-and-effect relationship between plasma levels of AIs or androstenedione and AIMSS has not yet been unraveled.

However, it is known that TRPA1 is amenable to sensitization by a variety of endogenous proinflammatory and proalgesic mediators (Bautista et al., 2013), and we previously reported that H_2O_2 or proteinase activated receptor-2 stimulation exaggerated TRPA1-dependent responses evoked by AIs. The present novel finding that the aromatase

substrate, androstenedione, activates TRPA1 proposes a novel paradigm to explain AIMSS generation. Multiple factors, which may concomitantly be present under the circumstances generated by breast cancer and AI administration, concur to engage TRPA1 and to cause the ensuing AIMSS-like behaviors. Letrozole (and likely other AIs) is the essential, although *per se* ineffective, initiating stimulus. However, its ability to slightly augment oxidative stress byproducts and androstenedione concentrations (Gallicchio et al., 2011) creates the condition for efficient TRPA1 signaling. Additional circumstances, such as prolonged AI treatment, may augment androstenedione levels (Gallicchio et al., 2011) and it should be underlined that the current hypothesis does not exclude that additional agents, able to activate or sensitize the TRPA1, may act along with AIs and androstenedione to reach the sufficient threshold for AIMSS generation. The present study, while showing that TRPV1 signaling negligibly contributes to androstenedione-evoked AIMSS-like behaviors, robustly underscores the paramount role of TRPA1.

Finally, we studied the role of TRPA1 in another painful condition which affect a large amount of population: migraine pain. Occupational exposure to, or treatment with, organic nitrates has long been known to provoke headaches (Thadani et al., 2006; Trainor et al., 1966). These observations have led to the clinical use of glyceryl trinitrate (GTN) as a reliable provocation test for migraine attacks (Olesen, 2008; Sicuteri et al., 1987). In most subjects, including healthy controls, GTN administration causes a mild headache that develops rapidly and is short-lived. However, after a remarkable time lag (hours) from GTN exposure, migraineurs develop severe headaches that fulfill the criteria of a typical migraine attack (Olesen, 2008; Sicuteri et al., 1987).

We report that the delayed and prolonged GTN-evoked PMA in mice is entirely TRPA1-dependent. Two chemically unrelated TRPA1 antagonists, but not TRPV1 or TRPV4 antagonists, completely reversed PMA. Furthermore, deletion of *Trpa1*, but not *Trpv1* or *Trpv4*, prevented the development of PMA. A recent report that TRPA1 antagonism attenuates GTN potentiation of formalin-evoked periorbital allodynia in rats is in line with our findings (Demartini et al., 2017). We exposed mice to a dose of GTN (10 mg/kg), but which exceeds the dose used in humans (~40 µg/kg, i.v.) (Iversen et al., 1996; Olesen, 2008). However, genetic deletion or pharmacological blockade of TRPA1 also suppressed PMA evoked by a low dose of GTN (1 mg/kg). The observation that, after correction for the mouse to man conversion factor (Reagan-Shaw et al., 2008), this

dose is only two-fold higher than the human dose, supports the translational relevance of the role of TRPA1 in GTN-evoked allodynia in mice.

NO activation of TRPA1, either directly, or indirectly *via* its byproducts, through nitrosylation of cysteinyl residues, is an important posttranslational mechanism of channel regulation. NO donors activate TRPA1 in cultured TG neurons and hTRPA1-HEK293 cells by distinct mechanisms. As Ca^{2+} -responses by SNAP, but not those by GTN, were inhibited by the NO scavenger, cPTIO, NO does not seem required for TRPA1 activation by GTN. It is possible that under *in vitro* conditions NO is released with insufficient velocity or in insufficient amounts to elicit TRPA1 gating, while the channel is engaged directly by GTN which binds to the same key cysteine/lysine residues required for channel activation by electrophilic and oxidant molecules.

In vivo GTN induces PMA *via* diverse anatomical pathways, mechanisms and time courses that depend from the route of administration. As the ALDH2 inhibitor, disulfiram, and the NO scavenger, cPTIO, blocked PMA elicited by systemic, but not local administration of GTN, local GTN likely causes allodynia by targeting TRPA1 by a direct, NO-independent mechanism, whereas systemic GTN by an indirect, NO dependent pathway. As a consequence, the ability of NO released from GTN to target TRPA1 requires that the conversion occurs distant from the site where NO engages the channel. Evidence that NO must have spent some time in the extracellular environment before leading to S-nitrosothiol formation supports this explanation. Furthermore, the observation that cPTIO and disulfiram prevent allodynia when administered before, but not after systemic GTN implies that NO is initially necessary, but is not subsequently sufficient, to sustain the allodynia. Attenuation by two different TRPA1 antagonists, HC-030031 or A967079, of GTN-evoked allodynia was a transient phenomenon, probably due to the limited half-lives of the antagonists in mice. These findings suggest that, to maintain allodynia, TRPA1 must be engaged continuously by one or more mediators generated by GTN/NO and whose identity and source are unknown.

GTN generates oxidative stress (Wenzl et al., 2009). The observation that pretreatment with the ROS scavengers, α LA or PBN, did not prevent GTN-evoked PMA, but attenuated allodynia from for 3-4 h after GTN, indicates that ROS do not initiate the response, but mediate the ensuing phase. However, additional TRPA1 agonists must contribute to the final phase of PMA, when antioxidants were ineffective. Carbonylic byproducts of oxidative stress, including 4-HNE, have half-lives longer than ROS (Brame

et al., 1999), and are known to target TRPA1 (Trevisani et al., 2007). PMA attenuation by NAC and L-carnosine, which efficiently quenches aldehydes, indicates that 4-HNE and/or related aldehydes engage TRPA1 to mediate the terminal phase of PMA, from 3-4 to 8 h after GTN.

Failure of local and efficacy of intrathecal antioxidants and TRPA1 antagonists to block PMA indicate that systemic GTN/NO does not target TRPA1 on cutaneous terminals of nociceptor and suggests the involvement of TRPA1 in a central site, such as the soma and central terminals in the brainstem of TG neurons. Assessment of GTN-induced oxidative stress showed no change in the dorsal brain stem, whereas a marked increase in H₂O₂ and 4-HNE levels were found in TGs. Remarkably, the time course of H₂O₂ formation (1-3 h) paralleled the ability of ROS scavengers to attenuate PMA, and the time course of increased 4-HNE staining (3-6 h) paralleled the ability of aldehyde scavengers to inhibit PMA.

Primary sensory neurons and associated SGCs are most abundant cell types in TG. The observation that resiniferatoxin, which defunctionalises TRPV1/TRPA1 expressing nociceptors, attenuated GTN-evoked H₂O₂ generation *in vivo*, suggests that TG neurons rather than SGCs generate oxidative stress. As pharmacological blockade of TRPA1, global TRPA1 deletion, selective deletion of TRPA1 in peripheral sensory neurons and TRPA1 knockdown all abrogated GTN-evoked oxidative stress and PMA, TRPA1 expressed by TG sensory neurons seems to be a critical step for PMA. Although various TRP channels can promote ROS release (Shimizu et al., 2014), to our knowledge this is the first evidence that TRPA1 expressed by cell bodies of primary sensory neurons increase the tissue burden of oxidative stress. Sensory neurons express several NOX isoforms that may mediate the GTN/NO/TRPA1 signal (Bedard et al., 2007). TG neurons, but not SGCs, co-express TRPA1 and NOX1, NOX2 and NOX4, and the NOX inhibitor apocynin reverses GTN-evoked mechanical allodynia, thus suggesting that NOXs expressed by TG neurons and located downstream from TRPA1 generate the pro-allodynic oxidative burden. NOX1 and NOX2 isoforms provide a major contribution, since the combination of selective NOX1 and NOX2 inhibitors afforded complete inhibition of allodynia. Notably, similar to α LA, the capacity of NOX inhibitors to suppress allodynia faded with time and was absent when the drugs were administered 3-4 h after GTN.

Several findings of the current study support the hypothesis that TRPA1/NOXs,

ROS and aldehydes sustain GTN-evoked PMA by an action that is confined to TGs. First, GTN induced ROS/HNE in TG but not the brain stem. In particular, failure to identify any increase in HNE staining in any specific brainstem area supports the hypothesis that oxidative stress is not generated at this level. Second, intrathecal administration of TRPA1 channel antagonists or antisense oligonucleotides attenuated this response. Third, both GTN-evoked PMA and ROS/HNE generation were attenuated by resiniferatoxin, which selectively desensitises TRPV1-expressing primary sensory neurons, a population that encompasses the TRPA1-positive subpopulation. Finally, similar attenuation was found in mice expressing Cre-recombinase from the locus of the primary sensory neuron-specific gene *Advillin*, resulting in a selective TRPA1 mRNA attenuation in nociceptors. Although our findings suggest a key role for TRPA1 in TG neurons, the present study did not systematically investigate the possibility that TRPA1 activation and oxidative stress in the central nervous system also contribute to GTN-evoked PMA. The ability of centrally administered NO-donors to affect the function of neurons of the spinal trigeminal nucleus (Koulchitsky et al., 2004; Koulchitsky et al., 2009) suggests that GTN can also act centrally. Furthermore, the cell bodies of TG neurons that mediate allodynia *via* TRPA1/NOX/oxidative stress may belong to meningeal nociceptors, which are known to contribute to the sensitisation process observed after exposure to inflammatory mediators or GTN (Levy et al., 2007; Strassman et al., 1996).

The beneficial action of CGRP/CGRP receptor blockade by small molecules or monoclonal antibodies indicate that CGRP is a major mediator of migraine headaches (Edvinsson, 2015; Ho et al., 2008). The observation that two different CGRP receptor antagonists, when administered by systemic or local routes, but not central administration, reduced GTN-evoked PMA suggests that CGRP acts at a peripheral site. One possible explanation is that excitation of the NO/TRPA1/NOX pathway in the soma of TG neurons generates antidromic action potentials, which ultimately invade cutaneous nerve terminals to promote local CGRP release. The observation that a CGRP monoclonal antibody, which does not cross the blood brain barrier and should act peripherally, attenuates PMA-induced by sodium nitroprusside plus sumatriptan in rats (Kopruszinski et al., 2017), supports the existence of a peripheral mechanism. However, further studies are required to examine the effects of GTN on antidromic transmission in TG neurons. Our findings that CGRP provides a limited and delayed contribution to the allodynia may explain the failure of BIBN4096BS to reduce GNT-evoked migraine-like pain in patients

(Tvedskov et al., 2010). Notably, we report that the early periorbital vasodilation elicited by GTN is entirely due to ALDH2-dependent NO formation, but neither TRPA1 nor CGRP are involved. Thus, vasodilatation and allodynia are temporally and mechanistically distinct. While vasodilatation is probably due to a direct NO action in the vascular smooth muscle, allodynia is a neuronal phenomenon mediated by TRPA1 activation and the ensuing oxidative stress.

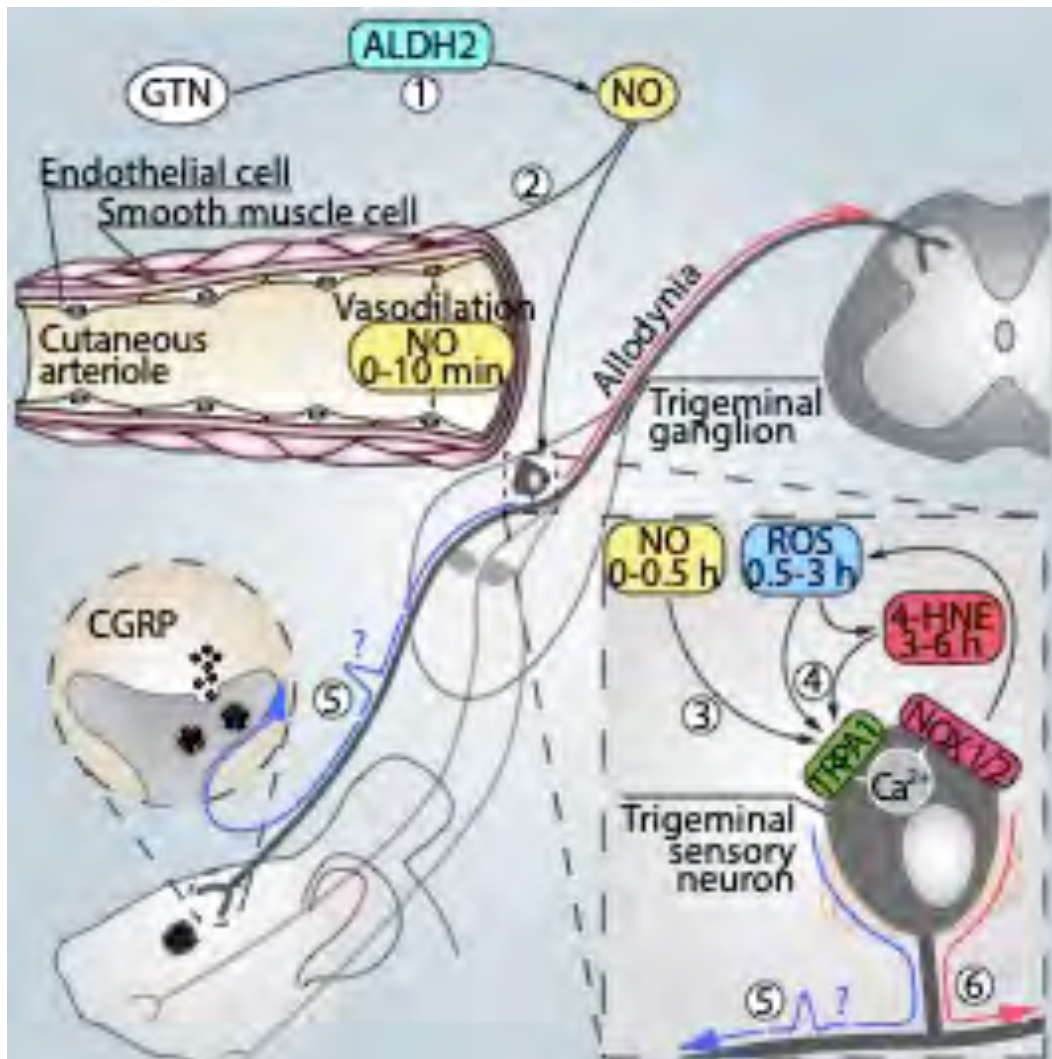
Our present results suggest that systemic GTN is converted by ALDH2 to NO that causes a transient vasodilatation unrelated to TRPA1 and most probably due to a direct action of the gaseous mediator on smooth muscle guanylyl cyclase. NO and/or its byproducts also target TRPA1/NOXs in the soma of TG neurons to increase ROS/RCS, thereby sustaining mechanical allodynia. In this view, the channel that triggers the oxidative burst is expressed by the same sensory neurons that potentially mediate the allodynia. Thus, it is not possible to discriminate whether TRPA1, in addition to generating the proalgesic oxidative stress, is also the final mediator of the hypersensitivity. Nevertheless, since TRPA1 is a major sensor of oxidative and carbonylic stress, it is possible that ROS/4-HNE, generated by TRPA1 activated by GTN/NO, target the same neuronal channel to signal allodynia.

In conclusion, our studies showed that different mechanisms identified TRPA1 as pharmacological targets for drug development in different condition, ranging from inflammatory to neuropathic pain. We showed that neuronal TRPA1 is essential in generating pain-like behaviors in a model of mechanical injury of the trigeminal nerve. We extend this observation to Schwann cells, which, *via* TRPA1, orchestrate neuroinflammation and ensuing neuropathic pain. Thus, amelioration of neuropathic pain by currently developed TRPA1 antagonists may derive from their ability to attenuate macrophage-dependent neuroinflammation.

Further, we showed the involvement of TRPA1 in another painful condition such as AIMSS induced by treatment with aromatase inhibitors. Data indicated that AIs *per se* or, most likely, in cooperation with other proinflammatory mediators, promote TRPA1-dependent neurogenic inflammation, mechanical hypersensitivity, and decreased grip force. This novel pathway may represent the main underlying mechanism responsible for pain and inflammatory symptoms associated with AI treatment.

In conclusion, our data clearly showed that TRPA1 antagonists, which are currently in clinical development, or established anti-migraine drugs, which have recently been

identified as selective channel inhibitors may be used to test whether a mechanism similar to the present one mediates the delayed attack evoked by GTN in migraineurs.



References

- Abrahamsen B, Zhao J, Asante CO, Cendan CM, Marsh S, Martinez-Barbera JP, *et al.* (2008). The cell and molecular basis of mechanical, cold, and inflammatory pain. *Science* 321: 702-705.
- Alemi F, Kwon E, Poole DP, Lieu T, Lyo V, Cattaruzza F, *et al.* (2013). The TGR5 receptor mediates bile acid-induced itch and analgesia. *J Clin Invest* 123: 1513-1530.
- Alessandri-Haber N, Dina OA, Joseph EK, Reichling DB, & Levine JD (2008). Interaction of transient receptor potential vanilloid 4, integrin, and SRC tyrosine kinase in mechanical hyperalgesia. *J Neurosci* 28: 1046-1057.
- Amin FM, Asghar MS, Ravneberg JW, de Koning PJ, Larsson HB, Olesen J, *et al.* (2013). The effect of sumatriptan on cephalic arteries: A 3T MR-angiography study in healthy volunteers. *Cephalalgia* 33: 1009-1016.
- Andre E, Campi B, Materazzi S, Trevisani M, Amadesi S, Massi D, *et al.* (2008). Cigarette smoke-induced neurogenic inflammation is mediated by alpha,beta-unsaturated aldehydes and the TRPA1 receptor in rodents. *J Clin Invest* 118: 2574-2582.
- Atoyan R, Shander D, & Botchkareva NV (2009). Non-neuronal expression of transient receptor potential type A1 (TRPA1) in human skin. *J Invest Dermatol* 129: 2312-2315.
- Bandell M, Story GM, Hwang SW, Viswanath V, Eid SR, Petrus MJ, *et al.* (2004). Noxious cold ion channel TRPA1 is activated by pungent compounds and bradykinin. *Neuron* 41: 849-857.
- Bang S, Kim KY, Yoo S, Kim YG, & Hwang SW (2007). Transient receptor potential A1 mediates acetaldehyde-evoked pain sensation. *Eur J Neurosci* 26: 2516-2523.

- Baraldi PG, Romagnoli R, Saponaro G, Aghazadeh Tabrizi M, Baraldi S, Pedretti P, *et al.* (2012). 7-Substituted-pyrrolo[3,2-d]pyrimidine-2,4-dione derivatives as antagonists of the transient receptor potential ankyrin 1 (TRPA1) channel: a promising approach for treating pain and inflammation. *Bioorg Med Chem* 20: 1690-1698.
- Barriere DA, Rieusset J, Chanteranne D, Busserolles J, Chauvin MA, Chapuis L, *et al.* (2012). Paclitaxel therapy potentiates cold hyperalgesia in streptozotocin-induced diabetic rats through enhanced mitochondrial reactive oxygen species production and TRPA1 sensitization. *Pain* 153: 553-561.
- Bautista DM, Jordt SE, Nikai T, Tsuruda PR, Read AJ, Poblete J, *et al.* (2006). TRPA1 mediates the inflammatory actions of environmental irritants and proalgesic agents. *Cell* 124: 1269-1282.
- Bautista DM, Pellegrino M, & Tsunozaki M (2013). TRPA1: A gatekeeper for inflammation. *Annu Rev Physiol* 75: 181-200.
- Bayliss WM (1901). On the origin from the spinal cord of the vaso-dilator fibres of the hind-limb, and on the nature of these fibres. *J Physiol* 26: 173-209.
- Bedard K, & Krause KH (2007). The NOX family of ROS-generating NADPH oxidases: physiology and pathophysiology. *Physiol Rev* 87: 245-313.
- Benemei S, Nicoletti P, Capone JG, De Cesaris F, & Geppetti P (2009). Migraine. *Handb Exp Pharmacol* 194: 75-89.
- Beretta M, Gruber K, Kollau A, Russwurm M, Koesling D, Goessler W, *et al.* (2008). Bioactivation of nitroglycerin by purified mitochondrial and cytosolic aldehyde dehydrogenases. *J Biol Chem* 283: 17873-17880.

- Bessac BF, Sivula M, von Hehn CA, Caceres AI, Escalera J, & Jordt SE (2009). Transient receptor potential ankyrin 1 antagonists block the noxious effects of toxic industrial isocyanates and tear gases. *Faseb J* 23: 1102-1114.
- Bessac BF, Sivula M, von Hehn CA, Escalera J, Cohn L, & Jordt SE (2008). TRPA1 is a major oxidant sensor in murine airway sensory neurons. *J Clin Invest* 118: 1899-1910.
- Bevan S, Hothi S, Hughes G, James IF, Rang HP, Shah K, *et al.* (1992). Capsazepine: a competitive antagonist of the sensory neurone excitant capsaicin. *Br J Pharmacol* 107: 544-552.
- Bhattacharya MR, Bautista DM, Wu K, Haeberle H, Lumpkin EA, & Julius D (2008). Radial stretch reveals distinct populations of mechanosensitive mammalian somatosensory neurons. *Proc Natl Acad Sci U S A* 105: 20015-20020.
- Bianchi BR, Zhang XF, Reilly RM, Kym PR, Yao BB, & Chen J (2012). Species comparison and pharmacological characterization of human, monkey, rat, and mouse TRPA1 channels. *J Pharmacol Exp Ther* 341: 360-368.
- Bolcskei K, Helyes Z, Szabo A, Sandor K, Elekes K, Nemeth J, *et al.* (2005). Investigation of the role of TRPV1 receptors in acute and chronic nociceptive processes using gene-deficient mice. *Pain* 117: 368-376.
- Bonet IJ, Fischer L, Parada CA, & Tambeli CH (2013). The role of transient receptor potential A 1 (TRPA1) in the development and maintenance of carrageenan-induced hyperalgesia. *Neuropharmacology* 65: 206-212.
- Brame CJ, Salomon RG, Morrow JD, & Roberts LJ, 2nd (1999). Identification of extremely reactive gamma-ketoaldehydes (isolevuglandins) as products of the isoprostane pathway and characterization of their lysyl protein adducts. *J Biol Chem* 274: 13139-13146.

- Burstein HJ, Prestrud AA, Seidenfeld J, Anderson H, Buchholz TA, Davidson NE, *et al.* (2010). American Society of Clinical Oncology clinical practice guideline: update on adjuvant endocrine therapy for women with hormone receptor-positive breast cancer. *J Clin Oncol* 28: 3784-3796.
- Caceres AI, Brackmann M, Elia MD, Bessac BF, Del Camino D, D'Amours M, *et al.* (2009). A sensory neuronal ion channel essential for airway inflammation and hyperreactivity in asthma. *Proc Natl Acad Sci U S A* 19: 19.
- Campana WM (2007). Schwann cells: activated peripheral glia and their role in neuropathic pain. *Brain Behav Immun* 21: 522-527. .
- Caspani O, Zurborg S, Labuz D, & Heppenstall PA (2009). The contribution of TRPM8 and TRPA1 channels to cold allodynia and neuropathic pain. *PLoS One* 4: e7383.
- Cavaletti G, & Marmiroli P (2010). Chemotherapy-induced peripheral neurotoxicity. *Nat Rev Neurol* 6: 657-666.
- Cevikbas F, Wang X, Akiyama T, Kempkes C, Savinko T, Antal A, *et al.* (2014). A sensory neuron-expressed IL-31 receptor mediates T helper cell-dependent itch: Involvement of TRPV1 and TRPA1. *J Allergy Clin Immunol* 133: 448-460.
- Chen J, Joshi SK, DiDomenico S, Perner RJ, Mikusa JP, Gauvin DM, *et al.* (2011). Selective blockade of TRPA1 channel attenuates pathological pain without altering noxious cold sensation or body temperature regulation. *Pain* 152: 1165-1172.
- Chen J, Zhang XF, Kort ME, Huth JR, Sun C, Miesbauer LJ, *et al.* (2008). Molecular determinants of species-specific activation or blockade of TRPA1 channels. *J Neurosci* 28: 5063-5071.
- Chung MK, Asgar J, Lee J, Shim MS, Dumler C, & Ro JY (2015). The role of TRPM2 in hydrogen peroxide-induced expression of inflammatory cytokine and chemokine in rat trigeminal ganglia. *Neuroscience* 297: 160-169.

Clapham DE (1995). Calcium signaling. *Cell* 80: 259-268.

Clapham DE (2003). TRP channels as cellular sensors. *D - 0410462* 426: 517-524.

Clapham DE, Montell C, Schultz G, & Julius D (2003). International Union of Pharmacology. XLIII. Compendium of voltage-gated ion channels: transient receptor potential channels. *Pharmacol Rev* 55: 591-596.

Connor C, & Attai D (2013). Adjuvant endocrine therapy for the surgeon: options, side effects, and their management. *Ann Surg Oncol* 20: 3188-3193.

Corey DP, Garcia-Anoveros J, Holt JR, Kwan KY, Lin SY, Vollrath MA, *et al.* (2004). TRPA1 is a candidate for the mechanosensitive transduction channel of vertebrate hair cells. *D - 0410462* 432: 723-730.

Crew KD, Greenlee H, Capodice J, Raptis G, Brafman L, Fuentes D, *et al.* (2007). Prevalence of joint symptoms in postmenopausal women taking aromatase inhibitors for early-stage breast cancer. *J Clin Oncol* 25: 3877-3883.

Csala M, Kardon T, Legeza B, Lizak B, Mandl J, Margittai E, *et al.* (2015). On the role of 4-hydroxynonenal in health and disease. *Biochim Biophys Acta* 1852: 826-838.

Cuzick J, Sestak I, Baum M, Buzdar A, Howell A, Dowsett M, *et al.* (2013). Effect of anastrozole and tamoxifen as adjuvant treatment for early-stage breast cancer: 10-year analysis of the ATAC trial. *Lancet Oncol* 11: 1135-1141.

da Costa DS, Meotti FC, Andrade EL, Leal PC, Motta EM, & Calixto JB (2010). The involvement of the transient receptor potential A1 (TRPA1) in the maintenance of mechanical and cold hyperalgesia in persistent inflammation. *Pain* 148: 431-437.

- Dai Y, Wang S, Tominaga M, Yamamoto S, Fukuoka T, Higashi T, *et al.* (2007). Sensitization of TRPA1 by PAR2 contributes to the sensation of inflammatory pain. *J Clin Invest* 117: 1979-1987.
- Dalle-Donne I, Aldini G, Carini M, Colombo R, Rossi R, & Milzani A (2006). Protein carbonylation, cellular dysfunction, and disease progression. *J Cell Mol Med* 10: 389-406.
- del Camino D, Murphy S, Heiry M, Barrett LB, Earley TJ, Cook CA, *et al.* (2010). TRPA1 contributes to cold hypersensitivity. *J Neurosci* 30: 15165-15174.
- Demartini C, Tassorelli C, Zanaboni AM, Tonsi G, Francesconi O, Nativi C, *et al.* (2017). The role of the transient receptor potential ankyrin type-1 (TRPA1) channel in migraine pain: evaluation in an animal model. *J Headache Pain* 18: 94.
- Desta Z, Kreutz Y, Nguyen AT, Li L, Skaar T, Kamdem LK, *et al.* (2011). Plasma letrozole concentrations in postmenopausal women with breast cancer are associated with CYP2A6 genetic variants, body mass index, and age. *Clin Pharmacol Ther* 90: 693-700.
- Diener HC (2003). RPR100893, a substance-P antagonist, is not effective in the treatment of migraine attacks. *Cephalalgia* 23: 183-185.
- Doerflinger NH, Macklin WB, & Popko B (2003). Inducible site-specific recombination in myelinating cells. *Genesis* 35: 63-72.
- Dunham JP, Kelly S, & Donaldson LF (2008). Inflammation reduces mechanical thresholds in a population of transient receptor potential channel A1-expressing nociceptors in the rat. *Eur J Neurosci* 27: 3151-3160.
- Edvinsson L (2015). CGRP receptor antagonists and antibodies against CGRP and its receptor in migraine treatment. *Br J Clin Pharmacol* 80: 193-199.

- Eid SR, Crown ED, Moore EL, Liang HA, Choong KC, Dima S, *et al.* (2008). HC-030031, a TRPA1 selective antagonist, attenuates inflammatory- and neuropathy-induced mechanical hypersensitivity. *Mol Pain* 4: 48.
- Fajardo O, Meseguer V, Belmonte C, & Viana F (2008). TRPA1 channels: novel targets of 1,4-dihydropyridines. *Channels (Austin)* 2: 429-438.
- Fanciullacci M, Alessandri M, Figini M, Geppetti P, & Michelacci S (1995). Increase in plasma calcitonin gene-related peptide from the extracerebral circulation during nitroglycerin-induced cluster headache attack. *Pain* 60: 119-123.
- Fernandes ES, Russell FA, Spina D, McDougall JJ, Graepel R, Gentry C, *et al.* (2011). A distinct role for transient receptor potential ankyrin 1, in addition to transient receptor potential vanilloid 1, in tumor necrosis factor alpha-induced inflammatory hyperalgesia and Freund's complete adjuvant-induced monoarthritis. *Arthritis Rheum* 63: 819-829.
- Ferrari LF, Levine JD, & Green PG (2016). Mechanisms mediating nitroglycerin-induced delayed-onset hyperalgesia in the rat. *Neuroscience* 317: 121-129.
- Gallicchio L, Macdonald R, Wood B, Rushovich E, & Helzlsouer KJ (2011). Androgens and musculoskeletal symptoms among breast cancer patients on aromatase inhibitor therapy. *Breast Cancer Res Treat* 130: 569-577.
- Gauchan P, Andoh T, Kato A, & Kuraishi Y (2009). Involvement of increased expression of transient receptor potential melastatin 8 in oxaliplatin-induced cold allodynia in mice. *Neurosci Lett* 458: 93-95.
- Gaudet R (2008). A primer on ankyrin repeat function in TRP channels and beyond. *Mol Biosyst* 4: 372-379.
- Geppetti P, & Holzer P (1996) *Neurogenic inflammation*. CRC Press: Boca Raton.

- Ghosh D, Griswold J, Erman M, & Pangborn W (2009). Structural basis for androgen specificity and oestrogen synthesis in human aromatase. *D - 0410462 457*: 219-223.
- Gibson L, Lawrence D, Dawson C, & Bliss J (2009). Aromatase inhibitors for treatment of advanced breast cancer in postmenopausal women. *Cochrane Database Syst Rev* 7: CD003370.
- Goldstein DJ, Wang O, Saper JR, Stoltz R, Silberstein SD, & Mathew NT (1997). Ineffectiveness of neurokinin-1 antagonist in acute migraine: a crossover study. *Cephalalgia* 17: 785-790.
- Guan Z, Kuhn JA, Wang X, Colquitt B, Solorzano C, Vaman S, *et al.* (2016). Injured sensory neuron-derived CSF1 induces microglial proliferation and DAP12-dependent pain. *Nat Neurosci* 19: 94-101.
- Guler AD, Lee H, Iida T, Shimizu I, Tominaga M, & Caterina M (2002). Heat-evoked activation of the ion channel, TRPV4. *J Neurosci* 22: 6408-6414.
- Guo R, Chen XP, Guo X, Chen L, Li D, Peng J, *et al.* (2008). Evidence for involvement of calcitonin gene-related peptide in nitroglycerin response and association with mitochondrial aldehyde dehydrogenase-2 (ALDH2) Glu504Lys polymorphism. *J Am Coll Cardiol* 52: 953-960.
- Hamilton, K K, E K, & Attwell (2016). Proton-gated Ca(2+)-permeable TRP channels damage myelin in conditions mimicking. *D - 0410462 529*: 523-527.
- Henry NL, Giles JT, & Stearns V (2008). Aromatase inhibitor-associated musculoskeletal symptoms: etiology and strategies for management. *Oncology (Williston Park)* 22: 1401-1408.
- Hill K, & Schaefer M (2007). TRPA1 is differentially modulated by the amphipathic molecules trinitrophenol and chlorpromazine. *J Biol Chem* 282: 7145-7153.

- Hinman A, Chuang HH, Bautista DM, & Julius D (2006). TRP channel activation by reversible covalent modification. *Proc Natl Acad Sci U S A* 103: 19564-19568.
- Ho TW, Edvinsson L, & Goadsby PJ (2010). CGRP and its receptors provide new insights into migraine pathophysiology. *Nat Rev Neurol* 6: 573-582.
- Ho TW, Ferrari MD, Dodick DW, Galet V, Kost J, Fan X, *et al.* (2008). Efficacy and tolerability of MK-0974 (telcagepant), a new oral antagonist of calcitonin gene-related peptide receptor, compared with zolmitriptan for acute migraine: a randomised, placebo-controlled, parallel-treatment trial. *Lancet* 372: 2115-2123.
- Hofmann T, Schaefer M, Schultz G, & Gudermann T (2002). Subunit composition of mammalian transient receptor potential channels in living cells. *Proc Natl Acad Sci U S A* 99: 7461-7466.
- Iversen HK, & Olesen J (1996). Headache induced by a nitric oxide donor (nitroglycerin) responds to sumatriptan. A human model for development of migraine drugs. *Cephalalgia* 16: 412-418.
- Iversen HK, Olesen J, & Tfelt-Hansen P (1989). Intravenous nitroglycerin as an experimental model of vascular headache. Basic characteristics. *Pain* 38: 17-24.
- Jaquemar D, Schenker T, & Trueb B (1999). An ankyrin-like protein with transmembrane domains is specifically lost after oncogenic transformation of human fibroblasts. *J Biol Chem* 274: 7325-7333.
- Jiang N, Li H, Sun Y, Yin D, Zhao Q, Cui S, *et al.* (2014). Differential gene expression in proximal and distal nerve segments of rats with sciatic nerve injury during Wallerian degeneration. *Neural Regen Res* 9: 1186-1194.

- Jin SJ, Jung JA, Cho SH, Kim UJ, Choe S, Ghim JL, *et al.* (2012). The pharmacokinetics of letrozole: association with key body mass metrics. *Int J Clin Pharmacol Ther* 50: 557-565.
- Jordt SE, Bautista DM, Chuang HH, McKemy DD, Zygmunt PM, Hogestatt ED, *et al.* (2004). Mustard oils and cannabinoids excite sensory nerve fibres through the TRP channel ANKTM1. *D - 0410462 427*: 260-265.
- Joseph EK, Chen X, Bogen O, & Levine JD (2008). Oxaliplatin acts on IB4-positive nociceptors to induce an oxidative stress-dependent acute painful peripheral neuropathy. *J Pain* 9: 463-472.
- Joseph EK, & Levine JD (2009). Comparison of oxaliplatin- and cisplatin-induced painful peripheral neuropathy in the rat. *J Pain* 10: 534-541.
- Jukanti R, Sheela S, Bandari S, & Veerareddy PR (2011). Enhanced bioavailability of exemestane via proliposomes based transdermal delivery. *J Pharm Sci* 100: 3208-3222.
- Julius D, & Basbaum AI (2001). Molecular mechanisms of nociception. *D - 0410462 413*: 203-210.
- Jung H, Toth PT, White FA, & Miller RJ (2008). Monocyte chemoattractant protein-1 functions as a neuromodulator in dorsal root ganglia neurons. *J Neurochem* 104: 254-263.
- Kao DJ, Li AH, Chen JC, Luo RS, Chen YL, Lu JC, *et al.* (2012). CC chemokine ligand 2 upregulates the current density and expression of TRPV1 channels and Nav1.8 sodium channels in dorsal root ganglion neurons. *J Neuroinflammation* 9: 189.
- Karashima Y, Talavera K, Everaerts W, Janssens A, Kwan KY, Vennekens R, *et al.* (2009). TRPA1 acts as a cold sensor in vitro and in vivo. *Proc Natl Acad Sci U S A* 106: 1273-1278.

- Kelly E, Lu CY, Albertini S, & Vitry A (2015). Longitudinal trends in utilization of endocrine therapies for breast cancer: an international comparison. *J Clin Pharm Ther* 40: 76-82.
- Kim HK, Park SK, Zhou JL, Taglialatela G, Chung K, Coggeshall RE, *et al.* (2004). Reactive oxygen species (ROS) play an important role in a rat model of neuropathic pain. *Pain* 111: 116-124.
- Kindt KS, Viswanath V, Macpherson L, Quast K, Hu H, Patapoutian A, *et al.* (2007). *Caenorhabditis elegans* TRPA-1 functions in mechanosensation. *Nat Neurosci* 10: 568-577.
- Koivisto A, Hukkanen M, Saarnilehto M, Chapman H, Kuokkanen K, Wei H, *et al.* (2012). Inhibiting TRPA1 ion channel reduces loss of cutaneous nerve fiber function in diabetic animals: sustained activation of the TRPA1 channel contributes to the pathogenesis of peripheral diabetic neuropathy. *Pharmacol Res* 65: 149-158.
- Kopruszinski CM, Xie JY, Eyde NM, Remeniuk B, Walter S, Stratton J, *et al.* (2017). Prevention of stress- or nitric oxide donor-induced medication overuse headache by a calcitonin gene-related peptide antibody in rodents. *Cephalalgia* 37: 560-570.
- Koulchitsky S, Fischer MJ, De Col R, Schlechtweg PM, & Messlinger K (2004). Biphasic response to nitric oxide of spinal trigeminal neurons with meningeal input in rat--possible implications for the pathophysiology of headaches. *J Neurophysiol* 92: 1320-1328.
- Koulchitsky S, Fischer MJ, & Messlinger K (2009). Calcitonin gene-related peptide receptor inhibition reduces neuronal activity induced by prolonged increase in nitric oxide in the rat spinal trigeminal nucleus. *Cephalalgia* 29: 408-417.

- Kremeyer B, Lopera F, Cox JJ, Momin A, Rugiero F, Marsh S, *et al.* (2010). A gain-of-function mutation in TRPA1 causes familial episodic pain syndrome. *Neuron* 66: 671-680.
- Kunkler PE, Ballard CJ, Oxford GS, & Hurley JH (2011). TRPA1 receptors mediate environmental irritant-induced meningeal vasodilatation. *Pain* 152: 38-44.
- Kwan KY, Allchorne AJ, Vollrath MA, Christensen AP, Zhang DS, Woolf CJ, *et al.* (2006). TRPA1 contributes to cold, mechanical, and chemical nociception but is not essential for hair-cell transduction. *Neuron* 50: 277-289.
- Kwan KY, Glazer JM, Corey DP, Rice FL, & Stucky CL (2009). TRPA1 modulates mechanotransduction in cutaneous sensory neurons. *J Neurosci* 29: 4808-4819.
- Laroche F, Coste J, Medkour T, Cottu PH, Pierga JY, Lotz JP, *et al.* (2014). Classification of and risk factors for estrogen deprivation pain syndromes related to aromatase inhibitor treatments in women with breast cancer: a prospective multicenter cohort study. *J Pain* 15: 293-303.
- Levy D, Burstein R, Kainz V, Jakubowski M, & Strassman AM (2007). Mast cell degranulation activates a pain pathway underlying migraine headache. *Pain* 130: 166-176.
- Lewis T (1937). The nocifensor system of nerves and its reactions. *Br Med J*.
- Li S, Liu Q, Wang Y, Gu Y, Liu D, Wang C, *et al.* (2013). Differential gene expression profiling and biological process analysis in proximal nerve segments after sciatic nerve transection. *PLoS One* 8: e57000.
- Lintermans A, Van Calster B, Van Hoydonck M, Pans S, Verhaeghe J, Westhovens R, *et al.* (2011). Aromatase inhibitor-induced loss of grip strength is body mass index dependent: hypothesis-generating findings for its pathogenesis. *Ann Oncol* 22: 1763-1769.

- Liu T, van Rooijen N, & Tracey DJ (2000). Depletion of macrophages reduces axonal degeneration and hyperalgesia following nerve injury. *Pain* 86: 25-32.
- Luiz AP, Schroeder SD, Chichorro JG, Calixto JB, Zamprônio AR, & Rae GA (2010). Kinin B(1) and B(2) receptors contribute to orofacial heat hyperalgesia induced by infraorbital nerve constriction injury in mice and rats. *Neuropeptides* 44: 87-92.
- Lundberg JM, & Saria A (1983). Capsaicin-induced desensitization of airway mucosa to cigarette smoke, mechanical and chemical irritants. *D - 0410462 302*: 251-253.
- Macpherson LJ, Geierstanger BH, Viswanath V, Bandell M, Eid SR, Hwang S, *et al.* (2005). The pungency of garlic: activation of TRPA1 and TRPV1 in response to allicin. *Curr Biol* 15: 929-934.
- Macpherson LJ, Xiao B, Kwan KY, Petrus MJ, Dubin AE, Hwang S, *et al.* (2007). An ion channel essential for sensing chemical damage. *J Neurosci* 27: 11412-11415.
- Malmberg AB, & Basbaum AI (1998). Partial sciatic nerve injury in the mouse as a model of neuropathic pain: behavioral and neuroanatomical correlates. *Pain* 76: 215-222.
- Mao JJ, Chung A, Benton A, Hill S, Ungar L, Leonard CE, *et al.* (2013). Online discussion of drug side effects and discontinuation among breast cancer survivors. *Pharmacoepidemiol Drug Saf* 22: 256-262.
- Materazzi S, Benemei S, Fusi C, Galdani R, De Siena G, Vastani N, *et al.* (2013). Parthenolide inhibits nociception and neurogenic vasodilatation in the trigeminovascular system by targeting the TRPA1 channel. *Pain* 154: 2750-2758.
- Materazzi S, Fusi C, Benemei S, Pedretti P, Patacchini R, Nilius B, *et al.* (2012). TRPA1 and TRPV4 mediate paclitaxel-induced peripheral neuropathy in mice via a glutathione-sensitive mechanism. *Pflugers Arch* 463: 561-569.

- May D, Baastrup J, Nientit MR, Binder A, Schunke M, Baron R, *et al.* (2012). Differential expression and functionality of TRPA1 protein genetic variants in conditions of thermal stimulation. *J Biol Chem* 287: 27087-27094.
- McGaraughty S, Chu KL, Perner RJ, Didomenico S, Kort ME, & Kym PR (2010). TRPA1 modulation of spontaneous and mechanically evoked firing of spinal neurons in uninjured, osteoarthritic, and inflamed rats. *Mol Pain* 6: 14.
- McKemy DD, Neuhausser WM, & Julius D (2002). Identification of a cold receptor reveals a general role for TRP channels in thermosensation. *D - 0410462 416: 52-58.*
- McNamara CR, Mandel-Brehm J, Bautista DM, Siemens J, Deranian KL, Zhao M, *et al.* (2007). TRPA1 mediates formalin-induced pain. *Proc Natl Acad Sci U S A* 104: 13525-13530.
- Miyamoto T, Dubin AE, Petrus MJ, & Patapoutian A (2009). TRPV1 and TRPA1 mediate peripheral nitric oxide-induced nociception in mice. *PLoS One* 4: e7596.
- Moilanen LJ, Laavola M, Kukkonen M, Korhonen R, Leppanen T, Hogestatt ED, *et al.* (2012). TRPA1 contributes to the acute inflammatory response and mediates carrageenan-induced paw edema in the mouse. *Sci Rep* 2: 380.
- Montell C, & Rubin GM (1989). Molecular characterization of the *Drosophila* trp locus: a putative integral membrane protein required for phototransduction. *Neuron* 2: 1313-1323.
- Moqrich A, Hwang SW, Earley TJ, Petrus MJ, Murray AN, Spencer KS, *et al.* (2005). Impaired thermosensation in mice lacking TRPV3, a heat and camphor sensor in the skin. *Science* 307: 1468-1472.

- Mouridsen HT (2006). Incidence and management of side effects associated with aromatase inhibitors in the adjuvant treatment of breast cancer in postmenopausal women. *Curr Med Res Opin* 22: 1609-1621.
- Mukhopadhyay I, Gomes P, Aranake S, Shetty M, Karnik P, Damle M, *et al.* (2011). Expression of functional TRPA1 receptor on human lung fibroblast and epithelial cells. *J Recept Signal Transduct Res* 31: 350-358.
- Nassenstein C, Kwong K, Taylor-Clark T, Kollarik M, Macglashan DM, Braun A, *et al.* (2008). Expression and function of the ion channel TRPA1 in vagal afferent nerves innervating mouse lungs. *J Physiol* 586: 1595-1604.
- Nassini R, Fusi C, Materazzi S, Coppi E, Tuccinardi T, Marone IM, *et al.* (2015). The TRPA1 channel mediates the analgesic action of dipyrene and pyrazolone derivatives. *Br J Pharmacol* 172: 3397-3411.
- Nassini R, Gees M, Harrison S, G DS, Materazzi S, N M, *et al.* (2011). Oxaliplatin elicits mechanical and cold allodynia in rodents via TRPA1 receptor. *Pain* 152: 1621-1631.
- Nassini R, Materazzi S, Andre E, Sartiani L, Aldini G, Trevisani M, *et al.* (2010). Acetaminophen, via its reactive metabolite N-acetyl-p-benzo-quinoneimine and transient receptor potential ankyrin-1 stimulation, causes neurogenic inflammation in the airways and other tissues in rodents. *Faseb J* 24: 4904-4916.
- Nassini R, Materazzi S, Benemei S, & Geppetti P (2014). The TRPA1 channel in inflammatory and neuropathic pain and migraine. *Rev Physiol Biochem Pharmacol* 167: 1-43.
- Nassini R, Materazzi S, Vriens J, Prenen J, Benemei S, De Siena G, *et al.* (2012a). The 'headache tree' via umbellulone and TRPA1 activates the trigeminovascular system. *Brain* 135: 376-390.

- Nassini R, Pedretti P, Moretto N, Fusi C, Carnini C, Facchinetti F, *et al.* (2012b). Transient receptor potential ankyrin 1 channel localized to non-neuronal airway cells promotes non-neurogenic inflammation. *PLoS One* 7: e42454.
- Niethammer P, Grabher C, Look AT, & Mitchison TJ (2009). A tissue-scale gradient of hydrogen peroxide mediates rapid wound detection in zebrafish. *D - 0410462* 459: 996-999. .
- Nilius B (2007). Transient receptor potential (TRP) cation channels: rewarding unique proteins. *Bull Mem Acad R Med Belg* 162: 244-253.
- Nilius B, Appendino G, & Owsianik G (2012). The transient receptor potential channel TRPA1: from gene to pathophysiology. *Pflugers Arch* 464: 425-458.
- Nilius B, & Szallasi A (2014). Transient Receptor Potential Channels as Drug Targets: From the Science of Basic Research to the Art of Medicine. *Pharmacol Rev* 66: 676-814.
- Obata K, Katsura H, Mizushima T, Yamanaka H, Kobayashi K, Dai Y, *et al.* (2005). TRPA1 induced in sensory neurons contributes to cold hyperalgesia after inflammation and nerve injury. *J Clin Invest* 115: 2393-2401.
- Okun A, Liu P, Davis P, Ren J, Remeniuk B, Brion T, *et al.* (2012). Afferent drive elicits ongoing pain in a model of advanced osteoarthritis. *Pain* 153: 924-933.
- Olesen J (2008). The role of nitric oxide (NO) in migraine, tension-type headache and cluster headache. *Pharmacol Ther* 120: 157-171.
- Owsianik G, D'Hoedt D, Voets T, & Nilius B (2006). Structure-function relationship of the TRP channel superfamily. *Rev Physiol Biochem Pharmacol* 156: 61-90.
- Peier AM, Moqrich A, Hergarden AC, Reeve AJ, Andersson DA, Story GM, *et al.* (2002). A TRP channel that senses cold stimuli and menthol. *Cell* 108: 705-715.

- Perkins NM, & Tracey DJ (2000). Hyperalgesia due to nerve injury: role of neutrophils. *Neuroscience* 101: 745-757.
- Persson MG, Agvald P, & Gustafsson LE (1994). Detection of nitric oxide in exhaled air during administration of nitroglycerin in vivo. *Br J Pharmacol* 111: 825-828.
- Petrus M, Peier AM, Bandell M, Hwang SW, Huynh T, Olney N, *et al.* (2007). A role of TRPA1 in mechanical hyperalgesia is revealed by pharmacological inhibition. *Mol Pain* 3: 40.
- Presant CA, Bosserman L, Young T, Vakil M, Horns R, Upadhyaya G, *et al.* (2007). Aromatase inhibitor-associated arthralgia and/ or bone pain: frequency and characterization in non-clinical trial patients. *Clin Breast Cancer* 7: 775-778.
- Ramachandran R, Bhatt DK, Ploug KB, Hay-Schmidt A, Jansen-Olesen I, Gupta S, *et al.* (2014). Nitric oxide synthase, calcitonin gene-related peptide and NK-1 receptor mechanisms are involved in GTN-induced neuronal activation. *Cephalalgia* 34: 136-147.
- Reagan-Shaw S, Nihal M, & Ahmad N (2008). Dose translation from animal to human studies revisited. *Faseb J* 22: 659-661.
- Renton T, Durham J, & Aggarwal VR (2012). The classification and differential diagnosis of orofacial pain. *Expert Rev Neurother* 12: 569-576.
- Reuter U, Bolay H, Jansen-Olesen I, Chiarugi A, Sanchez del Rio M, Letourneau R, *et al.* (2001). Delayed inflammation in rat meninges: implications for migraine pathophysiology. *Brain* 124: 2490-2502.
- Rezvanfar MA, Rezvanfar MA, Ahmadi A, Saadi HA, Baeri M, & Abdollahi M (2012). Mechanistic links between oxidative/nitrosative stress and tumor necrosis factor

alpha in letrozole-induced murine polycystic ovary: biochemical and pathological evidences for beneficial effect of pioglitazone. *Hum Exp Toxicol* 31: 887-897.

Sadofsky LR, Sreekrishna KT, Lin Y, Schinaman R, Gorka K, Mantri Y, *et al.* (2014). Unique Responses are Observed in Transient Receptor Potential Ankyrin 1 and Vanilloid 1 (TRPA1 and TRPV1) Co-Expressing Cells. *Cells* 3: 616-626.

Salvatore CA, Hershey JC, Corcoran HA, Fay JF, Johnston VK, Moore EL, *et al.* (2008). Pharmacological characterization of MK-0974 [N-[(3R,6S)-6-(2,3-difluorophenyl)-2-oxo-1-(2,2,2-trifluoroethyl)azepan-3-yl]-4-(2-oxo-2,3-dihydro-1H-imidazo[4,5-b]pyridin-1-yl)piperidine-1-carboxamide], a potent and orally active calcitonin gene-related peptide receptor antagonist for the treatment of migraine. *J Pharmacol Exp Ther* 324: 416-421.

Sawada Y, Hosokawa H, Matsumura K, & Kobayashi S (2008). Activation of transient receptor potential ankyrin 1 by hydrogen peroxide. *Eur J Neurosci* 27: 1131-1142.

Schaefer M (2005). Homo- and heteromeric assembly of TRP channel subunits. *Pflugers Arch* 451: 35-42.

Sestak I, Cuzick J, Sapunar F, Eastell R, Forbes JF, Bianco AR, *et al.* (2008). Risk factors for joint symptoms in patients enrolled in the ATAC trial: a retrospective, exploratory analysis. *Lancet Oncol* 9: 866-872.

Shapiro D, Deering-Rice CE, Romero EG, Huguen RW, Light AR, Veranth JM, *et al.* (2013). Activation of transient receptor potential ankyrin-1 (TRPA1) in lung cells by wood smoke particulate material. *Chem Res Toxicol* 26: 750-758.

Sherrington CS (1906) *The Integrative Action of the Nervous System* Scribner: New York.

Shimizu S, Takahashi N, & Mori Y (2014). TRPs as chemosensors (ROS, RNS, RCS, gasotransmitters). *Handb Exp Pharmacol* 223: 767-794.

- Sicuteri F, Del Bene E, Poggioni M, & Bonazzi A (1987). Unmasking latent dynociception in healthy subjects. *Headache* 27: 180-185.
- Story GM, Peier AM, Reeve AJ, Eid SR, Mosbacher J, Hricik TR, *et al.* (2003). ANKTM1, a TRP-like channel expressed in nociceptive neurons, is activated by cold temperatures. *Cell* 112: 819-829.
- Strassman AM, Raymond SA, & Burstein R (1996). Sensitization of meningeal sensory neurons and the origin of headaches. *D - 0410462 384*: 560-564.
- Sullivan MN, Gonzales AL, Pires PW, Bruhl A, Leo MD, Li W, *et al.* (2015). Localized TRPA1 channel Ca²⁺ signals stimulated by reactive oxygen species promote cerebral artery dilation. *Sci Signal* 8: ra2.
- Szallasi A, Cortright DN, Blum CA, & Eid SR (2007). The vanilloid receptor TRPV1: 10 years from channel cloning to antagonist proof-of-concept. *Nat Rev Drug Discov* 6: 357-372.
- Talavera K, Gees M, Karashima Y, Meseguer VM, Vanoirbeek JA, Damann N, *et al.* (2009). Nicotine activates the chemosensory cation channel TRPA1. *Nat Neurosci* 12: 1293-1299.
- Tassorelli C, Greco R, Wang D, Sandrini M, Sandrini G, & Nappi G (2003). Nitroglycerin induces hyperalgesia in rats--a time-course study. *Eur J Pharmacol* 464: 159-162.
- Tauzin S, Starnes TW, Becker FB, Lam PY, & Huttenlocher A (2014). Redox and Src family kinase signaling control leukocyte wound attraction and neutrophil reverse migration. *The Journal of cell biology* 207: 589-598.
- Thadani U, & Rodgers T (2006). Side effects of using nitrates to treat angina. *Expert Opin Drug Saf* 5: 667-674.

- Trainor DC, & Jones RC (1966). Headaches in explosive magazine workers. *Arch Environ Health* 12: 231-234.
- Trevisan G, Hoffmeister C, Rossato MF, Oliveira SM, Silva MA, Ineu RP, *et al.* (2013a). Transient receptor potential ankyrin 1 receptor stimulation by hydrogen peroxide is critical to trigger pain during monosodium urate-induced inflammation in rodents. *Arthritis Rheum* 65: 2984-2995.
- Trevisan G, Materazzi S, Fusi C, Altomare A, Aldini G, Lodovici M, *et al.* (2013b). Novel therapeutic strategy to prevent chemotherapy-induced persistent sensory neuropathy by TRPA1 blockade. *Cancer Res* 73: 3120-3131.
- Trevisani M, Siemens J, Materazzi S, Bautista DM, Nassini R, Campi B, *et al.* (2007). 4-Hydroxynonenal, an endogenous aldehyde, causes pain and neurogenic inflammation through activation of the irritant receptor TRPA1. *Proc Natl Acad Sci U S A* 104: 13519-13524.
- Tvedskov JF, Tfelt-Hansen P, Petersen KA, Jensen LT, & Olesen J (2010). CGRP receptor antagonist olcegepant (BIBN4096BS) does not prevent glyceryl trinitrate-induced migraine. *Cephalalgia* 30: 1346-1353.
- Van Steenwinckel J, Auvynet C, Sapienza A, Reaux-Le Goazigo A, Combadiere C, & Melik Parsadaniantz S (2014). Stromal cell-derived CCL2 drives neuropathic pain states through myeloid cell infiltration in injured nerve. *Brain Behav Immun* 45: 198-210.
- Vander Jagt DL (2008). Methylglyoxal, diabetes mellitus and diabetic complications. *Drug Metabol Drug Interact* 23: 93-124.
- Vannier B, Zhu X, Brown D, & Birnbaumer L (1998). The membrane topology of human transient receptor potential 3 as inferred from glycosylation-scanning mutagenesis and epitope immunocytochemistry. *J Biol Chem* 273: 8675-8679.

- Vergnolle N, Bunnett NW, Sharkey KA, Brussee V, Compton SJ, Grady EF, *et al.* (2001). Proteinase-activated receptor-2 and hyperalgesia: A novel pain pathway. *Nat Med* 7: 821-826.
- Voets T, Prenen J, Fleig A, Vennekens R, Watanabe H, Hoenderop JG, *et al.* (2001). CaT1 and the calcium release-activated calcium channel manifest distinct pore properties. *J Biol Chem* 276: 47767-47770.
- Vos BP, Strassman AM, & Maciewicz RJ (1994). Behavioral evidence of trigeminal neuropathic pain following chronic constriction injury to the rat's infraorbital nerve. *J Neurosci* 14: 2708-2723.
- Vriens J, Watanabe H, Janssens A, Droogmans G, Voets T, & Nilius B (2004). Cell swelling, heat, and chemical agonists use distinct pathways for the activation of the cation channel TRPV4. *Proc Natl Acad Sci U S A* 101: 396-401.
- Wang YY, Chang RB, Waters HN, McKemy DD, & Liman ER (2008). The nociceptor ion channel TRPA1 is potentiated and inactivated by permeating calcium ions. *J Biol Chem* 283: 32691-32703.
- Watanabe H, Vriens J, Suh SH, Benham CD, Droogmans G, & Nilius B (2002). Heat-evoked activation of TRPV4 channels in a HEK293 cell expression system and in native mouse aorta endothelial cells. *J Biol Chem* 277: 47044-47051.
- Wei EP, Moskowitz MA, Boccalini P, & Kontos HA (1992). Calcitonin gene-related peptide mediates nitroglycerin and sodium nitroprusside-induced vasodilation in feline cerebral arterioles. *Circ Res* 70: 1313-1319.
- Wei H, Koivisto A, & Pertovaara A (2010). Spinal TRPA1 ion channels contribute to cutaneous neurogenic inflammation in the rat. *Neurosci Lett* 479: 253-256.

- Wenzl MV, Beretta M, Gorren AC, Zeller A, Baral PK, Gruber K, *et al.* (2009). Role of the general base Glu-268 in nitroglycerin bioactivation and superoxide formation by aldehyde dehydrogenase-2. *J Biol Chem* 284: 19878-19886.
- Wilson SR, Gerhold KA, Bifolck-Fisher A, Liu Q, Patel KN, Dong X, *et al.* (2011). TRPA1 is required for histamine-independent, Mas-related G protein-coupled receptor-mediated itch. *Nat Neurosci* 14: 595-602.
- Yao X, Kwan HY, & Huang Y (2005). Regulation of TRP channels by phosphorylation. *Neurosignals* 14: 273-280.
- Zakrzewska JM (2013). Differential diagnosis of facial pain and guidelines for management. *Br J Anaesth* 111: 95-104.
- Zakrzewska JM, & Linskey ME (2014). Trigeminal neuralgia. *Bmj* 348: g474.
- Zappia KJ, O'Hara CL, Moehring F, Kwan KY, & Stucky CL (2017). Sensory Neuron-Specific Deletion of TRPA1 Results in Mechanical Cutaneous Sensory Deficits. *eNeuro* 4: 0069-0016.
- Zhang X, Kainz V, Zhao J, Strassman AM, & Levy D (2013). Vascular extracellular signal-regulated kinase mediates migraine-related sensitization of meningeal nociceptors. *Ann Neurol* 73: 741-750.
- Zhu MX (2005). Multiple roles of calmodulin and other Ca(2+)-binding proteins in the functional regulation of TRP channels. *Pflugers Arch* 451: 105-115.
- Zhu X, Fujita M, Snyder LA, & Okada H (2011). Systemic delivery of neutralizing antibody targeting CCL2 for glioma therapy. *J Neurooncol* 104: 83-92.
- Zurborg S, Piszczek A, Martinez C, Hublitz P, Al Banchaabouchi M, Moreira P, *et al.* (2011). Generation and characterization of an Advillin-Cre driver mouse line. *Mol Pain* 7: 66.

Zurborg S, Yurgionas B, Jira JA, Caspani O, & Heppenstall PA (2007). Direct activation of the ion channel TRPA1 by Ca²⁺. *Nat Neurosci* 10: 277-279.